THE UNIVERSITY
of EDINBURGH

Cellular and synaptic pathophysiology in a rat model of Fragile X syndrome

Adam Jackson B.Sc. (Hons)

A thesis submitted for the degree of Doctor of Philosophy at the University of Edinburgh

September 2016

Declaration

I hereby certify that this thesis and its composition are entirely my own work, with the exception of the following:

(1) Metabolic labelling experiments were performed with the assistance of Dr Stephanie Barnes

(2) Immunolabelling experiments were performed with the assistance of Siyan Dimitov when he was a MSc student in the lab

No part of the work contained in this thesis has been submitted for any other degree or professional qualification.

Signed …… Date..……..

Acknowledgements

I would like to thank the people who have helped me throughout the past 4 years. Firstly my supervisors, Prof Peter Kind and Prof David Wyllie, for providing excellent academic support and guidance throughout my PhD. I would also like to thank Prof Sumantra Chattarji (Shona) for hosting me in Bangalore, which was a great experience.

Secondly, to those who have helped me technically during my PhD, in particular Steph Barnes and Aleks Domanski who helped get me started in the world of electrophysiology. Additionally, I would like to thank Sonal Kedia, Sally Till, Antonis Asiminas, Mostafizur Rahman, Emma Perkins, Michael Daw, Siyan Dimitrov and Sam Booker for their help and advice.

I would also like to thank the friends I have made in CIP, especially those in room 101, who have made the lab such a great place to work. Special thanks to Sean for a memorable dance and Max for always letting me win at pool.

Finally, I would like to thank my family especially Laura who has been a great support through this process.

Abstract

Fragile X syndrome (FXS) is the most commonly inherited form of intellectual disability as well as a leading genetic cause of autism spectrum disorder. It is typically the result of a trinucleotide repeat expansion in the *Fmr1* gene which leads to loss of the encoded protein, fragile X mental retardation protein (FMRP).

Animal model studies over the past twenty years, mainly focusing on the *Fmr1* knockout (KO) mouse, have uncovered several cellular and behavioural phenotypes associated with the loss of FMRP. Seminal work using the *Fmr1* KO mouse found that metabotropic glutamate receptor mediated long-term depression (mGluR-LTD) in the hippocampus is both exaggerated (Huber et al., 2002) and independent of new protein synthesis (Nosyreva & Huber, 2006). These findings, together with studies focusing on other brain regions including the prefrontal cortex (Zhao et al., 2005) and amygdala (Suvrathan et al., 2010), have contributed to the 'mGluR theory of FXS' (Bear et al., 2004) which suggests that group 1 metabotropic receptor function is exaggerated in FXS.

The development of genetically modified rats allows the modelling of FXS in an animal model with more complex cognitive and social behaviours than has been previously available. It also provides an opportunity for comparison of phenotypes across mammalian species that result from FMRP deletion. While the study of *Fmr1* rats can significantly contribute to our understanding of FXS, we must first confirm the assumption that cellular phenotypes are conserved across mouse and rat models.

In this thesis, we first aimed to test if the key cellular and synaptic phenotypes that contribute to the 'mGluR theory of FXS' are conserved in both the hippocampus and amygdala of *Fmr1* KO rats. In agreement with mouse studies, we found mGluR-LTD was both enhanced and independent of new protein synthesis in *Fmr1* KO rats. Similarly, group 1 mGluR long-term potentiation (LTP) was significantly decreased at both cortical and thalamic inputs to the lateral amygdala.

Secondly, we investigated mPFC intrinsic excitability and synaptic plasticity in *Fmr1* KO rats. The mPFC plays a key role in several of the cognitive functions that are affected in fragile X patients including attention, cognitive flexibility and anxiety (Goto et al., 2010). The regulation of mPFC plasticity and intrinsic excitability has also been associated with mGluR signalling. Here we found that intralaminar LTP in the mPFC showed an age-dependent deficit in *Fmr1* KO rats. The mPFC also provides top down control of several cortical and subcortical regions through long-range connectivity. One pathway of interest in the study of FXS is mPFC-amygdala connectivity which is associated with fear learning and anxiety behaviours (Burgos-Robles et al., 2009). Using retrograde tracing, we showed layer 5 pyramidal neurons that provide long-range connections to the basal amygdala were intrinsically hypoexcitable in *Fmr1* KO rats. This phenotype could possibly be explained through homeostatic changes in the axon initial segment which regulates neuronal excitability.

This work provides the first evidence for conservation of cellular phenotypes associated with the loss of FMRP in mice and rats which will be key in the interpretation of future studies using *Fmr1* KO rats. We also provide evidence of deficits in mPFC long-range connectivity to the basal amygdala, a pathway that is associated with FXS relevant behaviours. Together this highlights how study of the rat model of FXS can complement existing studies of *Fmr1* KO mice as well as provide new insights into the pathophysiology resulting from the loss of FMRP. Some of this work was published in Till et al., 2015.

Lay abstract

Fragile X syndrome is a common form of intellectual disability that can also result in Autism spectrum disorder. Due to its prevalence and well understood genetic cause, Fragile X has been widely studied in an attempt to determine what changes in brain function result in this syndrome. Until recently, this work has mainly been carried out using a mouse model of Fragile X syndrome which lacks the same protein as affected humans. Work using this model has greatly increased our understanding of how brains are affected in Fragile X syndrome as well as highlighted possible treatments to try and help people with the disorder. Recent advances in genetic manipulation have made it possible to create a rat model of Fragile X syndrome. Rats have some significant advantages over mice for the study of human disorders as they are larger, more intelligent and respond to drugs in a similar way to humans. Therefore the rat model of Fragile X syndrome could become a very useful tool for studying the human disorder. However, before using the rat model we must first test if some of the key findings discovered using mice are also present in the rats as this will inform future studies.

In this thesis, I find that the main findings from studies of the Fragile X mouse which have led to clinical trials in human patients are also present in the new rat model of Fragile X syndrome. I also highlight changes in the function of multiple brain areas of the Fragile X rat that are involved in behaviours associated with Fragile X syndrome such as anxiety, memory and decision making. Overall, this work highlights that the rat is a good model for the study of Fragile X syndrome that will help inform future work on the disorder and potential treatments for human patients.

Contents

List of figures

List of tables

Abbreviations

Abbreviation	Definition
ACC	Anterior cingulate cortex
aCSF	Artificial cerebrospinal fluid
ADP	Afterdepolarisation
AHP	Afterhyperpolarisation
AMPA	α-amino-3-hydroxy-5-methyl-4-isoxazolepropionic acid
AP	Action potential
APV	2-amino-5-phosphonopentanoic acid
ASD	Autism spectrum disorder
BA	Basal amygdala
BLA	Basolateral amygdala
BSA	Bovine serum albumin
CA1	Cornu Ammonis 1
CA3	Cornu Ammonis 3
CDPPB	3-cyano-N-(1,3-diphenyl-1H-pyrazol-5-yl)benzamide
CHX	Cycloheximide
C_M	Membrane capacitance
CNQX	6-cyano-7-nitroquinoxaline-2,3-dione
CPM	Counts per minute
CTEP	2-chloro-4-[2-[2,5-dimethyl-1-[4-(trifluoromethoxy)phenyl] imidazol-4-yl]ethynyl]pyridine
DHPG	3,5-Dihydroxyphenylglycine
EDTA	Ethylenediaminetetraacetic acid
EGTA	ethylene glycol-bis(β-aminoethyl ether)-N,N,N',N'-tetraacetic acid
EPSC	Excitatory post-synaptic current
EPSP	Excitatory post-synaptic potential
ERK	Extracellular signal-regulated kinase
ESC	Embryonic stem cell
fAHP	Fast afterhyperpolarisation
fEPSP	Field excitatory post-synaptic potential
FMR1	Fragile X mental retardation gene 1
FMRP	Fragile X mental retardation protein
FXS	Fragile X syndrome
GABA	*gamma*-Aminobutyric acid
HCN	Hyperpolarisation-activated cyclic nucleotide gated
HEPES	4-(2-hydroxyethyl)-1-piperazineethanesulfonic acid
HFS	High frequency stimulation
I_h	H-current
$I_{K\text{-}FAST}$	Fast inactivating potassium current
$I_{K\text{-}SLOW}$	Slow inactivating potassium current
$I_{K\text{-}Sustained}$	Non-inactivating potassium current
$I_{K\text{-}WC}$	Whole-cell potassium current
IL	Infralimbic

IP_3	inositol 1,4,5-trisphosphate
iPSC	Induced pluripotent stem cell
IPSC	Inhibitory post-synaptic current
KO	Knockout
LA	Lateral amygdala
LE	Long Evans
LTD	Long term depression
LTP	Long term potentiation
mAHP	Medium afterhyperpolarisation
mEPSC	Mini excitatory post-synaptic current
mGluR	Metabotropic glutamate receptor
mIPSC	Mini inhibitory post-synaptic current
MPEP	2-Methyl-6-(phenylethynyl)pyridine
mPFC	Medial prefrontal cortex
mTOR	Mammalian target of rapamycin
NMDA	N-methyl-D-aspartate
PCR	Polymerase chain reaction
PIKE	PI3-kinase enhancer
PL	Prelimbic
PPF	Paired pulse facilitation
PPLFS	Paired pulse low frequency stimulation
PPR	Paired pulse ratio
PTX	Picrotoxin
R_{in}	Input resistance
RMP/V_M	Resting membrane potential
RM-ANOVA	Repeated measures ANOVA
SA	Spine apparatus
sAHP	Slow afterhyperpolarisation
SD	Sprague Dawley
sEPSC	Spontaneous excitatory post-synaptic current
sIPSC	Spontaneous inhibitory post-synaptic current
T_M	Membrane time constant
TTX	Tetrodotoxin
VGCC	Voltage-gated calcium channel
VGKC	Voltage-gated potassium channel
WT	Wild type

Chapter 1

Introduction

1.1 Intellectual disability

Intellectual disability (ID) is the most prevalent form of neurodevelopmental disorder (NDD) affecting between 1-3% of the population (Leonard & Wen 2002). It is characterized by an intelligence quotient (IQ) score of 70 or below at 18 years of age with cases ranging from mild (50-70) to severe (<50) (Ropers & Hamel 2005). ID can be caused by environmental influences including prenatal alcohol exposure, infection, birth complications or malnutrition but it is also known to have many genetic causes (Vissers et al. 2015). Genetic causes are thought to account for around 50% of ID cases however a genetic diagnosis is lacking in many cases with approximately 60% having no known cause (Rauch et al. 2012).

The clinical heterogeneity of ID is reflected in its genetic heterogeneity with several hundreds of ID related genes identified. The X chromosome has been a main focus of ID research because of the gender bias that exists in ID populations with significantly more males affected than females (Leonard & Wen 2002). X-linked mutations resulting in monogenic forms of ID have now been identified in over 100 genes which collectively comprise approximately 10% of ID in males (Lubs et al. 2012).

The identification of prevalent monogenic forms of ID has led to the generation of genetically engineered animal models to study the disorder. These models recapitulate many of the behavioural and physiological phenotypes associated with human mutations. This has allowed research into the underlying mechanism associated with ID causing mutations which allows us to identify potential therapeutic strategies. Given the significant phenotypic overlap of many distinct genetic causes of ID, it is possible that they may share common underlying pathophysiology that is amenable to common therapeutic intervention (Auerbach et al. 2011; Barnes et al. 2015). Therefore, in depth study of ID mutations that are available for animal modelling may provide key insight into the pathophysiology of a range of IDs.

1.2 Fragile X syndrome

Fragile X syndrome (FXS) is the most commonly inherited form of intellectual disability affecting approximately 1: 4,000 males and 1: 8,000 females (de Vries et al. 1997; Coffee et al. 2009). It was first identified by Martin & Bell in 1943 as a novel example of ID segregating in an X-linked fashion (Martin & Bell 1943). FXS is often first diagnosed in young children at 3 years of age on the basis of speech delay followed by genetic testing (Bailey et al. 2009). The severity of ID ranges from moderate to severe in some cases and is often found to worsen with age (Wright-Talamante et al. 1996; Utari et al. 2010).

FXS individuals present many physical features which become more obvious through development. Pre-pubertal males typically show normal growth but have larger head circumference. Infants may also present hypotonia, gastroesophageal reflux and middle ear infections that require medical attention (Hagerman & Hagerman 2002). Post-puberty features include a long face with prominent forehead and jaw as well as enlarged ears and macro-orchidism. Additional medical concerns can also include strabismus, seizures, joint hyperflexibility and excessive skin softness (Bagni et al. 2012).

The behaviour of FXS individuals is often associated with attention deficit hyperactivity disorder (ADHD), impulsivity, anxiety, repetitive language as well as poor eye contact (Cordeiro et al. 2011). These behaviours as well as social and language deficits often lead to the diagnosis of autism spectrum disorder (ASD) in FXS individuals. Approximately one-third of FXS individuals show concomitant diagnosis with ASD (Fombonne 2003). This accounts for ~0.5% of all ASD cases making the fragile X mutation the most common single gene cause of autism (Coffee et al. 2009). The precise link between FXS and ASD is unclear. Studies have identified that mutations in several FMRP interacting proteins such as cytoplasmic FMRP interacting protein 1 (CYFIP1) (Van Der Zwaag et al. 2010) and eukaryotic initiation factor 4E (eIF4E) (Neves-Pereira et al. 2009) can also result in ASD. Likewise, several

mRNA targets of FMRP encode proteins that are associated with ASD such as Neuroligin 3, Neurexin 1, SHANK3, PTEN, TSC2 and NF1 (Darnell et al. 2011). This overlap between FMRP and ASD linked genes may underlie the development of autistic phenotypes in FXS however it is still unknown why this affects only a subpopulation of individuals.

1.2.1 *Fmr1* gene

Early genetic diagnosis of FXS began under a microscope with identification of the 'marker X chromosome' which showed non-staining gaps near the long end of the X chromosome (Lubs 1969). This results in a constriction near the q27 site which is prone to breakage resulting in chromosomal lesion, hence the name 'Fragile X'. Using methods emerging from the human genome project both the mutation and gene associated with this fragile site were identified (Kremer et al. 1991; Verkerk et al. 1991). The gene, named fragile X mental retardation 1 (*FMR1*), contains a polymorphic CGG repeat in the 5' untranslated region of exon 1. It is the unstable expansion of this trinucleotide sequence that has been identified as the most common cause of FXS. *FMR1* has three allelic categories which vary depending on this triplet repeat expansion. Unaffected individuals carry alleles contain 5 to 44 repeats, with the most common allele comprising 29-30 repeats (Nelson et al. 2013) . Premutation alleles containing between 55-200 repeats and are associated with phenotypes that are not FXS related. Approximately 25% of female carriers are at risk of developing what is known as fragile X associated premature ovarian insufficiency (FXPOI) which results in ovarian dysfunction and early menopause (Conway et al. 1998). Premutation carriers can also develop fragile X associated tremor ataxia syndrome (FXTAS), a late onset neurodegenerative condition, however males are at a significantly greater risk (Jacquemont et al. 2004). Finally, full mutations contain in excess of 200 repeats. In all cases, full mutations are derived from maternal premutations with the length of the maternal premutation directly proportional to the risk of expansion in to the full mutation range (Fu et al. 1991). In this range, an epigenetic trigger occurs leading to hypermethylation of the gene resulting in transcriptional silencing and loss of the gene product, fragile X mental retardation protein (FMRP) (Pieretti et al. 1991). Null

mutations can also arise from conventional mutations that disrupt the *FMR1* gene however these are infrequently reported. Two reports of missense mutations have also been identified, I340N and R138Q (Feng et al. 1997), in screens of males suspected of FXS without the trinucleotide expansion however it is likely that several more exist.

1.2.2 Modelling FXS

The development of FXS animal models has greatly advanced our understanding of how the loss of FMRP gives rise to FXS phenotypes. The *FMR1* gene is highly conserved across multiple species (Verkerk et al. 1991). This has led to the generation of multiple animal models of FXS however the majority of studies have used the *Fmr1* KO mouse as their model. As in the human genome, the mouse *Fmr1* gene is located on the X chromosome and shows 97% amino acid sequence identity with human FMRP (Ashley et al. 1993). The expression level and location of FMRP is also similar in mouse tissue compared with human tissue (Bakker et al. 2000).

As human FXS is caused by the absence of FMRP, the initial strategy to make a mouse model of FXS was to disrupt the *Fmr1* gene. This was achieved by the Dutch-Belgian fragile X Consortium who created and initially characterised the *Fmr1* KO mouse (Bakker et al. 1994). This is in contrast to human FXS, which is typically caused by expansion of the *FMR1* gene and hypermethylation of the promoter region. However, mouse models generated with long CGG repeats (>200) show no increase in promoter methylation and FMRP is still expressed (Bontekoe et al. 2001).

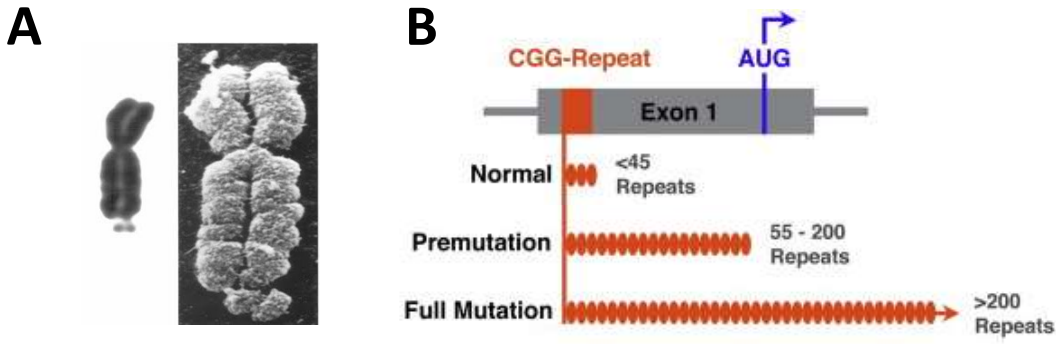

Figure 1.1 Fragile X mutation (A) Image of X chromosome of FXS individual. Constriction near the q27 site is prone to breakage resulting in chromosomal lesion, giving the name 'Fragile X'. (B) Polymorphic CGG repeat in the 5' untranslated region of exon 1 defines the transcription status of *FMR1* gene. <45 repeats allows normal transcription and translation of FMRP. Premutation alleles with 55-200 repeats can result in fragile X associated tremor ataxia syndrome (FXTAS) and fragile X associated premature ovarian insufficiency (FXPOI). Full mutation resulting from >200 CGG repeats leads to hypermethylation of the promoter region and transcriptional silencing of the *FMR1* gene. Figure adapted from Nelson et al., 2013.

1.2.3 Structure and function of FMRP

Since the discovery that the absence of FMRP is the cause of FXS, there has been a substantial effort to understand the function of FMRP and the consequences of its loss. The human *FMR1* gene is composed of 17 exons that undergo alternative splicing generating FMRP isoforms that can vary from 67-80kDa (Devys et al. 1993). FMRP is mainly cytoplasmic and is expressed throughout the body although most strongly in the neurons and testes (Verheij et al. 1993). It contains three domains associated with RNA binding; two KH domains and a RGG box (Siomi et al. 1993). Through these domains, FMRP is able to associate with polyribosomes via RNA binding (Stefani et al. 2004). This ability to associate with polyribosomes is clearly a key property of FMRP function as the point mutation I304N, which results in FXS (De Boulle et al. 1993), exists within the KH2 domain and results in loss of RNA binding (Zang et al. 2009).

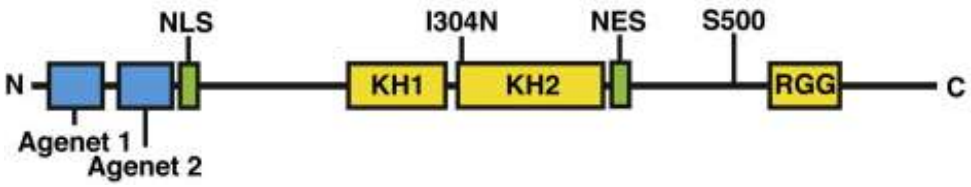

Figure 1.2 Structure of FMRP Two KH domains and an RGG box in the C-terminus act allow FMRP to interact with mRNA binding targets. I340N mutation in the KH2 domain prevents FMRP from binding mRNA and results in FXS phenotypes. Phosphorylation at S500 controls FMRPs ability to influence protein translation. Figure adapted from Nelson et al., 2013.

Through its interactions with polysomes, FMRP is widely thought to function as a negative regulator of translation (Nelson et al. 2013). The most commonly accepted mechanism is that FMRP directly associates with translational apparatus, stalling ribosomes and thereby preventing polypeptide elongation (Darnell et al. 2011). The ability of FMRP to influence protein translation is controlled by its phosphorylation state. Dephosphorylation of FMRP at serine 500 by PP2A relieves translation suppression and increases local protein synthesis (Narayanan et al. 2007). FMRP is then rephosphorylated by ribosomal s6 kinase 1 (S6K1) (Narayanan et al. 2008) allowing FMRP to bind to its mRNA target. The precise nature of FMRPs RNA selectivity is unknown. Analysis of FMRP interacting mRNAs suggested it is RNA structural components such as stem G-quartet loops and kissing complex motifs which are important for FMRP binding (Darnell et al. 2001; Darnell et al. 2005). However, more recent studies using HITS-CLIP mRNA cross linking techniques has identified 842 mRNA targets which show no enrichment of any particular structural elements (Darnell et al. 2011).

In total, FMRP can associate with approximately 4% of all mRNA in the brain which are enriched in both pre- and postsynaptic proteins (Darnell et al. 2011). Postsynaptic targets include ~30% of post-synaptic density proteins (PSD) including NMDA receptor subunits, PSD-95, SynGAP and calcium/calmodulin-dependent protein kinase II (CaMKII). FMRP can also regulate as much as 30% of presynaptic proteins including many structural elements, synaptic vesicle proteins and voltage-gated Ca^{2+}

channels. Therefore FMRP is clearly in a position to greatly influence synaptic function and plasticity.

1.3 FMRP role at the synapse

The majority of studies investigating the underlying pathophysiology of FXS have focused on the glutamatergic synapse. FMRP is located in dendritic spines, dynamically regulated by synaptic activity and a regulator of local protein synthesis (Weiler et al. 1997; Antar et al. 2004; Bassell & Warren 2008). These functions highlight FMRP as a key regulator of synaptic function and plasticity. The loss of FMRP is associated with a diverse set of behavioural phenotypes which suggests an underlying dysfunction of several functionally distinct brain regions. Here we will discuss the effects identified at glutamatergic synapses in various brain areas that appear to contribute to the FXS phenotype

A major hallmark of FXS is reduced cognitive ability. Synaptic plasticity, the ability of a synapse to modulate its strength in an activity-dependent manner, is thought to be the key molecular mechanism underlying memory and cognition. Therefore, many studies have investigated synaptic plasticity mechanism in FXS animal models. The association of synaptic plasticity and cognitive processing is often investigated within the hippocampus, a structure involved in many aspects of cognition such as learning and memory.

1.3.1 Hippocampal mGluR-LTD in *Fmr1* KO mice

Group 1 metabotropic glutamate receptors (mGluR) are seven transmembrane receptors which are canonically linked to Gq proteins, allowing receptor activation to stimulate downstream signalling pathways (Gladding et al. 2009). The group 1 subclass is comprised of $mGluR_1$ and $mGluR_5$ subtypes which show immunoreactivity throughout the brain (Ferraguti & Shigemoto 2006). In postsynaptic regions, group 1

mGluRs are localised perisynaptically where there activation is known to influence synaptic strength in a brain region-dependent manner (Lujan et al. 1996).

Activation of group 1 metabotropic glutamate receptors with the chemical agonist (R,S)-3,5-dihydroxyphenylglycine (DHPG) or paired-pulse low frequency stimulation (PP-LFS) results in a decrease in synaptic strength in CA1 hippocampus (Palmer et al. 1997; Huber 2000). This synaptic depression in long lasting and is mechanistically distinct from the classically described NMDA receptor dependent LTD at the same synapses (Palmer et al. 1997; Oliet et al. 1997). This form of plasticity was deemed particularly relevant to FXS as mGluR signalling is canonically linked to mRNA translation activation in excitatory neurons (Weiler & Greenough 1993). Crucially, the long term expression of mGluR-LTD has been shown to be dependent on rapid protein synthesis of pre-existing mRNAs within dendrites (Huber 2000; Huber et al. 2001). FMRP is also rapidly synthesised in response to mGluR activation on the same time scale (Weiler et al. 1997). This suggests that FMRP may play a role in regulating the long term expression of mGluR-LTD.

Studies investigating mGluR-LTD in CA1 hippocampus of *Fmr1* KO mice have found enhanced synaptic depression compared to wild-type controls (Huber et al. 2002; Hou et al. 2006). In addition, mGluR-LTD is also enhanced in *Fmr1* KO cerebellum which shares many of the same expression mechanisms (Koekkoek et al. 2005). Given FMRPs role as a translational suppressor, it was suggested that this enhanced depression was the result of increased levels of proteins that are required for mGluR-LTD in *Fmr1* KO synapses. As FMRP itself is synthesised in response to mGluR activation, it was suggested that FMRP may function as a negative feedback mechanism to limit mGluR stimulated translation of so called 'LTD proteins' thereby modulating synaptic depression. Therefore, in the absence of FMRP, unrepressed translation following mGluR-activation would lead to excess 'LTD protein' translation and exaggerated mGluR-LTD. This was termed the 'mGluR theory of

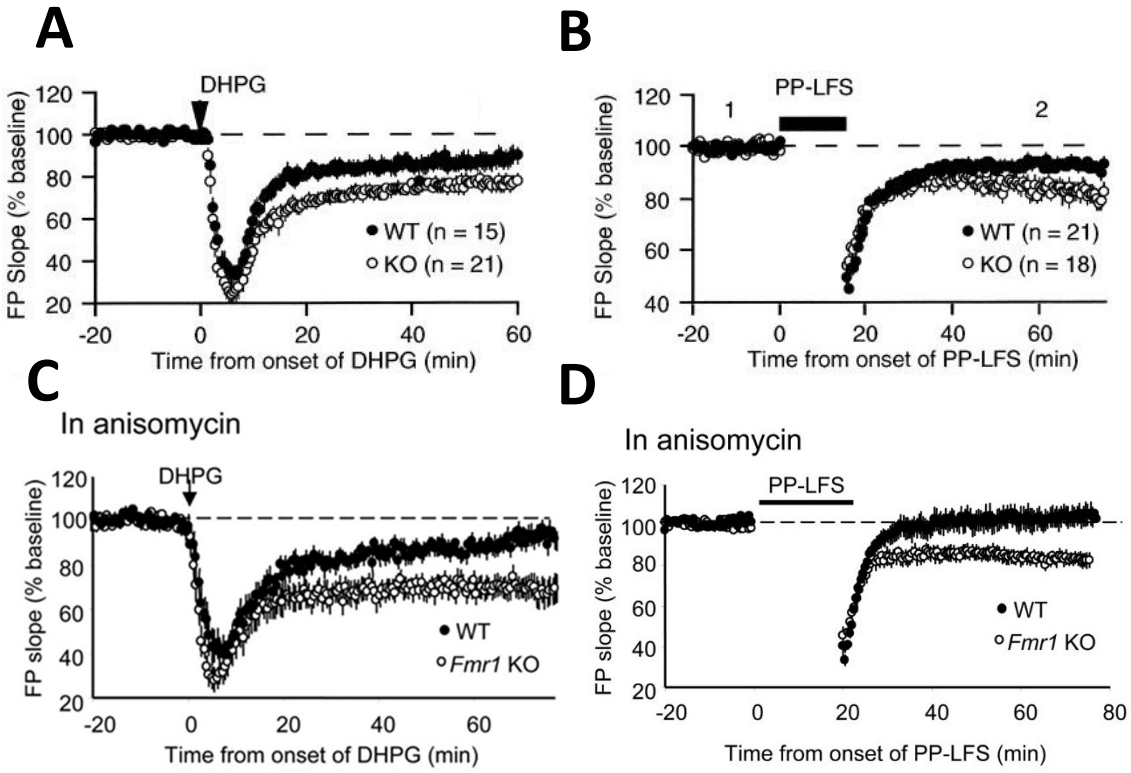

Figure 1.3 mGluR-dependent LTD is enhanced and independent of new protein synthesis in *Fmr1* KO mice (A) Chemical induction of mGluR-LTD with the group 1 mGluR agonist DHPG results in enhanced synaptic depression in *Fmr1* KO CA1 hippocampus (B) Synaptic induction of mGluR-LTD with 900 paired pulses at 1Hz frequency results in enhanced synaptic depression in *Fmr1* KO mice (C and D) Both chemical and synaptic mGluR-LTD require new protein synthesis for long-term expression in WT mice. mGluR-LTD is independent of new protein synthesis in *Fmr1* KO mice. Figures from Huber et al., 2002 and Nosyreva & Huber, 2006.

FXS' (Bear et al. 2004) which proposed that many of the phenotypes associated with FXS are the result of excess protein translation downstream of group 1 mGluRs.

Contrary to this hypothesis, mGluR-stimulated protein synthesis is absent in *Fmr1* KO mice (Todd et al. 2003; Weiler et al. 2004; Osterweil et al. 2010). This suggests that the basal levels of 'LTD proteins' in *Fmr1* KO dendrites are sufficient for the expression of mGluR-LTD. Consistent with its role as a negative regulator of protein translation, *in vivo* and *in vitro* basal protein synthesis levels are exaggerated in *Fmr1* KO mice (Qin 2005; Dölen et al. 2007). This includes the upregulation of several

proteins that are vital to proper synaptic function including PSD-95, AMPAR subunits and CaMKII (Muddashetty et al. 2007; Osterweil et al. 2010). Therefore it was hypothesised mGluR-LTD, which is normally blocked in the presence of protein synthesis inhibitors, will persist in *Fmr1* KO mice as the necessary proteins are already present at the synapse. This was confirmed experimentally as mGluR-LTD is insensitive to protein synthesis blockade in the absence of FMRP (Nosyreva & Huber 2002).

1.3.2 mGluR-regulated protein synthesis in *Fmr1* KO mice

The finding that mGluR activation does not result in new protein synthesis in FXS (Osterweil et al. 2010), suggests dysfunction of the signalling pathways which link mGluR activation to protein synthesis. One potential explanation could be that mGluR signalling is uncoupled from protein translational machinery in the absence of FMRP. Another explanation, which has gathered more experimental evidence, is that enhanced basal protein synthesis levels in the *Fmr1* KO mice may cause a ceiling effect such that further stimulation of mGluR is ineffective (Qin et al. 2005; Osterweil et al. 2010).

mGluR activation is believed to be linked to protein translation machinery via two intracellular signalling pathways, the mammalian target of rapamycin (mTOR) pathway and the ERK/MAPK pathway. mGluRs stimulate translation intiation through the formation of the eukaryotic initiation factor complex 4F (eIF4F) (Banko 2006). This complex requires phosphorylation of eIF4E binding protein (4E-BP) via activation of the mTOR signalling pathway and phosphorylation of eIF4E by Mnk, a component of the ERK/MAPK pathway (Banko et al. 2006). Both pathways also activate p70 S6 kinase which activates the ribosomal protein S6, stimulating translation of 5' terminal oligopyrimidine tract (TOP) containing mRNAs which typically encode components of translation machinery thereby increasing the translational capacity of a cell (Dufner & Thomas 1999; Antion et al. 2008).

1.3.3 mTOR signalling in *Fmr1* KO mice

Although $mGluR_5$ expression is normal in the absence of FMRP, $mGluR_5$ shows reduced association with the scaffolding protein Homer (Giuffrida et al. 2005). mGluR-Homer interactions are also necessary for coupling mGluR activity with the PI3K-mTOR pathway (Ronesi & Huber 2008). In agreement with this, mGluR activation fails to activate components of the mTOR pathway in *Fmr1* KO mice suggesting mGluR is uncoupled from mTOR signalling and is therefore unable to trigger protein translation (Ronesi & Huber 2008). However other groups have found that the steady state levels of mTOR and Akt phosphorylation are enhanced in *Fmr1* KO mice (Gross et al. 2010; Sharma et al. 2010). This is thought to be the result of increased PIKE levels in *Fmr1* KO neurons, whose mRNA normally associates with FMRP (Darnell et al. 2011; Gross et al. 2010; Sharma et al. 2010). PIKE binds and activates PI3K and Akt in response to mGluR activation leading to increased mTOR signalling. These differences may stem from the background strain of the animals used, FVB (Sharma et al. 2010) or C57BL/6 (Ronesi & Huber 2008) however this effect has not been investigated further.

Several studies have found that the expression of mGluR-LTD is sensitive to rapamycin suggesting mTOR signalling is necessary for the synthesis of new proteins in response to mGluR activation (Hou & Klann 2004; but see below). Furthermore, rapamycin also reduces steady state protein synthesis suggesting mTOR signalling also regulates basal mRNA translation (Muddashetty et al. 2007). However in *Fmr1* KO mice, mGluR-LTD is insensitive to rapamycin treatment (Sharma et al. 2010). mTOR activation in response to mGluR activation is also absent in *Fmr1* KO mice which is consistent with the finding that mGluR is uncoupled from the mTOR signalling (Ronesi & Huber 2008) or could mean that the phosphorylated state of mTOR in *Fmr1* KO synapses is increased to a state that it is insensitive to further mGluR activation (Sharma et al. 2010). Nevertheless, these results are consistent with the view that overactive basal protein synthesis in *Fmr1* KO mice results in the accumulation of synaptic proteins that are sufficient for the expression of mGluR-LTD. However, a study which examined mTOR activation under the experimental

conditions that revealed altered mGluR-dependent synaptic plasticity in CA1 hippocampus of *Fmr1* KO mice found no differences in steady state mTOR signalling in *Fmr1* KO mice suggesting this pathway is not responsible for the increased basal protein synthesis in the absence of FMRP (Osterweil et al. 2010). In agreement with this, rapamycin had no effect on basal protein synthesis rates in either genotype (Osterweil et al. 2010). The differences in these studies may stem from differences in tissue preparation. Whilst Sharma et al (2010) used acutely dissected tissue in their study, Osterweil et al (2010) allowed tissue to incubate for 4 hours to reach a stable level of protein synthesis. Therefore, it is unclear if results from Sharma and colleagues reflects the early post-mortem state of *Fmr1* KO mTOR signalling or if these effects stem from differential response of *Fmr1* KO tissue to acute tissue preparation. These results raise questions about the role of mTOR signalling in mGluR-LTD and mGluR-driven protein synthesis and how it contributes to FXS pathology.

1.3.4 ERK/MAPK signalling in *Fmr1* KO mice

Activation of mGluR also stimulates the ERK1/2 pathways (Gallagher 2004; Osterweil et al. 2010). The dual phosphorylation and activation of ERK1/2 is also associated with and necessary for mGluR-LTD expression in WT CA1 hippocampus (Gallagher et al. 2004; Banko et al. 2006; Hou et al. 2006). Studies have reported that steady state levels of ERK phosphorylation are increased in *Fmr1* KO animals suggesting enhanced ERK signalling may contribute to the FXS phenotype (Hou et al. 2006). Consistent with this, preincubation with U0126 normalises basal protein synthesis levels to WT levels in *Fmr1* KO mice (Osterweil et al. 2010). However, this study did not observe any differences in steady state or mGluR-driven ERK activation in *Fmr1* KO animals compared to WT controls suggesting that hypersensitivity of $mGluR_5$ or ERK signalling do not contribute to enhanced basal protein synthesis. Therefore, altered protein synthesis rates in *Fmr1* KO mice may be the result of hypersensitive response of protein translation machinery in the absence of FMRP rather than changes in upstream signalling (Osterweil et al. 2010).

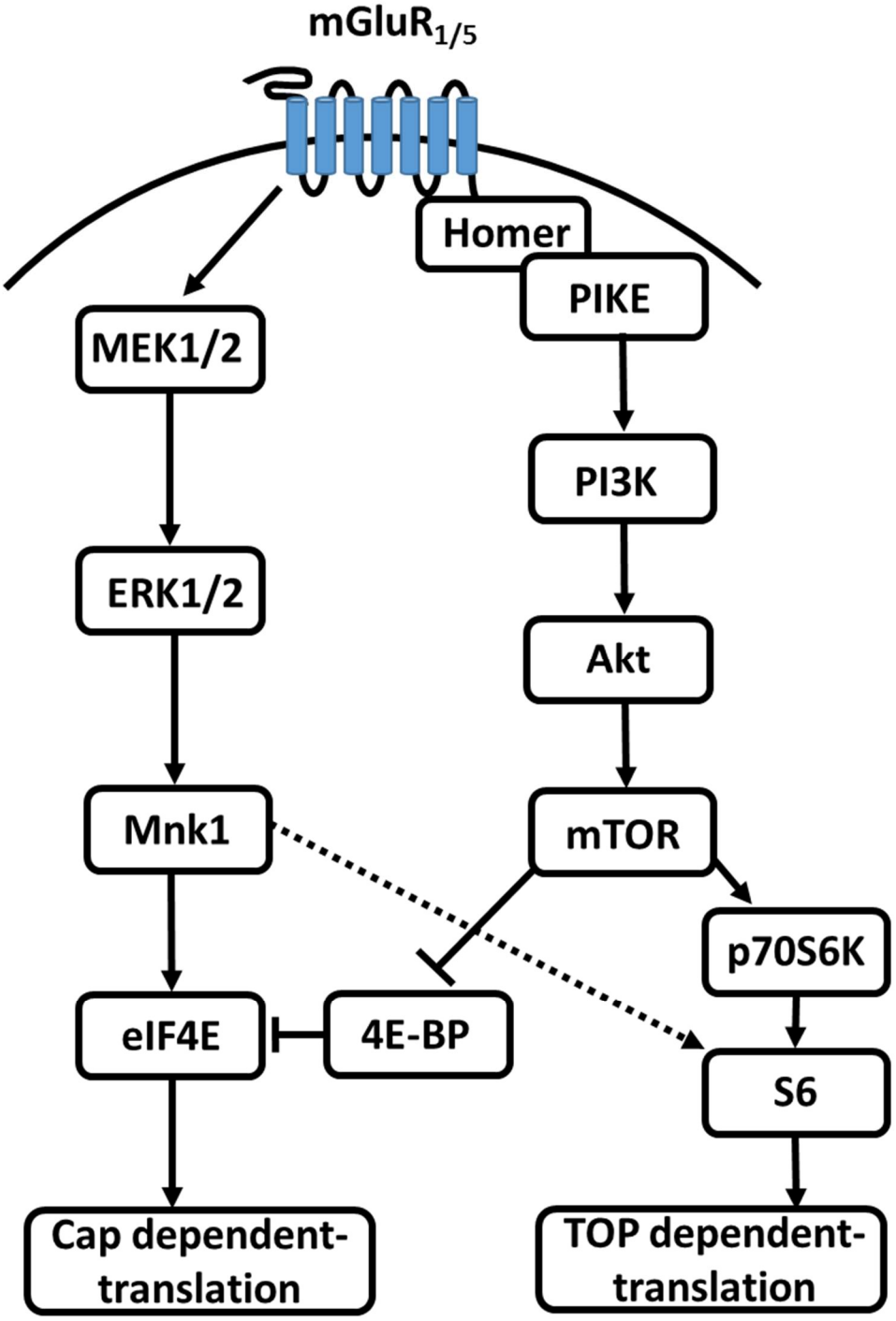

Figure 1.4 Group 1 mGluR signalling links to protein translation machinery
Stimulation of $mGluR_{1/5}$ activates local protein translation through mammalian target of rapamycin (mTOR) pathway and extracellular signal-regulated kinase (ERK) pathway. Both pathways result in Cap dependent-translation of local mRNAs as well as TOP dependent mRNA translation which increases the translational capacity of the neuron.

1.3.5 mGluR theory of FXS

Taken together, the findings that FMRP is normally synthesised in response to mGluR activation, basal protein synthesis is exaggerated in the absence of FMRP, that mGluR-LTD requires new protein synthesis and that mGluR-LTD is enhanced and independent of new protein synthesis in *Fmr1* KO mice have contributed to the mGluR theory of FXS (Bear et al. 2004). This theory suggests that in the absence of FMRP, exaggerated protein synthesis downstream of mGluR-signalling results in enhanced mGluR-LTD that no longer requires new protein synthesis in *Fmr1* KO mice. This theory also suggests that many of the phenotypes associated with FXS may be the result of exaggerated responses to mGluR activation. In agreement with this, studies targeting group 1 mGluR signalling either genetically or pharmacologically have shown significant amelioration of many phenotypes in *Fmr1* KO mice. Reducing $mGluR_5$ signalling restores both basal protein synthesis levels and mGluR-LTD magnitude to WT levels (Dölen et al. 2007; Michalon et al. 2012). This strategy has also corrected phenotypes at many levels of analysis including spine density phenotypes and ocular dominance plasticity in the visual cortex as well as behaviours including exaggerated inhibitory avoidance extinction, increased audiogenic seizure susceptibility and hyperactivity in open field tests (Yan et al. 2005; Nakamoto et al. 2007). Interestingly many of these phenotypes could still be rescued when therapeutics were administered at 1 month of age indicating these therapeutics may still be beneficial to FXS patients when started late in development (Michalon et al. 2012).

1.3.6 NMDAR-dependent plasticity in *Fmr1* KO mice

As well as mGluR-LTD, NMDAR-dependent forms of plasticity have also been investigated in the hippocampus of *Fmr1* KO mice. Some forms of NMDAR-dependent LTP are also reliant on new protein synthesis such as late phase LTP (L-LTP), a persistent form of LTP that last in excess of 4 hours. The induction of L-LTP is independent of protein synthesis however its long term maintenance requires it (Stanton & Sarvey 1984). Due to FMRPs role in translation regulation, L-LTP was

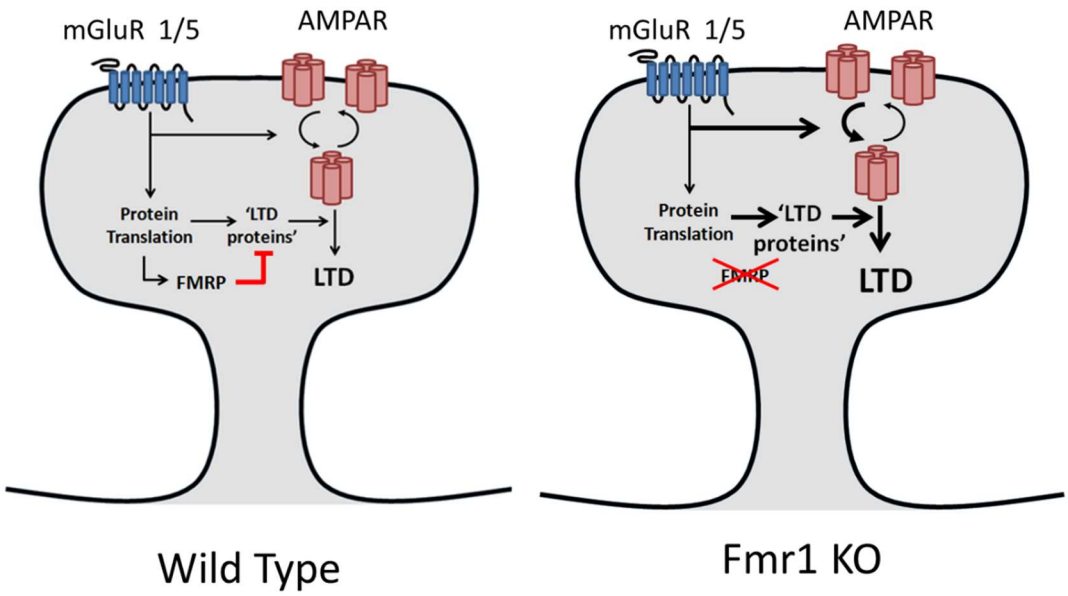

Figure 1.5 The mGluR theory of fragile X syndrome Model designed to explain experimental observations of mGluR-dependent phenotypes in *Fmr1* KO mice. In WT dendritic spine, group 1 mGluR activation results in the synthesis of local protein synthesis including FMRP which acts as a repressor of local mRNA translation. In *Fmr1* KO dendritic spines, basal levels of 'LTD proteins' are increased in the absence of FMRP leading to excess AMPAR removal in response to mGluR activation. These excess levels are also sufficient to mediate synaptic depression meaning new protein synthesis is no longer required for the long term expression of mGluR-LTD in the absence of FMRP.

also investigated in *Fmr1* KO mice however no difference was observed between genotypes (Paradee et al. 1999; Zhang et al. 2009). As FMRP loss affects protein-synthesis dependent LTD but not LTP, this suggests that FMRP may specifically regulate proteins required for LTD expression. Alternatively, FMRP may be specifically required for the regulation of dendritic protein synthesis. L-LTP is induced by multiple trains of high frequency tetanus that rely on neuron wide transcription and translation (Abraham & Williams 2003). In contrast, L-LTP induced using a weaker theta burst protocol which is solely dependent on dendritic mRNA translation revealed reduced LTP in *Fmr1* KO mice (Lauterborn et al. 2007). This indicates that FMRP may only regulate local mRNA translation at dendritic sites. Protein-synthesis independent forms of NMDA-receptor dependent plasticity have also been investigated. Hippocampal NMDAR-dependent LTD is unaffected in *Fmr1* KO mice

(Huber et al. 2000) suggesting the enhanced synaptic depression is specific to mGluR-LTD. Similarly early-phase NMDAR-dependent LTP, which is independent of protein synthesis, is comparable to WT levels in *Fmr1* KO mice (Godfraind et al. 1996; Li et al. 2002; Larson et al. 2005). This suggests that NMDAR function and signalling are unaffected in the hippocampus of *Fmr1* KO mice.

1.4 Amygdala synaptic plasticity

FXS individuals exhibit a common incidence of gaze avoidance, high anxiety and elevated acute stress levels consistent with amygdala dysfunction (Hessl et al. 2004). In agreement with this, evidence from human neuroimaging studies has shown that sensitisation of the amygdala is part of the aberrant emotional response in FXS individuals (Watson et al. 2008). Consistent with observations in humans, studies in *Fmr1* KO mice have revealed changes in amygdala dependent behaviours including anxiety and fear learning (McNaughton et al. 2008; Paradee et al. 1999).

The amygdala forms a key component of the brains fear circuitry. The neurobiology of fear circuitry has typically been investigated using fear conditioning paradigms in rodents. Evidence from lesion and pharmacological studies points to the amygdala as the neural system involved in many aspects of fear learning. As the responses to fear conditioning paradigms resemble the behavioural and physiological symptoms of human fear, an understanding of the neurobiology of fear memories is thought to have clinical relevance to human conditions associated with altered fear responses (LeDoux 2003).

In classical fear conditioning paradigms, a conditioned stimulus (CS), such as a tone, is paired with an aversive unconditioned stimulus (US) leading to their association. At a neurobiological level, CS and US carrying inputs converge in the lateral amygdala (LA) arising from thalamic and cortical synapses respectively (Romanski & LeDoux 1993). This convergence results in enhanced processing of CS inputs believed to be

the result of LTP at thalamic inputs to the LA (Blair et al. 2001; Bauer et al. 2002). Crucially for the study of FXS, whilst $mGluR_5$ signalling results in LTD in CA1 hippocampus, $mGluR_5$ mediates LTP at thalamic inputs to the LA (Rodrigues et al. 2002). Based on the mGluR theory of FXS, excessive mGluR signalling may be expected to result in exaggerated mGluR-LTP in the LA of *Fmr1* KO mice. However given the observed deficits in fear learning in *Fmr1* KO mice (Paradee et al. 1999) this suggests that mGluR-LTP is diminished. This has been confirmed experimentally with the finding that mGluR-dependent LTP is lost at thalamic inputs to the LA in the absence of FMRP (Zhao 2005; Suvrathan et al. 2010). Contrary to plasticity deficits in the hippocampus, acute treatment with mGluR antagonists does not rescue this phenotype in *Fmr1* KO mice (Suvrathan et al. 2010). However, chronic administration does rescue this phenotype (personal communication, Professor Shona Chattarji, inSTEM). Whilst this provides further evidence on group 1 mGluR dysfunction in FXS, it suggests that synaptic phenotypes vary with brain region.

As well as thalamic inputs, plasticity at cortical inputs to the LA can also mediate CS-US association during fear conditioning (Tsvetkov et al. 2002). Synaptic strengthening of the cortical input to the LA also shows a requirement for group 1 mGluR signalling (Cho et al. 2011). This form of plasticity uses an induction protocol which mirrors the timing of convergent thalamic and cortical input activation *in vivo* which suggests it may have behavioural relevance. Plasticity at this pathway remains unexplored in animal models of FXS but, given the involvement of group 1 mGluR signalling, could represent a further cellular correlate for the deficits in fear learning.

1.5 Cortical synaptic plasticity

1.5.1 Synaptic plasticity in Primary sensory cortical areas

The activity-dependent plasticity rules that govern learning and memory as well as cognition also play a role in refining developing networks in response to experience. This mechanism is of particular importance during developmental critical periods. Critical periods are developmental time windows in which the ability of experience to influence the connectivity of a developing network is greatly enhanced. After this period ends, the ability of activity to influence synapses becomes much reduced as they become less plastic. Critical periods have been heavily studied in the cortex in particular in sensory cortical areas which typically undergo this period of heightened plasticity early in an animal's development. Disruptions in network activity during developmental critical periods can drastically alter the ability of a network to respond to sensory input resulting in permanent sensory processing deficits. Perhaps the most famous example of this phenomenon comes from the work of Hubel & Wiesel (1970) which showed that deprived visual experience during the visual critical period of cats results in reduced visual acuity in adulthood.

Sensory processing deficits are a common feature across many ASDs including FXS (Fagiolini & Leblanc 2011). Studies in *Fmr1* KO mice have revealed changes in critical period plasticity in cortical areas underlying several sensory modalities. As FMRP is expressed in very early development, in a way that is regulated by neuronal activity, it is in a key position to regulate activity dependent plasticity of cortical areas during early critical periods (Agulhon et al., 1999; Todd et al. 2003). This has been highlighted in the somatosensory cortex (S1) where the critical period for NMDAR-dependent LTP at thalamocortical afferents on to layer IV spiny stellates usually occurs early in the postnatal week (Crair & Malenka 1995). The closure of this critical period coincides with the time point of peak FMRP expression in S1 (Till et al. 2012). In *Fmr1* KO mice, this critical period is delayed continuing into the second postnatal week (Harlow et al. 2010). A similar delay in the development of translaminar connectivity in S1 of *Fmr1* KO mice has also been observed. Ascending connections

from layer 4 to layer 2/3 pyramidal neurons typically develop in the second postnatal week following the closure of the layer 4 critical period. However in the absence of FMRP, this pathway is weakened and shows reduced connection probability at this stage of development (Bureau et al. 2008). These phenotypes are temporally restricted to these early developmental time points, showing a return to WT levels by the third postnatal week suggesting they may be the result of a delay in the maturation of S1 cortical circuits in *Fmr1* KO mice.

Visual experience also drives the expression of *Fmr1* mRNA suggesting FMRP may play a role in visual cortex development (V1) (Gabel et al. 2004). Evidence of visual critical period deficits in *Fmr1* KO mice comes from studies of ocular dominance plasticity. In WT mice, brief 3 day monocular deprivation at P28 results in depression of deprived eye responses in the binocular region of V1, followed by potentiation of responses from the non-deprived eye 4 days later (Frenkel & Bear 2004). In contrast, *Fmr1* KO V1 exists in a 'hyperplastic state' showing immediate potentiation of responses to the non-deprived eye (Dölen et al. 2007). *In vitro* electrophysiological analysis of *Fmr1* KO V1 has revealed loss of LTP in juvenile mice, which may contribute to this ocular dominance phenotype (Wilson & Cox 2007). Interestingly, these phenotypes in *Fmr1* KO mice are normalised to WT levels by either genetic or pharmacological reduction of $mGluR_5$ signalling (Dölen et al. 2007; Wilson & Cox 2007). This suggests that the exaggerated mGluR signalling proposed by work in the hippocampus may also contribute to changes in sensory cortex development.

1.5.2 Synaptic plasticity in Integrative cortical areas

As well as primary sensory cortical areas, integrative cortical areas also undergo synaptic plasticity throughout development. An example with particular relevance to FXS is the prefrontal cortex (PFC). Deficits in attention, inhibitory control and cognitive flexibility are all common symptoms reported in FXS individuals that are associated with PFC function (Royall et al. 2002). Similarly there have been reports of deficits in PFC-related behaviours in *Fmr1* KO mice suggesting FMRP plays a key

role in PFC function (Krueger et al. 2011; Gantois et al. 2013; Kramvis et al. 2013; Sidorov et al. 2014).

Unlike primary sensory areas, PFC synapses remain plastic well into adulthood. In early adulthood, studies in *Fmr1* KO mice have revealed LTP deficits in multiple PFC subregions including the anterior cingulate cortex (ACC), medial PFC (mPFC) and piriform cortex (Zhao et al. 2005; Meredith et al. 2007; Wang et al. 2008). An interesting observation in PFC plasticity of *Fmr1* KO mice is an age-dependent loss of LTP in some subregions, with LTP intact in juvenile animals but deficits appearing in adulthood (Larson et al. 2005; Martin et al. 2015). Given the increasing ID associated with ageing in FXS, this progressive LTP loss has been proposed as a potential synaptic mechanism of this cognitive deficit. As with sensory areas, acute pharmacological blockade with MPEP, a group 1 mGluR negative allosteric modulator, has been shown to restore LTP to WT levels in the ACC and mPFC (Xu et al. 2012; Martin et al. 2015) suggesting excessive mGluR signalling can contribute to cortical deficits in adult *Fmr1* KO animals as well as during development.

1.6 Synaptic connectivity in FXS

1.6.1 Dendritic spines

Dendritic spines are postsynaptic compartments where excitatory synaptic contacts are formed. The morphology of dendritic spines influences the compartmentalisation of signalling cascades as well as synaptic function (Yuste 2011). Therefore, both the density of dendritic spines and their shape can influence circuit function. Alterations in spine density and morphology have been commonly reported across many cognitive disorders (Kaufmann & Moser 2000). Post-mortem analysis of human FXS tissue has revealed an increase in spine density, with the majority in an elongated and filopodial state (Rudelli et al. 1985; Hinton et al., 1991; Irwin et al. 2001). Given the difficulties of performing adequately controlled studies with human tissue in neurodevelopmental disorders e.g. age matching, post-mortem interval, and patient medical history; it is

unclear if these differences truly reflect the effects of FMRP loss. However, a series of studies have identified similar deficits in *Fmr1* KO mice. A transient elevation in spine density and spine length has been observed in S1 and mPFC neurons in juvenile *Fmr1* KO mice (Nimchinsky et al. 2001; Testa-Silva et al. 2012). This phenotype then reappears in adulthood with increased spine density and immature morphology reported in several cortical cell types (Comery et al. 1997; Dölen et al. 2007). However, some more recent studies investigating spine density across development in various different cell types have failed to repeat these findings (Meredith et al. 2007; Cruz-Martín et al. 2010; Harlow et al. 2010; Wijetunge et al. 2014). These inconsistencies may arise from differences in methodology e.g. Golgi vs intracellular labelling, as it has been suggested Golgi labelling may preferentially label a subset neurons which may show spine abnormalities in FXS (Nimchinsky et al. 2001). These results could also stem from differences in analysis as some investigators use *n* as number of analysed dendrites or neurons for statistical analysis therefore the use of non-independent replicates could result in falsely significant results.

Original studies in human tissue first identified the increased presence of abnormally, long and thin dendritic spines in FXS tissue (Rudelli et al. 1985; Hinton et al. 1991; Irwin et al. 2001). These abnormally thin and tortuous spines are reminiscent of immature spine precursors suggesting a delay in synapse development or pruning (Bagni & Greenough 2005). Subsequent studies in *Fmr1* KO mice have revealed similar immature spine phenotypes across multiple cell types (Meredith et al. 2007; Levenga et al. 2011; Qin et al. 2011). As well as suffering from the limitations in analysis already discussed these studies have typically examined spine morphology using diffraction limited microscopy techniques that lack the spatial resolution to image many parameters of spine morphology such as head width, neck length and neck width. A recent study using stimulated emission depletion (STED) microscopy, a technique with allows imaging with ~50nm spatial resolution, has revealed that the developmental trajectory of spine morphology is largely intact in *Fmr1* KO mice (Wijetunge et al. 2014). This study only identified nanoscale changes in spine morphology in a region and age dependent manner with no changes in spine density.

Whilst this data raises doubts about the presence of immature spine phenotypes in FXS, spine morphology in fixed tissue alone provides a limited view of spine maturity and function. Dendritic spines are dynamic structures which undergo structural transformations over time at rates which vary with maturity (Bonhoeffer & Yuste 2002). Real-time imaging of spine dynamics using *in vivo* two photon microscopy in *Fmr1* KO somatosensory cortex did not observe any changes in spine motility but did find increased spine turnover on L2/3 pyramidal neurons at P10-12, a critical period in somatosensory circuit development where functional synaptic defects have also been reported (see below; Cruz-Martin et al. 2010). Higher spine turnover has also been reported in L5 pyramidal neurons of somatosensory cortex at P20 and P30 in the absence of FMRP (Pan et al. 2010). These data suggest that spine instability in early circuit development, which may persist in some cell types in *Fmr1* KO mice, which would likely contribute to altered circuit dynamics in FXS.

Together, these data display the brain region and development specificity of spine phenotypes in the absence of FMRP but also highlight the flawed methodology of past studies in assessing spine density and morphology. It is difficult to suggest what these effects may have on neuronal function but it is clear that even subtle perturbations in spine morphology could result in large changes at the circuit level.

1.6.2 Functional connectivity

Abnormal neuronal connectivity is proposed to underlie the cognitive and behavioural deficits in many neurodevelopmental disorders. Functional magnetic resonance (fMRI) studies in ASDs have revealed increased local connectivity with impaired long-range synchronisation (Geschwind & Levitt 2007). Abnormalities in dendritic spine number and dynamics as well as multiple synaptic plasticity phenotypes suggests that functional changes in synaptic connectivity may also exist in FXS circuits.

Studies investigating layer 5 pyramidal neuron local connectivity in both mPFC and S1 have revealed a hyperconnected state in the early development of *Fmr1* KO mice (Testa-Silva et al. 2012; Patel et al. 2014). This hyperconnectivity could drive excessive feedback excitation resulting in circuit hyperexcitability. Interestingly these phenotypes, similar to spine deficits in the same cortical areas, are developmentally transient with normal functional connectivity returning by postnatal week 5. Given the observation that increased spine density reappears in many cortical areas in adult *Fmr1* KO mice (Comery et al. 1997; Dölen et al. 2007) this raises the possibility that adult *Fmr1* KO circuits may also exist in a hyperconnected state however this has not been explored experimentally.

Whilst the postsynaptic role of FMRP has been extensively investigated, FMRP also plays a role in regulating presynaptic function which can also affect synaptic connectivity. A study using mosaic *Fmr1* female mice revealed that WT presynaptic neurons form synaptic connections at higher rates than neurons lacking FMRP in hippocampal organotypic cultures (Hanson & Madison 2007). This effect was independent of postsynaptic identity. As FMRP is expressed in axons and growth cones of hippocampal neurons, its loss results in altered axonal growth (Antar et al. 2006). This effect may result in the reduced connectivity observed in mosaic studies as the ability of *Fmr1* KO axons to target postsynaptic neurons and form synaptic connections is unaffected.

As well as through the loss of physical connectivity, synaptic release probability can also have a major effect on presynaptic function. This is commonly assessed using measurements of paired pulse ratio (PPR), which inversely correlates with synaptic release probability (Zucker & Regehr 2002). No changes in PPR have been reported in the majority of studies of *Fmr1* KO mice which focus on hippocampal and cortical excitatory synapses (Pfeiffer & Huber 2007; Gibson et al. 2008; Deng et al. 2011) suggesting FMRP does not affect basal presynaptic release in these structures. In contrast, Suvrathan et al (2010) have reported enhanced PPR at thalamic inputs to the LA as well as a decreased mEPSC frequency on to LA principal neurons suggesting

loss of FMRP results in decreased presynaptic release probability in the LA. This presynaptic effect was rescued with acute treatment of MPEP suggesting this reduced release probability is the result of excessive group 1 mGluR signalling. As $mGluR_5$ expression is localised postsynaptically in the LA (Rodrigues et al. 2002) the most probable explanation for this effect is through modulation of retrograde signalling such as endocannabinoids (eCB). eCBs are released from postsynaptic terminals in response to mGluR activation and diffuse across the synaptic cleft where they act upon presynaptic terminals causing a reduction in presynaptic release (Alger 2002; Chevaleyre et al. 2006). Whilst eCB signalling has been heavily investigated in the hippocampus and cortex, little is known about its role in the amygdala. However as $mGluR_5$ signalling has been proposed to be constitutively active in *Fmr1* KO mice (Ronesi & Huber 2008) as well as showing enhanced coupling to eCB mobilisation (Zhang & Alger 2010), this could provide a potential mechanism for the therapeutic action of mGluR antagonism on presynaptic release in the LA.

1.7 Neuronal excitability in FXS

In addition to ID phenotypes, FXS is also associated with a generalised over-arousal to sensory stimuli. This has been noted across multiple modalities. In auditory processing, FXS individuals exhibit reduced prepulse inhibition (PPI) showing increased responsiveness to auditory cues and reduced attenuation of startle responses (Frankland et al. 2004). Sufferers also present tactile defensiveness as well as avoidance of innocuous tactile stimuli suggesting hypersensitivity of touch (Baranek et al., 2008). Sensitivity to visual stimuli, which manifests as gaze aversion, has also been noted in approximately 90% of FXS males (Merenstein et al. 1996). This hypersensitivity to normal sensory stimuli results in hyperarousal of FXS individuals and also contributes to the ASD symptoms associated with the condition such as social withdrawal (Kronk et al. 2010).

The described sensory hypersensitivity is a common feature of ASD and reflects an underlying hypersensitivity of cortical circuits to sensory input. Consistent with this, event-related potentials in the auditory cortex in response to auditory stimulation are

increased in FXS individuals (Castren et al. 2003). This hypersensitivity also results in incidences of seizure in 10-20% of FXS individuals (Berry-Kravis 2002). Similarly, *Fmr1* KO mice exhibit increased auditory circuit activity as well as a reduced threshold for audiogenic seizures (Chen & Toth 2001; Musumeci et al. 2000). This hypersensitivity is thought to be the result of circuit hyperexcitability in the absence of FMRP. Circuit hyperexcitability can arise through changes at multiple levels of analysis i.e. molecular, synaptic, cellular, network (Contractor et al. 2015). Given the functional complexity of FMRP and its wide range of mRNA targets, changes in both the intrinsic physiology of individual neurons as well as synapse-level alterations have been proposed as one of multiple mechanisms leading to circuit hyperexcitability have been identified in *Fmr1* KO animals.

1.7.1 Translation dependent effects of FMRP loss on excitability

CNS neurons convert synaptic input from both excitatory and inhibitory synapses into an output signal generated as an action potential. This input-output relationship can be influenced by changes in the intrinsic membrane properties of a neuron. These properties are dependent on the combination and properties of ion channels expressed throughout the neuron. Through its role in mRNA trafficking and translation, FMRP is able to influence neuronal intrinsic excitability through regulation of many proteins related to membrane properties, ionic homeostasis and action potential firing.

A variety of K^+ channels that modulate intrinsic membrane properties have been identified as targets of FMRP (Darnell et al. 2011). Changes in K^+ channel result in increased input resistance of L4 stellate cells in the somatosensory cortex, resulting in neuronal hyperexcitability (Gibson et al. 2008). However this is a transient effect as neuronal excitability is normalised by 4 weeks of age. Surprisingly, this is the only

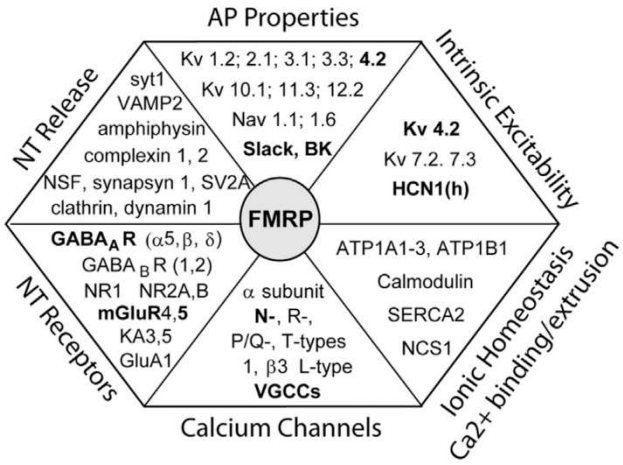

Figure 1.6 FMRP regulation of neuronal excitability Table representing the various ways FMRP is able to modulate neuronal excitability through proteins whose expression is altered by FMRP loss. Those in bold have been experimentally validated to have an effect on neuronal excitability in *Fmr1* KO mice. Figure from Contractor et al., 2015.

report of somatic changes in intrinsic membrane properties in *Fmr1* KO mice. Other studies investigating pyramidal neurons in CA1 hippocampus as well as entorhinal and somatosensory cortex (S1) have observed no changes in intrinsic membrane properties in the somatic compartment (Deng et al. 2013; Desai et al. 2006; Zhang et al. 2014).

Whilst pyramidal neurons appear largely unaffected in *Fmr1* KO mice from somatic recordings, recordings in the dendritic compartment of neurons has revealed significant alterations in intrinsic membrane properties. These changes are associated with changes in ion channel expression throughout the dendritic tree in the absence of FMRP. Dendritic ion channels can affect neuronal excitability in various ways and are key in mediating somatic integration, synaptic plasticity as well as neuronal firing (Beck & Yaari 2008).

One channel that is prominent in regulating dendritic excitability is the hyperpolarisation activated cyclic nucleotide gated channel (HCN). These channels mediate the I_h current, a non-inactivating cation conductance that is activated in response to membrane hyperpolarisation. HCN channels are also active at rest and

therefore can influence resting membrane potential and input resistance (Shah 2014). HCN also plays an important role in the summation of dendritic potentials. It is expressed in an increasing gradient towards the distal dendrites and the presence of I_h results in marked attenuation of EPSP summation (Berger et al. 2001). FMRP has been shown to interact with HCN1 mRNA thereby regulating its expression (Darnell et al. 2011). In agreement with the theory that FMRP represses mRNA translation, I_h currents are increased in CA1 dendrites of *Fmr1* KO mice (Brager et al. 2012). This increased current is associated with a decreased input resistance making dendrites less excitable in the absence of FMRP. In contrast, L5 pyramidal neurons in S1 and medial prefrontal cortex (mPFC) show reduced dendritic I_h in *Fmr1* KO mice resulting in increased excitability.

Another channel that is translationally controlled by FMRP is the K+ channel $K_v4.2$ (Darnell et al. 2011). This channel mediates the A-type K^+ current and display a characteristic expression gradient along the somatodendritic axis, increasing with distance from the soma (Hoffman et al. 1997). It is activated by subthreshold potential and attenuated propagating signals such as EPSP and bAP thereby acting as a powerful regulator of dendritic excitability. There have been conflicting reports regarding the expression of $K_v4.2$ channels in *Fmr1* KO CA1 pyramidal neuron dendrites. Work from Gross et al. (2011) suggested that, in contrast to FMRPs role as a negative regulator of translation, $K_v4.2$ mRNA and protein expression levels were reduced in CA1 dendrites of *Fmr1* KO mice. Consistent with this, measurement of A-type current in the dendritic compartment confirmed a reduction in current density in CA1 dendrites resulting in enhanced Ca^{2+} currents in response to bAP (Routh et al. 2013). However, Lee et al. (2011) demonstrated $K_v4.2$ was upregulated in the same compartment of *Fmr1* KO mice. The reason for the conflicting results of these studies is not clear. Both used biochemical techniques to assess the expression levels of Kv4.2 protein as well as its effect on LTP threshold. An additional study by Routh et al (2013) also found increased Kv4.2. currents in proximal dendrites of CA1 pyramidal neurons (<200µm from soma). Therefore the difference in results could stem from differential changes in Kv4.2 expression in subsections of the dendritic tree in *Fmr1* KO neurons.

In agreement with studies of I_h, opposing phenotypes of $K_v4.2$ currents in dendrites have been observed between pyramidal neurons in CA1 hippocampus (Routh et al. 2013) and L5 mPFC where levels were decreased (Kalmbach et al. 2015). These results highlight the brain region specific differences in FXS phenotypes and how the typically held view that neurons are hyperexcitable cannot be universally applied. It also suggests that the observed differences in ion channel expression may not be the result of mis-translation due to loss of FMRP but may reflect homeostatic or activity dependent changes in intrinsic properties. Given the varied circuit dynamics of the hippocampus and cortex, this mechanism could explain how FMRP loss can result in opposing effects in different brain regions depending on their local activity and synaptic input.

1.7.2 Non-canonical role for FMRP: Protein-protein interactions

Whilst FMRP is mainly thought of as a regulator of protein translation, several actions of FMRP are also mediated through direct protein-protein interactions. This role includes the direct modulation of some ion channels known to modulate neuronal excitability. The first example of this was presented by Brown et al. (2010) when they showed that FMRP directly interacts with sodium-activated K^+ channel 'Slack' in the auditory brainstem. This interaction is mediated by amino acids 1-298 in the N-terminus of FMRP, a region which does not interact with ribosomes. Slack channels regulate many features of neuronal excitability such as adaptation during sustained firing which is crucial for the fidelity of signal processing (Brown et al. 2010). Mutations in Slack channels have been linked to seizure events and result in severe cases of ID in humans (Kim & Kaczmarek 2014). This suggests that loss of regulation by FMRP may contribute to excitability defects in FXS auditory processing.

FMRP also regulates neuronal excitability through a direct interaction with the BK K^+ channel. This effect has been shown in both hippocampal and cortical pyramidal neurons (Deng et al. 2013; Myrick et al. 2015). BK channels are activated by Ca^{2+} entry following membrane depolarisation helping to repolarise action potentials,

produce fast-afterhyperpolarisation (fAHP) and close Ca^{2+} channels (Lee & Cui 2010). FMRP binding increases BK channel activity thereby modulating both neurotransmitter release and burst firing characteristics of a neuron. Loss of FMRP results in excessive presynaptic Ca^{2+} influx during repetitive activity causing excess glutamate release (Deng et al. 2013). FMRP is able to modulate BK channel activity by interacting with its β4 subunit (Deng et al. 2013). This protein-protein interaction was highlighted by the *FMR1* missense mutation R138Q which was identified in a patient presenting FXS phenotypes (Collins et al. 2010). Whilst this mutation is in the KH RNA binding domain, it does not interfere with FMRPs mRNA binding capability. However this mutation prevents FMRP from interacting with the BK channel and rendered FMRP unable to modulate action potential duration (Deng et al. 2013).

Finally, FMRP has also been shown to directly bind to presynaptic N-type voltage gated Ca^{2+} channels via its carboxy terminus (Ferron et al. 2014). This interaction does not affect channel activity but does regulate its surface expression. Loss of FMRP results in reduced presynaptic Ca^{2+} currents in *Fmr1* KO neurons which has been shown to have a major impact on neurotransmitter release in dorsal root ganglion neurons (Ferron et al. 2014).

1.7.3 mGluR and neuronal excitability

mGluR activation is commonly studied in relation to synaptic plasticity in FXS however mGluRs can also influence neuronal excitability. Whilst it is clear that excessive protein translation downstream of mGluR signalling can cause changes in excitability, acute mGluR activation can also modulate neuronal excitability. Consistent with this, the group 1 mGluR agonist DHPG can transform normal neuronal activity intro prolonged epileptiform bursting in CA3 hippocampus (Chuang et al 2005). This epileptiform activity is the result of a voltage gated cation conductance, termed $I_{mGluR(V)}$, which depolarises excitatory neurons thereby increasing neuronal activity (Bianchi et al. 2009). Once induced by agonist stimulation, $I_{mGluR(V)}$ remains undiminished for several hours following agonist washout. Whilst this effect can only be induced by DHPG activation in WT circuits, in the absence of FMRP synaptically

released glutamate provides sufficient mGluR activation to drive CA3 epileptiform activity (Chuang et al. 2005; Bianchi et al. 2009).

Evidence suggests that as well as excess translation downstream of $mGluR_5$ activation, $mGluR_5$ function may also be altered in *Fmr1* KO mice. $mGluR_5$ is reduced in post-synaptic density (PSD) fractions of *Fmr1* KO synapses due to an altered balance of $mGluR_5$ association with different isoforms of the post-synaptic scaffolding protein Homer (Giuffrida et al. 2005). The N-terminal domain of Homer binds with the intracellular C-terminal tail of group 1 mGluRs, influencing the localisation and function of mGluRs within the synapse (Shiraishi-Yamaguchi & Furuichi 2007). Long isoforms of Homer localise mGluRs to the PSD through interactions with the synaptic protein SHANK. Homer 1a, the activity induced short form of Homer, disrupts $mGluR_5$ binding with the long Homer isoform. This alters mGluR localisation and causes constitutive, agonist independent activation of group 1 mGluRs (Ango et al. 2001). In *Fmr1* KO mice, $mGluR_5$ is found in association with H1a at a higher rate than in WT controls rendering $mGluR_5$ constitutively active (Giuffrida et al. 2005). This phenotype appears to contribute to several protein synthesis independent phenotypes of FXS including neocortical hyperexcitability (Ronesi et al. 2012). As H1a bound $mGluR_5$ shows agonist independent activity, this suggests that the therapeutic action of $mGluR_5$ antagonists in *Fmr1* KO mice may partly be the result of inhibition of constitutively active $mGluR_5$.

The ability of $mGluR_5$ signalling to modulate excitatory transmission has been well established in pyramidal neurons of the mPFC due to their dysfunction in neuropsychiatric disorders such as Schizophrenia (Goto et al. 2010). $mGluR_5$ is highly expressed on postsynaptic terminals of layer 5 pyramidal neurons (Muly et al. 2003). mGluR agonists are able to drive increased network dependent excitatory spontaneous activity in these neurons through a mechanism that is blocked by $mGluR_5$ antagonists (Marek & Zhang 2008). Similarly, the orthosteric $mGluR_5$ agonist CHPG increases intrinsic bursting of layer 5 pyramidal neurons in the mPFC (Fontanez-Nuin et al. 2011). Therefore, if $mGluR_5$ exists in a constitutively active state in *Fmr1* KO neurons,

this could result in significant changes in the intrinsic excitability of layer 5 mPFC pyramidal neurons.

As well as integrating inputs from various brain regions, the mPFC provides top-down control of various cortical and subcortical regions through long range excitatory connections allowing it to influence many different behaviours (Vertes 2004). Layer 5 pyramidal neurons, which form the primary output layer of the mPFC, exist as a heterogeneous population exhibiting differing intrinsic properties, neuromodulation and synaptic connectivity depending on their long range targets (Wang et al. 2006; Brown & Hestrin 2009; Dembrow et al. 2010). This suggests that subnetworks exist within the mPFC that modulate specific mPFC-dependent behaviours.

Through its anatomical connectivity with the amygdala, the mPFC is able to exert executive control over emotional processing as well as influence fear behaviours (Euston et al. 2012). The mPFC is formed by two distinct subregions, the ventral portion consists of the prelimbic region (PL) whilst the ventral portion consists of the infralimbic cortex (IL), which show distinct connectivity (Vertes 2004; Gabbott et al. 2005; Hoover & Vertes 2007). These two regions also appear to play distinct roles in fear learning. The inactivation of PL results in impairment of fear acquisition, consolidation and expression (Choi et al. 2010; Vidal-Gonzalez et al. 2006; Corcoran & Quirk 2007) whilst IL activity is required for extinction memory (Hefner et al. 2008; Muigg et al. 2008). Therefore, proper function of these cortical regions and their connectivity with the amygdala are clearly important for appropriate fear behaviour. This suggests that changes in the neuronal excitability of mPFC subnetworks could result in significant changes in various aspects of fear learning. As *Fmr1* KO animals show deficits in learned fear expression (Paradee et al. 1999), changes in the intrinsic properties of PL subnetworks that project to the amygdala may contribute to this phenotype. The effects of FMRP loss on this circuit are unexplored in FXS however given the exaggerated function of $mGluR_5$ in *Fmr1* KO brains and observed behavioural deficits, this appears to be a potential affect that may contribute to the FXS phenotype.

1.7.4 Inhibitory circuits in FXS

Inhibitory transmission, acting through the neurotransmitter GABA, can also influence neuronal excitability by balancing circuit activity. Disruption of excitatory/inhibitory circuit balance is thought to be a common feature of ASDs (Gogolla et al. 2009). Whilst most studies in FXS have focused on excitatory neurotransmission, several components of the GABAergic system are also regulated by FMRP expression. Studies in *Fmr1* KO mice have shown expression of various $GABA_A$ subunit mRNA are downregulated across multiple brain regions (El Idrissi et al. 2005; Gantois et al. 2006; D'Hulst et al. 2006; Curia et al. 2009). Despite these extensive changes in $GABA_AR$ expression, synaptic GABA currents are largely unaffected in *Fmr1* KO neurons (Paluszkiewicz et al. 2011; Curia et al. 2009).

One area that shows large deficits in inhibitory circuits in *Fmr1* KO brains is the basal amygdala (BA), a sub-nuclei of the amygdala. Immunostaining for the synthetic enzyme for GABA is reduced in *Fmr1* KO mice as well as a decrease in the number of inhibitory connections (Olmos-Serrano et al. 2010). This is reflected in a decrease in both the amplitude and frequency of action potential dependent and independent inhibitory synaptic potentials in both the adult (Olmos-Serrano et al. 2010) and developing BA of *Fmr1* KO mice (Vislay et al. 2013). As well as deficits in synaptic inhibitory transmission, there are also deficits in tonic GABAergic transmission on to excitatory neurons in both the BA and striatum (Martin et al. 2014; Olmos-Serrano et al. 2010; Centonze et al. 2008). Tonic GABA signalling is mediated by extrasynaptic $GABA_ARs$ and can influence neuronal excitability through shunting inhibition (Semyanov et al. 2004). Therefore, diminished tonic GABA conductance in the BA results in intrinsic hyperexcitability of *Fmr1* KO principal neurons (Olmos-Serrano et al. 2010). Thus changes in GABAergic tonic inhibition has been proposed as a potential therapeutic candidate for the treatment of FXS (Olmos-Serrano et al. 2010; Heulens et al. 2012; Martin et al. 2014).

1.8 Generation of a rat model of FXS

Genetically modified mice have proved to be an invaluable tool in the investigation of human mutations which result in neurological disorders. However advances in genome manipulation tools have now allowed the development of genetically engineered rats opening a new avenue of investigation. The use of zinc finger nucleases, a class of engineered DNA binding proteins, can facilitate targeted editing of the genome by creating a double strand break in DNA allowing the insertion or deletion of desired DNA sequences.

Rats possess several advantages over mice as a model for the study of NDDs. They exhibit more complex social and cognitive behaviours allowing extended modelling of several key aspects of ASDs. Additionally, the larger body and brain size of rats can facilitate investigations by allowing more complex surgical experimentation, greater tissue sample collection as well as non-invasive imaging such as function magnetic resonance imaging (fMRI). fMRI uses changes in blood oxygen level as an indirect measure of neuronal activation allowing real-time *in vivo* imaging of brain activity (Harris et al. 2015). Due to its non-invasive nature, fMRI has been commonly used to investigate the neural systems underlying sensory, cognitive and emotional processing in the human brain and the effect that genetic mutations can have on their activity. As such, fMRI represents a valuable clinical tool in the study of human disorders such as FXS. Finally, rats metabolic physiology is also closer to humans than that of mice making the rat a better model for studying the pharmacokinetics/pharmacodynamics characteristics of drugs. Therefore, the use of fMRI in rodent models of FXS will be useful for the translation of findings into humans, making rats a potentially valuable preclinical model.

Despite their common features, mice and rats separated in evolution 12-24 million years ago and show very divergent behaviours (Gibbs et al. 2004). Whilst rats will clearly become a useful tool in the future of FXS research, experimental interpretation will be prone to the untested assumption that cellular phenotypes identified in *Fmr1*

KO mice are conserved across mammalian species. Therefore, it is vital to establish if the core physiological deficits associated with FXS from studies using *Fmr1* KO mice are also present in rat models.

A key cellular phenotype associated with the loss of FMRP in mice is the theory that excessive group 1 mGluR signalling is a core pathophysiology of FXS (Bear et al. 2004). This phenotype has been displayed in many different brain regions, resulting in various deficits in synaptic plasticity and neuronal signalling (Huber et al. 2002; Noyreva & Huber 2006; Suvrathan et al. 2010; Wilson & Cox 2007; Martin et al. 2015). Similarly, genetic or pharmacological reduction $mGluR_5$ signalling has been shown to ameliorate many cellular and behavioural phenotypes in *Fmr1* KO mice highlighting $mGluR_5$ as a potential target for the treatment of FXS (Yan et al. 2005; Dölen et al. 2007; Osterweil et al. 2010; Michalon et al. 2012; Michalon et al. 2014). A role of mGluRs has also been identified in Drosophila that lack the ortholog of FMRP, suggesting this pathophysiology is conserved across species (McBride et al. 2005). However investigation of these core mGluR-dependent phenotypes in *Fmr1* KO rats would also provide cross-mammalian evidence of the effects of FMRP loss for the first time that will be important when attempting to translate findings from fundamental basic research into therapeutic treatments.

1.9 Aims of this thesis

The generation of the *Fmr1* KO rat model has the potential to become a key tool for future research of FXS. However in order to inform future studies, we must first establish if the key cellular phenotypes identified over the past 20 years of research using the *Fmr1* KO mouse are conserved in rats. Equally, this provides a unique opportunity to investigate the conservation of these phenotypes across mammalian species (Till et al. 2015). Seminal work from Bear and colleagues identified that protein synthesis downstream of mGluR signalling is exaggerated in *Fmr1* KO mice resulting in hippocampal mGluR-LTD that is both enhanced and independent of new protein synthesis, culminating in the ‘mGluR theory of FXS’ (Huber et al. 2002;

Nosyreva & Huber 2006; Osterweil et al. 2010). Therefore, the initial focus of this thesis was to investigate the key cellular deficits in the hippocampus that result from FMRP deletion are conserved in rats. Next we investigated mGluR-dependent LTP in the LA as well as excitatory and inhibitory circuitry of the subnuclei of the basolateral amygdala (BLA). Finally, we investigated age dependent deficits in translaminar LTP in the PL mPFC as well as the intrinsic properties of the subnetwork of L5 pyramidal neurons that project to the BLA, a pathway that is important for behaviours affected in *Fmr1* KO animals.

Chapter 3 Investigate synaptic and chemical mGluR-LTD in *Fmr1* KO rats to test if:

1. mGluR-LTD is enhanced
2. $mGluR_5$ antagonism can rescue changes in mGluR-LTD
3. mGluR-LTD is protein synthesis independent
4. Protein synthesis levels are exaggerated in the hippocampus
5. NMDAR-dependent plasticity mechanisms are affected in the hippocampus

Chapter 4 Investigate synaptic plasticity and excitatory/inhibitory synaptic transmission in the basolateral amygdala to test if in *Fmr1* KO rats:

1. mGluR-dependent LTP is absent at thalamic inputs to the LA
2. mGluR-dependent LTP is absent at cortical inputs to the LA
3. Presynaptic release probability is reduced in the LA
4. Inhibitory and excitatory neurotransmission are affected in the BA

Chapter 5 Investigate synaptic plasticity in the PL mPFC and long-range connectivity with the BLA in *Fmr1* KO rats to test if:

1. Translaminar LTP in the PL mPFC shows age-dependent deficit
2. Subpopulation of L5 pyramidal neurons in the PL that project to the BLA have changes in intrinsic excitability

3. If these neurons show differences in excitatory and inhibitory synaptic neurotransmission.

Chapter 2

Methods

2.1 Animals

2.1.1 Housing and Breeding

All experimental animals were male and housed in cages under a 12:12hr light dark cycle with *ad libitum* access to food and water and in accordance with UK Home Office regulations.

2.1.2 Generation of *Fmr1* SD rats

Fmr1 mutant rats were constructed on an outbred Sprague Dawley background by SAGE laboratories. They were generated using zinc-finger nuclease technology to make a 122bp deletion across intron 7/exon 8 junction resulting in loss of FMR1 gene protein product (Hamilton et al., 2009)

2.1.3 Generation of *Fmr1* LEH rats

Fmr1 mutant rats were constructed on the Long-Evans hooded background by SAGE laboratories. They were generated using zinc-finger nuclease technology to insert an eGFPnlsSV40pA cassette in the coding region of exon 1 resulting in loss of FMRP expression.

2.2 Genotyping

2.2.1 DNA extraction

Tissue was collected in the form of ear clips at weaning for animal identification and genotyping. DNA was extracted using the Hot Shot method. Tissue samples were placed in 600 µl NaOH (50 mM) and heated to 100ºC for 45 mins. This solution was then neutralised with 50µl Tris-HCl (1 M, pH 8.0) and heated at 100°C for a further 2mins. Samples were centrifuged at 13,000 x g for 20 mins and then stored at 4°C.

2.2.2 *Fmr1* SD primers

Single reaction:

Forward: 5’ – TGGCATAGACCTTCAGTAGCC – 3’

Reverse: 5’ – TATTTGCTTCTCTGAGGGGG – 3’

2.2.3 *Fmr1* LEH primers

Two separate PCRs were required for *Fmr1* LEH genotyping, one for the WT allele and one for the KO allele

Wild-type reaction:

WT forward: 5’- CGA GGA AGG ACG AGA AGA TG -3’

WT reverse: 5’- CCG CTT CCC TGA CTG AAC T -3’

Knockout reaction:

KO forward: 5’- ACG TAA ACG GCC ACA AGT TC -3’

KO reverse: 5’- ATG CCG TTC TTC TGC TTG TC -3’

2.2.4 Polymerase chain reaction

Each reaction consisted of 6µl Promega GoTaq master mix, 1µl extracted DNA, 1µl forward primer, 1µl reverse primer and 3µl ddH_20. The thermocycler conditions for all listed primer sets are shown in Table 2.1. PCR products were run on a 2% agarose gel containing Sybersafe at 50mV for 30 mins with a 100bp DNA ladder (New England Biolabs).

Step 1	95°C for 5 mins
Step 2	95°C for 30 secs
Step 3	60°C for 30 secs
Step 4	68°C for 30 secs
Go to **Step 2** 34x	
Step 5	68°C for 5 mins
Step 6	4°C forever

Table 2.1 Thermocycling conditions used for all listed primer sets

2.3 Electrophysiology preparation

2.3.1 Solutions

All chemicals were purchased from Sigma-Aldrich (St Louis, MO, US) or Abcam biochemicals (Cambridge, UK)

Extracellular

Table 2.2 External solution composition (in mM)

	Modified slicing aCSF solution	**Recording aCSF solution**
NaCl	86	124
NaH_2PO_4	1.2	1.2
KCl	2.5	2.5
$NaHCO_3$	25	25
D-glucose	25	20
Sucrose	75	
$CaCl_2$	0.5	2
$MgCl_2$	7	1

Solutions were saturated with continuous carbogen bubbling (95% O_2 : 5% CO_2)

Intracellular

Table 2.3 Cs-gluconate internal solution composition (in mM)

	K-gluconate internal
K-gluconate	120
KCl	20
HEPES	10
NaCl	4
Mg-ATP	4
Na-GTP	0.3
pCreatine	10

Solutions were adjusted to pH 7.25 with KOH, osmolarity 295mOsm.L^{-1}

Table 2.4 K-gluconate internal solution composition (in mM)

	Cs-gluconate internal
CsOH	110
D-gluconic acid	110
CsCl	20
HEPES	10
NaCl	4
QX314	5
Mg-ATP	4
Na-GTP	0.3
EGTA	0.2
pCreatine	10

Solutions were adjusted to pH 7.25 with CsOH, osmolarity 295mOsm.L^{-1}

Table 2.5 High chloride internal solution composition (in mM)

CsCl	140
HEPES	10
MgCl2	2
QX314	5
Mg-ATP	5
Na-GTP	1
EGTA	0.5
pCreatine	10

Solutions were adjusted to pH 7.25 with CsOH, osmolarity 295mOsm.L^{-1}

2.3.2 Tissue slicing

Rats were anaesthetised using isoflurane and decapitated. The brain was quickly dissected out and placed in ice-cold (<4°C) modified slicing aCSF solution (Table 2.2). Brains were prepared depending on experimental brain region required (Table 2.6) and mounted to a vibroslice stage. Slices were cut in ice-cold modified slicing aCSF solution using a vibratome (UK: VT1200S, Leica, UK; India: VT1000, Leica, UK) and transferred to a holding chamber containing recording aCSF solution (Table 2.2) where they were maintained at 35°C for 30 mins. For hippocampus experiments, CA3 was microdissected from slices before transferring to holding chamber. Slices were left to recover for a further 30 mins at room temperature prior to the start of experimentation.

Table 2.6 Slice preparation protocols for different brain regions

Brain region	**Slice plane**	**Animal age**	**Slice thickness**
Hippocampus	Horizontal	P21-P35	400µm
Lateral Amygdala	Coronal	4-8 weeks	400µm
Prelimbic mPFC	Coronal	4-16 weeks	300µm

2.4 Extracellular recordings

Slices were placed in a submerged recording chamber heated to 31°C and perfused with pre-warmed carbogenated recording aCSF solution at a rate of 4-5ml/min. fEPSP were recorded via aCSF filled micropipettes (1-3MΩ) prepared from boroscillate glass capillaries (Harvard apparatus, UK) using a horizontal puller (P-97 Flaming Brown, Sutter Instruments, US). Synaptic responses were evoked every 30 secs using a bipolar nichrome (80/20) stimulating wire attached to a constant current stimulus isolator (Digitimer, UK) delivering a 200μs pulse unless stated elsewhere.

For hippocampus, the recording electrode were placed in the *stratum radiatum* of CA1 and the stimulating wire was placed on the Schaffer collateral.

For mPFC, recording electrodes were placed in layer 5 of the Prelimbic region and the stimulating wire was placed in layer 2/3. Stimulating and recording electrodes were staggered to prevent direct antidromic stimulation.

2.4.1 Stimulation paradigms

Before the initiation of any stimulation paradigm, a stable baseline of at least 20 mins was acquired. DHPG, APV, Cycloheximide, Anisomycin, Picrotoxin and CDPPB were all purchased from Abcam biochemical. CTEP was purchased from Axon Medchem. For all experiments, baseline stimulation intensity was selected as 40-60% of the minimum amplitude at which a population spike appeared.

<u>Input output - Hippocampus</u>

Basal synaptic transmission was investigated by increasing current intensity to give fibre volley amplitudes ranging from 0.05 – 0.5 mV in 0.05 mV increments. Corresponding fEPSP slope measurements were taken for each fibre volley amplitude and plotted to give an input-output curve.

Paired pulse facilitation - Hippocampus

Paired pulse facilitation was generated by delivering a pair of successive stimulations with a varying inter-stimulus interval (25 – 1000ms). Paired pulse ratios were calculated by dividing the slope of the second fEPSP by the slope of the first fEPSP.

Chemically induced LTD - Hippocampus

DHPG-LTD was induced by perfusing slices with the group 1 mGluR agonist DHPG (50μM or 100μM) for 5 mins. Slices were then perfused with aCSF for a further 60 mins. For experiments testing DHPG-LTD in the presence of Picrotoxin, Anisomycin, Cycloheximide or CTEP, slices were pre-incubated for a minimum of 20 mins prior to DHPG wash-on.

Synaptically induced LTD - Hippocampus

PP-LFS LTD was induced using 900 paired pulses with an inter-stimulus interval of 50ms at a frequency of 1Hz (0.4ms pulse duration). APV 50μM was present throughout the recording to prevent activation of NMDAR which can lead to another form of synaptic depression.

NMDA-LTD was induced using 900 single pulses at a frequency of 1Hz.

Synaptically induced LTP - Hippocampus and mPFC

In the hippocampus, LTP was induced using a 1s 100Hz high frequency train. For these experiments the CA3 area was not microdissected from the hippocampal slice.

In the mPFC, LTP was induced using 5 trains of 300Hz (0.5s, 0.05ms pulse duration) at 3 min intervals (Huang et al., 1999).

2.4.2 Data Analysis

Signal waveforms were amplified 1000x, low-pass filtered at 1.3kHz (npi electronics) and digitized at 20kHz (National Instruments). Data was collected and analysed using WinLTP (University of Bristol) before being exported to Microsoft Excel. fEPSP slopes were normalised to baseline values. Normalised data were averaged across experimental groups and reported as mean ± SE. Significant differences between groups were determined using Student's t-test ($p < 0.05$) or repeated measures ANOVA ($p < 0.05$) in Graphpad Prism software. Statistical tests were performed using n as animals unless stated.

2.5 Intracellular recording

For whole-cell recordings, slices were transferred to a recording chamber of an upright microscope (UK: S-SCOPE-II, Scientifica, UK; India: Olympus BX51WI, Olympus, Japan). Slices were perfused with carbogenated recording aCSF solution at a rate of 4-5ml/min. Temperature was set depending on the experimental paradigm (24 – 30°C) but was maintained using an HPT-2 inline heater (ALA Scientific, NY, US). Cells were visualised with IR-DIC video microscopy using a camera (UK: Watec cameras, NY, US; India: HD-210U, Dage, IN, US). Patch pipettes (2.5-3.5MΩ) were prepared from boroscillate glass capillaries (Harvard apparatus, UK) using a horizontal puller (UK: P-97 Flaming Brown, Sutter Instruments, US; India: P-97 Flaming Brown, Sutter Instruments, US) and filled with the experimentally appropriate internal solution.

When an appropriate neuron was visually identified (CA1 pyramidal neuron, lateral amygdala principle neuron or prelimbic mPFC layer 5 pyramidal neuron with retrobead labelling (see SURGERY) whole-cell recording was established. Following the application of positive pressure, the recording electrode was advanced towards the cell using a motor micromanipulator (UK: Patchstar, Scientifica, UK; India: MPC-200, Sutter Instruments, US). Pipette resistance was monitored using the Clampfit membrane test function (-5 mV test step, 10Hz). When an increase in pipette resistance and a visible dimple in the target cell was observed, positive pressure was released and

negative pressure applied until a giga-ohm seal was achieved (>1GΩ). Pipette capacitance was compensated before whole-cell configuration was achieved through the application of short, sharp bursts of negative pressure. Following membrane rupture, access resistance was monitored throughout experiments. Cells were accepted with resting membrane potential lower than -60mV and access resistance <25MΩ. If access resistance or holding current changed by >25% during a recording it was terminated.

2.5.1 Recording paradigms

Passive membrane properties - Hippocampus and mPFC

Resting membrane potential (V_M) was recorded by switching the amplifier to I=0 configuration and recording for 60s. Cells were then maintained at a set membrane potential of -70mV. Membrane time constant (T_M) was calculated by fitting a single exponential to 10-90% of the membrane charging curve following -25pA injection. Input resistance (R_{in}) was calculated as the slope of the linear fit of the current-voltage plot generated from a family of current injections (500ms, -100pA to 100pA, Δ25pA) and the steady-state voltage response. Capacitance (C_M) was calculated using $C_M = T_M / R_{in}$.

I_h current is mediated by HCN channels and results in a pronounced 'Sag' current when the cell is hyperpolarised. The peak hyperpolarised potential and the steady-state voltage response were measured from a -250pA step. Sag ratio was then calculated using (peak – steady-state / (peak * 100)).

Active membrane properties – Hippocampus and mPFC

Neuron firing characteristics were investigated using a family of current steps (500ms, 0-400pA, Δ25pA). Number of action potentials per 500ms was plotted against injected current. Rheobase was measured as the first current step to elicit at least one action potential.

The properties of the first action potential at a current intensity that resulted in 3-4 action potentials was used to calculate waveform properties. AP peak was defined as the maximal spike response and was measured from threshold to peak. AP width was measured as the width at half the maximal spike response. AP phase plots were generated using the first derivative of the AP signal against membrane voltage. AP threshold was classified as the membrane voltage where dvdt exceeded $10ms.mV^{-1}$.

Four different after spike potentials were analysed. Fast AHP (fAHP) was measured as the most negative potential following an AP waveform. Medium AHP (mAHP) was measured as the maximum negative potential following a train of 5 AP evoked at frequencies ranging from 20-100Hz using a 2ms, 2nA current pulse. Slow AHP (sAHP) was measured as the negative potential 1s after the last AP of a train of 15 AP at 50Hz using a 2ms, 2nA current pulse. After-spike depolarising potential (ADP) was measured as the maximum depolarised potential following an AP elicited using a 2ms, 2nA current pulse.

Whole-cell K^+ currents - mPFC

To isolate whole-cell K^+ currents, 1µM TTX and 2mM $MnCl_2$ were added to the recording aCSF solution with 0 Ca^{2+} and 0 Na_2HPO_4 to block Na^+, Ca^{2+} and Ca^{2+} - activated K^+ currents. K-gluconate internal solution was used for all experiments. Total I_K currents ($I_{K\text{-}WC}$) were recorded with a 4 sec -100mV pre-pulse, to deinactivate any inactivated voltage gated K^+ channels, followed by a test step to +50mV. Non-inactivating K^+ currents ($I_{K\text{-}Sustained}$) were isolated using a 30 sec pre-pulse to +20mV, to ensure inactivation of components of the current with slow inactivation kinetics, followed by a test step to +50mV. Slowly inactivating K^+ current ($I_{K\text{-}SLOW}$) was isolated by digital subtraction of $I_{K\text{-}Sustained}$ from $I_{K\text{-}WC}$. 'A-type' K^+ current ($I_{K\text{-}FAST}$) was isolated using the subtraction method. A 4 sec -100mV pre-pulse was followed by a test pulse to +50mV to elicit $I_{K\text{-}WC}$. In the second part of this protocol, following the -100mV pre-pulse, membrane potential was stepped to +20mV for 200ms and then to +50mV. This brief 200ms step is designed to inactivate $I_{K\text{-}FAST}$ which has very fast inactivation kinetics, on the order of tens of ms. Therefore, the step to +50mV will only be composed of $I_{K\text{-}SLOW}$ and $I_{K\text{-}Sustained}$ which can be digitally subtracted from $I_{K\text{-}}$

$_{WC}$ to give a pure $I_{K\text{-}FAST}$ current. Recovery of $I_{K\text{-}FAST}$ was tested in the same way using two test pulses separated by an interval of 10-100ms (Δ10ms).

Synaptic events – Hippocampus, mPFC and lateral amygdala

Cells were allowed 5mins to stabilise following membrane rupture before postsynaptic currents were acquired. Spontaneous currents were recorded using normal recording aCSF and AP independent currents (mEPSC/mIPSC) were recorded in normal recording aCSF containing 300nM TTX. Excitatory postsynaptic currents (EPSC) were measured at -70mV using Cs-gluconate internal solution (Table 2.3) with 75µM picrotoxin present in the external solution to block inhibitory currents. Inhibitory postsynaptic currents (IPSC) were measure at -70mV using High chloride internal solution (Table 2.5) with 20µM CNQX present in the external solution to block excitatory currents. Postsynaptic currents were recorded at 10kHz and bessel filtered at 2kHz.

Synaptic currents - mPFC

Synaptic currents were evoked by a bipolar cluster electrode (FHC, ME, US) placed in layer 2/3 of prelimbic mPFC. For AMPA/NMDA ratios, excitatory currents were measured at membrane potentials of -70mV and +40mV in the presence of 75µM picrotoxin to block GABAergic transmission. AMPA currents were measured as the peak current at -70mV. NMDA currents were measured 50ms after the peak current at +40mV. At this time any AMPAR mediated current should have decayed leaving a pure NMDA component. For GABA/AMPA ratios, IV plots were performed to calculate excitatory and inhibitory reversal potentials. Excitatory currents were pharmacologically isolated using 75µM picrotoxin and tested at membrane potentials -80 – 50mV. Inhibitory currents were pharmacologically isolated using 20µM CNQX and 50µM APV and tested at membrane potentials -100 - -30mV. Using this method, AMPA currents were recorded at -60mV and GABA currents were recorded at +10mV. For all currents, the average of 20 traces was used.

Paired pulse facilitation – mPFC and lateral amygdala

Paired pulse facilitation was generated by delivering a pair of successive stimulations with a varying interstimulus interval (25-100ms). Paired pulse ratios were calculated by dividing the peak amplitude of the second EPSC by the peak amplitude of the first EPSC. An average of 5 sweeps was used for each interstimulus interval.

Synaptically induced LTP - mPFC

In lateral amygdala, high frequency stimulation consisted of two trains of 100 pulse at 30Hz or 100Hz, separated by 20s. Experiments were performed in 75µM picrotoxin. Test pulses were delivered to thalamic inputs at 0.05Hz using a bipolar cluster electrode (FHC, ME, US). LTP was quantified by normalising EPSP 10-90% slope to baseline levels.

2.5.2 Data analysis

Signal waveforms were acquired using a Multiclamp 700B amplifier and Clampex software (Molecular Devices, CA, US). Signals were filtered at 10kHz using the built-in bessel filter of the amplifier and digitized at 20kHz (Digidata 1440, Molecular Devices, CA,US). Data were analysed offline using Clampfit software (Molecular Devices, CA, US). Synaptic event data were analysed using the template function in Clampfit software.

2.6 Stereotaxic injections

2.6.1 Anaesthesia and preparation

Before surgery, 10-14 week old rats were placed in a plexiglass chamber and anaesthetised using a mixture of air and isoflurane (5%, 0.4l/min). When breathing rate slowed to approximately 1Hz, rats were transferred to a stereotaxic frame (David Kopf, CA, US) where anaesthesia was continued through a mask (1.5 – 3%, 0.4l/min).

Anaesthesia level was constantly monitored throughout the experiment through observation of breathing rate and loss of toe pinch reflex. Ear bars were placed into the skull indentation on the interaural line to fix the head in place. The fur on the head was removed using an electric razor and the scalp swabbed with iodine solution. Petroleum jelly added to the eyes to prevent drying. All surgical tools were washed with Dettol and 70% ethanol before sterilisation using a bead steriliser. Injection pipettes were produced from boroscillate glass capillaries (Harvard apparatus, UK) using a horizontal puller (P-1000 Flaming Brown, Sutter Instruments, US).

2.6.2 Stereotaxic surgery

A small incision was made along the medial axis of the scalp and the skull exposed by clamping the skin with forceps. The skull was cleaned to expose the lambda and bregma with any ruptured blood vessels cauterised. The skull and surrounding skin was kept hydrated using saline solution throughout the experiment. Bregma and lambda co-ordinates were established and the nose bar adjusted to ensure they were in the same horizontal plane. Sterotaxic co-ordinates from Paxinos & Watson (2006) for the injection site were identified relative to the Bregma and the skull thinned using a microdrill. A small gauge needle was used to perforate the skull and carefully removed it. Any blood flow was cleaned and stemmed before preceeding with injection.

Retrobeads IX (Lumafluor) diluted 1:4 with saline were infused bilaterally in the basolateral amygdala (AP -3.3mm, ML ±5.0mm, DV -8.1mm). Retrobeads were infused at a rate of 100nl/min using a Picospritzer III (Parker Hannifin, NH, US). After the infusion of 1 – 1.5ul, injection was stopped and the pipette left in place for a further 10mins before removing it from the brain. Skull was sealed using bone wax and the scalp sutured (Mersilk 5-0, Ethicon) and treated with povidone-iodine solution. Animals were transferred to a cage and allowed to recover before oral administration of paracetamol suspension (1ml, 50mg/ml). This was repeated for four days post-surgery. Animals were allowed at least 2 weeks to recover before further experimentation.

2.7 Metabolic labelling

2.7.1 Tissue preparation

Brains were collected from WT and *Fmr1* KO rats (P25-32) as previously described and whole hippocampi dissected out. Transverse hippocampal slices (500µm) were prepared using a Stoeling tissue slice and stored in netwells (Corning, Sigma-Aldrich) submerged in oxygenated aCSF at 30ºC. Following a minimum 4 hour incubation, slices were transferred to a second recovery chamber of oxygenated aCSF at 30 ºC containing actinomycin D (25µM; Tocris) for 30mins to inhibit protein transcription. Slices were then incubated in aCSF containing ~0.37 MBq/ml of ^{35}S-Met/Cys protein labelling mix (Perkin Elmer) +/- DHPG 100µM for 5mins before transferring to oxygenated aCSF containing ~0.37 MBq/ml of ^{35}S-Met/Cys protein labelling mix for a further 40mins. Slices were snap frozen on dry ice and then stored at -80ºC until further processing. aCSF control samples were taken for further analysis.

2.7.2 Tissue processing

Slices were thawed and homogenised in 150µl homogenising buffer containing (in mM)10 HEPES pH 7.4, 2 EDTA, 2 EGTA, 1% Triton X-100, protease and phosphatase inhibitors (Sigma-Aldrich). Proteins were precipitated using 12.5% Trichloroacetic acid (Sigma-Aldrich), vortexed and put on ice for 10mins before spinning at 13,000x for 5mins at 4ºC. Supernatant was discarded and replaced with 150µl 1M NaOH and incubated at 37ºC until the pellet dissolved. pH was adjusted using 50µl 0.33M HCl. 50µl of sample was added to scintillation vials containing 10ml scintillation cocktail (Promega). Sample vials were loaded in a scintillation counter reading ^{35}S at 2 minutes per sample. Each sample was run in triplicate.

2.7.3 BSA protein assay

Protein concentration for each sample was measured using a Bio-Rad DC kit. BSA standards were made using a 2mg/ml BSA stock (New England Bio Labs). Serial dilutions ranging from 2mg/ml to 0.0625mg/ml were made using ddH_2O. 5µl of either BSA standard or protein sample were added to a 96 well plate in triplicate. 25µl of reagent A was added to each well followed by 200µl of reagent B. Samples were then incubated at room temperature for 15mins before being read at an absorbance of 740nm on a FluoStar Optima plate reader (BMG Labtech). Protein concentrations for each sample were calculated based on the measure BSA standard curve.

2.7.4 Analysis of protein samples

Scintillation counts for each sample were divided by its protein concentration to give counts per minute/µg protein (CPM/µg). The value for each sample was normalised to the CPM of the aCSF control sample and the volume of sample added to the scintillation vial (50µl for all samples). The average CPM/µg/µl was calculated for each triplicate sample and mean calculated for each animal. The average protein synthesis for each animal was expressed as percentage of the WT control. Statistics were performed using each animal as *n*. Significant differences were determined by paired Student's t-test ($p>0.05$).

2.8 Immunofluorescent labelling

Following acute slicing (see section 2.3.2), slices were allowed to recover for 1 hour before being fixed in 4% paraformaldehyde at 4ºC for 1 hour. Slices were then washed 3 times with 0.1M phosphate buffer (PB) and stored in PB at 4ºC for a minimum of 1 week until further processing. Immediately prior to processing, slices were washed 3 times in 0.1M PB for 10-20 minutes each wash. Slices were then washed 3 times in phosphate buffered saline (PBS) (0.025M PB + 0.9% NaCl) for 10-20 minutes each wash. Slices were then transferred to a 24-well plate containing 0.5ml blocking solution containing 10% normal goat serum (NGS), 0.3% Triton-X and 0.05% Sodium

azide for 1 hour. Blocking solution was then removed and primary antibody solution of 5% NGS, 0.3% Triton-X and 0.05% Sodium azide in PBS containing 1:200 Anti-AnkG (Rabbit) and 1:100) Anti NeuN (mouse). Slices were then incubated for 72 hours before washing with PBS, 3 times for 15-20 minutes. Secondary antibody solution of PBS containing 3% NGS, 0.1% Triton-X, 0.05% Sodium azide, goat anti-mouse 633nm antibody 1:500 and goat anti-rabbit 468nm 1:500 was then added to slices and incubated at 4ºC overnight. Slices were then washed 3 times with PBS, followed by two washes in PB for 10-20mins and one wash for 60-90mins. Slices were then mounted on to glass slides and stored at 4ºC until imaging.

2.8.1 Imaging

Images were taken using a Zeiss AxiovertLSM 510 inverted confocal microscope with native software. A 63x magnification, numerical aperture 1.5 lens was used to image z-stacks with 1µm step sizes. 10 axon initial segments (AIS) were imaged from each animal across two slices. AISs were traced using FIJI software (ImageJ). Length was manually measured as distance from the distal to proximal end of the AIS. Distance from soma was measured as distance from NeuN staining to the proximal end of the AIS. 10 measurements were averaged to give an animal average for each measure. Statistical significance was tested using a Student's t-test, with *n* as number of animals.

2.9 Statistics

Significant differences between groups were determined using Student's t-test ($p < 0.05$) or two-way ANOVA ($p < 0.05$) in Graphpad Prism software. Statistical tests were performed using *n* as animals unless stated. Significance was reported as * $p<0.05$, ** $p<0.01$, ***$p<0.001$.

Chapter 3

Translating the mGluR theory of FXS to the *Fmr1* KO rat

3.1 Introduction

Fragile X syndrome (FXS) is a common form of intellectual disability and autism spectrum disorder (ASD). It is the result of the transcriptional silencing of fragile X mental retardation protein (FMRP) (Kremer et al. 1991) which leads to a range of cognitive, behavioural and physical symptoms. The generation of the *Fmr1* KO mouse has been a key tool in the investigation of FXS as it has been shown to reproduce many of the phenotypes presented by human patients (Bakker et al. 1994).

Advances in transgenic technologies have allowed the generation of genetic models of central nervous system disorders in a range of species including rats (Hamilton et al. 2014). Whilst mice have been invaluable tools in the study of neurodevelopmental disorders, rats possess several advantages such as being more flexible to novel situations and having more extensive social interactions. These qualities are particularly useful in the study of FXS and ASD where patients exhibit deficits in social behaviours as well as anxiety disorders. Rat's richer behavioural repertoire allows testing of more complex cognitive processes which will be key in better understanding the aetiology of human intellectual disabilities. Rats also maintain the experimental advantages over large mammals by having short gestation periods and large litter sizes, typically larger than mice, making them an ideal experimental model.

With the advent of the *Fmr1* KO rat, it is crucial to establish whether the key cellular deficits identified in other FXS models are conserved in this new model of FXS. Studies using the *Fmr1* KO mouse have elucidated many cellular processes that appear to be aberrant in the absence of FMRP. Changes in group 1 metabotropic dependent plasticity (mGluR-LTD) (Huber et al. 2002; Nosyreva & Huber. 2006) as well as elevated basal protein synthesis rates in CA1 hippocampus (Osterweil et al. 2010; Barnes et al. 2015) have led to the hypothesis that many aspects of FXS are the result of exaggerated group 1 mGluR signalling, specifically $mGluR_5$ (Bear et al. 2004).

These results have also led to the development of potential therapeutic strategies that target $mGluR_5$ and its downstream signalling pathways (Dölen et al. 2007; Osterweil et al. 2013) which have shown the reversal of some phenotypes of *Fmr1* KO mice.

These preclinical findings have also led to large scale human clinical trials targeting $mGluR_5$ signalling as a treatment for FXS. Therefore, the generation of a new rat model of FXS provides the opportunity to establish if these phenotypes are conserved across mammalian species. This would provide cross-mammalian evidence for the 'mGluR theory of FXS' in species that separated in evolution over 12-24 million years ago, validating its targeting as a treatment strategy in human FXS (Gibbs et al. 2004). The establishment of these core phenotypes will also provide an important foundation for the design and interpretation of future studies that take advantage of the *Fmr1* KO rats behavioural and technical benefits.

Therefore in this chapter, I aimed to establish if the key electrophysiological findings reported in *Fmr1* KO mice hippocampus can be recapitulated in the *Fmr1* KO rat model. I investigated mGluR-LTD using both chemical and synaptic induction. I also tested the effect of new generation $mGluR_5$ negative allosteric modulators on mGluR-LTD in *Fmr1* KO rats. Next, I investigated the protein synthesis dependency of mGluR-LTD in rat models of FXS. I also investigated if any differences exist in the induction of chemical v synaptically induced mGluR-LTD in both genotypes. Finally, I examined NMDA-dependent plasticity mechanisms to test if FMRP's role in regulating plasticity is specific to mGluR-dependent forms.

3.2 Results

3.2.1 mGluR-LTD at CA3 – CA1 synapses

Extracellular recordings were made from the *stratum radiatum* of CA1 pyramidal neurons where electrical stimulation of Schaffer collaterals produces a fEPSP. This

pathway is commonly used for investigations into synaptic plasticity as the laminated structure of inputs and outputs of the hippocampus make it highly amenable to this form of experiment. The application of a single pulse to this pathway resulted in a fEPSP with a smooth rising phase (Fig 3.1). The slope of this rising phase was used for quantification as it has a linear relationship with synaptic conductance whereas the peak fEPSP amplitude, which can be contaminated by population spikes and polysynaptic activity, has a non-linear relationship with synaptic conductance. By plotting fEPSP slope against time, changes in synaptic strength in response to drug application or stimulus patterns can be investigated (Fig 3.1 C and D).

3.2.2 mGluR-LTD can be reliably induced both chemically and electrically at CA3-CA1 synapses

Several forms of plasticity, with different mechanisms of induction, have been reported to be present at hippocampal CA3 – CA1 synapses. mGluR-dependent LTD can be induced at these synapses both chemically, using the group I mGluR agonist DHPG (DHPG-LTD), or synaptically by application of 900 paired pulses at 1Hz frequency (PP-LFS LTD). Here I found that both DHPG-LTD and PP-LFS LTD could be reliably induced in juvenile (P21-35) WT animals (Fig 3.1 B and C). DHPG-LTD (5 mins, DHPG 100μM) resulted in an acute depression during wash-on which recovered to a stable synaptic depression (Fig 3.1 B). Initial attempts to induce PP-LFS LTD using 200μs pulse width gave very inconsistent levels of synaptic depression. Increasing pulse width to 400μs during the induction protocol resulted in stable synaptic depression (Fig 3.1 D). Therefore, this protocol was used for any further PP-LFS LTD experiments.

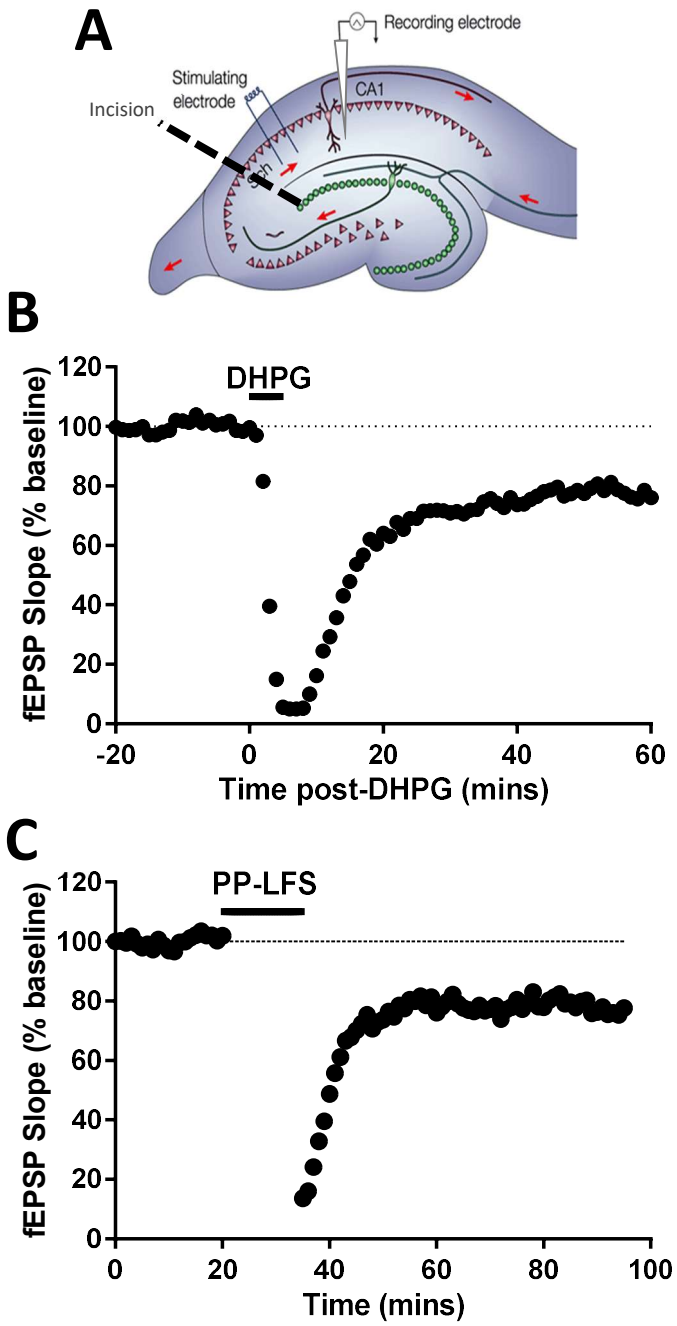

Figure 3.1 mGluR dependent LTD in CA1 hippocampus
(A) Schematic illustrating experimental set up. Horizontal hippocampal slices were taken from P21-P35 WT and *Fmr1* KO rats. A stimulating electrode was placed in the Schaeffer collateral pathway and fEPSP recorded in the stratum radiatum of CA1. An incision was made at the CA3-CA1 to prevent contamination by recurrent CA3 activity. (B) Example timecourse of DHPG-LTD recording. 5 min DHPG (100µM) wash-on resulted in significant LTD in WT hippocampal slices. (C) Example timecourse of PPLFS-LTD recording. 900 paired-pulse at 1Hz frequency resulted in significant LTD in WT hippocampal slices. Panel A is adapted from Kim et al. (2002).

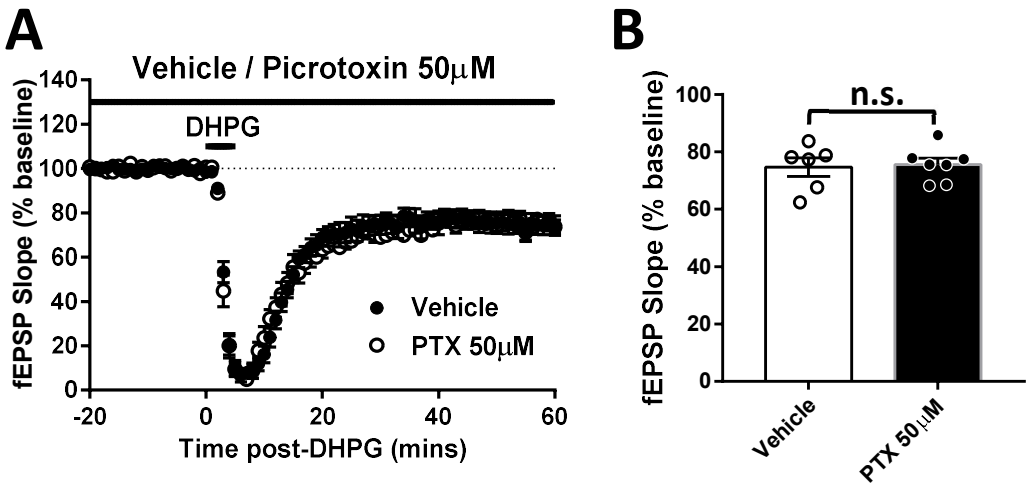

Figure 3.2. DHPG-LTD is not influenced by $GABA_A$ receptor inhibition

(A) Timecourse of DHPG-LTD recording in the presence of vehicle or picrotoxin 75μM. (B) DHPG-LTD was not significantly different in the presence of picrotoxin (Vehicle: 74.72 ± 3.25%, n=6 slices/6 animals; PTX: 75.58 ± 2.28%, n=6 slices/6 animals; p>0.05, Student unpaired *t*-test).

3.2.3 DHPG-LTD is not influenced by GABAA receptor inhibition

Early studies into the mechanisms of mGluR-LTD found that its expression was facilitated by the presence of $GABA_A$ receptor ($GABA_AR$) antagonists. Blocking inhibition resulted in an enhancement of DHPG-LTD which was attributed to an increase in tissue excitability as a similar result was found in 'Mg^{2+}-free' aCSF (Palmer et al. 1997). However other studies have been unable to reproduce these results suggesting that the effect of $GABA_AR$ antagonism on DHPG-LTD may be dependent on animal age as well as experimental design (Oliet et al. 1997; Pavlov et al. 2004; Rohde et al. 2009). To investigate the effect of disinhibition on DHPG-LTD, slices were pre-incubated in the $GABA_AR$ antagonist picrotoxin (50μM) for at least 20mins prior to LTD induction. The presence of picrotoxin had no effect on the magnitude of LTD in WT slices (Fig 3.2 B; Vehicle: 74.72 ± 3.25%, n=6; PTX: 75.58 ± 2.28%, n=6; p>0.05). This result indicates that DHPG-LTD is not influenced by $GABA_AR$ inhibition in our experimental design and was not used in further experiments.

3.3 Basal synaptic and cellular properties in CA1 of *Fmr1* KO LEH rats

3.3.1 Basal excitatory transmission at Schaeffer collateral inputs to CA1 is unaffected in *Fmr1* KO LEH rats

Previous studies in *Fmr1* KO mice have reported no alterations in basal synaptic transmission at CA3 – CA1 synapses (Godfraind et al. 1996, Paradee et al. 1999; Huber et al. 2002). To ensure that no differences in basal synaptic transmission exist in the *Fmr1* KO LEH rats that could confound further investigation, I examined both the input/output relationship and presynaptic release probability of CA3 – CA1 synapses. No change in basal synaptic strength were observed in *Fmr1* KO LEH rats (Fig 3.3 A; $F(1,6)=1.20$; $p=0.32$). Paired pulse ratio was not significantly different at any of the measured inter-stimulus intervals (Fig 3.3 B; $F(1,10)=0.139$; $p=0.72$) suggesting that basal release probability is largely unaffected in *Fmr1* KO LEH rats. These results indicate that basal excitatory transmission at CA3 – CA1 synapses is intact in the absence of FMRP.

3.3.2 CA1 intrinsic properties are unchanged in *Fmr1* KO LEH CA1 pyramidal neurons

There have been no reports of changes in whole-cell intrinsic properties in CA1 pyramidal neurons in *Fmr1* KO mice (Pilpel et al. 2009; Brager et al. 2012). In agreement with this, no changes were found here in any passive membrane intrinsic properties (Fig 3.4 A, B, C; Input resistance: WT: 94.23 ± 6.95MΩ, n=8, KO: 94.76 ± 4.80MΩ, n=12, $p > 0.05$; Capacitance: WT: 215.16 ± 15.99pF, n=8, KO: 231.03 ± 9.67pF, n=12, $p > 0.05$; Membrane time constant: WT: 19.39 ± 0.98ms, n=8, KO: 21.63 ± 0.65ms, n=12, $p > 0.05$). There was also no change in the active properties of CA1 pyramidal neurons (Fig 3.4 D). *Fmr1* KO LEH neurons showed no differences in the number of action potentials fired in response to current injection (Fig 3.4 D; $F(1,18)=0.124$; $p=0.729$). The amount of current required to elicit a single action potential was also comparable between genotypes (Fig 3.4 E; WT: 154.17 ± 9.65pA, n=8; KO: 150 ± 8.69pA, n=12, $p > 0.05$). Together, these results show that loss of

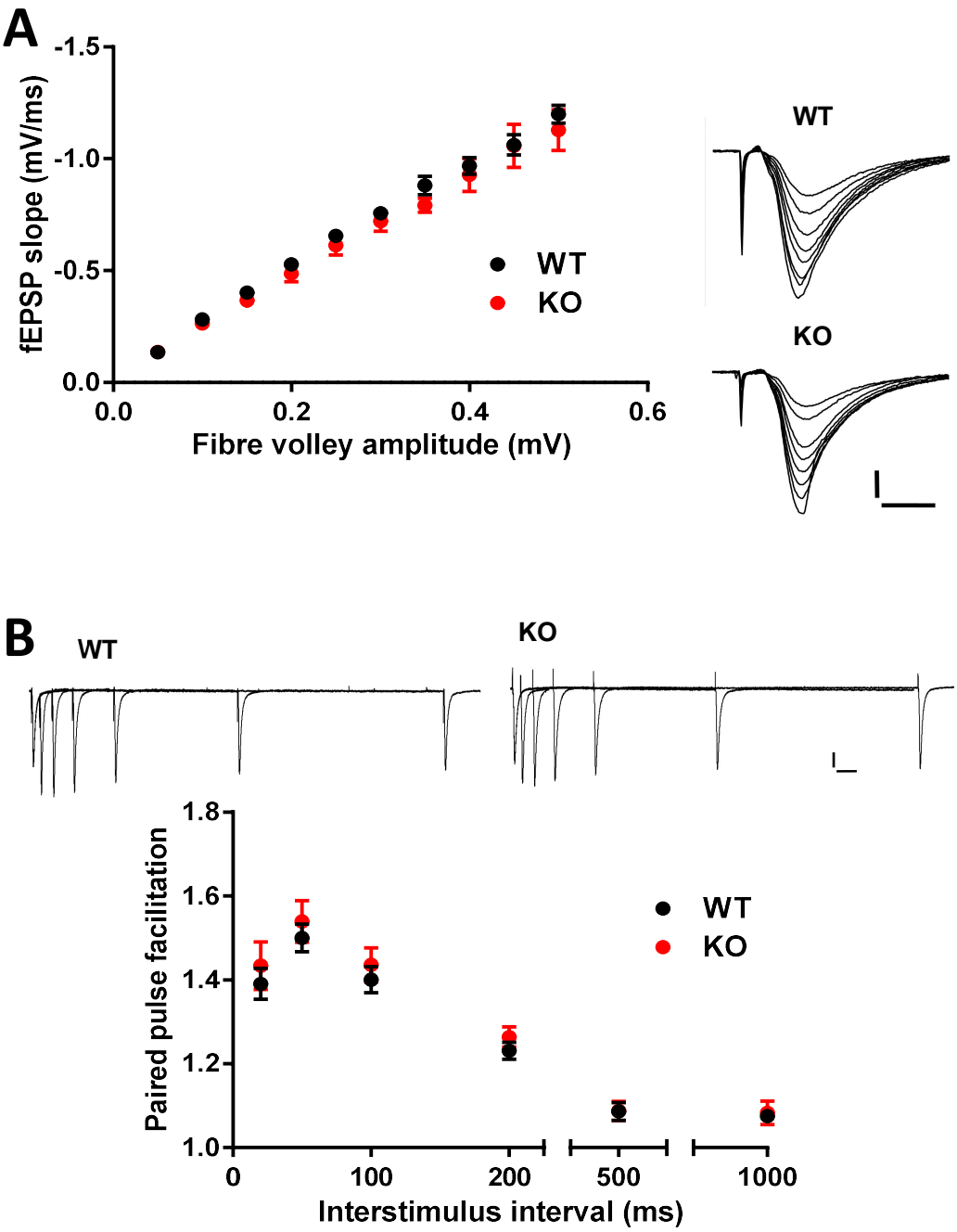

Figure 3.3 Basal excitatory synaptic transmission is unaffected at CA3-CA1 synapses in *Fmr1* KO LEH rats (A) Input-output function was measured at CA3-CA1 synapses by comparison of fibre volley amplitude and fEPSP slope. No significant differences were observed between genotypes ($F(1,6)=1.20$; $p=0.32$, Two-way RM-ANOVA). Example traces from each genotype showing fEPSP at various stimulation strengths. Scale 100µV, 20ms. (B) Paired pulse facilitation was tested using two concurrent pulses at multiple inter-stimulus intervals (25-1000ms). Paired pulse facilitation was comparable between WT controls and *Fmr1* KO LEH rats ($F(1,10)=0.139$; $p=0.72$, Two-way RM-ANOVA). Example traces from each genotype showing paired pulse facilitation at all tested intervals. Scale 100µV, 50ms.

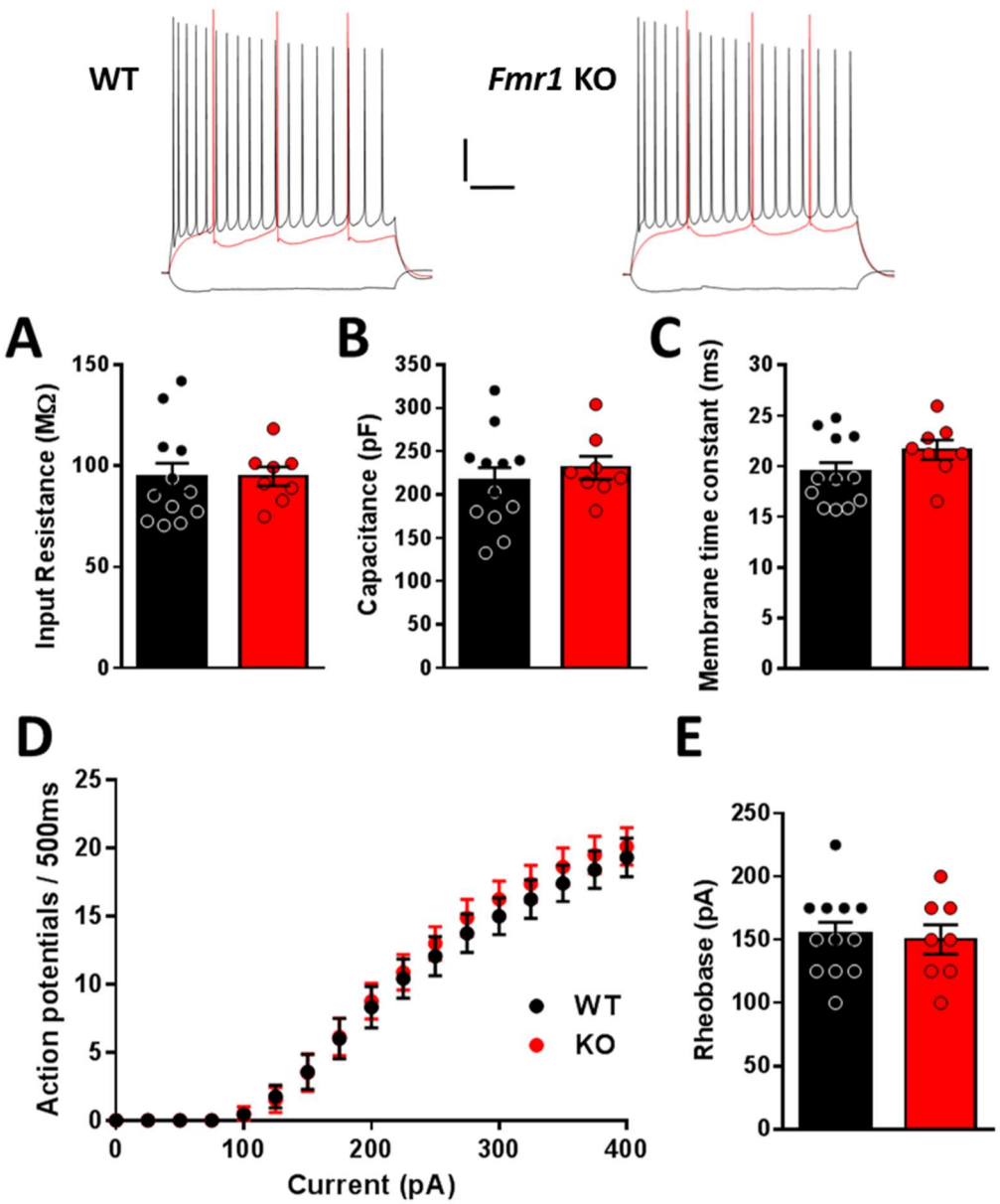

Figure 3.4 Intrinsic properties are unaltered in *Fmr1* KO LEH CA1 pyramidal neurons Whole cell electrophysiological recordings revealed no changes in (A) input resistance (WT: 94.23 ± 6.95MΩ, n=8 cells/4 animals, KO: 94.76 ± 4.80MΩ, n=12 cells/4 animals; $p > 0.05$, Student unpaired *t*-test) (B) Capacitance (WT: 215.16 ± 15.99pF, n=8 cells/4 animals, KO: 231.03 ± 9.67pF, n=12 cells/4 animals; $p > 0.05$, Student unpaired *t*-test) (C) Membrane time constant (WT: 19.39 ± 0.98ms, n=8 cells/4 animals, KO: 21.63 ± 0.65ms, n=12 cells/4 animals; $p > 0.05$, Student unpaired *t*-test. (D) Current-firing responses showed no differences in the number of action potentials fired in response to current injection in *Fmr1* KO LEH neurons ($F(1, 18)=0.124$; $p=0.729$, Two way RM-ANOVA). (E) Rheobase was comparable between genotypes (WT: 154.17 ± 9.65pA, n=8 cells/4 animals, KO: 150.00 ± 8.69pA, n=12 cells/4 animals; $p > 0.05$, Student unpaired *t*-test). Example traces of WT and *Fmr1* KO neurons voltage responses to -100pA, rheobase and 2x rheobase current steps. Scale 100ms, 20mV.

FMRP does not affect either the passive or active membrane properties in CA1 pyramidal neurons.

3.4 mGluR-dependent plasticity at CA3-CA1 synapses in *Fmr1* KO LEH rats

3.4.1 DHPG-LTD is enhanced in *Fmr1* KO LEH rats

mGluR-LTD in CA1 of the hippocampus is both exaggerated and independent of new protein synthesis in *Fmr1* KO mice (Huber et al. 2002; Nosyreva & Huber 2006). These results contributed to the 'mGluR theory of Fragile X syndrome' (Bear et al. 2004) which suggested that aberrant $mGluR_5$ signalling contributed to the pathophysiology associated with Fragile X syndrome. Therefore, I investigated whether these animals showed the same phenotypes following the induction of mGluR-LTD using the group 1 agonist DHPG. As shown previously in *Fmr1* KO mice, application of DHPG (50μM) resulted in synaptic depression that was significantly greater in *Fmr1* KO LEH animals than in WT controls (Fig 3.5 A; WT: 89.60 ± 2.30%, n=10; KO: 82.96 ± 1.80%, n=11; p=0.034). This effect was also seen when a higher concentration of DHPG (100μM) was used for DHPG-LTD induction (Fig 3.5 B; WT: 74.73 ± 3.97%, n=8; KO: 57.46 ± 4.89%, n=8; p=0.016). These results show that DHPG-LTD is enhanced in *Fmr1* KO LEH rat's relative to WT controls.

For DHPG-LTD induction in WT slices, synaptic depression was found to be more reliable when DHPG 100μM rather than DHPG 50μM was used (Fig 3.5 B, DHPG 100μM: 7 out of 8 slices had LTD >10%; Fig 3.5 A, DHPG 50μM: 3 out of 10 slices had LTD >10%). Therefore for all future *Fmr1* LEH experiments, DHPG-LTD was induced using DHPG 100μM.

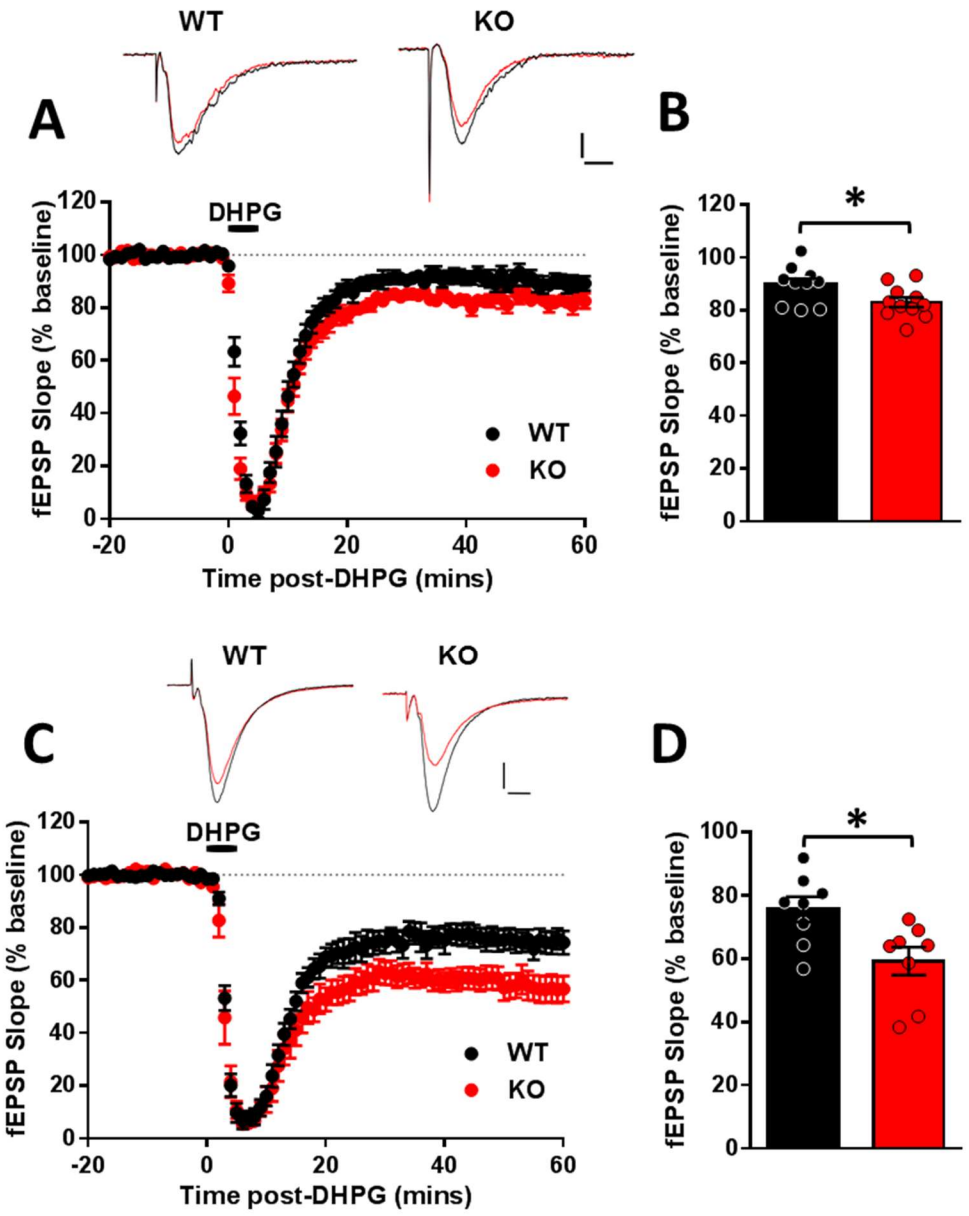

Figure 3.5 DHPG-LTD is enhanced in *Fmr1* KO LEH rats (A) Timecourse showing DHPG-LTD (DHPG 50µM) in WT and *Fmr1* KO LEH rats. Example traces showing fEPSP from baseline (black) and 60mins post-DHPG (red). Scale 100µV, 10ms. (B) DHPG-LTD was significantly greater in *Fmr1* KO LEH slices than WT controls (WT: 89.60 ± 2.30%, n=10 slices/10 animals; KO: 82.96 ± 1.80%, n=11 slices/11 animals; p=0.034, Student unpaired *t*-test). (C) Timecourse showing DHPG-LTD (DHPG 100µM) in WT and *Fmr1* KO LEH rats. Example traces showing fEPSP from baseline (black) and 60mins post-DHPG (red). Scale 100µV, 10ms. (D) DHPG-LTD was also significantly greater in *Fmr1* KO LEH slices with DHPG 100µM (WT: 74.73 ± 3.97%, n=8 slices/8 animals; KO: 57.46 ± 4.89%, n=8 slices/8 animals; p=0.016, Student unpaired *t*-test).

3.4.2 Presynaptic release is reduced following DHPG-LTD in *Fmr1* KO rats

Previous studies have given conflicting reports on whether DHPG-LTD has both a presynaptic and postsynaptic locus. The discrepancy in results could be due to differences in experimental design, animal age or experimental technique. Studies in *Fmr1* KO mice have highlighted a presynaptic role of FMRP (Deng et al., 2013) as well as a role in regulating retrograde signalling that can influence presynaptic release. Therefore, I monitored presynaptic release probability in response to DHPG-LTD in *Fmr1* KO LEH rats. In this study, DHPG-LTD resulted in no change in paired pulse ratio in WT animals (Fig 3.6; WT Baseline: 1.52 ± 0.05; WT 50-60mins: 1.55 ± 0.05; n=7; $p > 0.05$). In contrast, DHPG-LTD resulted in a significant increase in paired pulse ratio in KO animals (Fig 3.6; KO Baseline: 1.60 ± 0.04; KO 50-60mins: 1.72 ± 0.04; n=8; p=0.0009). This result suggests that while there is no apparent presynaptic component to DHPG-LTD in WT animals, DHPG-LTD results in a significant decrease in presynaptic release probability in *Fmr1* KO rats that may contribute to the exaggerated synaptic depression.

3.4.3 CTEP corrects enhanced DHPG-LTD in *Fmr1* KO LEH rats

Both pharmacological and genetic strategies focusing on $mGluR_5$ signalling have been found to be successful in ameliorating some of the phenotypes shown in *Fmr1* KO mice (Chuang et al. 2005; Yan et al. 2005; Osterweil et al. 2010; Dölen et al. 2007). Here I examined if pre-incubation in the $mGluR_5$ negative allosteric modulator CTEP (10μM) could restore the level of DHPG-LTD shown by *Fmr1* KO LEH rats to WT levels. CTEP incubation significantly reduced the magnitude of DHPG-LTD in *Fmr1* KO LEH animals to WT levels (Fig 3.7 D; WT: 84.72 ± 4.61%; n=4; KO: 74.21 ± 4.75%; $p>0.05$). CTEP incubation also prevented the reduction in presynaptic release probability in *Fmr1* KO LEH rats following DHPG-LTD (Fig 3.7 E; WT CTEP Baseline: 1.51 ± 0.003; WT CTEP 50-60mins: 1.53 ± 0.01; n=4; $p > 0.05$; KO CTEP Baseline: 1.51 ± 0.05; KO CTEP 50-60mins: 1.54 ± 0.06; n=7; $p > 0.05$). These data

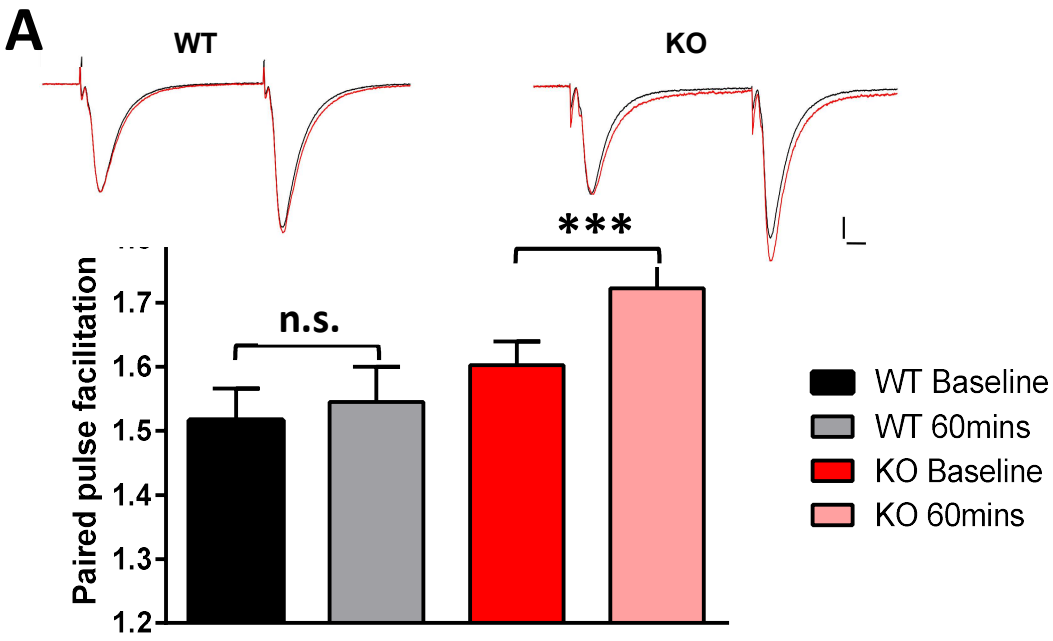

Figure 3.6 Presynaptic release is reduced following DHPG-LTD in *Fmr1* KO LEH rats (A) Paired pulse facilitation was unaffected by DHPG-LTD in WT LEH rats (WT Baseline: 1.52 ± 0.05; WT 50-60mins: 1.55 ± 0.05; n=7 slices/7 animals; p > 0.05) but was significantly increased in *Fmr1* KO LEH rats (KO Baseline: 1.60 ± 0.04; KO 50-60mins: 1.72 ± 0.04; n=8 slices/8 animals; p=0.0001. Statistics performed using Two way RM-ANOVA with Bonferroni correction. Example traces showing fEPSP from baseline (black) and 60mins post-stimulation (red). First fEPSP in red trace has been scaled to baseline for visualisation of PPF. Scale 100µV, 10ms

suggest that the enhanced DHPG-LTD shown in these animals is due to exaggerated $mGluR_5$ signalling which can be corrected by pharmacological inhibition.

3.4.4 PP-LFS LTD magnitude is unaltered in Fmr1 KO rats

Previous studies have shown that mGluR-dependent LTD can also be induced electrically using different patterns of synaptic stimulation. The most commonly used of these stimulation paradigms is PPLFS-LTD where 900 paired pulses (50ms interstimulus interval) are delivered at a rate of 1Hz (Kemp & Bashir 1999). Studies using *Fmr1* KO mice have found PP-LFS LTD is enhanced in slices where FMRP is absent (Huber et al. 2002). Therefore, I investigated whether this mGluR-dependent

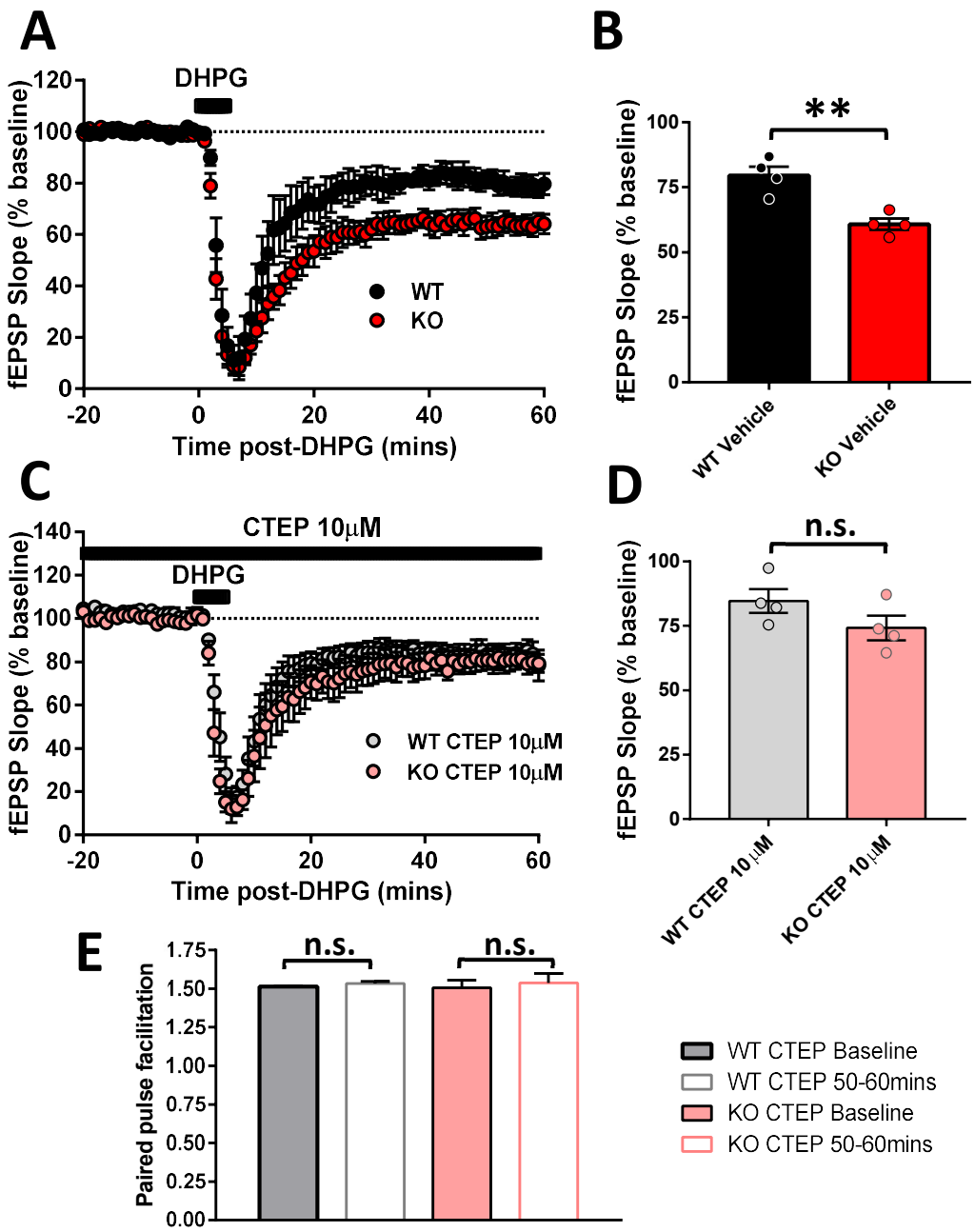

Figure 3.7 CTEP corrects enhanced DHPG-LTD in *Fmr1* KO LEH rats (A) Timecourse showing DHPG-LTD in WT and *Fmr1* KO LEH rats. (B) DHPG-LTD was significantly increased in *Fmr1* KO LEH rats (WT: 79.53 ± 3.47%; n=4 slices/4 animals; KO: 60.79 ± 2.15%; n=4 slices/4 animals; p=0.01, Student unpaired *t*-test). (C) Timecourse showing DHPG-LTD in WT and *Fmr1* KO LEH rats in the presence of CTEP 10μM. (D) DHPG-LTD was comparable between genotypes in the presence of CTEP 10μM (WT: 84.72 ± 4.61%; n=4 slices/4 animals; KO: 74.21 ± 4.75%; p>0.05, Student unpaired *t*-test). (E) PPF was not significantly different following DHPG-LTD in both WT (WT Baseline: 1.51 ± 0.003; WT 50-60mins: 1.53 ± 0.01; n=4 slices/4 animals; p > 0.05) or *Fmr1* KO slices in presence of CTEP (KO Baseline: 1.51 ± 0.05; KO 50-60mins: 1.54 ± 0.06; n=4 slices/4 animals; p > 0.05, Two way RM-ANOVA with Bonferroni correction).

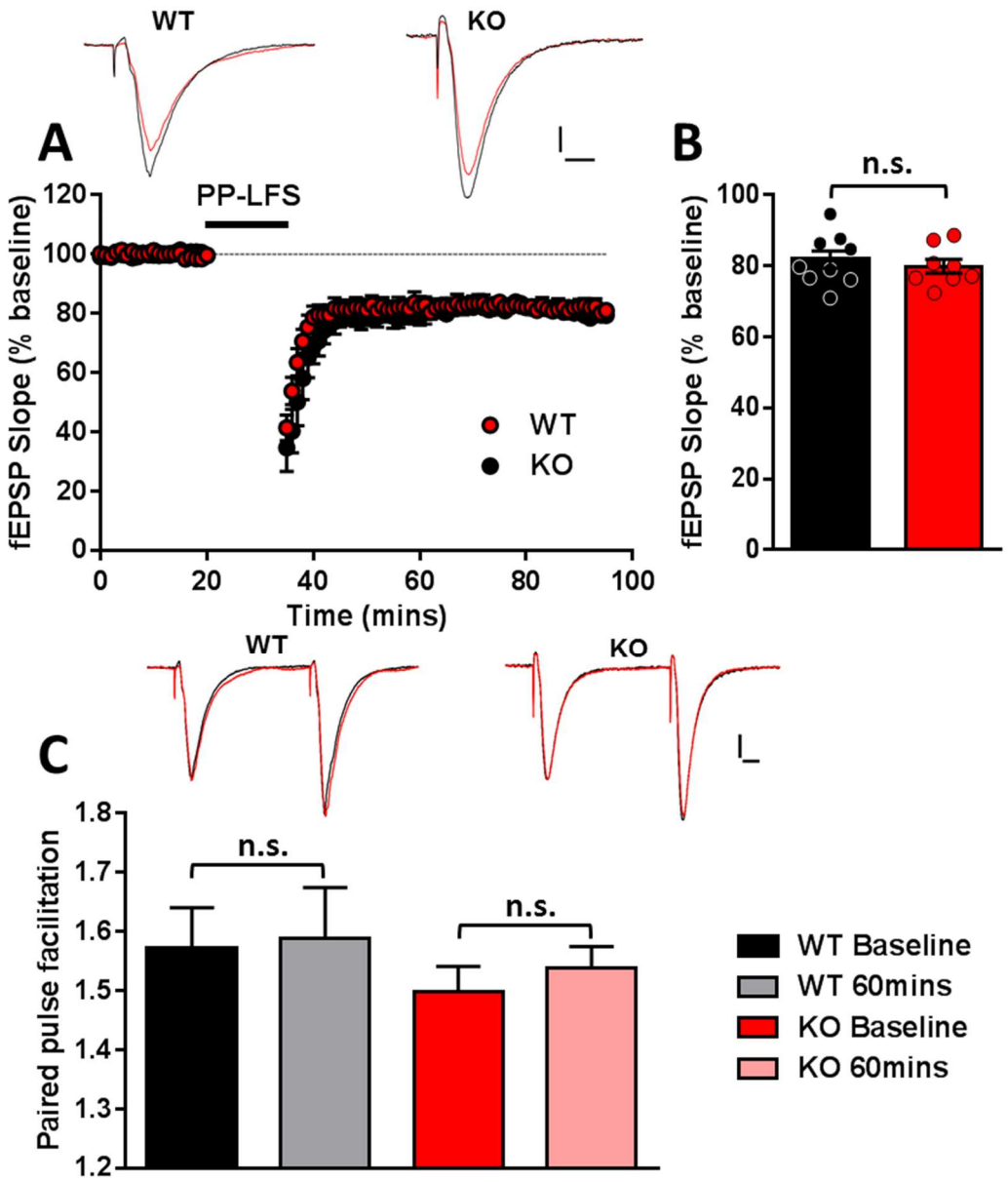

Figure 3.8 PPLFS-LTD is comparable between genotypes and shows no presynaptic effect (A) Timecourse of PPLFS-LTD induced with 900 paired-pulses at 1Hz in the presence of APV 50µM in WT and *Fmr1* KO LEH animals. Example traces showing fEPSP from baseline (black) and 60mins post-stimulation (red). Scale 100µV, 10ms (B) PPLFS-LTD magnitude was comparable between genotypes (WT: 81.58 ± 2.37%; n=9 slices/9 animals; KO: 80.70 ± 1.87%; n=8 slices/8 animals; p> 0.05, Student unpaired *t*-test). (C) Paired pulse facilitation was unaffected by PPLFS-LTD in both genotypes (WT Baseline: 1.48 ± 0.05; WT 85-95mins: 1.50 ± 0.06; n=7 slices/7 animals; p > 0.05; KO Baseline: 1.52 ± 0.06; KO 85-95mins: 1.56 ± 0.07; n=8 slices/8 animals; p > 0.05, Two way RM-ANOVA with Bonferroni correction). Example traces showing fEPSP from baseline (black) and 60mins post-stimulation (red). First fEPSP in red trace has been scaled to baseline for visualisation of PPF. Scale 100µV, 10ms

form of LTD is also enhanced in *Fmr1* KO LEH rats. Here I found no significant difference in the magnitude of PP-LFS LTD between genotypes (Fig 3.8 B; WT: 81.58

± 2.37%; n=9; KO: 80.70 ± 1.87%; n=8; p> 0.05). However unlike DHPG stimulation, induction of PP-LFS LTD did not affect presynaptic release probability in either genotype (Fig 3.8 C; WT Baseline: 1.48 ± 0.05; WT 85-95mins: 1.50 ± 0.06; n=7; p > 0.05; KO Baseline: 1.52 ± 0.06; KO 85-95mins: 1.56 ± 0.07; n=8; p > 0.05). These results suggest that despite both being group 1 mGluR-dependent, DHPG-LTD and PP-LFS LTD possess distinct expression mechanisms.

3.5 Protein synthesis dependency of mGluR-LTD in rat models of Fragile X syndrome

3.5.1 DHPG-LTD is protein synthesis independent in both WT LEH and *Fmr1* KO LEH rats

The pathophysiology associated with Fragile X syndrome is hypothesised to result, in part from of elevated basal protein synthesis downstream from $mGluR_5$-regulated signalling pathways (Osterweil et al. 2010). This elevated protein synthesis is believed to result in the enhanced and protein-synthesis independent mGluR-LTD that has been reported in *Fmr1* KO mice (Huber et al. 2002; Nosyreva et al. 2006). Therefore, based on the presence of enhanced DHPG-LTD in *Fmr1* KO LEH rats, I hypothesised that DHPG-LTD would also be independent of new protein synthesis in this animal model of Fragile X syndrome. To investigate this I pre-incubated hippocampal slices in protein synthesis inhibitor Cycloheximide (100μM) for at least 30mins prior to DHPG-LTD induction. Contrary to previous results, I found that DHPG-LTD was independent of new protein synthesis in both WT animals (Fig 3.9 B; WT: 79.52 ± 1.32%; n=3; $p_{WTvBaseline} > 0.05$) and KO animals (Fig 3.9 D; KO: 61.34 ± 2.86%; n=4; $p_{WTvBaseline} > 0.05$). This was consistent when a different protein synthesis inhibitor, Anisomycin (20μM), was tested (Fig 3.9 B; WT: 79.55 ± 1.86%; n=4; $p_{WTvBaseline} > 0.05$; Fig 3.9 D; KO: 59.77 ± 6.00%; n=4; $p_{WTvBaseline} > 0.05$). These results are consistent with the hypothesis that DHPG-LTD is protein synthesis independent in the *Fmr1* KO LEH rats however this is confounded by the finding

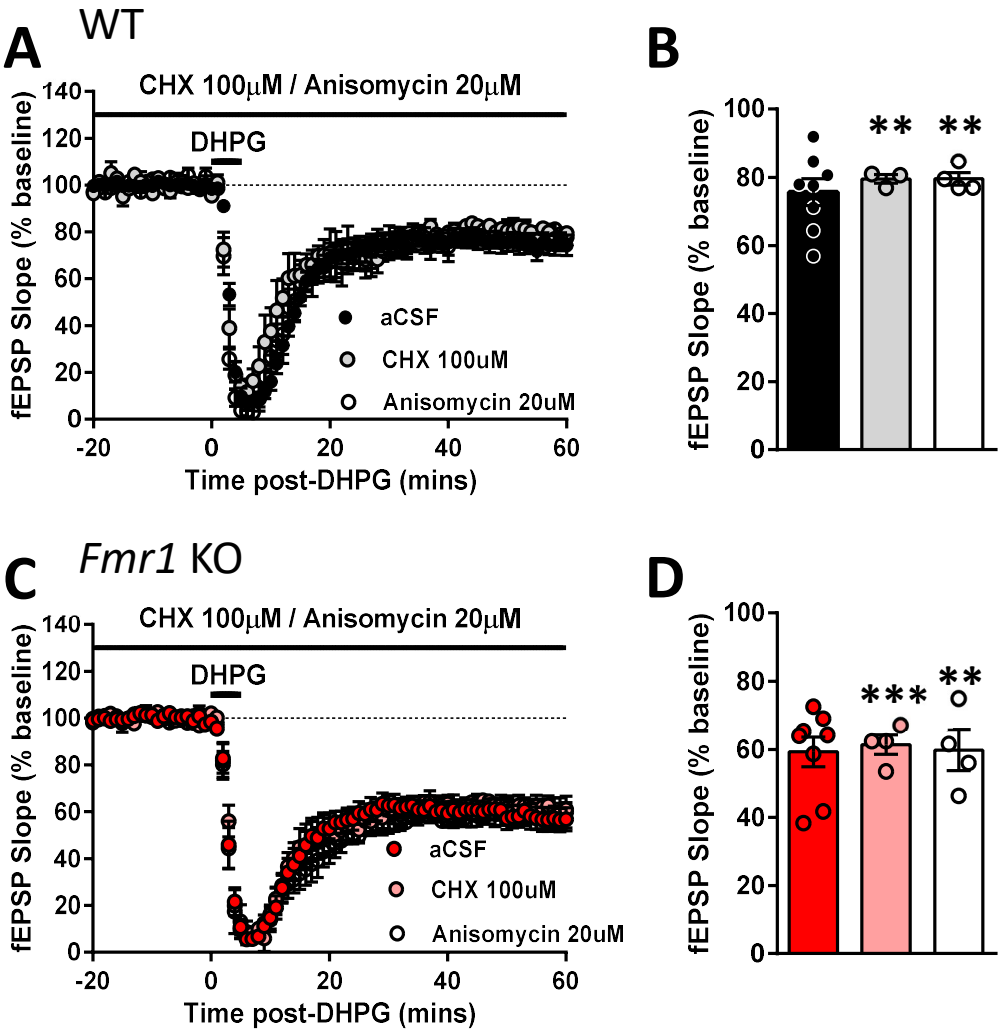

Figure 3.9 Protein synthesis inhibitors had no effect on DHPG-LTD in either genotype. (A) Timecourse showing DHPG-LTD in WT LEH animals in the presence of cycloheximide (100μM) or anisomycin (20μM). (B) DHPG-LTD caused significant synaptic depression in the presence of protein synthesis inhibitors in WT LEH animals (WT CHX: 79.52 ± 1.32%; n=3 slices/3 animals; p=0.004, Student paired *t*-test; WT Aniso: 79.55 ± 1.86%; n=4 slices/4 animals; p=0.002, Student paired *t*-test). (C) Timecourse showing DHPG-LTD in *Fmr1* LEH KO animals in the presence of cycloheximide (100μM) or anisomycin (20μM). (D) DHPG-LTD caused significant synaptic depression in the presence of protein synthesis inhibitors in *Fmr1* KO LEH animals (KO CHX: 61.34 ± 2.86%; n=4 slice/4 animals; p=0.0009, Student paired *t*-test; KO Aniso: 59.77 ± 6.00%; n=4 slices/4 animals; p=0.007, Student paired *t*-test).

that WT LEH rats also exhibited protein synthesis independent DHPG-LTD. The addition of protein synthesis inhibitors also had no effect on the decrease in presynaptic release probability in *Fmr1* KO LEH rats (Fig 3.10 A and B; Cycloheximide WT Baseline: 1.57 ± 0.09; Cycloheximide WT 50-60mins: 1.62 ± 0.1; n=3; $p > 0.05$; Cycloheximide KO Baseline: 1.52 ± 0.54; Cycloheximide KO 50-60mins: 1.70 ± 0.07; n=4; p=0.01; Anisomycin WT Baseline: 1.53 ± 0.78; Anisomycin WT 50-60mins: 1.57 ± 0.08; n=4; $p > 0.05$; Anisomycin KO Baseline: 1.49 ± 0.07; Anisomycin KO 50-60mins: 1.64 ± 0.08; n=4; p=0.0006). These findings show that inhibition of new protein synthesis has no effect on either the magnitude or mechanism of DHPG-LTD in either genotype.

3.5.2 Basal protein synthesis is not elevated in *Fmr1* KO LEH rats and is not affected by DHPG treatment in either genotype

Previous reports in *Fmr1* KO mice have found that exaggerated and protein synthesis independent DHPG-LTD is associated with an increase in basal protein synthesis (Dölen et al. 2007). Therefore, I used metabolic labelling to assess basal protein synthesis levels in our *Fmr1* KO LEH rats and WT controls. Here I found a subtle but not significantly different increase in protein synthesis levels in hippocampal slice from *Fmr1* KO rats (Fig 3.11; WT: 100.00 ± 0.00%; n=8; KO: 113.63 ± 7.56%; n=8; $p>0.05$). This suggests that exaggerated basal protein synthesis levels do not contribute to the exaggerated DHPG-LTD observed in *Fmr1* KO rats.

It has previously been shown that the protocol used to induce DHPG-LTD in hippocampal slices results in a significant increase in protein synthesis rates in WT animals that is not observed in *Fmr1* KO mice (Osterweil et al. 2010). This DHPG-induced protein synthesis is thought to represent the rapid translation of proteins responsible for the long-term expression of DHPG-LTD. Therefore, I tested the effected of DHPG stimulation on protein synthesis levels in our *Fmr1* LEH rats, where neither genotype show protein synthesis dependent DHPG-LTD. Application of DHPG 100µM during the first 5mins of metabolic labelling did not result in a

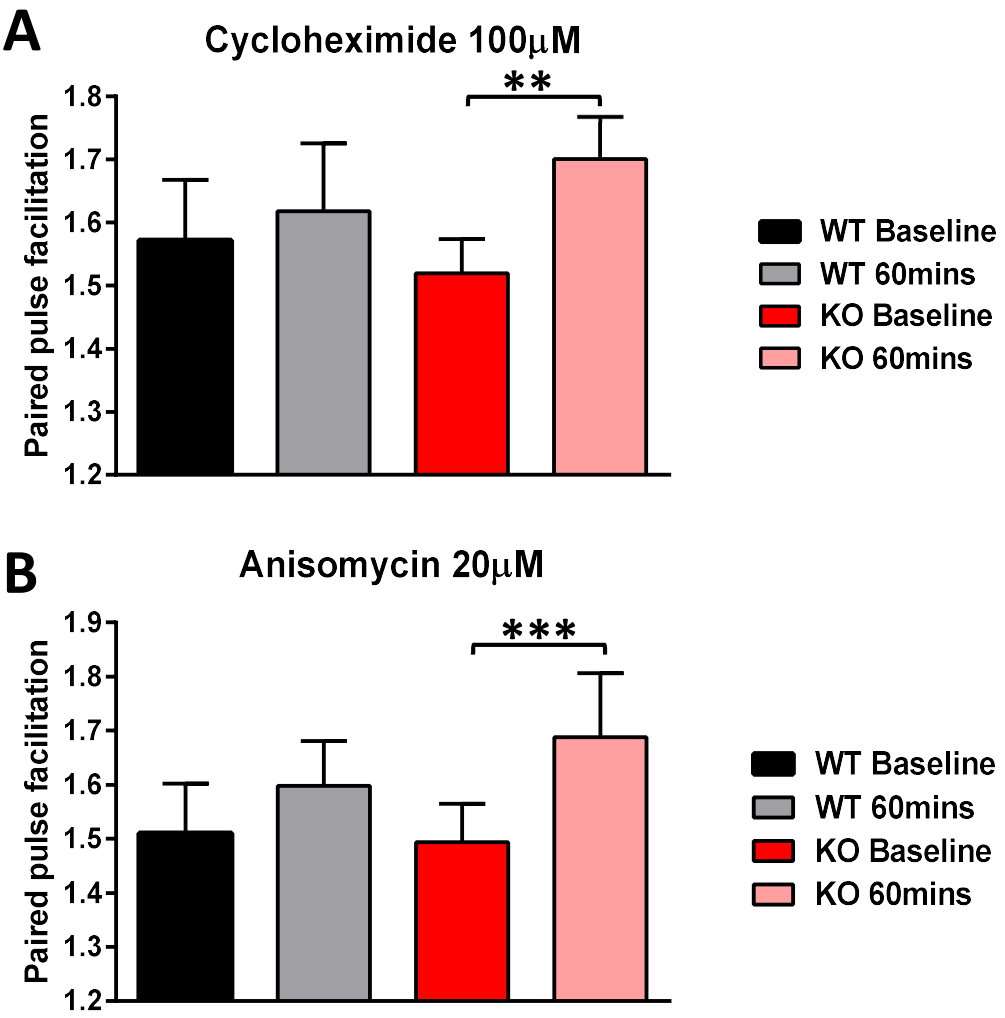

Figure 3.10 Incubation with protein synthesis inhibitors does not affect PPF increase following DHPG-LTD in *Fmr1* LEH KO rats (A) Paired pulse facilitation was unaffected by DHPG-LTD in presence of Cycloheximide 100μM in WT LEH rats (WT Baseline: 1.57 ± 0.09; WT 50-60mins: 1.62 ± 0.1; n=3 slices/3 animals; $p > 0.05$) but was significantly increased in *Fmr1* KO LEH rats (KO Baseline: 1.52 ± 0.54; KO 50-60mins: 1.70 ± 0.07; n=4 slice/4 animals; $p=0.01$). (B) Paired pulse facilitation was unaffected by DHPG-LTD in presence of anisomycin 20μM in WT LEH rats (WT Baseline: 1.53 ± 0.78; WT 50-60mins: 1.57 ± 0.08; n=4 slices/4 animals; $p > 0.05$) but was significantly increased in *Fmr1* KO LEH rats (KO Baseline: 1.49 ± 0.07; KO 50-60mins: 1.64 ± 0.08; n=4 slices/4 animals; $p=0.0006$). Statistics performed using Two-way ANOVA with Bonferroni correction.

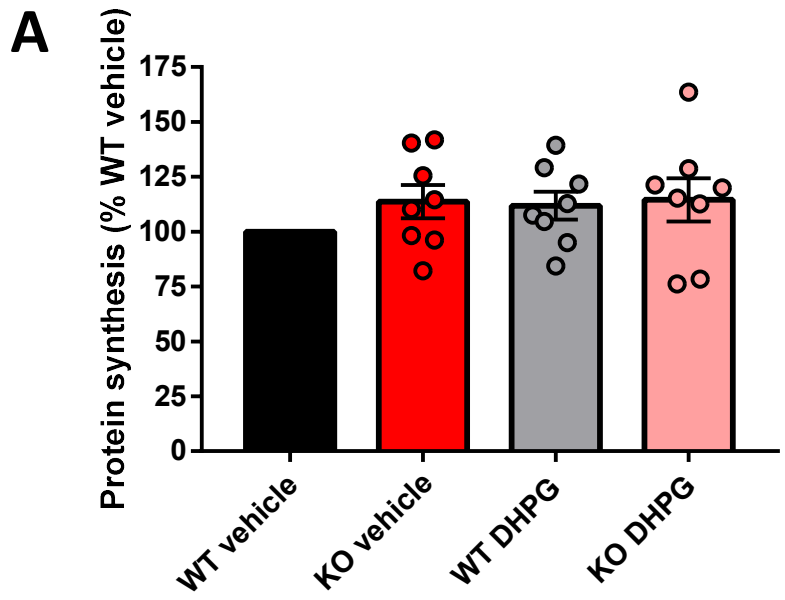

Figure 3.11 Basal protein synthesis is not elevated in *Fmr1* KO LEH rats and is not affected by DHPG treatment in either genotype (A) Basal protein synthesis was not significantly enhanced in *Fmr1* KO LEH rats (WT: 100.00 ± 0.00%; n=8 animals; KO: 113.63 ± 7.56%; n=8 animals; p>0.05). DHPG did not significantly increase protein synthesis rates in either genotype (WT vehicle: 100.00 ± 0.00%; n=8 animals; WT DHPG: 111.83 ± 6.35%; n=8 animals; p>0.05; KO vehicle: 113.63 ± 7.56%; n=8 animals; KO DHPG: 114.50 ± 9.86%; n=8 animals; p>0.05). Statistics performed using Two-way ANOVA with Bonferroni correction.

significant increase in protein synthesis rates compared to vehicle control in either genotype (Fig 3.11; WT vehicle: 100.00 ± 0.00%; n=8; WT DHPG: 111.83 ± 6.35%; n=8; p>0.05; KO vehicle: 113.63 ± 7.56%; n=8; KO DHPG: 114.50 ± 9.86%; n=8; p>0.05). This data suggests that the absence of protein synthesis dependent DHPG-LTD in this colony may be the result of an inability of group 1 mGluR activation to trigger downstream protein synthesis in these rats

3.5.3 Harlan WT LEH rats show protein synthesis dependent DHPG-LTD

The protein synthesis dependence of DHPG-LTD in wild-type animals is a well reported phenotype across the field in both mouse and rat studies (Huber et al. 2000; Barnes et al. 2015, Auerbach et al. 2011, Tian et al. 2015). It has been noted previously that the genetic background strain of animals can have an effect on the protein

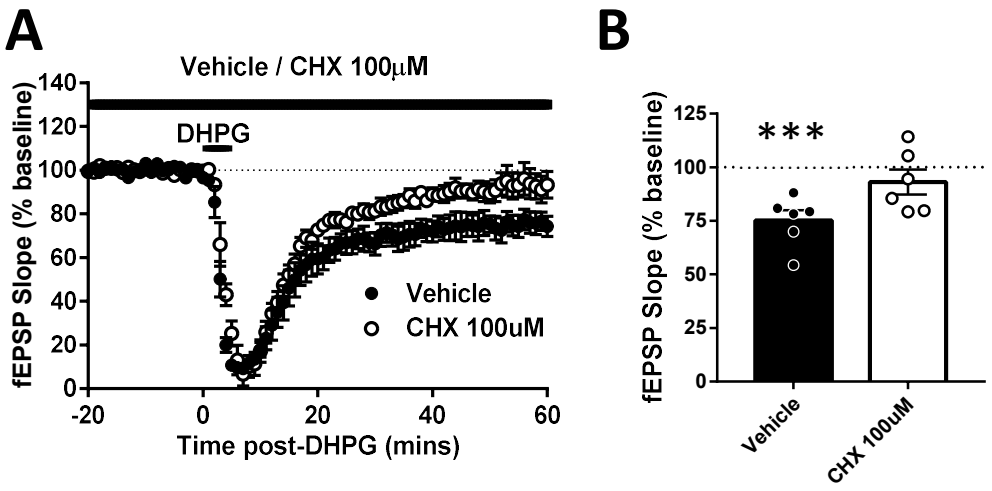

Figure 3.12 DHPG-LTD is protein synthesis dependent in WT LEH rats from a different vendor (A) Timecourse showing DHPG-LTD in WT LEH rats from a different vendor in the presence of cycloheximide 100μM. (B) DHPG-LTD was dependent on new protein synthesis in these WT LEH rats (aCSF: 75.12 ± 4.80%; n=6 slices/6 animals; p = 0.004, Student paired *t*-test; CHX: 93.08 ± 5.86%; n=6 slices/6 animals; p> 0.05, Student paired *t*-test).

synthesis dependency of DHPG-LTD (Personal communication, Professor K. Huber, University of Texas Southwestern). Therefore, I tested the effect of a protein synthesis inhibitor on DHPG-LTD in Blue Spruce Long Evans rats sourced from Harlan laboratories. In these animals I found that the magnitude of DHPG-LTD was not significantly different from baseline in the presence of the protein synthesis inhibitor Cycloheximide (Fig 3.12; aCSF: 75.12 ± 4.80%; n=6; $p_{aCSFvBaseline}$ = 0.004; CHX: 93.08 ± 5.86%; n=6; $p_{CHXvBaseline}$ > 0.05). This result suggests that the lack of protein synthesis dependent DHPG-LTD that I see in our *Fmr1* LEH colony could be due to their genetic background strain.

3.5.4 DHPG-LTD is enhanced and independent of new protein synthesis in Sprague Dawley *Fmr1* KO rats

During the course of this investigation I was also given access to an *Fmr1* KO rat bred on the Sprague Dawley (SD) genetic strain, created by Horizon laboratories (Till et al. 2015). This strain was first used to confirm our finding that DHPG-LTD was enhanced in *Fmr1* KO rats. Here, hippocampal DHPG-LTD was examined in juvenile (P21-32) WT and *Fmr1* KO SD rats. Consistent with findings in *Fmr1* KO LEH rats, application

of DHPG (50μM, 5 mins) resulted in synaptic depression that was significantly greater than WT littermate controls (Fig 3.13 A; WT: 78.64 ± 3.70%, n=17; KO: 67.53 ± 4.11%, n=17; p=0.023). Next, I investigated the protein synthesis dependency of mGluR-LTD in both genotypes of the *Fmr1* SD rats. Hippocampal slices were pre-incubated in the protein synthesis inhibitor Cycloheximide (100μM) for a minimum of 30 mins prior to DHPG-LTD induction, which then remained present for the remainder of the experiment. The inhibition of new protein synthesis prevented the maintenance of DHPG-LTD in WT slices (Fig 3.13 D; WT: 98.08 ± 8.35%, n=11; $p_{WTvBaseline}$>0.05). In contrast, DHPG-LTD was independent of new protein synthesis in *Fmr1* KO rats (Fig 3.13 D; KO: 74.22 ± 7.42%, n=11; $p_{KOvBaseline}$=0.022). Therefore, in agreement with findings in *Fmr1* KO mice, DHPG-LTD was both exaggerated and independent of new protein synthesis in *Fmr1* KO SD rats compared to WT littermate controls.

3.5.5 Basal excitatory transmission at Schaeffer collateral inputs to CA1 is unaffected in Sprague Dawley *Fmr1* KO rats

As changes in basal synaptic strength or release probability could affect the induction or expression of synaptic plasticity (Palmer et al. 1997), I investigated these parameters in the *Fmr1* SD rat model. Here, the input/output relationship of this synapse was investigated by incrementally increasing stimulus intensity and plotting the evoked fibre volley amplitude against fEPSP slope. In agreement with other Fragile X models, no change in basal synaptic strength were observed at CA3 – CA1 synapses in *Fmr1* KO SD rats (Fig 3.14 A; F(1,14)=0.09; p=0.77). Next, I investigated paired pulse ratios by applying two stimulus pulses with a varying inter-stimulus interval (20-1000ms) which has been interpreted as a measure of pre-synaptic release probability (Zucker & Regehr 2002). Paired pulse ratio was not significantly different at any of the measured inter-stimulus intervals (Fig 3.14 B; F(1,18)=0.195; p=0.664) suggesting that basal release probability is largely unaffected in *Fmr1* KO SD rats. From these results it can be suggested that differences in basal synaptic properties do not account

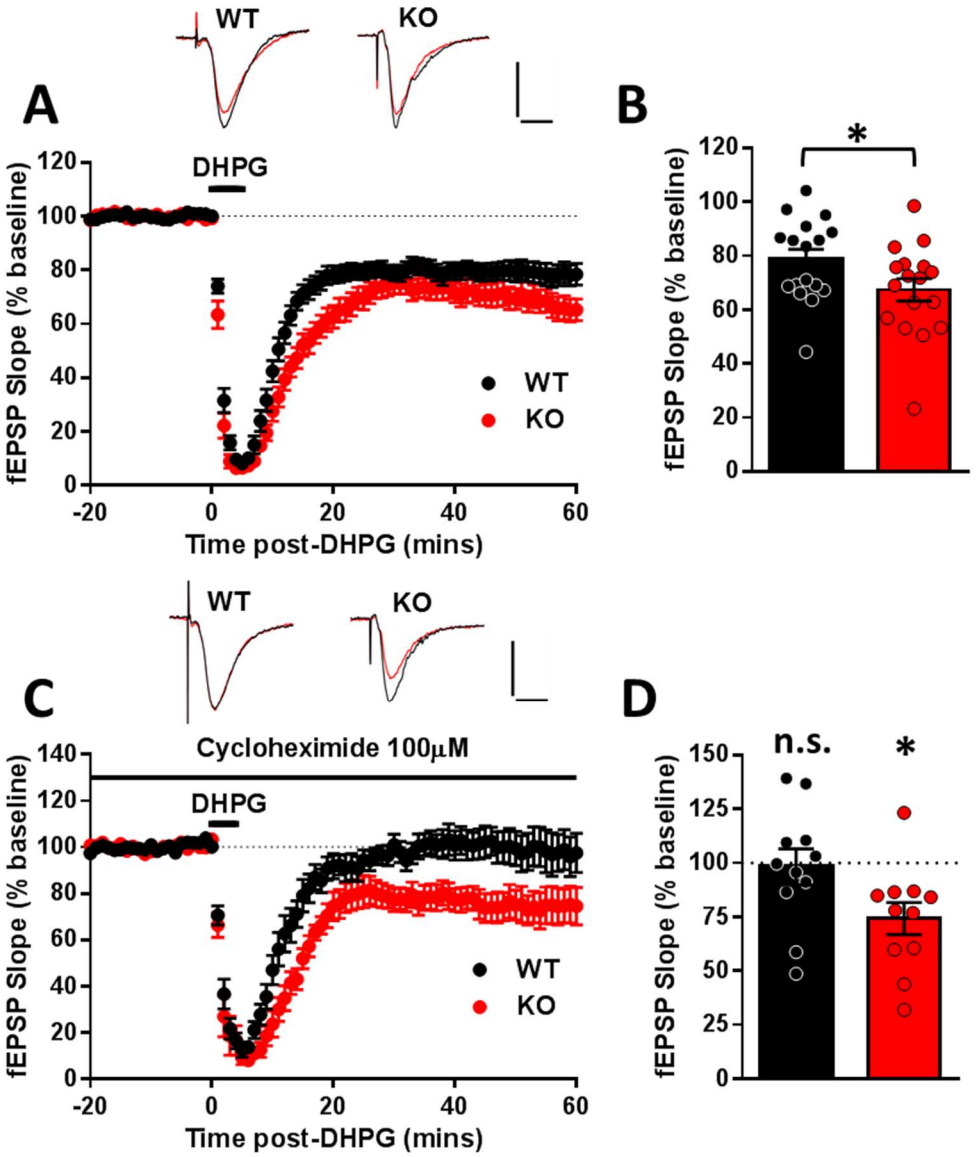

Figure 3.13 DHPG-LTD is enhanced and independent of new protein synthesis in Sprague Dawley *Fmr1* KO rats (A) Timecourse showing DHPG-LTD (DHPG 50µM) in WT and *Fmr1* KO SD rats. Example traces showing fEPSP from baseline (black) and 60mins post-DHPG (red). Scale 0.5mV, 10ms. (B) DHPG-LTD was significantly greater in *Fmr1* KO SD slices than WT controls (WT: 78.64 ± 3.70%, n=17 slices/ 17 animals; KO: 67.53 ± 4.11%, n=17 slices/ 17 animals; p=0.023, Student unpaired *t*-test). (C) Timecourse showing DHPG-LTD (DHPG 50µM) in WT and *Fmr1* KO SD rats in the presence of Cycloheximide 100µM. Example traces showing fEPSP from baseline (black) and 60mins post-DHPG (red). Scale 0.5mV, 10ms. (D) Inhibition of new protein synthesis prevented the maintenance of DHPG-LTD in WT slices (WT: 98.08 ± 8.35%, n=11 slices/ 11 animals; p=0.82, Student paired *t*-test). In contrast, DHPG-LTD was independent of new protein synthesis in *Fmr1* KO rats (KO: 74.22 ± 7.42%, n=11 slices/ 1 animals; p=0.022, Student paired *t*-test).

for any plasticity differences between the two Fragile X Syndrome rat models.

3.5.6 PP-LFS LTD is protein-synthesis dependent in WT LEH rats but protein synthesis independent in *Fmr1* KO LEH rats

Synaptically induced mGluR-LTD has also been shown to be protein synthesis dependent in WT animals as well as protein synthesis independent in *Fmr1* KO mice (Nosyreva & Huber 2006). Here I tested the protein synthesis-dependency of PP-LFS LTD in *Fmr1* LEH rats. In contrast to DHPG-LTD, PPLFS-LTD was not significantly different from baseline when new protein synthesis was inhibited in WT slices (Fig 3.15 B; WT aCSF: 81.71 ± 2.89%; n=7; CHX: 94.12 ± 3.48%; n=7; $p_{CHXvBaseline} > 0.05$). However, PPLFS-LTD cause significant synaptic depression in *Fmr1* KO LEH rats in the presence of Cycloheximide (Fig 3.15 D; KO aCSF: 77.34 ± 0.68%; n=5; KO CHX: 78.66 ± 4.23%; n=5; $p_{CHXvBaseline} = 0.007$). This data is in direct agreement with studies in the *Fmr1* KO mice that have shown PP-LFS LTD is independent of new protein-synthesis in the absence of FMRP (Nosyreva & Huber 2006). This data also provides further evidence that a difference in the mechanism of DHPG-LTD and PP-LFS LTD expression may exist.

3.7 NMDA-dependent plasticity mechanisms are unaffected in the absence of FMRP

Previous studies in *Fmr1* KO mice have found no changes in NMDA-dependent plasticity mechanisms in CA1 hippocampus (Godfraind et al. 1996; Paradee et al. 1999; Huber et al. 2002). Here I investigated two forms of plasticity in *Fmr1* LEH rats, NMDA-dependent LTD and NMDA-dependent LTP. No significant differences were observed in the magnitude of LTD induced by 900 single pulses at a frequency of 1Hz (Fig 3.16 A; WT: 81.16 ± 3.11%; n=6; KO: 80.25 ± 4.93%; n=5; $p > 0.05$). Similarly no significant differences were observed in the magnitude of NMDA-

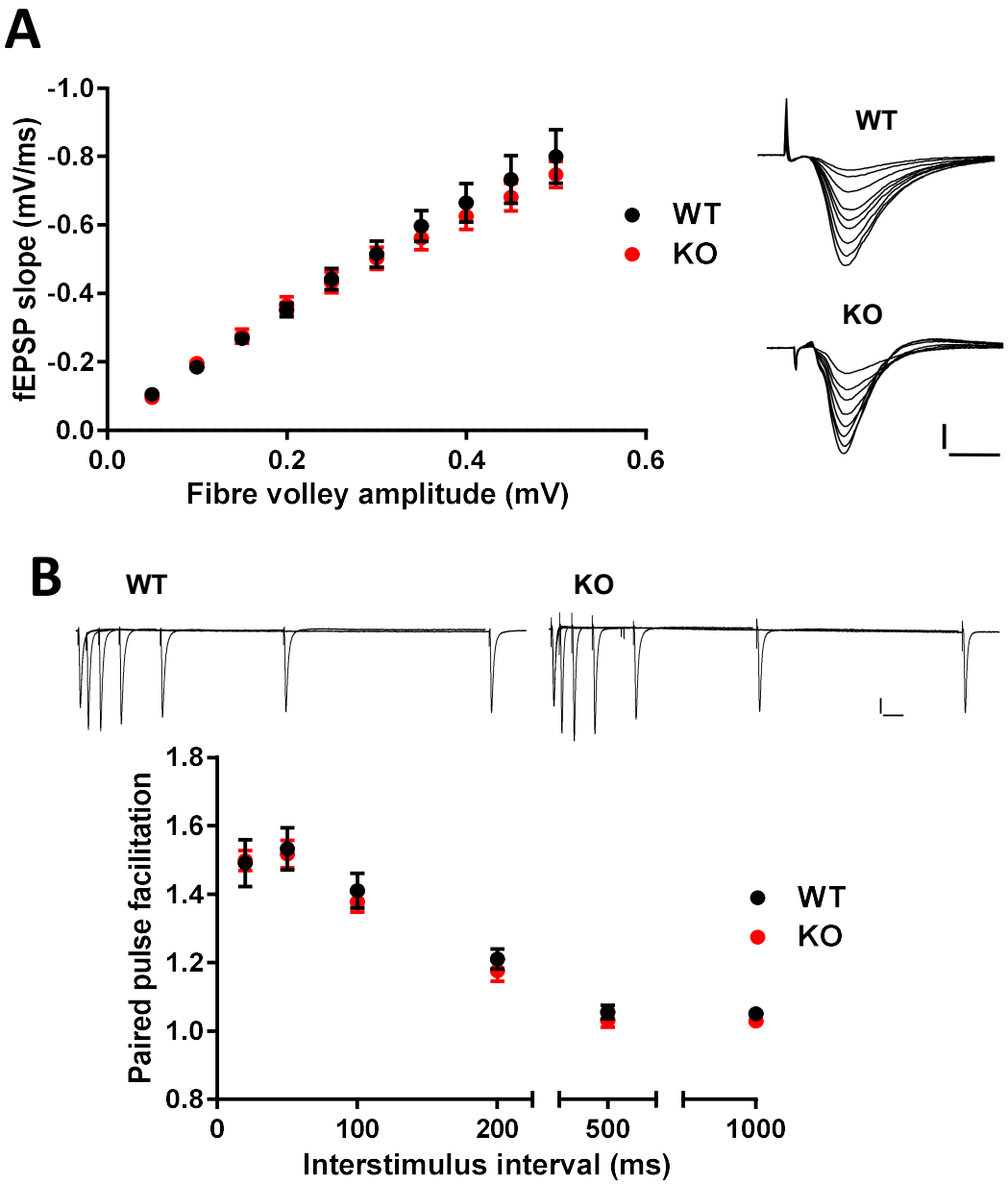

Figure 3.14 Basal excitatory synaptic transmission is unaffected at CA3-CA1 synapses in *Fmr1* KO SD rats (A) Input-output function was measured at CA3-CA1 synapses by comparison of fibre volley amplitude and fEPSP slope. No significant differences were observed between genotypes ($F(1,14)=0.091$; $p=0.7678$, Two way RM-ANOVA). Example traces from each genotype showing fEPSP at various stimulation strenths. Scale 100µV, 20ms. (B) Paired pulse facilitation was tested using two concurrent pulses at multiple interstimulus intervals (25-1000ms). Paired pulse facilitation was comparable between WT controls and *Fmr1* KO SD rats ($F(1,18)=0.1945$; $p=0.6644$, Two way RM-ANOVA). Example traces from each genotype showing paired pulse facilitation at all tested intervals. Scale 100µV, 50ms.

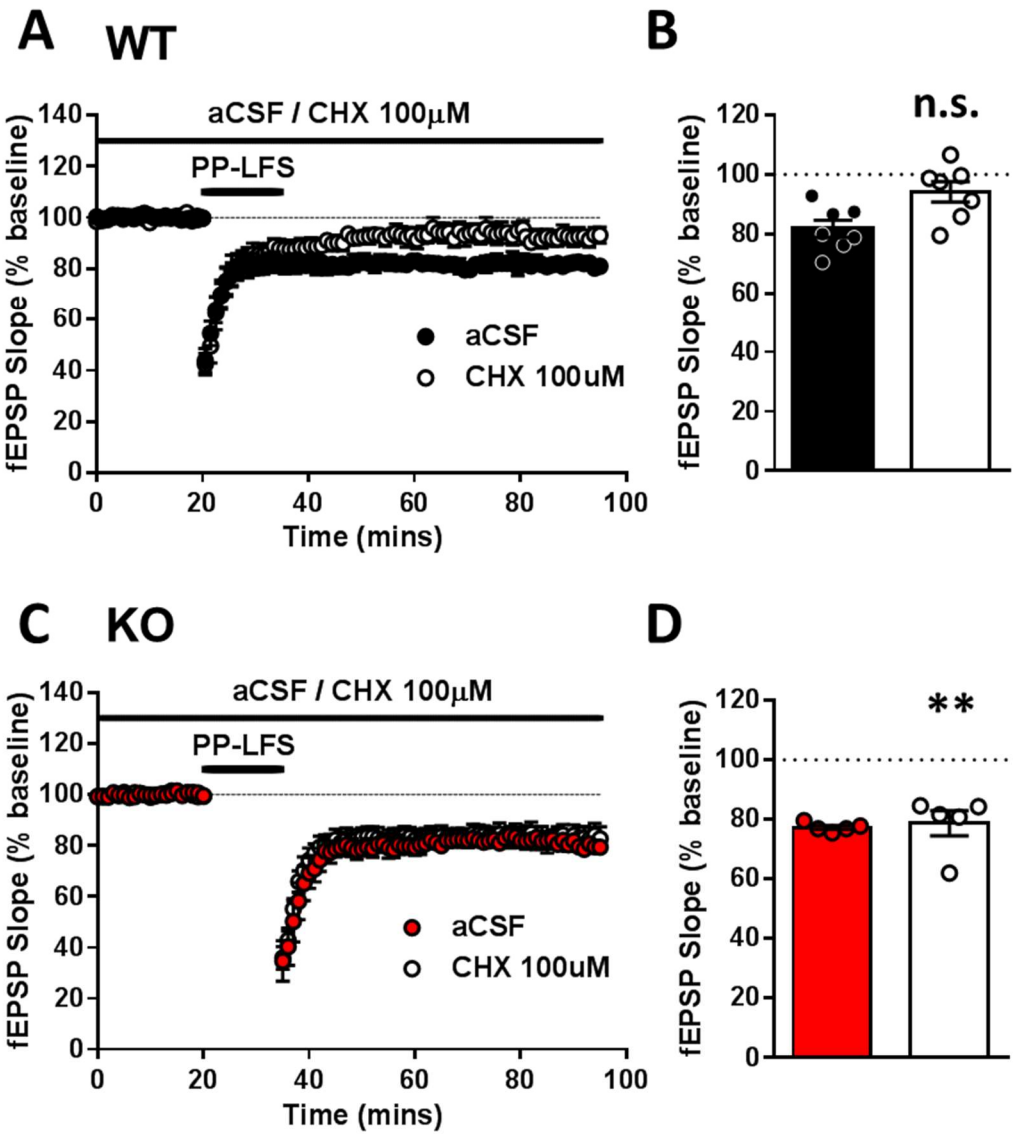

Figure 3.15 PPLFS-LTD is protein synthesis independent in *Fmr1* LEH KO rats
(A) Timecourse showing PPLFS-LTD in WT LEH animals in the presence of cycloheximide (100µM).(B) PPLFS-LTD was dependent on new protein synthesis in WT LEH rats (WT aCSF: 81.71 ± 2.89%; n=7 slices/ 7 animals; CHX: 94.12 ± 3.48%; n=7 slices/ 7 animals; p> 0.05, Student paired *t*-test). (C) Timecourse showing DHPG-LTD in WT LEH animals in the presence of cycloheximide (100µM). (D) PPLFS-LTD was independent of new protein synthesis in *Fmr1* LEH KO rats (KO aCSF: 77.34 ± 0.68%; n=5 slices/ 5 animals; KO CHX: 78.66 ± 4.23%; n=5 slices/ 5 animals; p= 0.007, Student paired *t*-test).

dependent LTP between genotypes (Fig 3.16 B; WT: 152.68 ± 15.38%; n=4; KO: 146.09 ± 10.54%; n=4; $p > 0.05$).

3.8 Discussion

In this chapter, the core physiological hippocampal phenotypes identified in *Fmr1* KO mice that have contributed to the 'mGluR theory of FXS' have been assessed in *Fmr1* KO rats. I have shown that DHPG-LTD is enhanced in two separate rat models of FXS relative to control animals and this appears to be corrected by incubation with $mGluR_5$ negative allosteric modulators. In contrast to previous studies, I did not observe a protein synthesis dependent component to DHPG-LTD in LEH WT rats. This appears to be restricted to this outbred LEH strain as protein synthesis dependent DHPG-LTD was observed in WT animals from a separate LEH colony and also SD rats. In line with studies in *Fmr1* KO mice, *Fmr1* SD KO rats showed protein synthesis independent DHPG-LTD. Using *Fmr1* LEH rats, no difference in the magnitude of PPLFS-LTD was observed between genotypes. However this form of plasticity was found to be dependent on new protein synthesis in WT rats but independent of new protein synthesis in *Fmr1* KO LEH rats. This data suggests that DHPG-LTD and PPLFS-LTD have distinct mechanisms of expression. Together, this work highlights the conservation of mGluR dependent phenotypes caused by the loss of FMRP between mice and rats

3.8.1 Induction of mGluR-LTD in CA1 hippocampus

Long-term depression resulting from the stimulation of group 1 mGluRs has been commonly studied at Schaeffer collateral synapses onto CA1 pyramidal neurons. A common method is through application of DHPG, an agonist of $mGluR_{1/5}$, which produces a stable synaptic depression lasting in excess of 1hr. Early studies into the mechanisms of DHPG-LTD found that its expression was enhanced when tissue excitability was increased either by the presence of $GABA_AR$ antagonists or using Mg^{2+}-free aCSF (Palmer et al. 1997). I found that increasing tissue excitability via

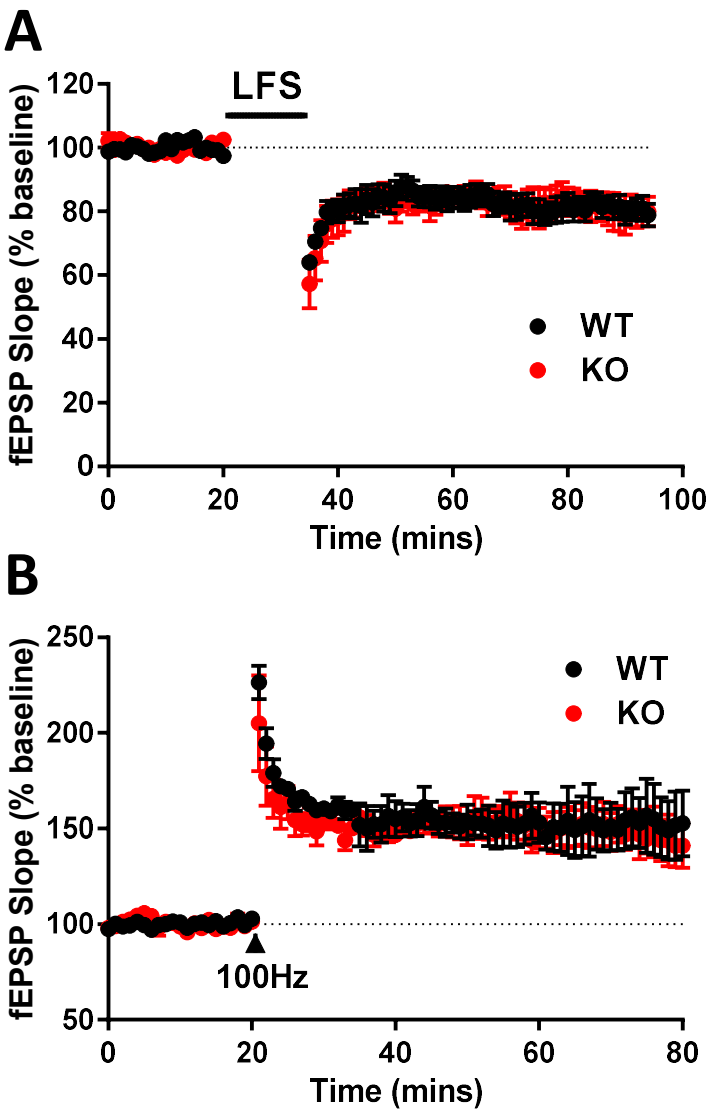

Figure 3.16 NMDAR-dependent plasticity mechanisms were unaffected by the loss of FMRP. (A) Timecourse showing NMDAR-dependent LTD induced with 900 pulses at 1Hz frequency resulted in equal magnitude synaptic depression in both genotypes (WT: 81.16 ± 3.11%; n=6 slices/ 6 animals; KO: 80.25 ± 4.93%; n=5 slices/5 animals; $p > 0.05$, Student unpaired *t*-test). (B) Timecourse showing NMDAR-dependent LTP induced with 1s, 100Hz train resulted in equal magnitude synaptic potentiation in both genotypes (WT: 152.68 ± 15.38%; n=4 slices/4 animals; KO: 146.09 ± 10.54%; n=4 slices/4 animals; $p > 0.05$, Student unpaired *t*-test).

disinhibition had no effect on DHPG-LTD magnitude. This may be caused by differences in experimental design as this previous study used adult, female rats as well as using the 'grease-gap' recording method where the recording electrode is placed in the alveus of CA1 hippocampus. The recordings shown here were performed in CA1 *stratum radiatum*, as were those in another study that showed no effect of disinhibition on DHPG-LTD (Rohde et al. 2009). Therefore differences in GABAergic innervation or the activity of interneurons in different lamina could explain the differences in mechanism observed here as has previously been hypothesised for NMDA-LTD on CA1 apical dendrites (Parvez et al. 2010).

3.8.2 Mechanistic differences in chemical v synaptic induction of mGluR-LTD

mGluR-LTD can be induced using both patterned synaptic stimulation as well as chemical agonists such as DHPG. Chemical stimulation is most commonly used in the study of the mechanism of mGluR-LTD because of the ability to perform complimentary molecular and biochemical analysis. Classically, the mechanisms of both chemical (DHPG-LTD) and synaptic mGluR-LTD (PPLFS-LTD) are thought to be analogous. Several studies have shown the long term expression of both DHPG-LTD and PPLFS-LTD to be dependent on $mGluR_5$ signalling (Huber et al. 2000; Moult et al. 2008; Faas et al. 2002). Both forms have been shown to be dependent on similar signalling pathways involving activation of mitogen activated protein kinase (MAPK), protein tyrosine phosphatases (PTP) and Jun N-term kinase (Gallagher 2004; Huang et al. 2004; Moult et al. 2008; Li et al. 2007). Similarly, studies have shown that both forms of mGluR-LTD are dependent on new protein synthesis (Huber et al. 2000; Nosyreva and Huber 2006). Both DHPG-LTD and PPLFS-LTD have also been shown to occlude one another at some developmental ages which also suggests a shared mechanism (Huber et al. 2001).

Whilst these findings suggest that both chemical and synaptic mGluR-LTD share one mechanism, the data in this chapter provide evidence of the contrary. Firstly, when comparing mGluR-LTD between genotypes in our *Fmr1* LEH colony, DHPG-LTD

was found to be exaggerated in *Fmr1* KO LEH rats whereas the magnitude of PPLFS-LTD was unaffected. This suggests that the loss of FMRP affects the expression of DHPG-LTD through a mechanism that is not involved in PPLFS-LTD. The magnitude of mGluR-LTD in CA1 hippocampus has previously been linked with the level of basal protein synthesis (Osterweil et al. 2010) however I observed no significant difference in this between WT controls and *Fmr1* KO LEH rats, although repeat experiments are required to confirm this (Fig 3.11). This suggests that elevated basal protein synthesis is not the cause of the observed exaggerated DHPG-LTD in *Fmr1* LEH KO rats.

One possible explanation for the exaggerated DHPG-LTD in the absence of FMRP could be through an additional presynaptic depression. DHPG wash on resulted in a significant increase in paired pulse facilitation (PPF), which is associated with a reduction in synaptic release probability, in *Fmr1* LEH KO slices. I saw no long term effect on PPF following DHPG wash-on in WT controls suggesting DHPG-LTD is expressed postsynaptically in WT animals. No change in PPF was observed in either genotype following PPLFS-LTD induction (Fig 3.8) suggesting that the reduction in release probability following DHPG-LTD in *Fmr1* KO LEH slices may contribute to the exaggerated synaptic depression. This is further supported by preliminary data showing the normalisation of DHPG-LTD magnitude as well as PPF in the absence of FMRP following incubation with the $mGluR_5$ negative allosteric modulator CTEP (Fig 3.7). As group 1 mGluR expression in CA1 hippocampus is typically restricted to the postsynaptic terminal, this reduction in presynaptic release could be mediated by a retrograde signalling mechanism such as endocannabinoid (eCB) release.

Following postsynaptic depolarisation and mGluR activation, eCBs are release from the postsynaptic terminal into the synaptic cleft where they act upon presynaptic afferents (Chevaleyre et al. 2006). The eCB receptor subtype cannabinoid 1 receptor (CB1R) is expressed in many brain regions including the hippocampus and its activation is thought to lead to a reduction in the probability of neurotransmitter release (Alger 2002). Whilst CB1R activation is not typically thought to be involved in LTD

at excitatory synapses, CB1R antagonism has been shown to reduce the acute short-term depression following DHPG application suggesting eCB release plays a role in mGluR-LTD (Rouach & Nicoll 2003). Group 1 mGluR activation has also been shown to be required for eCB-mediated plasticity at inhibitory terminals in CA1 hippocampus highlighting an important regulatory role of mGluR signalling in eCB release (Varma et al. 2001). In *Fmr1* KO mice, $mGluR_5$ signalling has been found to be both constitutively active as well as showing enhanced coupling with eCB mobilization (Ronesi et al. 2012; Zhang & Alger 2010). This has been shown to lead to alterations in eCB-mediated plasticity mechanisms in several brain areas (Zhang & Alger 2010; Maccarrone et al. 2010; Jung et al. 2012). Therefore, one could hypothesise that enhanced $mGluR_5$ signalling and eCB release at *Fmr1* LEH KO synapses could result in depression of vesicle release at presynaptic terminals, resulting in enhanced DHPG-LTD in the absence of FMRP. This could be further investigated by testing the effects of CB1R antagonism on DHPG-LTD in *Fmr1* LEH KO rats.

Whilst an increase in PPF is indicative of reduction in presynaptic release probability, it can also be explained through other mechanisms. The locus of expression of mGluR-LTD has raised some controversy in the field since it was first identified. Some work in adolescent WT animals has suggested a presynaptic effect through observations of increased PPF and a reduction in mEPSC frequency, but not amplitude, following DHPG application (Oliet et al. 1997; Faas et al. 2002; Fitzjohn et al. 1999) whereas others have proposed postsynaptic effect through AMPAR internalisation in a process that is dependent on postsynaptic protein synthesis (Snyder et al. 2001; Huber et al. 2000). These presynaptic changes could also be explained through a postsynaptic mechanism if AMPAR internalisation took place preferentially at synapses that have a higher probability of glutamate release than average, counter to a mechanism previously suggested for postsynaptic LTP (Poncer & Malinow 2001). However this mechanism would likely require the activation of both mGluR and AMPAR. Given that DHPG-LTD can be induced without concurrent synaptic stimulation (Fitzjohn et al. 1999; Huber et al. 2001) this is unlikely to explain the increased PPF observed here.

3.8.3 Protein synthesis dependency of mGluR-LTD in *Fmr1* rats

Several lines of evidence suggest that the expression of mGluR-LTD is dependent on rapid dendritic protein synthesis (Huber et al. 2000; Huber et al. 2001). Contrary to this, in this thesis I found that DHPG-LTD was independent of new protein synthesis in WT LEH rats (Fig 3.9). It has been suggested that some rodent background strains may contain genetic mutations which result in protein synthesis independent plasticity (Professor Kimberly Huber, personal communication, University of Texas Southwestern). In agreement with this I saw protein synthesis dependent DHPG-LTD in two other strains of WT rat under the same recording conditions. The stimulation of mGluRs has been shown to increase protein synthesis levels in conditions that induce LTD in the hippocampus (Osterweil et al. 2010). This new protein synthesis is thought to represent the expression of proteins which lead to AMPAR internalisation and depression of synaptic transmission, of which there are several candidates (Zhang et al. 2008; Davidkova & Carroll 2007). Metabolic labelling revealed that DHPG did not cause a significant increase in protein synthesis rates in WT LEH rats (Fig 3.11). One potential explanation for this finding is that protein synthesis levels are already saturated in this strain of WT animals. As proposed for *Fmr1* KO mice, elevated basal protein synthesis downstream of mGluRs could lead to protein synthesis independent LTD as the existing protein pool is sufficient to support the expression of synaptic depression. Analysis using RNA sequencing to compare the transcriptomes of these different rat strains may provide information on the underlying cause of these differences in DHPG-LTD mechanism.

In contrast to DHPG-LTD, I found PPLFS-LTD was abolished in the presence of protein synthesis inhibitors in WT LEH rats (Fig 3.15) suggesting the expression of chemical and synaptic mGluR-LTD are supported by different populations of proteins in these animals. PPLFS-LTD may be acting through a different group of receptors than DHPG-LTD which is the result of group 1 mGluR activation with a specific agonist. In agreement with this, Volk et al. (2006) showed that PPLFS-LTD can persist in systems where group 1 mGluRs are both genetically deleted or blocked

pharmacologically. This LTD could be mediated by other G_q coupled receptors such as M_1 muscarinic acetylcholine receptors (mAChRs) which is also dependent on new protein synthesis (Volk et al. 2007). Interestingly, disruption of mGluR interactions with the protein Homer, which is thought to link mGluR activation with downstream protein synthesis, disrupts DHPG-LTD whilst having no effect on PPLFS-LTD (Ronesi & Huber 2008). This supports the hypothesis that whilst DHPG-LTD is independent of new protein synthesis due to an unknown mutation in this WT strain resulting in saturated protein synthesis downstream of mGluR signalling, PPLFS-LTD is unaffected as it is being mediated through a different set of synaptic receptors, potentially mAChRs, which requires a different subpool of proteins for its expression. Future experiments addressing the protein synthesis dependency of carbachol induced-LTD and its ability to stimulate new protein synthesis in this strain of WT animals could also inform this hypothesis.

3.8.4 Translating the 'mGluR theory' to a rat model of FXS

The 'mGluR theory of FXS' is based on the observation that mGluR-LTD in CA1 hippocampus is both exaggerated and independent of new protein synthesis in *Fmr1* KO mice (Huber et al. 2002; Nosyreva & Huber 2006). These phenotypes are thought to be the result of exaggerated basal protein synthesis caused by aberrant $mGluR_5$ signalling (Osterweil et al. 2010). These findings have contributed to the hypothesis that many aspects of FXS are the result of exaggerated group 1 mGluR signalling (Bear et al. 2004).

The generation of rat models of FXS has enabled us to investigate if these hippocampal phenotypes are conserved across mammalian species. Using the SD *Fmr1* rat generated by Horizon laboratories, I found DHPG-LTD was both enhanced and independent of new protein synthesis (Fig 3.13). Basal protein synthesis rates were also enhanced in *Fmr1* SD KO rats relative to WT controls (Till et al. 2015). These results are in good agreement with the original findings in *Fmr1* KO mice. Experiments using a second rat model of FXS on a different genetic background, the

Fmr1 LEH rat, have revealed some intriguing findings however this most likely a result of WT strain issues. DHPG-LTD was once again found to be enhanced in *Fmr1* LEH KO rats (Fig 3.5) and PPLFS-LTD was independent of new protein synthesis (Fig 3.15). Whilst the protein synthesis independency of DHPG-LTD in WT animals from this colony provide a confounding factor, the finding of protein synthesis dependent DHPG-LTD in WT LEH rats from a separate supplier suggests that genetic backcrossing may be a potential solution. This would allow us to then test the effect of FMRP loss on protein synthesis dependent DHPG-LTD.

3.8.5 Summary

In summary, the data presented in this chapter provide good evidence of shared cellular pathophysiology associated with the loss of FMRP in CA1 hippocampus of mice and rats. The core phenotypes identified in *Fmr1* KO mice that have informed the 'mGluR theory of FXS' (1) exaggerate mGluR-LTD, (2) protein synthesis independent mGluR-LTD and (3) enhanced basal protein synthesis, have all been displayed. I have also shown that a pharmacological strategy targeting $mGluR_5$ is able to normalise the enhanced DHPG-LTD adding to the findings in *Fmr1* KO mice that therapeutics targeting group 1 mGluRs can ameliorate some of the phenotypes associated with the loss of FMRP. This work provides the first cross-mammalian evidence for mGluR-dependent cellular phenotypes in models of FXS and can act as a foundation for future investigations into hippocampal function in rat models of FXS that would otherwise rely of interpretations and assumptions from *Fmr1* KO mouse data.

Chapter 4

Neuronal excitability and synaptic deficits in the FXS amygdala

4.1 Introduction

Although intellectual disability is often seen as the defining feature of FXS it is often co-occuring with a range of emotional features, which are the most debilitating aspects for many families. These features include anxiety, gaze avoidance and elevated stress (Hessl et al. 2004). These behaviours are consistent with amygdala dysfunction, a key component of the brains fear circuitry involved in both the acquisition, expression and storage of fear memories (Davis 2006). Consistent with this, amygdala abnormalities have been identified in FXS patients using functional and structural MRI studies (Watson et al. 2008; Gothelf et al. 2008; Kates et al. 1997; Hazlett et al. 2009). Behavioural studies using *Fmr1* KO mice have also identified abnormalities in social behaviour, anxiety and fear conditioning (McNaughton et al. 2008; Paradee et al. 1999; Spencer et al. 2008) highlighting the importance of FMRP in amygdala function.

The neurocircuitry of fear responses has classically been studied in rodents using fear conditioning paradigms. Many species including humans, primates and rodents are able to acquire conditioned fear reactions following the association of a neutral stimulus with a noxious event (LeDoux 2003). As these fear responses closely resemble the behavioural and physiological symptoms of human fear responses, they are thought to have clinical relevance to the understanding of the underlying neurobiology of fear pathology in human conditions such as FXS.

Several studies have identified the basolateral amygdala (BLA); which is composed of the basal (BA) and lateral amygdala (LA) nuclei; as a key component in fear learning across species (LeDoux et al. 1990). The LA receives direct sensory input from both the thalamus and cortex (Pitkänen et al. 1997). Studies showing that long-term potentiation (LTP) at these inputs is occluded by fear learning has led to the hypothesis that this may represent the cellular correlate of the acquisition of fear memories (Blair et al. 2001; Tsvetkov et al. 2002). These forms of plasticity have particular relevance to FXS as group 1 mGluR-dependent forms of LTP have been identified at both of these inputs (Rodrigues et al. 2002; Cho et al. 2011). In line with the mGluR signalling

dysfunction in FXS, studies in *Fmr1* mice have identified deficits in mGluR-LTP at thalamic inputs to the LA (Suvrathan et al. 2010; Zhao et al. 2005). This is accompanied by deficits in fear learning in *Fmr1* KO mice (Paradee et al. 1999). Another well characterised component fear and anxiety related circuit is the BA which serves in the storage and expression of fear memories (Gale et al. 2004; Anglada-Figueroa 2005). Several studies in *Fmr1* mice have revealed significant defects in inhibitory signalling within the BA that could also contribute to the described deficits in amygdala mediated behaviours (Olmos-Serrano et al. 2010; Olmos-Serrano et al. 2011; Kratovac & Corbin 2013; Martin et al. 2014; Vislay et al. 2013).

Recent work in our lab has revealed that *Fmr1* KO rats show deficits in cued fear conditioning (Dr Sally Till, University of Edinburgh, personal communication) suggesting an underlying pathology in amygdala function of *Fmr1* KO rats. LTP at both cortical and thalamic inputs to the LA underlies this form of learning in rats and is regulated by group 1 mGluR signalling (Rodrigues et al. 2002; Cho et al. 2011). As I have shown in my work in the CA1 hippocampus (Chapter 3), group 1 mGluR signalling is affected in *Fmr1* KO rats. Therefore, I wanted to test the fidelity of mGluR-LTP at the two major inputs to the LA in *Fmr1* KO rats using previously established protocols. The loss of FMRP is also associated with cellular hyperexcitability in the BA as a result of deficits in inhibitory signalling. This circuit excitability affects amygdala output which can lead to changes in amygdala dependent behaviours. Therefore, I next examined the intrinsic excitability of principal neurons in both major nuclei of the BLA as well as their excitatory/inhibitory synaptic balance.

4.2 Results

4.2.1 mGluR-dependent LTP at thalamic inputs is impaired in the lateral amygdala of *Fmr1* KO rats

Long-term potentiation at auditory thalamic inputs of the lateral amygdala is believed to represent the cellular correlate of auditory fear learning. Tetanic stimulation of axons in the internal capsule, where the inputs from the auditory thalamus are believed to enter the lateral amygdala, results in a form of LTP that is dependent on both NMDA-receptors and $mGlu_5$-receptor activation (Rodrigues et al. 2002; Bauer et al. 2002). Here, I investigated if this mGluR-dependent form of synaptic plasticity is intact in our rat model of Fragile X syndrome. Tetanic stimulation of thalamic inputs to the lateral amygdala at 30Hz resulted in a form of LTP in WT animals that was significantly impaired in *Fmr1* KO rats (Fig 4.1 B; WT: 132.41 ± 4.57%; n=7; KO: 110.77 ± 5.36%; n=6; p=0.01). Some forms of LTP have been shown to be absent in animal models of Fragile X syndrome due to changes in the threshold for induction (Meredith et al. 2007). Thus I repeated these experiments with an increased tetanic stimulation frequency of 100Hz (Humeau et al. 2007). Even with this more robust form of induction, LTP was still significantly impaired in *Fmr1* KO rats (Fig 4.1 D; WT: 156.94 ± 9.80%; n=8; KO: 119.17 ± 3.63%; n=8; p=0.003). Therefore, in line with studies from *Fmr1* KO mice, mGluR-dependent plasticity is impaired at thalamic inputs to the lateral amygdala.

4.2.2 mGluR-dependent LTP at cortical inputs to the LA is absent in *Fmr1* KO rats

As well as thalamic inputs, the LA also receives synaptic inputs arising from various cortical regions. As these inputs can undergo plasticity independently, it is likely that synaptic potentiation at either input is sufficient for fear learning (Tsvetkov et al. 2004; Romanski & LeDoux 1992). *In vivo* studies have suggested that associative interaction of these two inputs in the LA could facilitate the formation of fear memories (Doyere et al. 2003). *In vitro* studies have shown that paired stimulation of

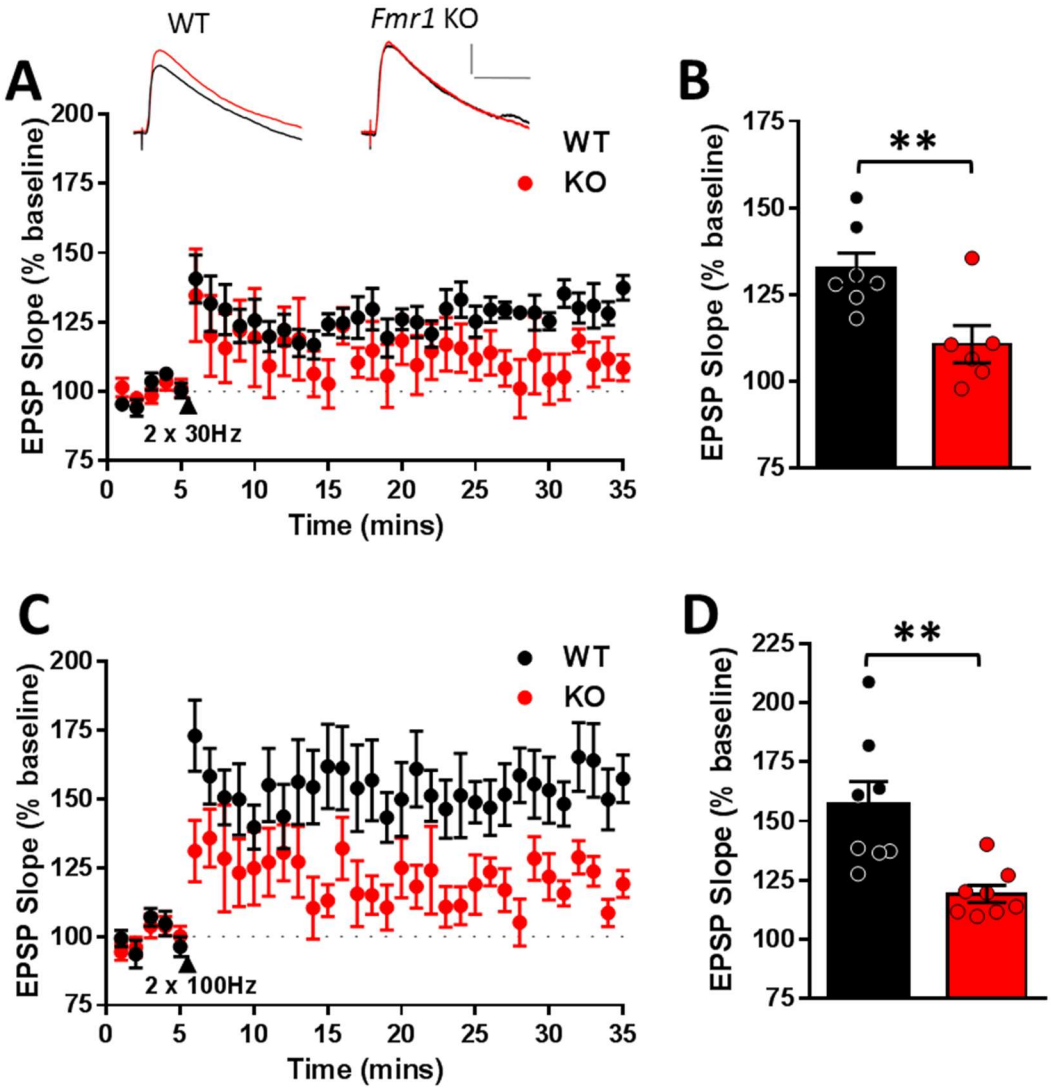

Figure 4.1 mGluR-dependent LTP at thalamic inputs to the LA is impaired in *Fmr1* KO rats (A) Timecourse showing LTP induced with 2 trains of 100 pulses @ 30Hz in WT and *Fmr1* KO rats. Example traces of EPSP in WT and *Fmr1* KO recordings showing baseline (black) and 30 mins post-stimulation (red). (B) LTP (30Hz) was significantly reduced in *Fmr1* KO slices compared to controls (WT: 132.41 ± 4.57%; n=7 slices/7 animals; KO: 110.77 ± 5.36%; n=6 slices/6 animals; p=0.01, Student unpaired *t*-test). (C) Timecourse showing LTP induced with 2 trains of 100 pulses @ 100Hz in WT and *Fmr1* KO rats. (D) LTP (100Hz) was significantly reduced in *Fmr1* KO slices compared to controls (WT: 156.94 ± 9.80%; n=8 slices/8 animals; KO: 119.17 ± 3.63%; n=8 slices/8 animals; p=0.003, Student unpaired *t*-test)

thalamic and cortical inputs to the LA, using temporal delays that have been observed *in vivo* (Quirk et al. 1997), result in LTP at cortico-amygdala synapses (Cho et al.

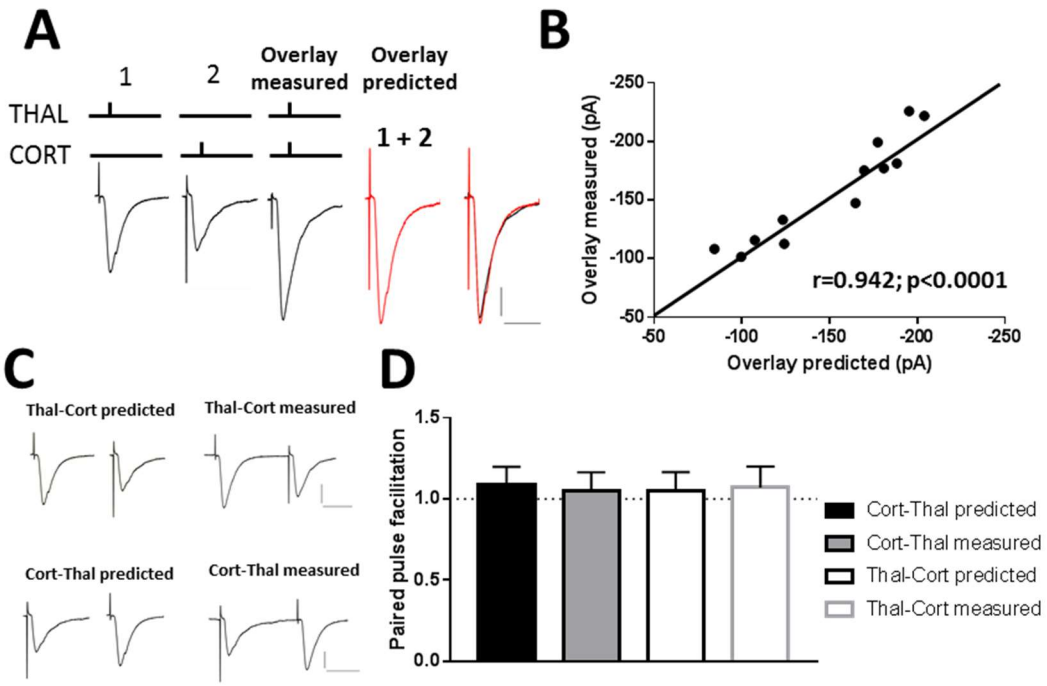

Figure 4.2 Cortical and thalamic inputs to LA principal neurons can be independently activated (A) Example traces showing EPSCs evoked by stimulation of thalamic (1) or cortical (2) inputs and simultaneous stimulation (Overlay measured) compared with predicted EPSC based on arithmetic sum (Overlay predicted, 1+2). Scale 50pA, 20ms (B) Amplitudes of measured EPSC and predicted EPSC showed linear relationship (r=0.942, Pearson's correlation coefficient). (C) Example traces showing paired pulses (50ms interval) of cortical and thalamic stimulation compared with predicted traces based on absence of cross facilitation. (D) No significant cross facilitation was shown in cortical and thalamic inputs (Cort-Thal predicted: 1.09 ± 0.11; n=13 cells/6 animals; Cort-Thal measured: 1.05 ± 0.11; n=13 cells/6 animals; p>0.05, Student paired *t*-test; Thal-Cort predicted: 1.05 ± 0.12; n=13 cells/6 animals; Thal-Cort measured: 1.07 ± 0.13; n=13 cells/6 animals; p>0.05, Student paired *t*-test).

2011). This form of LTP was also found to be dependent on group 1 mGluR signalling (Cho et al. 2011). As I have shown deficits in other mGluR-dependent synaptic plasticity mechanisms in *Fmr1* KO rats, here I investigated if this form of plasticity was also affected by the loss of FMRP.

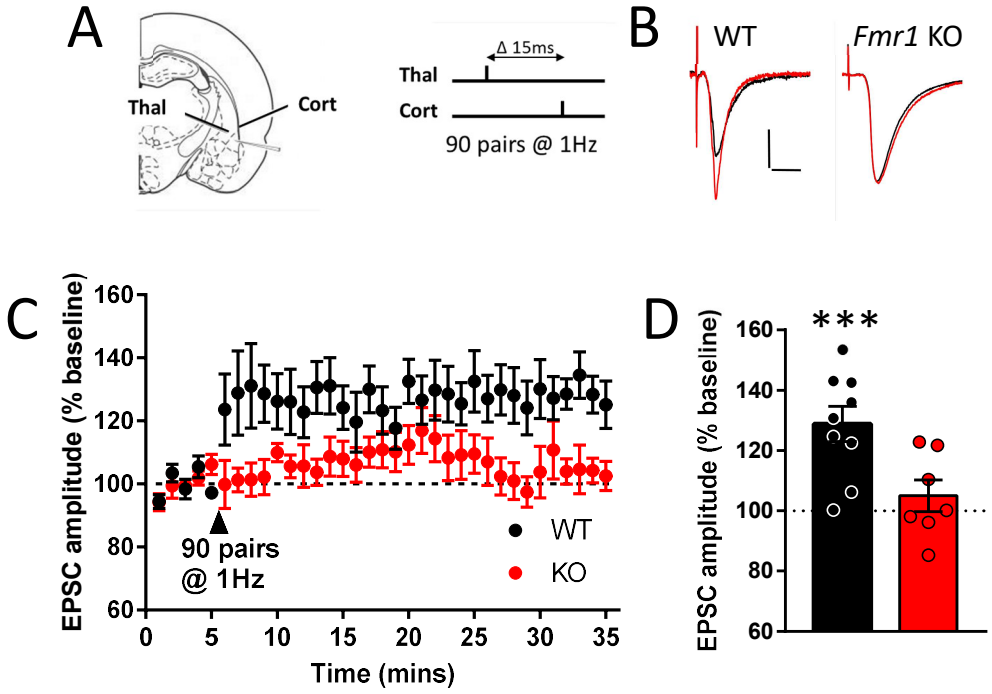

Figure 4.3 mGluR-dependent LTP at cortical inputs to the LA is reduced in *Fmr1* KO rats (A) Schematic of experimental design. Stimulating electrodes placed in external and internal capsule to stimulate cortical and thalamic inputs respectively. LTP was induced with 90 pairs of thalamic and cortical stimuli with 15ms interval at 1Hz. (B) Example EPSC traces from WT and *Fmr1* KO recordings showing baseline (black) and 30mins post-stimulation (red). Scale 50pA, 10ms. (C) Timecourse showing LTP induced at cortical inputs in WT and *Fmr1* KO rats. (D) This protocol induced significant LTP in WT rats (WT: 128.83 ± 5.84%; n=9 slices/9 animals; p=0.001, Student paired *t*-test) but was no LTP in *Fmr1* KO rats (104.97 ± 5.27%; n=7 slices/7 animals; p>0.05, Student paired *t*-test).

Initially, I tested if I could independently activate thalamic and cortical inputs. I activated cortical and thalamic inputs to principal neurons of the LA to elicit EPSCs using stimulating electrodes placed in the external capsule and internal capsule respectively (Fig 4.2). Comparison of the arithmetic sum of EPSCs elicited by separate activation of cortical or thalamic inputs was found to strongly correlate with responses when both inputs were simultaneously stimulated (Fig 4.2 B; r=0.942). Furthermore, no paired pulse facilitation was observed between inputs with a 50ms inter-pulse interval (Fig 4.2 D). These findings confirm that using this strategy is able to independently activate cortical and thalamic inputs to the LA.

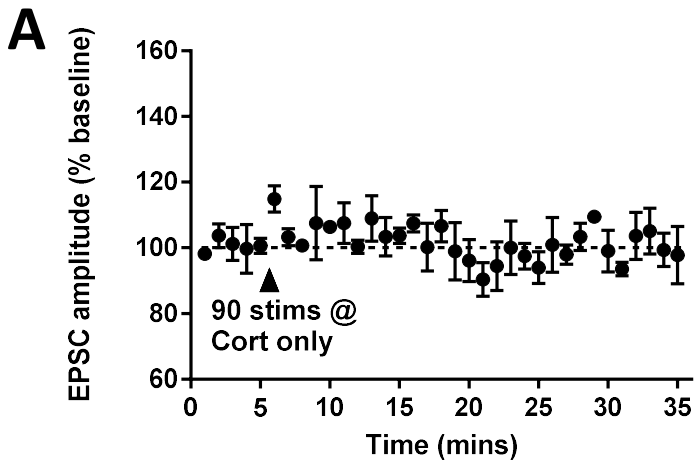

Figure 4.4 LTP at cortical input in WT animals requires paired thalamic stimulation (A) Timecourse of LTP induction with 90 stimulations, 1Hz at cortical inputs only. No significant LTP was induced in WT rats with only cortical stimulation (WT cortical: 99.28 ± 5.71%; n=3 slices/3 animals; p>0.05, Student paired *t*-test).

Next, I induced LTP using paired stimulation of thalamic and cortical inputs for 90 seconds at 1Hz frequency. Thalamic inputs were stimulated 15ms prior to cortical inputs to mimic the suggested timing of inputs to the lateral amygdala recorded *in vivo* (Quirk et al. 1997). Using this protocol, significant potentiation of EPSC amplitude was seen in WT cortico-amygdala pathway (Fig 4.3 D; WT: 128.83 ± 5.84%; n=9; p=0.001). The induction of LTP in WT cortical inputs required paired thalamic stimulation as stimulation of cortical inputs alone for 90 seconds at 1Hz showed no potentiation (Fig 4.4; WT cortical: 99.28 ± 5.71%; n=3; p>0.05). However when this protocol was performed in *Fmr1* KO slices, no LTP was found in cortico-amygdala pathway (Fig 4.3 D; KO: 104.97 ± 5.27%; n=7; p>0.05). This data shows that as well as a loss of mGluR-dependent LTP at thalamic synapses to the LA, cortico-amygdala mGluR-dependent LTP is also absent in *Fmr1* KO rats.

	WT (n=21 cells/7 animals)			*Fmr1* KO (n=16 cells/6 animals)			p-value
	Mean	SD	SEM	Mean	SD	SEM	
RMP (mV)	-70.60	2.80	0.63	-72.16	3.01	0.80	0.13
Rin (MΩ)	200.30	52.22	11.40	193.79	28.71	7.18	0.66
Cm (pF)	178.38	47.69	10.66	179.00	32.24	8.06	0.93
Tm (ms)	33.93	5.50	1.23	34.74	8.09	2.02	0.69
Sag (%)	4.36	2.38	0.53	4.32	2.06	0.52	0.85

Table 4.1 Summary of subthreshold properties of WT and *Fmr1* KO LA principal neurons. Statistics were performed using Student unpaired *t*-test.

4.2.3 Intrinsic properties were unchanged in principal neurons off the lateral amygdala in *Fmr1* KO rats

Next, I examined if the observed deficits in LTP could be the result of abnormal intrinsic physiology of the postsynaptic LA neuron. No changes were observed in any passive membrane intrinsic properties (Table 4.1). Furthermore, active properties measured using a family of current steps did not differ between genotypes (Fig 4.6; $F(1,35)=0.007$; $p=0.93$). The amount of current required to elicit an action potential was also comparable between genotypes (Fig 4.6 B; WT: 115.00 ± 8.96pA; n=21; KO: 103.13 ± 5.53pA; n=16; $p>0.05$). These results suggest that changes in postsynaptic excitability are not responsible for the observed deficits in LTP induction in the LA.

4.2.4 mEPSC frequency is increased, but amplitude unchanged, in the absence of FMRP

As well as mGluR-dependent deficits in synaptic plasticity in the lateral amygdala of *Fmr1* KO animals, there have also been suggestions of changes in presynaptic release probability at excitatory synapses on to LA principal neurons (Suvrathan et al. 2010). Therefore, I compared the frequency and amplitude of mEPSCs in lateral amygdala neurons between our genotypes. Whole cell recordings were performed of LA principal neurons at -70mV in the presence of 300nM tetrodoxin and 75µM picrotoxin to block $GABA_A$ mediated transmission. Here I found a significant decrease in the frequency of mEPSCs in *Fmr1* KO animals (Fig 4.6 C; WT: 2.68 ±

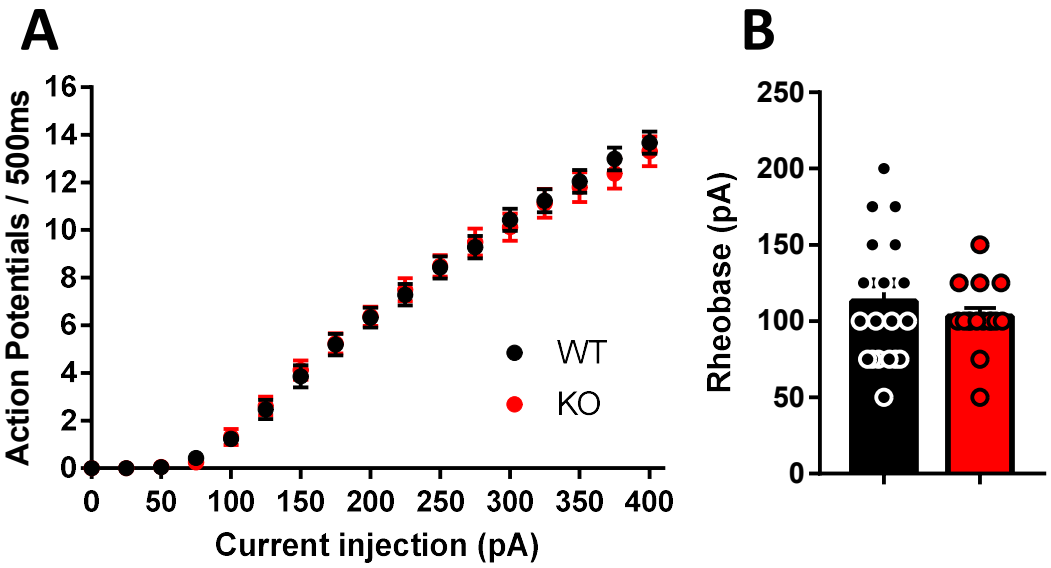

Figure 4.5 Neuronal excitability in *Fmr1* KO LA principal neurons is unaffected
(A) Current-firing responses showed no differences in the number of action potentials fired in response to various current injections in *Fmr1* KO neurons (F(1,35)=0.007; p=0.93, Two way RM-ANOVA). (B) Rheobase current was comparable between genotypes (WT: 115.00 ± 8.96pA; n=21 cells/7 animals; KO: 103.13 ± 5.53pA; n=16 cells/6 animals; p>0.05, Student unpaired *t*-test).

0.25Hz; n=5; KO: 1.65 ± 0.16Hz; p=0.009) however mEPSC amplitude was unchanged (Fig 4.6 A; WT: -20.68 ± 0.47pA; n=5; KO: -21.36 ± 0.67pA; n=5; p>0.05). No changes were observed in mEPSC kinetics (Fig 4.6 E; WT rise time: 1.08 ± 0.05ms; n=5; KO rise time: 1.02 ± 0.08ms; n=5; p>0.05; Fig 4.6 F; WT decay time: 4.76 ± 0.24ms; n=5; KO decay time: 4.70 ± 0.11ms; n=5; p>0.05). These results suggest that presynaptic release probability onto lateral amygdala principal neurons is decreased in *Fmr1* KO rats whilst postsynaptic conduction is unchanged.

To further test the possibility that presynaptic release is reduced in *Fmr1* KO rats, I measured paired pulse ratios (PPR) at both thalamic and cortical inputs to the LA. At thalamic synapses, I found PPRs of evoked EPSCs to be significantly larger in KO rats compared to WT rats across multiple inter-pulse intervals, indicating a reduction in release probability in the absence of FMRP (Fig 4.7 A; F(1,9)=15.27; p=0.004). Similarly, PPRs were found to be increased in KO rats at cortical synapses compared

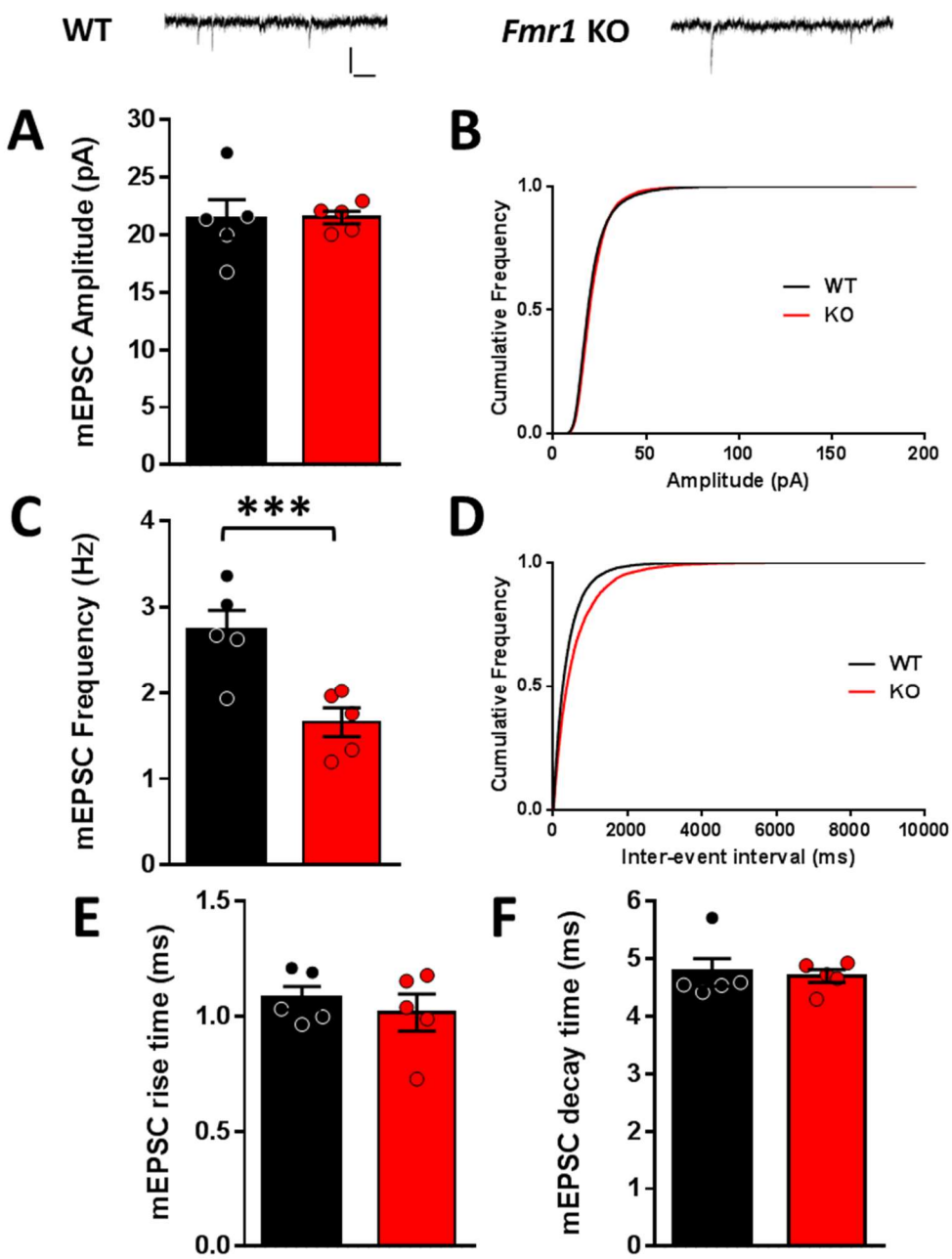

Figure 4.6 mEPSC frequency is reduced in *Fmr1* LE LA principal neurons (A) mEPSC amplitude was unaffected between genotypes (WT: 20.68 ± 0.47pA; n=5 animals/21 cells; KO: 21.36 ± 0.67pA; n=5 animals/18 cells; p>0.05). (B) Cumulative frequency of mEPSC amplitudes in WT and *Fmr1* KO neurons. (C) mEPSC frequency was significantly reduced in *Fmr1* KO neurons (WT: 2.68 ± 0.25Hz; n=5 animals/21 cells; KO: 1.65 ± 0.16Hz; n=5 animals/18 cells; p=0.009). (D) Cumulative frequency of mEPSC inter-event intervals in WT and *Fmr1* KO neurons. (E) No differences were observed in mEPSC rise time (WT: 1.08 ± 0.05ms; n=5 animals/21 cells; KO: 1.02 ± 0.08ms; n=5 animals/18 cells; p>0.05) or (F) decay time (WT: 4.76 ± 0.24ms; n=5 animals/21 cells; KO: 4.70 ± 0.11ms; n=5 animals/18 cells; p>0.05). Statistics were performed using Student unpaired t-test. Example traces scale 20pA, 100ms.

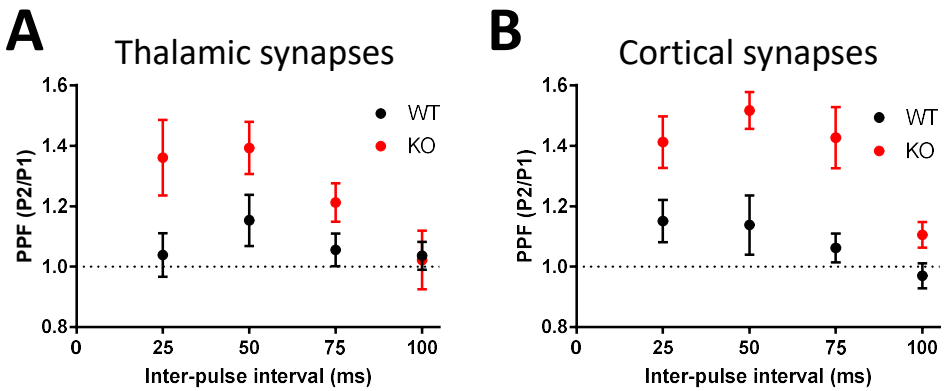

Figure 4.7 Release probability in reduced at both thalamic and cortical inputs on to LA principal neurons (A) Paired pulse facilitation at thalamic inputs to *Fmr1* KO LA principal neurons was increased at a range of inter-pulse intervals (F(1,9)=15.27; p=0.004, Two way RM-ANOVA). (B) Paired pulse facilitation at cortical inputs to *Fmr1* KO LA principal neurons was increased at a range of inter-pulse intervals (F(1,7)=22.04; p=0.002, Two way RM-ANOVA).

to WT controls (Fig 4.7 B; F(1,7)=22.04; p=0.002). The observed reduction in mEPSC frequency and changes in PPR at both inputs to the LA provide strong evidence that presynaptic release is reduced in *Fmr1* KO rats.

4.2.5 Inhibitory synapses on to principal neurons of the LA are unaffected in Fmr1 KO rats

FMRP expression has been shown in GABAergic interneurons throughout the brain (Feng et al. 1997; Olmos-Serrano et al. 2010) suggesting an involvement in interneuron function. Given the observed alterations in the lateral amygdala excitatory circuitry of *Fmr1* KO rats, I next investigated if inhibitory transmission is similarly affected in lateral amygdala principal neurons. Here, recordings of LA principal neurons were performed at -70mV using modified Cl^- internal (see methods) in the presence of 300nM TTX and 10µM CNQX to block AMPAR mediated transmission. I observed no significant alterations in mIPSC amplitude (Fig 4.8 A; WT: -41.32 ± 8.23pA; n=5; KO: -43.63 ± 2.26pA; n=5; p>0.05), frequency (Fig 4.8 C; WT: 8.13 ± 0.72Hz; n=5; KO: 7.37 ± 0.94Hz; n=5; p>0.05), rise time (Fig 4.8 E; WT: 1.88 ± 0.25ms; n=5; KO: 1.90 ± 0.16ms; n=5; p>0.05) and decay time (Fig 4.8 F; WT: 11.41

± 0.44ms; KO: 12.16 ± 0.54ms; n=5; p>0.05). This analysis revealed no changes in mIPSC frequency or kinetics suggesting that inhibitory neurotransmission is unaffected in the LA of *Fmr1* KO rats.

4.2.6 Basal amygdala excitatory and inhibitory circuitry are unaffected in *Fmr1* KO rats

As well as the LA, the basal amygdala (BA) has been shown to play a role in fear and anxiety behaviours, serving as a storage for fear memories (Ehrlich et al. 2009; Anglada-Figueroa 2005; Gale et al. 2004). FXS has been increasingly linked with excitatory/inhibitory imbalances associated with dysfunction of inhibitory transmission in several brain regions (Gibson et al. 2008; Selby et al. 2007). Previous studies in *Fmr1* KO mice have revealed significant deficits in inhibitory synapse formation and function resulting in hyperexcitability of BA principal neurons (Olmos-Serrano et al. 2010; Vislay et al. 2013). Here, I investigated both mEPSC and mIPSCs on to BA principal neurons as indicators of excitatory and inhibitory neurotransmission. Contrary to findings in the LA, I observed no significant differences in mEPSC frequency in *Fmr1* KO BA principal neurons (Fig 4.9 C; WT: 7.60 ± 0.84Hz; n=6; KO: 7.64 ± 1.04Hz; n=5; p>0.05). Similarly, mEPSC amplitude (Fig 4.9 A; WT: -18.61 ± 1.55pA; n=6; KO: -19.69 ± 1.33pA; n=5; p>0.05), rise time (Fig 4.9 E; WT: 1.14 ± 0.03ms; n=6; KO: 1.25 ± 0.07ms; n=5; p>0.05) and decay time (Fig 4.9F; WT: 3.57 ± 0.06ms; n=6; KO: 3.54 ± 0.02ms; n=5; p>0.05) were comparable between genotypes. In contrast to reports in *Fmr1* KO mice (Olmos-Serrano et al. 2010; Martin et al. 2014), no significant differences were observed in mIPSC amplitude (Fig 4.10 A; WT: -30.89 ± 2.79pA; n=4; KO: -32.35 ± 2.44pA; n=4; p>0.05) or frequency (Fig 4.10 C; WT: 8.85 ± 0.86Hz; n=4; KO: 7.33 ± 1.23pA; n=4; p>0.05). mIPSC kinetics were also unaltered in *Fmr1* KO neurons (Fig 4.10 E; WT rise time: 2.23 ± 0.07ms; n=4; KO rise time: 2.19 ± 0.17ms; n=4; p>0.05; Fig 4.10 F; WT decay time: 12.45 ± 0.56ms; n=4; KO decay time: 12.21 ± 0.51ms; n=4; p>0.05). This data indicates that GABAergic synaptic transmission is intact in the BA of *Fmr1* KO rats at the age tested.

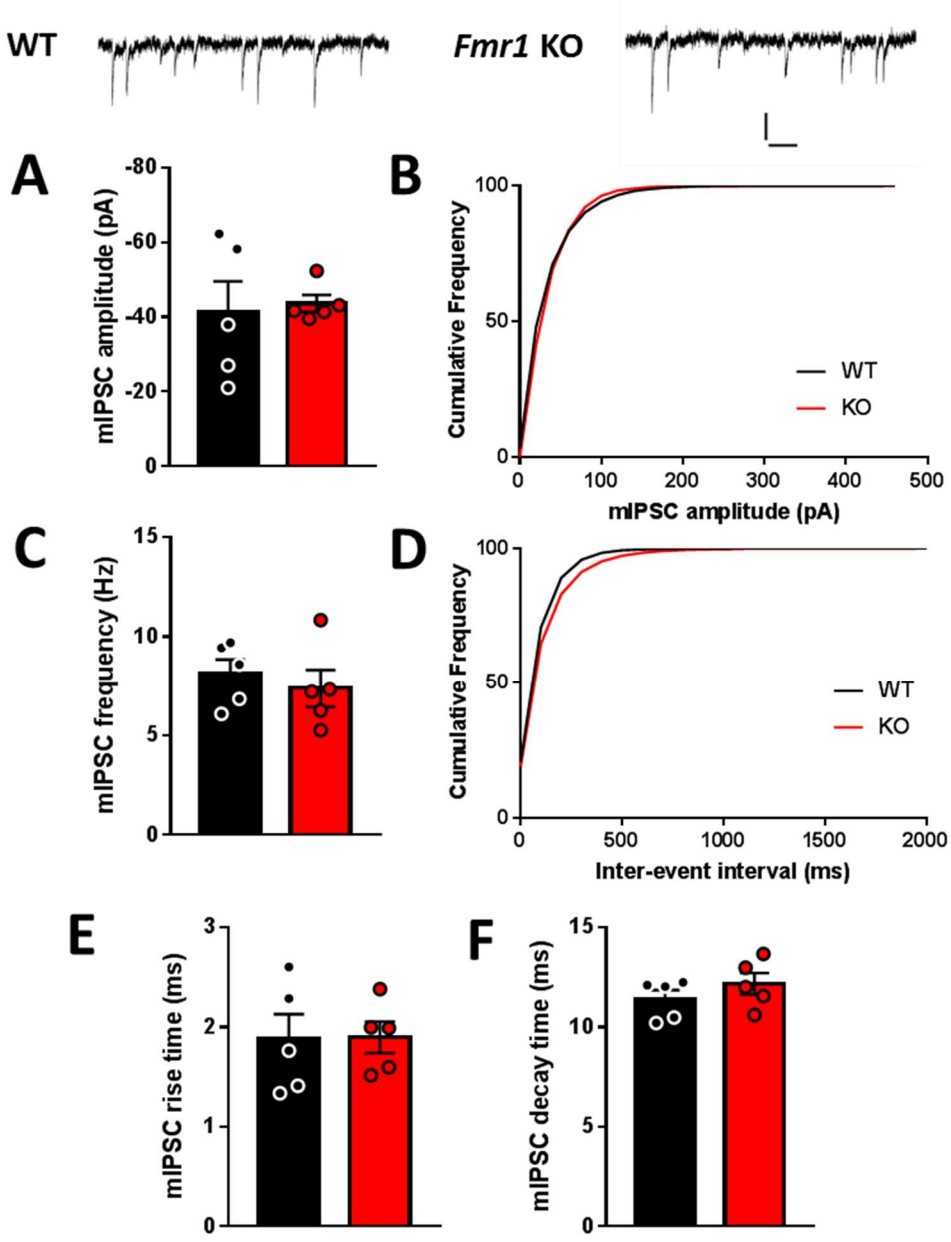

Figure 4.8 mIPSCs are unaffected in *Fmr1* LE LA principal neurons (A) mIPSC amplitude was unaffected between genotypes (WT: -41.32 ± 8.23pA; n=5 animals/5 cells; KO: -43.63 ± 2.26pA; n=5 animals/5 cells; p>0.05). (B) Cumulative frequency of mIPSC amplitudes in WT and *Fmr1* KO neurons. (C) mIPSC frequency was unaffected in *Fmr1* KO neurons (WT: 8.13 ± 0.72Hz; n=5 animals/5 cells; KO: 7.37 ± 0.94Hz; n=5 animals/5 cells; p>0.05). (D) Cumulative frequency of mIPSC inter-event intervals in WT and *Fmr1* KO neurons. (E) No differences were observed in mIPSC rise time (WT: 1.88 ± 0.25ms; n=5 animals/5 cells; KO: 1.90 ± 0.16ms; n=5 animals/5 cells; p>0.05) or (F) decay time (WT: 11.41 ± 0.44ms; n=5 animals/5 cells; KO: 12.16 ± 0.54ms; n=5 animals/5 cells; p>0.05). Statistics were performed using Student unpaired t-test. Example traces scale 20pA, 100ms.

4.2.7 *Fmr1* KO BA principal neurons are hyperexcitable compared to WT controls

Excitatory/inhibitory balances can also manifest as a result of changes in the intrinsic properties of neurons as well as synaptic abnormalities. Here, I tested the intrinsic properties of BA principal neurons in *Fmr1* KO rats. I found that input resistance was significantly greater in *Fmr1* KO BA neurons compared to WT controls but all other measured parameters were comparable (Table 4.2). In line with this, *Fmr1* KO neurons fired more action potentials in response to a family of current steps compared to WT controls (Fig 4.11 A; p=0.02). This was associated with a decrease in rheobase in the absence of FMRP (Fig 4.11 B; WT: 248.61 ± 7.69pA; n=18; KO: 222.22 ± 9.67pA; n=18; p=0.04). This data suggests that despite excitatory and inhibitory circuits being intact in *Fmr1* KO BA nuclei, principal neurons are intrinsically hyperexcitable in the absence of FMRP.

4.3 Discussion

4.3.1 mGluR-dependent phenotypes in the lateral amygdala

As well as intellectual disability, FXS is also associated with a range of emotional features including anxiety, gaze avoidance and elevated stress (Hessl et al. 2004). These behaviours are consistent with amygdala dysfunction, a key component of brain circuitry responsible for fear learning. Studies using *Fmr1* KO mice have highlighted abnormalities in the acquisition of amygdala-dependent behaviours such as fear learning (Paradee et al. 1999). A large body of evidence has shown the LA to be the neural centre for fear conditioning (Shin & Liberzon 2010).

During auditory fear conditioning, the integration of a conditioned (CS) and unconditioned stimulus (US) within the LA results in the acquisition of fear

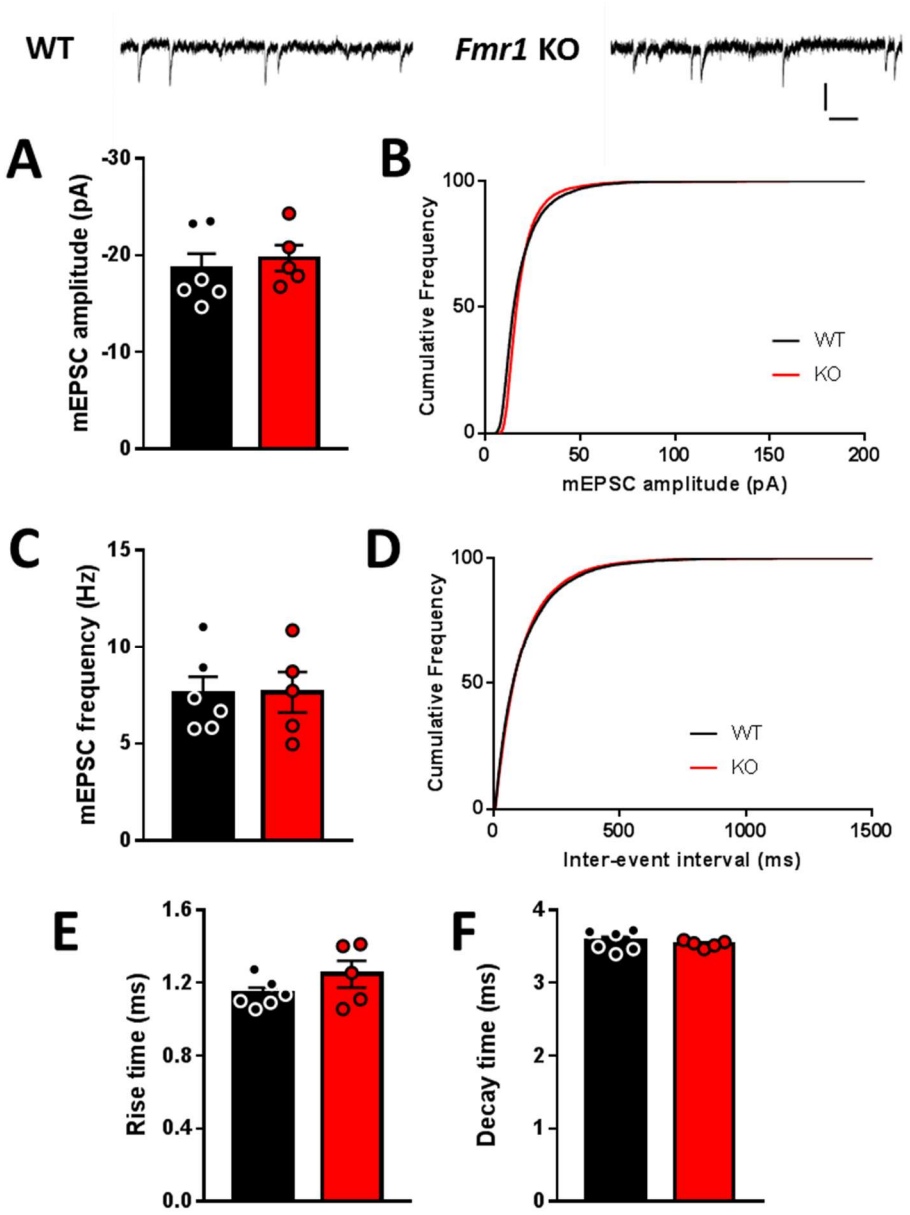

Figure 4.9 mEPSCs are unaffected in *Fmr1* LE BA principal neurons (A) mEPSC amplitude was unaffected between genotypes (WT: -18.61 ± 1.55pA; n=6 animals/6 cells; KO: -19.69 ± 1.33pA; n=5 animals/5 cells; p>0.05). (B) Cumulative frequency of mEPSC amplitudes in WT and *Fmr1* KO neurons. (C) mEPSC frequency was unaffected in *Fmr1* KO neurons (WT: 7.60 ± 0.84Hz; n=6 animals/6 cells; KO: 7.64 ± 1.04Hz; n=5 animals/5 cells; p>0.05). (D) Cumulative frequency of mEPSC inter-event intervals in WT and *Fmr1* KO neurons. (E) No differences were observed in mEPSC rise time (WT: 1.14 ± 0.03ms; n=6 animals/6 cells; KO: 1.25 ± 0.07ms; n=5 animals/5 cells; p>0.05) or (F) decay time (WT: 3.57 ± 0.06ms; n=6 animals/6 cells; KO: 3.54 ± 0.02ms; n=5 animals/5 cells; p>0.05). Statistics were performed using Student unpaired t-test. Example traces scale 20pA, 100ms.

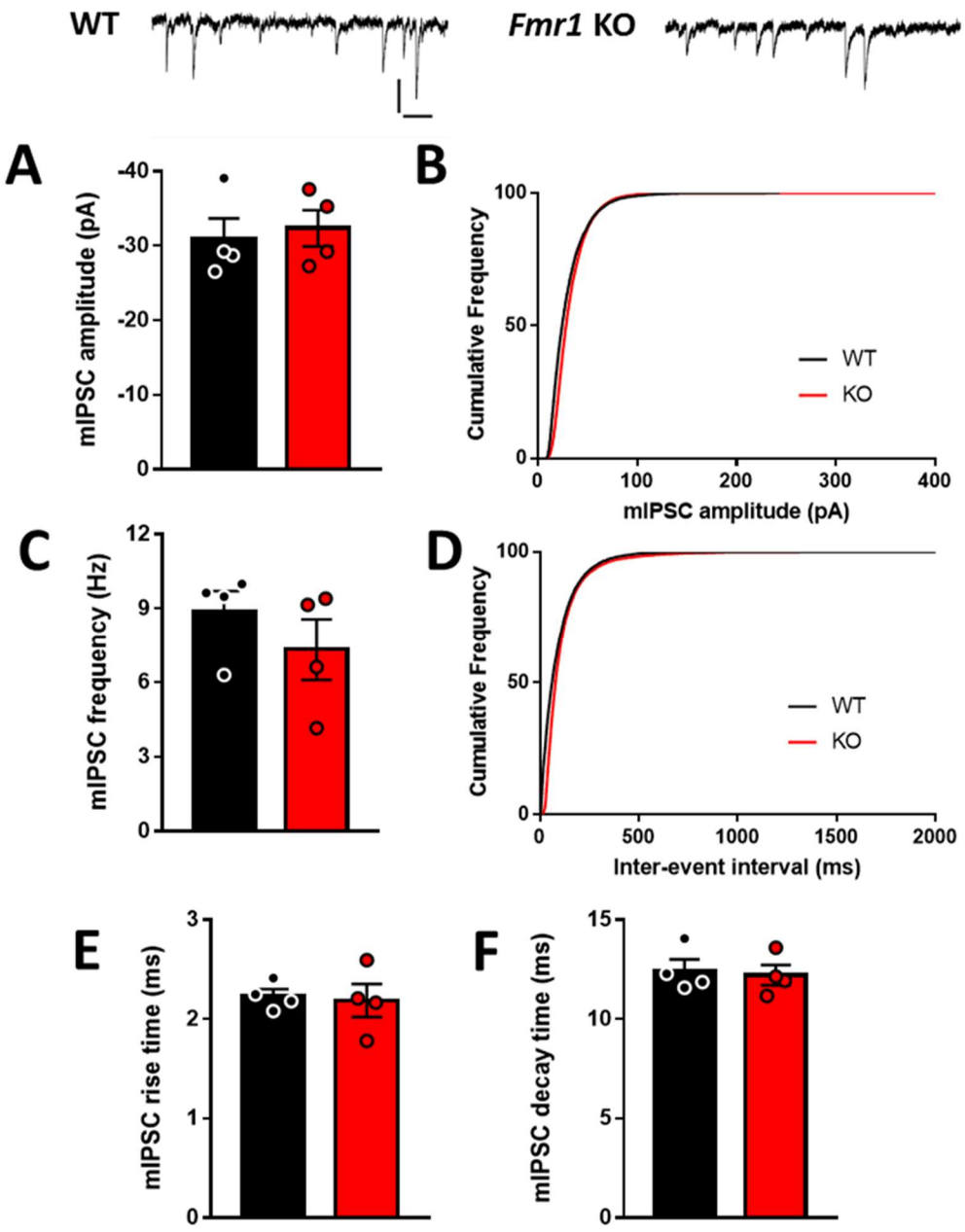

Figure 4.10 mIPSCs are unaffected in *Fmr1* LE BA principal neurons (A) mIPSC amplitude was unaffected between genotypes (WT: -30.89 ± 2.79pA; n=4 animals/4 cells; KO: -32.35 ± 2.44pA; n=4 animals/4 cells; p>0.05). (B) Cumulative frequency of mIPSC amplitudes in WT and *Fmr1* KO neurons. (C) mIPSC frequency was unaffected in *Fmr1* KO neurons (WT: 8.85 ± 0.86Hz; n=4 animals/4 cells; KO: 7.33 ± 1.23pA; n=4 animals/4 cells; p>0.05). (D) Cumulative frequency of mIPSC inter-event intervals in WT and *Fmr1* KO neurons. (E) No differences were observed in mIPSC rise time (WT: 2.23 ± 0.07ms; n=4 animals/4 cells; KO: 2.19 ± 0.17ms; n=4 animals/4 cells; p>0.05) or (F) decay time (WT: 12.45 ± 0.56ms; n=4 animals/4 cells; KO: 12.21 ± 0.51ms; n=4 animals/4 cells; p>0.05). Statistics were performed using Student unpaired t-test. Example traces scale 20pA, 100ms.

	WT (n=18 cells/6 animals)			*Fmr1* KO (n=18 cells/6 animals)			p-value
	Mean	SD	SEM	Mean	SD	SEM	
RMP (mV)	-70.04	3.40	0.82	-70.35	2.09	0.52	0.76
Rin (MΩ)	75.66	10.08	2.37	86.89	19.59	4.62	* 0.04
Cm (pF)	280.19	70.17	16.54	285.26	67.45	15.90	0.83
Tm (ms)	22.05	6.46	1.52	24.72	6.63	1.56	0.23
Sag (%)	13.96	4.07	0.96	12.56	5.29	1.25	0.38

Table 4.2 Summary of subthreshold properties of WT and *Fmr1* KO BA principal neurons. Statistics were performed using Student unpaired *t*-test.

memories (LeDoux 2003). This process has been shown to be impaired in transgenic mice lacking $mGluR_5$ as well as by local application of the $mGluR_5$ antagonist MPEP *in vivo* (Schulz et al. 2001; Rodrigues et al. 2002). *In vitro* work has also shown that LTP at thalamic inputs to the LA, believed to represent a cellular correlate of fear learning, is dependent on $mGluR_5$ signalling (Rodrigues et al. 2002). Based on the observation that group 1 mGluR signalling is altered in the absence of FMRP, previous studies in *Fmr1* KO mice have identified deficits in mGluR-LTP at these synapses consistent with the observed deficits in fear learning (Zhao et al. 2005; Suvrathan et al. 2010; Paradee et al. 1999). Here I observed a similar deficit in mGluR-dependent plasticity at thalamic inputs to the LA of *Fmr1* KO rats. No differences were observed in the intrinsic excitability of principal neurons in the LA suggesting this did not contribute to the deficit in LTP. This is in agreement with the finding that fear acquisition is affected in these animals (Dr Sally Till, personal communication) and provides further evidence of the translation of group 1 mGluR-dependent phenotypes from mouse to rat FXS models.

In this chapter, I also investigated LTP at cortical inputs to the LA, a pathway that has not previously been investigated in *Fmr1* KO mice. Using low-frequency paired activation of thalamic and cortical inputs to the LA, LTP was induced at cortico-amygdala synapses that has been shown to be dependent on group 1 mGluR signalling (Cho et al. 2011). This induction protocol is designed to mimic the temporal pattern of synaptic activation that occurs in the LA *in vivo* during fear conditioning paradigms, leading to LTP of the cortical input which carries CS driven signals. Consistent with the notion that this form of plasticity is crucial for fear

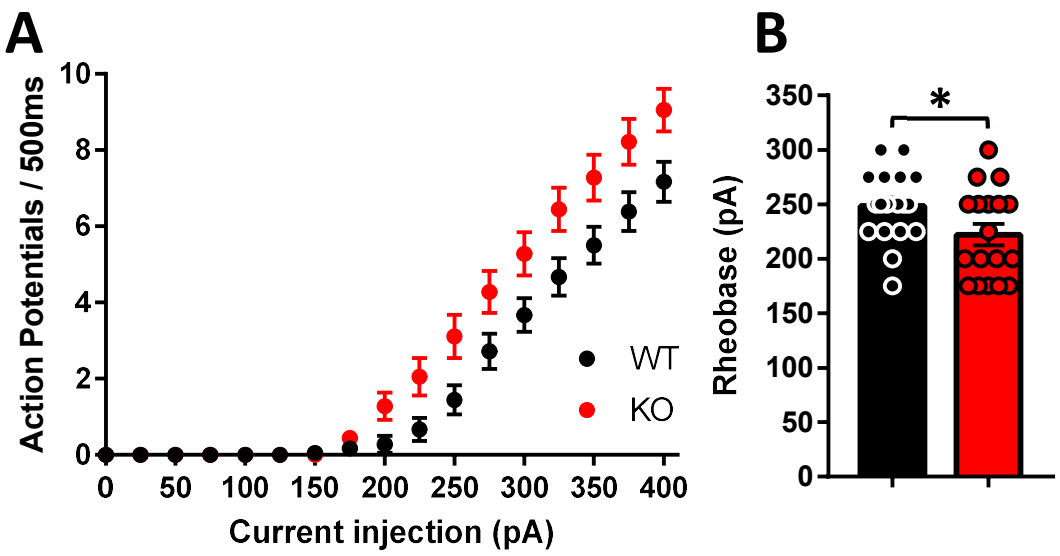

Figure 4.11 *Fmr1* KO BA principal neurons are hyperexcitable (A) *Fmr1* KO neurons fire significantly more action potentials in response to various current injections ($F(1,34)=5.922$; $p=0.02$, Two way RM-ANOVA). (B) Rheobase current was significantly reduced in *Fmr1* KO neurons (WT: 248.61 ± 7.69pA; n=18 cells/6 animals; KO: 222.22 ± 9.67pA; n=18 cells/6 animals; $p=0.04$, Student unpaired *t*-test).

learning, it has also been shown to be occluded in slices from fear conditioned rats (Cho et al. 2011). Here, I found this form of mGluR-LTP was also absent in the LA of *Fmr1* KO rats. Together with results from the thalamic pathway, this suggests that alterations in group 1 mGluR signalling in the absence of FMRP are preventing the expression of LTP in pathways that are crucial for fear memory formation.

Although one may hypothesise that alterations in mGluR-dependent LTP would exist in *Fmr1* KO animals in light of the 'mGluR theory of FXS', the contrasting roles of mGluRs in synaptic plasticity in the hippocampus and amygdala highlight the complications of translating this theory across brain regions. Work from the hippocampus showing that $mGluR_5$ signalling is enhanced in *Fmr1* KO animals would suggest that mGluR-LTP in the LA of *Fmr1* KO rats may be exaggerated, as was observed with hippocampal mGluR-LTD. Yet both here and in studies of *Fmr1* KO mice (Suvrathan et al., 2010; Zhao et al., 2005) we find it to be absent. This is in agreement with observations of impaired fear memory in FXS animal models. A

potential explanation for this effect could be through $mGluR_5$s interaction with NMDARs. $mGluR_5$ in the LA has been shown to be predominantly expressed on the postsynaptic terminal where they interact with other glutamate receptors, in particular NMDARs (Naisbitt et al., 1999). In agreement with this, mGluR agonists have been shown to potentiate NMDAR currents (Fitzjohn et al., 1996; Pisani et al., 2001) through a mechanism that is inhibited by $mGluR_5$ deletion or pharmacological inhibition (Mannaioni et al., 2001; Pisani et al., 2001). Thus $mGluR_5$ is in a critical position to modulate synaptic plasticity through modulation of NMDARs. $mGluR_5$ and NMDARs interact physically through scaffolding proteins. One known interaction is via Homer proteins which have been shown to bind with Shank, a protein that exists as part of the NMDAR associated PSD-95 complex (Naisbitt et al., 1999; Hayashi et al., 2009). As $mGluR_5$-Homer interactions are thought to be disrupted in *Fmr1* KO mice (Giuffrida et al., 2005; Ronesi & Huber, 2008), the ability of mGluRs to modulate NMDAR signalling may be lost in the absence of FMRP. As LTP at thalamic inputs is also dependent on NMDAR signalling (Rodrigues et al., 2002), one could hypothesise that it is this mechanism that underlies the absence of mGluR-dependent LTP at thalamic inputs in the LA of *Fmr1* KO rats. Future experiments investigating the ability of mGluR activation to modulate NMDAR currents in *Fmr1* KO neurons would complement this. Also, this hypothesis could be further tested through addition of a peptide that mimics the C-terminal tail of $mGluR_5$ to the intracellular solution used during whole cell recordings of WT neurons. This strategy has previously been used to disrupt $mGluR_5$-Homer interactions (Ronesi & Huber, 2008) which would reveal if this interaction was necessary for LTP induction in this pathway.

Whilst the described hypothesis may be applicable to the observed LTP deficit at thalamic inputs to the LA, it is unlikely that this could explain the plasticity deficit at cortical inputs as this form of plasticity is not dependent on NMDAR signalling (Cho et al., 2013). This deficit is most likely due to an insufficient rise in intracellular Ca^{2+} concentration to reach a threshold for LTP induction in *Fmr1* KO neurons. Previous studies in *Fmr1* KO mPFC pyramidal neurons has revealed deficits in spike time dependent plasticity related to reduced Ca^{2+} signalling (Meredith et al., 2007).

However these studies suggested a role of L-type voltage gated Ca^{2+} channels (VGCC) which do not contribute to the form of plasticity studied here (Cho et al., 2012). As insufficient postsynaptic depolarisation takes place during the induction of mGluR-dependent cortical LTP to activate NMDAR or VGCC, intracellular Ca^{2+} increases may arise from mGluR driven release of internal stores via IP_3 signalling. Consistent with this, Xestospongin-C, a compound which inhibits release from IP_3-sensitive Ca^{2+} stores, blocks plasticity of this pathway (Cho et al., 2012).

It is unknown how IP_3 signalling is affected in animal models of FXS however evidence from human fibroblast studies has shown that Ca^{2+} release is depressed through IP_3-receptors (IP_3R) in the absence of FMRP (Schmunk et al., 2015). IP_3Rs are enriched in the spine apparatus (SA), a specialised region of the endoplasmic reticulum which extends into dendritic spines where it acts as a local intracellular Ca^{2+} store (Fifkova et al., 1983). Long isoforms of Homer, containing a C-terminal domain coiled-coil structure, cross-link group 1 mGluRs in the postsynaptic membrane to IP_3Rs in the SA which results in rapid, spatially localised Ca^{2+} in response to mGluR activation (Tu et al., 1998). Homer 1a, which does not contain the coiled-coil domain, is unable to crosslink these two receptors. Consistent with this, upregulation of Homer 1a in cerebellar purkinje neurons reduces and delays mGluR-triggered release of intracellular Ca^{2+} (Tu et al., 1998). Given that $mGluR_5$ is more associated with Homer 1a in the absence of FMRP and shows reduced association with long Homer isoform (Ronesi et al., 2012), this could result in reduced Ca^{2+} release from intracellular stores following mGluR activation in *Fmr1* KO neurons. Alternatively, changes in calcium buffering or extrusion could also contribute to changes in postsynaptic calcium concentration however these effects have not previously been reported in any neurons lacking FMRP. Comparison of Ca^{2+} signals using two photon imaging of dendritic spines during plasticity induction may reveal if deficits in Ca^{2+} signalling play a role in the absence of cortical LTP in *Fmr1* KO rats.

4.3.2 Nucleus specific changes in excitability of amygdala

Inhibitory circuits of the amygdala are the major determinant of activity within the LA and BA nuclei (Olmos-Serrano & Corbin, 2011). Interneurons comprise approximately 20% of neurons within these nuclei and play roles in gating plasticity as well as modulating principal neuron output (Kemppainen & Pitkänen, 2000; Quirk & Gehlert, 2003). FXS has been increasingly linked with E/I imbalances associated with dysfunction of inhibitory transmission in several brain regions (Gibson et al., 2008; Selby et al., 2007). FMRP is expressed in the majority of interneurons in the BA (Olmos-Serrano et al., 2010) and its absence results in multiple deficits in GABAergic signalling. Work in *Fmr1* KO mice, has identified deficits in synaptic transmission at inhibitory synapses on to BA principal neurons including reduced mIPSC frequency and amplitude (Olmos-Serrano et al., 2010; Vislay et al., 2013). This effect was developmentally regulated with deficits appearing at P10, showing no effect at P14-16, but then reappearing in the third postnatal week. However here I found that mIPSCs were unaffected in both LA and BA nuclei of 4-6 week old *Fmr1* KO rats suggesting that GABAergic synaptic transmission is unaffected. As studies in *Fmr1* KO mice identified deficits at earlier ages, it is possible that these effects have normalised by this time point. Therefore, future experiments investigating the development of inhibitory neurotransmission in both the LA and BA may reveal significant effects in *Fmr1* KO rats.

As well as deficits in phasic inhibition, there have been several reports of reduced tonic GABA activity in *Fmr1* KO BA principal neurons (Olmos-Serrano et al., 2010; Martin et al., 2015). Tonic GABA activation results in shunting inhibition on excitatory neurons thereby constraining neuronal excitability (Semyanov et al., 2004). Therefore reduced tonic GABA activation results in hyperexcitability of principal neurons in the BA of *Fmr1* KO mice (Olmos-Serrano et al., 2010). Here, I observed a similar hyperexcitability of BA principal neurons in *Fmr1* KO rats suggesting a reduction in tonic GABA conductances may be also be present. Deficient inhibitory tone in the amygdala could lead to overexpression of fear responses producing pathological stated

of anxiety as shown by FXS individuals (Quirk & Gehlert, 2003). However this is only one potential explanation for this effect therefore future experiments investigating the state of tonic GABA signalling in *Fmr1* KO rats BA are necessary.

4.3.3 Summary

In summary, the loss of FMRP results in deficient LTP at both of the major inputs to the LA associated with the formation of fear memories. Excitatory inputs to the LA also show a reduced release probability in *Fmr1* KO rats. In the BA, no deficits were observed in excitatory or inhibitory neurotransmission in *Fmr1* KO rats. However, BA principal neurons were hyperexcitable in the absence of FMRP which has previously been associated with reduced tonic inhibition. Interestingly, these effects are constrained to the BA as no changes in neuronal excitability were observed in the LA of *Fmr1* KO rats. This data provides further evidence of the distinct effects FMRP loss can have on circuit function even in closely associated brain regions highlighting the complications in designing a therapeutic strategy to target the wide range of phenotypes associated with FXS.

Chapter 5

Age-dependent LTP deficits and neuronal hypoexcitability in the prelimbic mPFC of *Fmr1* KO rats

5.1 Introduction

The prefrontal cortex (PFC) is a cortical region that plays a key role in higher order cognitive functions such as attention, working memory and cognitive flexibility (Miller 2000). Many of these functions associated with the PFC are affected in neurodevelopmental disorders such as FXS. Studies using *Fmr1* KO mice have revealed changes in several PFC mediated behaviours (Moon et al. 2006; Krueger et al. 2011; Sidorov et al. 2014; Kramvis et al. 2013; Dansie et al. 2013) as well as significant biochemical and physiological phenotypes in this cortical region (Liu et al. 2011; Paul et al. 2013; Testa-Silva et al. 2012). Changes in translaminar long term plasticity (LTP) have been observed in several of PFC subregions in *Fmr1* KO mice as well as changes in local connectivity (Larson et al. 2005; Meredith et al. 2007; Wang et al. 2008; Koga et al. 2015; Martin et al. 2015; Testa-Silva et al. 2012).

As well as local connectivity, the PFC also provides long-range excitatory outputs to other brain structures in a subregion dependent manner (Hoover & Vertes 2007). The main cortical output layer, layer 5 (L5), contains pyramidal neurons that can be distinguished based on their long-range target. These neurons show distinct intrinsic physiology as well as different intralaminar connections suggesting they can form distinct subnetworks depending on their long-range target (Wang et al. 2006; Brown & Hestrin 2009; Dembrow et al. 2010).

The PFC is composed of many functionally and anatomically distinct subregions. One PFC subregion of particular interest in the study of FXS is the prelimbic medial PFC (PL). The PL primarily innervates limbic sites allowing it to modulate various aspects of cognitive behaviour (Vertes 2004). A key projection target is the basolateral amygdala (BLA) which shows robust reciprocal connectivity with the PL (Mcdonald 1998; Little & Carter 2013). This pathway has been implicated in both the acquisition and expression of fear learning (Corcoran & Quirk 2007; Laviolette 2005; Vidal-Gonzalez et al. 2006), behaviours which have been found to be affected in *Fmr1* KO rats.

Interestingly for the study of FXS, activation of group 1 mGluR subtypes has been found to modulate the excitability of L5 mPFC pyramidal neurons and enhance mPFC output (Kalmbach et al. 2013; Kiritoshi et al. 2013; Fontanez-Nuin et al. 2011; Marek, G.J; Zhang 2009). Some of these effects have also been shown to be dependent on the long-range projection target of the pyramidal neuron (Kalmbach et al. 2013). Therefore, I hypothesised that the constitutive activation of $mGluR_5$ suggested by work in *Fmr1* KO mice (Giuffrida et al. 2005; Ronesi et al. 2012; Osterweil et al. 2010) could lead to significant changes in L5 pyramidal neuron excitability and connectivity. As the timing and fidelity of PL activity has been shown to play a role in both the acquisition and expression of fear learning (Vidal-Gonzalez et al. 2006; Burgos-Robles et al. 2009), changes in the intrinsic properties of PL subnetworks that project to the BLA could contribute to the deficits in fear learning shown in *Fmr1* KO animals.

Here I investigated both local and long-range connectivity of PL L5 pyramidal neurons in *Fmr1* KO rats. First, I tested LTP at layer 2/3 (L2/3) to L5 synapses in both the PL of juvenile and adult *Fmr1* rats. Next, I used retrograde labelling to identify specific L5 pyramidal neurons with long-range projections to the BLA. I then used whole cell electrophysiological recordings to assess the intrinsic physiology as well as excitatory and inhibitory circuit properties of this subset of neurons in *Fmr1* KO rats.

5.2 Results

5.2.1 Age-dependent LTP deficit in prelimbic mPFC of *Fmr1* KO rats

Several studies have identified LTP deficits in various subregions of the mPFC in *Fmr1* KO mice (Meredith et al. 2007; Zhao et al. 2005; Martin et al. 2015). Some of these phenotypes also show age-dependency, with LTP intact in juvenile animals but deficits appearing during adulthood (Larson et al. 2005; Martin et al. 2015). Here I studied layer 2/3 to layer 5 synapses of the prelimbic (PL) of the mPFC. Firstly, we wanted to test if LTP was intact in 4-6 week old *Fmr1* KO rats. No significant difference was observed in the magnitude of LTP at this age (Fig 5.1 D; WT: 118.06 ± 5.76%; n=6; KO: 116.37 ± 3.95%; n=6; $p>0.05$). However when I tested the same paradigm in 10-12 week old rats I observed a clear LTP deficit in *Fmr1* KO rats compared to WT controls (Fig 5.1 F; WT: 119.43 ± 5.28%; n=7; KO: 98.43 ± 3.99%; n=7; $p=0.008$). These data show that whilst LTP is supported across these ages in WT animals, the ability to express LTP is impaired with age in *Fmr1* KO rats.

5.2.2 Age-dependent LTP deficit is also observed in *Fmr1* Sprague Dawley rat model

Next I tested if the age-dependent LTP deficit I observe in our Long Evans *Fmr1* KO rats is present in the Sprague Dawley (SD) *Fmr1* KO rat model. As found previously, no significant difference was observed in the magnitude of LTP between genotypes at 4-6 weeks (Fig 5.2 B; WT: 118.04 ± 4.07%; n=5; KO: 119.78 ± 6.31%; n=5; $p>0.05$) but LTP was absent in 10-12 week old SD *Fmr1* KO rats (Fig 5.2 D; WT: 129.66 ± 5.99%; n=7; KO: 100.57 ± 6.46%; n=6; $p=0.007$). These findings are in agreement with data from the *Fmr1* KO LEH rats indicating that in the absence of FMRP, LTP in the prelimbic mPFC is lost in an age-dependent manner.

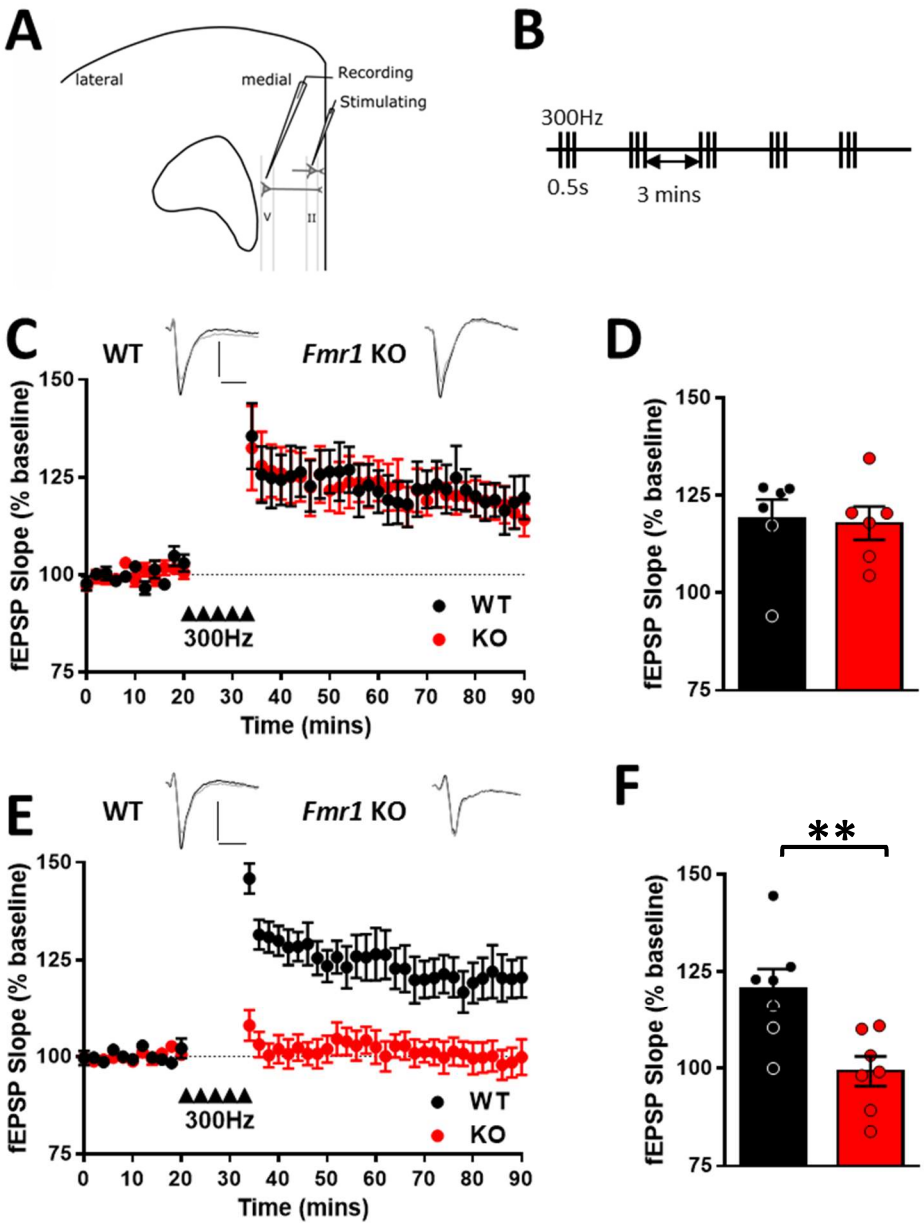

Figure 5.1 Age-dependent deficit of LTP in *Fmr1* KO rat prelimbic mPFC (A) A stimulating electrode was placed in layer 2/3 of prelimbic mPFC and fEPSP recorded in layer 5. (B) LTP induction protocol consisted of 5 trains of 500ms at 300Hz frequency with an inter-train interval of 3mins. (C) Timecourse showing LTP induction in 4-6 week old WT and *Fmr1* KO rats. (D) No significant difference was observed in magnitude of LTP between genotypes (WT: 118.06 ± 5.76%; n=6 slices/6 animals; KO: 116.37 ± 3.95%; n=6 slices/6 animals; p>0.05, Student unpaired *t*-test). (E) Timecourse showing LTP induction in 10-12 week old WT and *Fmr1* KO rats. (F) LTP was significantly reduced in *Fmr1* KO rats compared to WT controls at 10-12 weeks (WT: 119.43 ± 5.28%; n=7 slices/7 animals; KO: 98.43 ± 3.99%; n=7 slices/7 animals; p=0.008, Student unpaired *t*-test). Example traces Grey=baseline, Black= 80-90mins; scale 0.5mV, 5ms

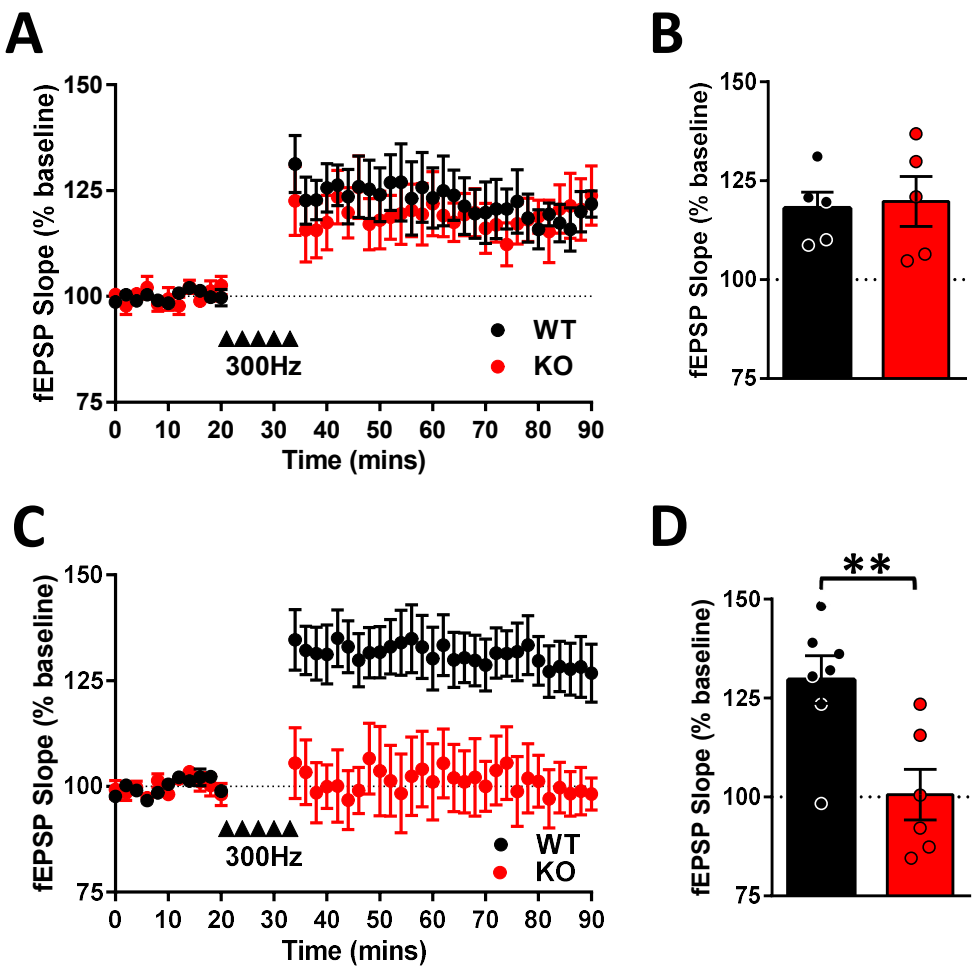

Figure 5.2 Age-dependent deficit of LTP in SD *Fmr1* KO rat prelimbic mPFC (A) Timecourse showing LTP induction in 4-6 week old WT and *Fmr1* KO SD rats. (D) No significant difference was observed in magnitude of LTP between genotypes (WT: 118.04 ± 4.07%; n=5 slices/5 animals; KO: 119.78 ± 6.31%; n=5 slices/5 animals; p>0.05, Student unpaired *t*-test). (D) Timecourse showing LTP induction in 10-12 week old WT and *Fmr1* KO rats. (E) LTP was significantly reduced in *Fmr1* KO rats compared to WT controls at 10-12 weeks (WT: 129.66 ± 5.99%; n=7 slices/7 animals; KO: 100.57 ± 6.46%; n=6 slices/6 animals; p=0.007, Student unpaired *t*-test).

5.2.3 Basal synaptic strength is unaffected at L2 excitatory inputs onto L5 neurons in Fmr1 KO rats

A recent study in *Fmr1* KO mice similarly found age-dependent deficits in mPFC LTP which they linked to an increase in AMPA/NMDA ratio resulting from a decrease in NMDA currents (Martin et al. 2015). Therefore, I tested AMPA/NMDA ratio at L2/3

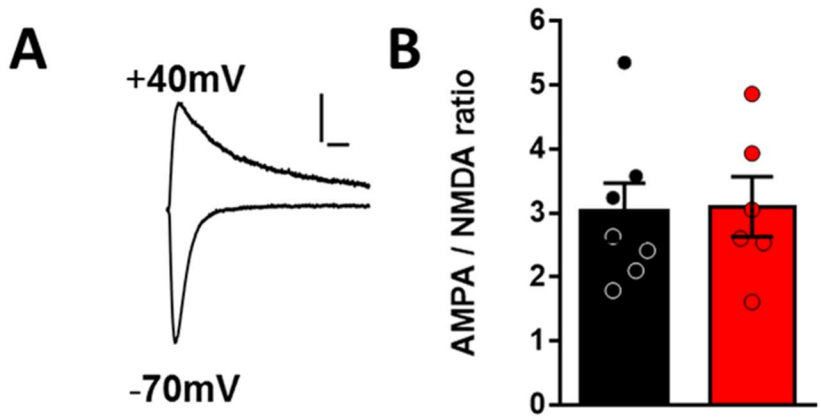

Figure 5.3. No changes in AMPA/NMDA ratio at L2/3 to L5 synapses on to *Fmr1* KO PL-BLA projection neurons (A) Example traces showing NMDAR currents measured at +40mV and AMPAR currents at -70mV. (B) No significant difference in AMPA/NMDA ratios was observed in *Fmr1* KO neurons (WT: 3.02 ± 0.45; n=7 cells/ 4 animals; KO: 3.10 ± 0.47; n=6 cells/3 animals; p>0.05, Student unpaired *t*-test).

synapses on to L5 pyramidal neurons. AMPAR and NMDAR mediated responses were evoked at -70mV and +40mV respectively. I found no significant difference in AMPA/NMDA ratio at these synapses in *Fmr1* KO rats (Fig 5.3 B; WT: 3.02 ± 0.45; n=7; KO: 3.10 ± 0.47; n=6; p>0.05). Power analysis of this data revealed that 2770 cells/genotype would need to be analysed in order to observe a significant effect. This data suggests that basal synaptic function is unaffected at L2 inputs to L5 pyramidal neurons in adult *Fmr1* KO rats. In contrast to studies of *Fmr1* KO mice, it also suggests that a change in AMPA/NMDA ratio does not contribute to the loss of LTP in *Fmr1* KO PL mPFC.

5.3 Intrinsic cell physiology and synaptic connectivity in mPFC neurons that project to the basolateral amygdala of *Fmr1* rats

5.3.1 Investigation of prelimbic layer V circuits that project to the basolateral amygdala in *Fmr1* KO rats

As well as its local translaminar connectivity, the mPFC is in a position to provide top-down control to several other cortical and subcortical regions by influencing their

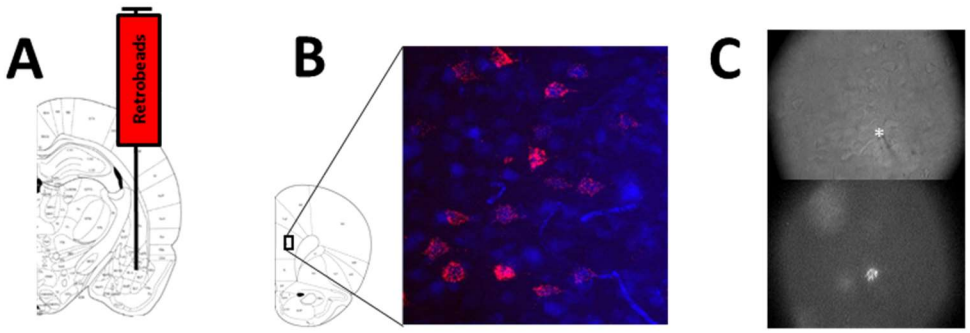

Figure 5.4 Strategy for visualisation of PL-BLA projection neurons (A) Red retrobeads (1µL) were stereotaxically injected in the BLA of *Fmr1* rats (B) Acute slices were taken containing prelimbic mPFC for electrophysiological recordings. Confocal image showing red retrobead signal in PL-BLA projection neurons in L5 prelimbic mPFC and NeuN immunofluorescence. (C) Top: DIC image showing whole cell electrophysiological recording from a PL-BLA projection neuron. * denotes recorded cell. Bottom: Same cell visualised using fluorescence microscopy showing presence of red retrobeads.

activity through long range projections. It does this through a variety of pyramidal neurons with different long-range targets that form the main output layer of the mPFC. Importantly, the intrinsic physiology and local connectivity of pyramidal neurons in layer 5 mPFC is greatly influenced by their long range connectivity. Therefore, when assessing neuronal excitability or synaptic connectivity in these circuits, it is important to distinguish neurons based on their projection targets.

One key projection target is the basolateral amygdala (BLA), which shows strong reciprocal connectivity with the PL mPFC (Little & Carter 2012; Little & Carter 2013). This pathway has been implicated in both the acquisition and expression of fear learning, behaviours which have been found to be affected in *Fmr1* KO rats. Therefore, I adopted a strategy that would allow us to restrict our electrophysiological analysis to the specific subset of neurons that provide input to the BLA. Here I stereotaxically injected retrobead tracers into the BLA of 3-4 month old *Fmr1* rats (Fig 5.3 A). Following animal recovery for a minimum of 1 week, acute slices containing prelimbic mPFC were taken and cell somas containing retrobeads identified using confocal

microscopy. Labelled projection neurons were distributed throughout both L2-3 and L5 in both the prelimbic and infralimbic mPFC as found in previous studies (Gabbott et al. 2005) however for this study recordings were limited to prelimbic L5 neurons. This confirmed the presence of a subset of L5 pyramidal neurons that project to the BLA (PL-BLA projection neurons).

5.3.2 Layer 5 contains two classes of PL-BLA projections neurons

Whole cell electrophysiological recordings were performed from retrobead containing L5 PL neurons visualised using fluorescence microscopy (Fig 5.3). Neuronal excitability was investigated using a series of ascending depolarising current steps. At rheobase, the current injection required to generate a single action potential, neurons could be classified as either regular spiking neurons (RS) or burst spiking neurons (BS) (Van Aerde & Feldmeyer 2015). RS neurons were defined as neurons able to generate a single action potential in response to a suprathreshold current. BS neurons were defined as neurons that fired a burst of two or more action potentials in an all or none manner in response to suprathreshold current. These two subsets of neurons were observed in both WT and *Fmr1* KO animals at similar ratios. However due to the low number of BS neurons in both genotypes, experiments were restricted to RS neurons where possible i.e. could not be done in experiments where action potential firing was blocked due to external/internal solution composition.

5.3.3 Regular spiking PL-BLA projection neurons are hypoexcitable in *Fmr1* KO rats

The intrinsic properties of L5 pyramidal neurons can be modulated by $mGluR_5$ activation (Kiritoshi et al. 2013). As $mGluR_5$ is suggested to be constitutively active in animal models of FXS, I tested the intrinsic excitability of L5 PL-BLA in *Fmr1* KO rats. I found that *Fmr1* KO neurons were hypoexcitable compared to WT controls. PL-BLA projection neurons fired significantly fewer action potentials in response to a series of depolarising current steps from 25-400pA (Fig 5.4 B; $F(1,56)=23.3$;

p=0.0001). Rheobase was also significantly larger in *Fmr1* KO animals (Fig 5.4 C; WT: 100.00 ± 5.00pA; n=26; KO: 124.22 ± 5.78pA; n=32; p=0.003). This data indicates that PL-BLA projection neurons have reduced intrinsic excitability in the absence of FMRP.

5.3.4 Hypoexcitability in PL-BLA projection neurons is not due to alterations in subthreshold intrinsic properties

Some studies that have found changes in neuronal intrinsic excitability in *Fmr1* KO animals have linked this phenotype to a change in membrane input resistance (Gibson et al. 2008; Olmos-Serrano et al. 2010). To explore the underlying mechanism of the reduction in intrinsic neuronal excitability, intrinsic membrane properties of PL-BLA projection neurons were compared between genotypes. Surprisingly, input resistance was comparable between the two genotypes (Fig 5.5 A; WT: 134.94 ± 7.47MΩ; n=26; KO: 123.66 ± 5.12MΩ; n=32; p>0.05). Power analysis of this data revealed that 148 cells/genotype would be required to see a significant decrease in *Fmr1* KO PL-BLA projection neuron input resistance. Additionally no significant differences were observed in any intrinsic membrane properties (Fig 5.5 B; WT time constant: 28.01 ± 1.17ms; n=26; KO time constant: 30.70 ± 1.57ms; n=32; p>0.05; Fig 5.5 C; WT capacitance: 222.63 ± 13.87pF; n=26; KO capacitance: 255.62 ± 12.40pF; n=32; p>0.05; Fig 5.5 D; WT Sag: 8.74 ± 0.77%; n=26; KO Sag: 10.97 ± 0.83%; n=32; p>0.05) however *Fmr1* KO neurons were slightly but significantly depolarised at rest (Fig 5.5 E; WT RMP: -71.70 ± 0.49mV; n=26; KO RMP: -69.68 ± 0.59mV; n=32; p=0.01).

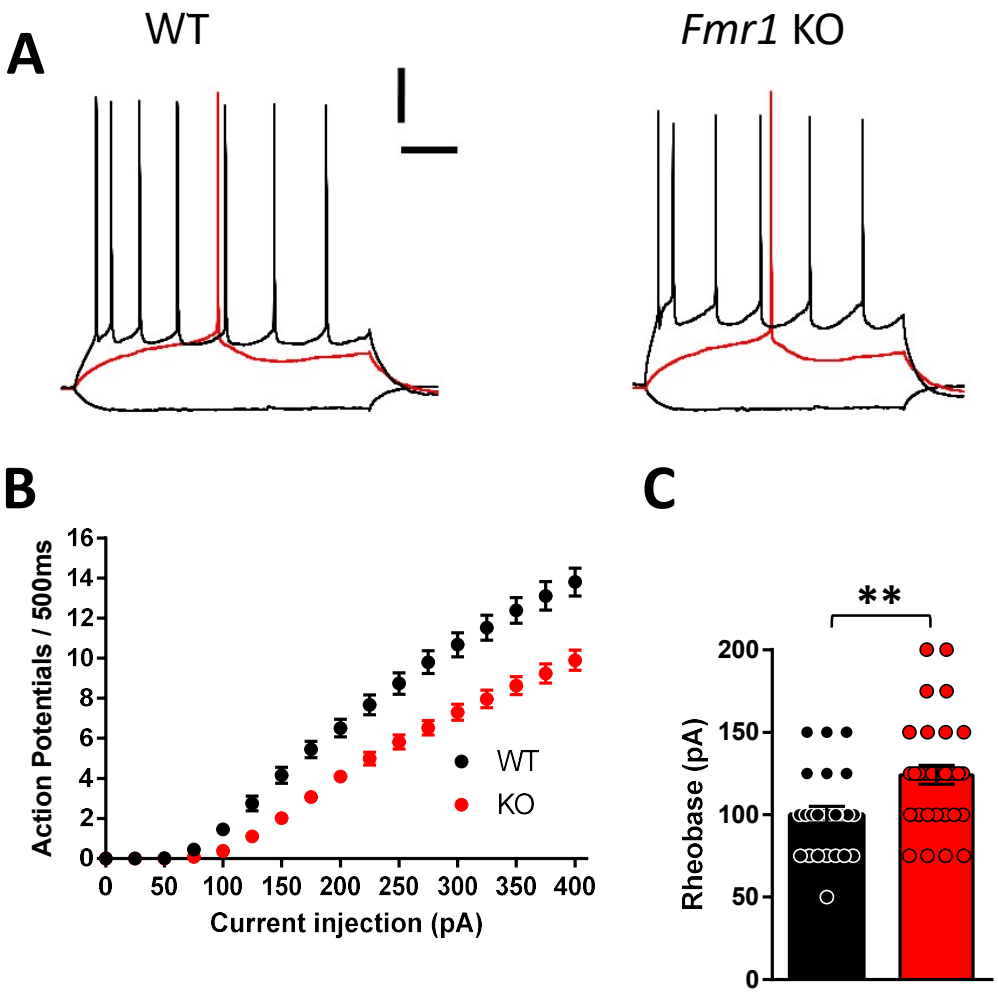

Figure 5.5 PL-BLA projection neurons are hypoexcitable in *Fmr1* KO rats
(A) Example traces of WT and *Fmr1* KO neurons voltage responses to -100pA, rheobase (WT: 100pA, KO: 125pA) and 2x rheobase current steps. Scale 100ms, 20mV. (B) PL-BLA projection neurons fire significantly fewer action potentials in response to a series of depolarising current steps from 25-400pA ($F(1,56)=23.3$; $p=0.0001$, Two way RM-ANOVA). (C) Rheobase was significantly larger in *Fmr1* KO neurons compared to WT controls (WT: 100.00 ± 5.00pA; n=26 cells/11 animals; KO: 124.22 ± 5.78pA; n=32 cells/16 animals; $p=0.003$, Student unpaired *t*-test).

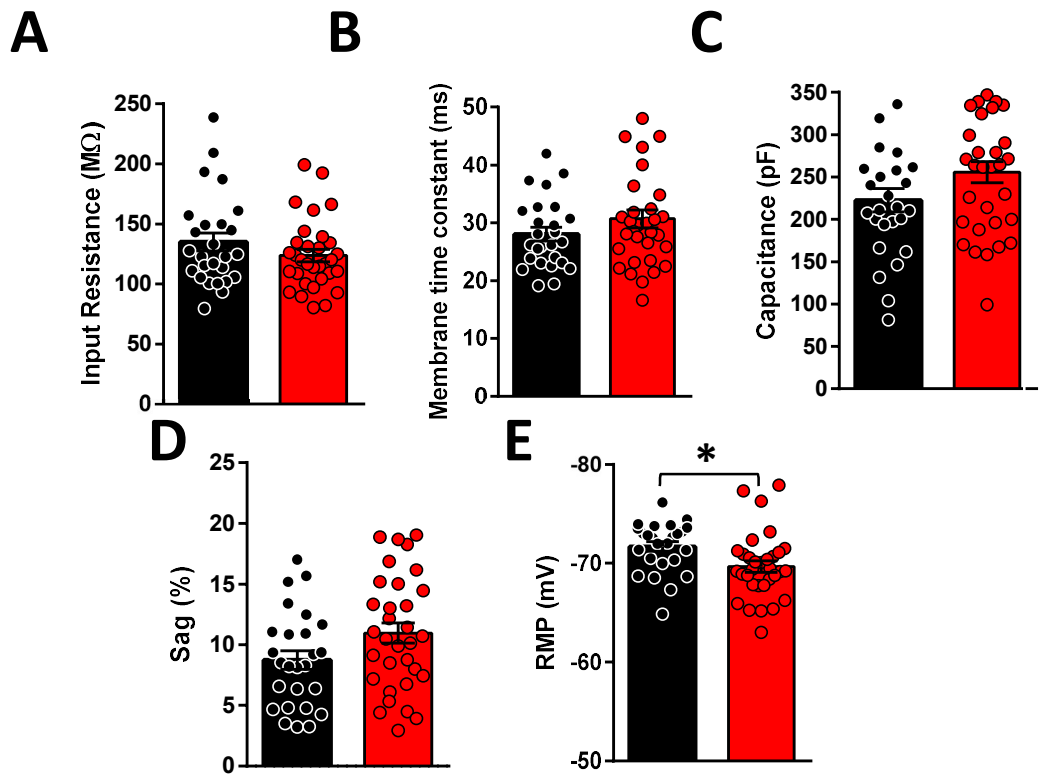

Figure 5.6 Hypoexcitability in PL-BLA projection neurons is not due to alterations in subthreshold intrinsic properties (A) Input resistance not significantly different between genotypes (WT: 134.94 ± 7.47MΩ; n=26 cells/11 animals; KO: 123.66 ± 5.12MΩ; n=32 cells/16 animals; p>0.05). (B) Membrane time constant is unaffected in *Fmr1* KO PL-BLA projection neurons (WT: 28.01 ± 1.17ms; n=26 cells/11 animals; KO: 30.70 ± 1.57ms; n=32 cells/16 animals; p>0.05). (C) Membrane capacitance was not significantly different between genotypes (WT: 222.63 ± 13.87pF; n=26 cells/11 animals; KO: 255.62 ± 12.40pF; n=32 cells/16 animals; p>0.05). (D) Sag, a measure of Ih current, was comparable between genotypes (WT: 8.74 ± 0.77%; n=26 cells/11 animals; KO: 10.97 ± 0.83%; n=32 cells/16 animals; p>0.05). (E) *Fmr1* KO PL-BLA projection neurons are significantly depolarised at rest compared to WT controls (WT: -71.70 ± 0.49mV; n=26 cells/11 animals; KO: -69.68 ± 0.59mV; n=32 cells/16 animals; p=0.01). Statistical tests performed with Student unpaired *t*-test.

5.3.5 Post action potential currents are not affected by loss of FMRP

Trains of action potentials are followed by an afterhyperpolarisation (AHP) which is an important regulator of cell excitability (McKay et al. 2009). Post-burst AHPs consist of two components which can be distinguished based on their timing. The medium AHP (mAHP) is activated immediately following an action potential train and

has a decay time of <200ms. mAHP amplitude is affected by both the number of action potentials in a train as well as their frequency (Abel et al. 2004). In order to control for this effect, I evoked mAHP using a train of 5 action potentials at fixed frequencies ranging from 20-100Hz. I found that the absence of FMRP had no significant effect on mAHP amplitude at this range of frequencies (Fig 5.6 A; ($F(1,26)=2.836$; $p=0.1042$). The slow AHP (sAHP) reaches its peak after the mAHP has decayed and has a timecourse of several seconds (Sah & Faber 2002). sAHP was evoked using 15 action potentials at 50Hz (McKay et al. 2009) and measured 1 second after the end of the train. Here I also saw no significant difference between WT and *Fmr1* KO neurons (Fig 5.6 B; WT: -1.31 ± 0.18mV; n=12; KO: 1.34 ± 0.14mV; n=16; $p>0.05$). The afterdepolarisation (ADP) that follows a single action potential was also compared between genotypes. No significant change in ADP amplitude was observed in *Fmr1* KO neurons (Fig 5.6 C; WT: 21.04 ± 0.99mV; n=12; KO: 20.84 ± 0.89mV; n=17; $p>0.05$). This suggests that post action potential currents do not play a role in the observed hypoexcitability of *Fmr1* KO PL-BLA neurons.

5.3.6 Loss of FMRP results in changes in action potential kinetics

As well as changes in intrinsic membrane properties, changes in active cation conductances that underlie the firing of an action potential can also influence neuronal excitability. Previous studies have revealed both a direct and indirect role of FMRP in regulating some of these ion channels (Brown et al. 2010; Deng et al. 2013). Therefore, I investigated action potential waveform and kinetics in our WT and *Fmr1* KO PL-BLA projection neurons to see if these factors could contribute to the observed change in intrinsic excitability. In line with the hypoexcitability of *Fmr1* KO neurons, action potential threshold was significantly depolarised in the absence of FMRP (Fig 5.7 C; WT: -40.31 ± 0.66mV; n=26; KO: -38.18 ± 0.48; n=32; $p=0.01$). Threshold voltage was significantly correlated with the maximum number of action potentials fired ($p=0.04$). Further analysis of action potential waveform revealed no significant differences in action potential height (Fig 5.7 D;

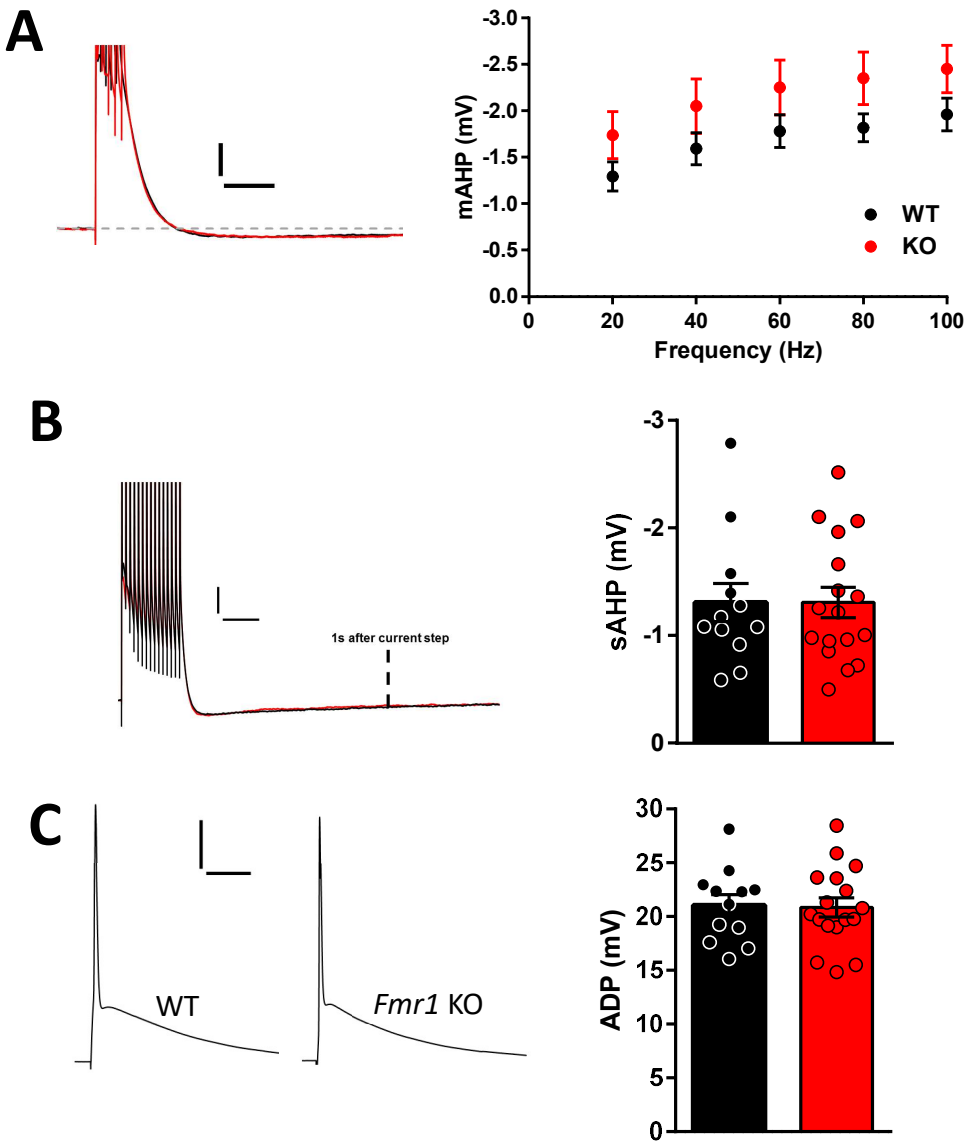

Figure 5.7 Post burst AHP are not affected by loss of FMRP (A) Example trace of mAHP, the maximum hyperpolarisation following a train of action potentials, evoked by a train of 5 action potentials at various frequencies (20-100Hz). Scale 50ms, 5mV. No significant difference in mAHP was found between genotypes ($F(1,26)=2.836$; $p=0.1042$, Two way RM-ANOVA). (B) Example trace of sAHP, measured as hyperpolarisation 1s after train of 15 action potentials at 50Hz. Scale 100ms, 5mV. No significant difference in sAHP magnitude was observed between genotypes (WT: -1.31 ± 0.18mV; n=12 cells/6 animals; KO: -1.34 ± 0.14mV; n=17 cells/10 animals; $p>0.05$, Student unpaired *t*-test). (C) Example traces of ADP following a single action potential Scale 10ms, 20mV. No significant difference in ADP magnitude was observed between genotypes (WT: 21.04 ± 0.99mV; n=12 cells/6 animals; KO: 20.84 ± 0.89mV; n=17 cells/10 animals; $p>0.05$, Student unpaired *t*-test).

WT: 83.57 ± 0.96mV; n=26; KO: 81.64 ± 0.96; n=32; p>0.05) or width (Fig 5.7 E; WT: 1.02 ± 0.02; n=26; KO: 1.07 ± 0.03; n=32; p>0.05). Phase plot analysis revealed significant differences in action potential kinetics between genotypes (Fig 5.7 F). *Fmr1* KO action potentials had a slower maximum depolarisation speed (Fig 5.7 G; WT: 317.06 ± 8.50mV/ms; n=26; KO: 289.47 ± 9.22mV/ms; n=32; p=0.035) as well as a slower maximum repolarisation speed (Fig 5.7 H; WT: -75.92 ± 2.08mV/ms; n=26; KO: -69.63 ± 1.66mV/ms; n=32; p=0.02). This data suggests that whilst passive currents at rest are not affected in *Fmr1* KO neurons, ionic conductances that underlie action potential firing are altered.

5.3.7 Axon initial segments are significantly shorter in *Fmr1* KO PL-BLA projection neurons

Changes in action potential threshold and maximum dv/dt indicate changes in the underlying Na^+ conductances in *Fmr1* KO neurons. Action potentials are initiated by the axon initial segment (AIS). This highly specialised structure contains a high density of Na^+ channels which are recruited and stabilised in the membrane by the structural protein Ankyrin-G (Zhuo et al., 1998). AIS length and distance from soma have been shown to regulate action potential threshold as well as action potential waveform (Kole & Stuart 2008; Kole et al. 2008). As Ankyrin G is highly enriched in the AIS, I used immunocytochemistry to examine the morphology of the AIS in PL-BLA projection neurons in *Fmr1* rats. I observed a significant decrease in AIS length in *Fmr1* KO rats compared to WT controls (Fig 5.8 B; WT: 30.90 ± 1.31µm; n=4; KO: 24.60 ± 0.72µm; n=4; p=0.03). No significant difference in AIS distance from soma was found between genotypes (Fig 5.8 C; WT: 2.79 ± 0.20µm; n=4; KO: 2.82 ± 0.45µm; n=4; p>0.05). As AIS length is known to regulate action potential threshold and neuronal excitability (Kole & Stuart 2008) this morphological change results in hypoexcitability of *Fmr1* KO PL-BLA projection neurons.

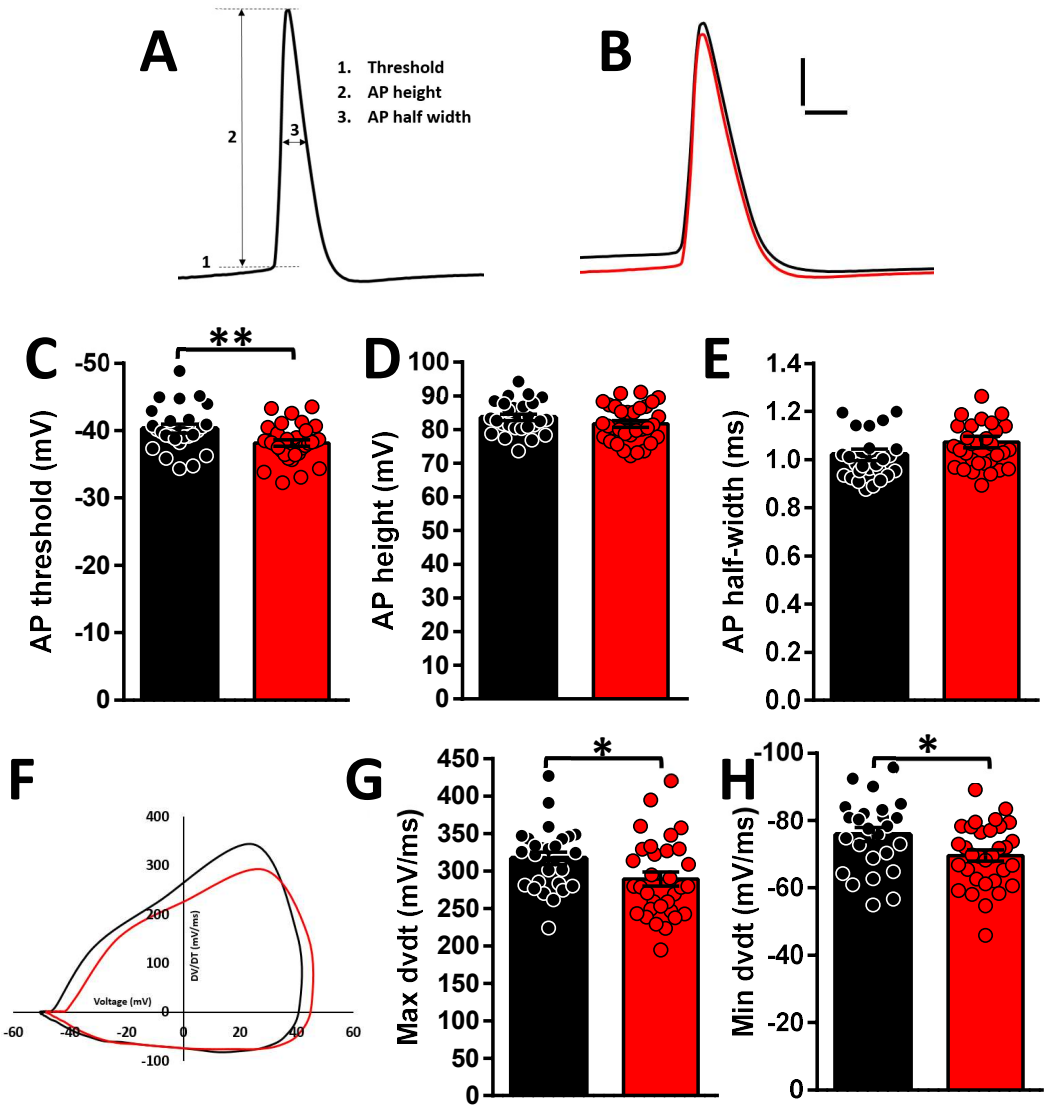

Figure 5.8 Loss of FMRP affects action potential waveform in *Fmr1* KO PL-BLA projection neurons (A) Schematic showing measurements of action potential waveform. (B) Example traces of action potential from WT and *Fmr1* KO neuron. Scale 20mV, 1ms. (C) Action potential threshold was significantly depolarised in *Fmr1* KO neurons (WT: -40.31 ± 0.66mV; n=26 cells/ 11 animals; KO: -38.18 ± 0.48; n=32 cells/16 animals; p=0.01). (D) Action potential height was not significantly different between genotypes (WT: 83.57 ± 0.96mV; n=26 cells/ 11 animals; KO: 81.64 ± 0.96; n=32 cells/16 animals; p>0.05). (E) Action potential half-width was not significantly different between genotypes (WT: 1.02 ± 0.02; n=26 cells/ 11 animals; KO: 1.07 ± 0.03; n=32 cells/16 animals; p>0.05). (F) Phase plot of action potential in WT and *Fmr1* KO neuron. (G) Max dvdt was significantly reduced in *Fmr1* KO neurons compared to WT controls (WT: 317.06 ± 8.50mV/ms; n=26 cells/ 11 animals; KO: 289.47 ± 9.22mV/ms; n=32 cells/16 animals; p=0.035). (H) Min dvdt was significantly increased in *Fmr1* KO neurons compared to WT controls (WT: -75.92 ± 2.08mV/ms; n=26 cells/ 11 animals; KO: -69.63 ± 1.66mV/ms; n=32 cells/16 animals; p=0.02). Statistical tests performed with Student unpaired *t*-test.

5.3.8 K^+ conductances are unaffected in *Fmr1* KO neurons

Layer 5 mPFC pyramidal neurons contain several classes of voltage gated K^+ channels (VGKC) (Dong & White 2003). K^+ channels also influence many aspects of neuronal excitability including action potential threshold, resting membrane potential and shaping action potentials (Kang et al. 2000). These properties suggest that alterations in K^+ conductances could also contribute to the hypoexcitability of *Fmr1* KO neurons. Previous studies have identified at least three classes of K^+ current in rat layer 5 mPFC pyramidal neurons that can be isolated based on their biophysical properties using different protocols (Dong & White, 2003, Kalmbach et al. 2015). Sustained K^+ currents such as non-inactivating K current ($I_{K\text{-}Sustained}$) and the slow-inactivating K current ($I_{K\text{-}SLOW}$) play roles in action potential duration whereas the rapidly inactivating 'A-type' K^+ current ($I_{K\text{-}FAST}$) have effects on firing frequency, action potential repolarisation and fAHP (Kang et al. 2000).

Total whole-cell VGKC currents ($I_{K\text{-}WC}$) were evoked using 4s pre-pulse to -100mV to deinactivate any inactivated K^+ channels followed by a depolarising step to +50mV. No significant differences were observed in total VGKC currents between genotypes (Fig 5.9 A; WT: 50.69 ± 4.73pA/pF; n=8; KO: 52.04 ± 5.66pA/pF; n=6; $p>0.05$). A second protocol was used to isolate the $I_{K\text{-}Sustained}$ component of this current. A prolonged 30s depolarising prepulse to +20mV was used initially to inactivate any current components that showed inactivation kinetics. This was followed by a test step to +50mV which elicited a small non-inactivating current ($I_{K\text{-}Sustained}$). Again no significant differences were observed in this current component between genotypes (Fig 5.9 B; WT: 10.75 ± 0.82pA/pF; n=8; KO: 10.77 ± 1.60pA/pF; n=6; $p>0.05$). To isolate the $I_{K\text{-}FAST}$ current component, a brief prepulse to +20mV was used to inactivate this fast inactivating current without significantly altering the slow-inactivating or sustained components. Digital subtraction of this current from the total VGKC current revealed a rapidly inactivating current termed $I_{K\text{-}Fast}$. A-type K^+ currents were not significantly different in *Fmr1* KO neurons compared to WT controls (Fig 5.9 D; WT: 12.95 ± 1.78pA/pF; n=8; KO: 15.84 ± 3.03pA/pF; n=6; $p>0.05$). Finally, the slow-inactivating current ($I_{K\text{-}SLOW}$) was calculated by digital subtraction of I_K from the total VGKC current. No significant differences were observed in this component PL-BLA

projection neuron K^+ current (Fig 5.9 C; WT: 26.80 ± 3.68pA/pF; n=8; KO: 25.20 ± 4.54pA/pF; n=6; p>0.05). As expected from this data, no significant differences were observed in the relative contribution of the three K^+ current components between genotypes (Fig 5.9 E; F(1,12)=0.161; p=0.695). Together, these data show that no differences in any component of the whole cell VGKC current of PL-BLA projection neurons exist between WT and *Fmr1* KO rats suggesting that changes in whole-cell K^+ currents do not play a role in the altered intrinsic excitability of *Fmr1* KO neurons.

5.3.9 Kv4 component of A-type K^+ current was comparable between genotypes

Macroscopic currents are composed of distinct channels with comparable kinetics (Korngreen & Sakmann 2000). Kv1 or Kv4 subunits can contribute to A-type K^+ currents. These two conductances can be separated by their kinetics of recovery from inactivation (Coetzee et al. 1999). Kv4 subunits show full recovery following inactivation within 100ms however Kv1 subunits are an order of magnitude slower (Routh et al. 2013). As changes in Kv4.2 conductances has been implicated in various cell types in *Fmr1* KO mice (Routh et al. 2013; Gross et al. 2011; Kalmbach et al. 2015) I tested the relative contribution of these two components of the A-type K^+ current. Using an interstimulus interval ranging from 10-100ms to recover K^+ channels from inactivation, two 200ms test steps from -100mV to +50mV were used to isolate the A-type K^+ current as previously described. Using this method, I found the time course of recovery of A-type K^+ current was comparable between genotypes (Fig 5.10). With a 100ms recovery time, A-type K^+ currents had recovered equally in both WT and *Fmr1* KO neurons (Fig 5.10 B; WT: 87.38 ± 2.73%; n=7; KO: 88.24 ± 1.99%; n=8; p>0.05). Based on their kinetics of recovery from inactivation, this second current should be mediated by Kv4 channels only, therefore, this data suggests that Kv1 and Kv4 currents are unaffected in *Fmr1* KO PL-BLA neurons.

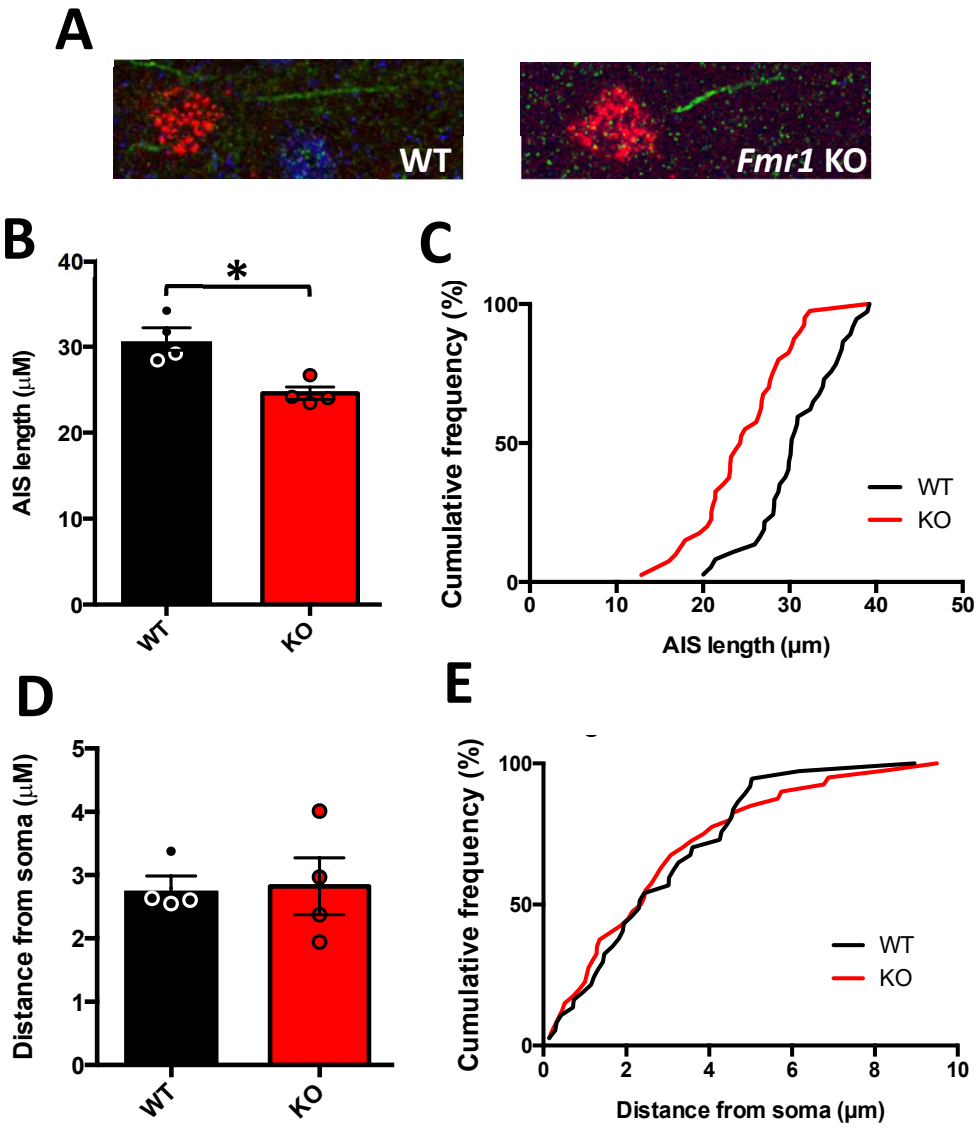

Figure 5.9 Axon initial segment is significantly shorter in *Fmr1* KO PL-BLA projection neurons (A) Confocal image of bead labelled soma showing immunocytochemistry for axon initial segment (AIS) specific Ankyrin-G (green) and NeuN (blue). (B) AIS length is significantly increased in *Fmr1* KO rats (WT: 30.90 ± 1.30µm; n=4 animals; KO: 24.60 ± 0.72µm; n=4 animals; p=0.03, Student unpaired *t*-test) (C) Cumulative distribution of AIS length data. (D) No difference between genotypes was observed in AIS distance from soma (WT: 2.79 ± 0.20µm; n=4 animals; KO: 2.82 ± 0.45µm; n=4 animals; p=0.95, Student unpaired *t*-test). (E) Cumulative distribution of AIS distances from soma.

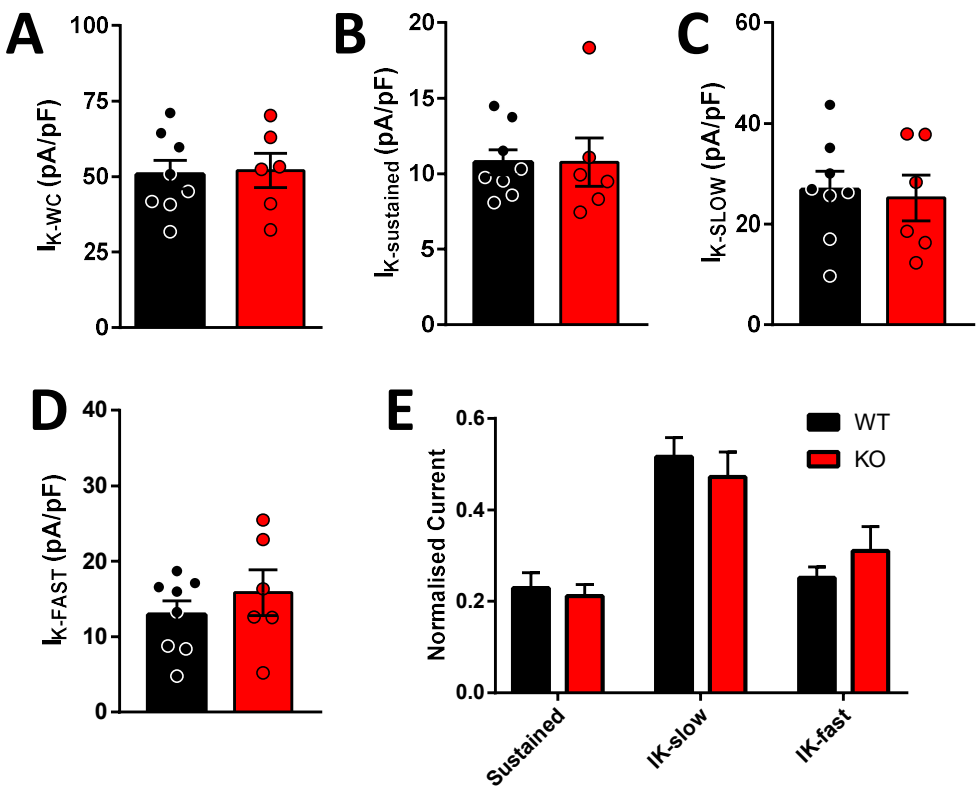

Figure 5.10 No changes in any component of whole-cell K^+ current in *Fmr1* KO PL-BLA neurons (A) No significant difference in whole-cell K^+ current in *Fmr1* KO neurons (WT: 50.69 ± 4.73pA/pF; n=8 cells/4 animals; KO: 52.04 ± 5.66pA/pF; n=6 cells/3 animals; p>0.05, Student unpaired *t*-test). (B) No significant difference in sustained K^+ current in *Fmr1* KO neurons (WT: 10.75 ± 0.82pA/pF; n=8 cells/4 animals; KO: 10.77 ± 1.60pA/pF; n=6 cells/3 animals; p>0.05, Student unpaired *t*-test). (C) No significant difference in slow-inactivating K^+ current in *Fmr1* KO neurons (WT: 26.80 ± 3.68pA/pF; n=8 cells/4 animals; KO: 25.20 ± 4.54pA/pF; n=6 cells/3 animals; p>0.05, Student unpaired *t*-test). (D) No significant difference in fast-inactivating K^+ current in *Fmr1* KO neurons (WT: 12.95 ± 1.78pA/pF; n=8 cells/4 animals; KO: 15.84 ± 3.03pA/pF; n=6 cells/3 animals; p>0.05, Student unpaired *t*-test). (E) No significant difference in relative contribution of different current components to whole cell K^+ current in *Fmr1* KO neurons ($F(1,12)=0.161$; p=0.695, Two way ANOVA).

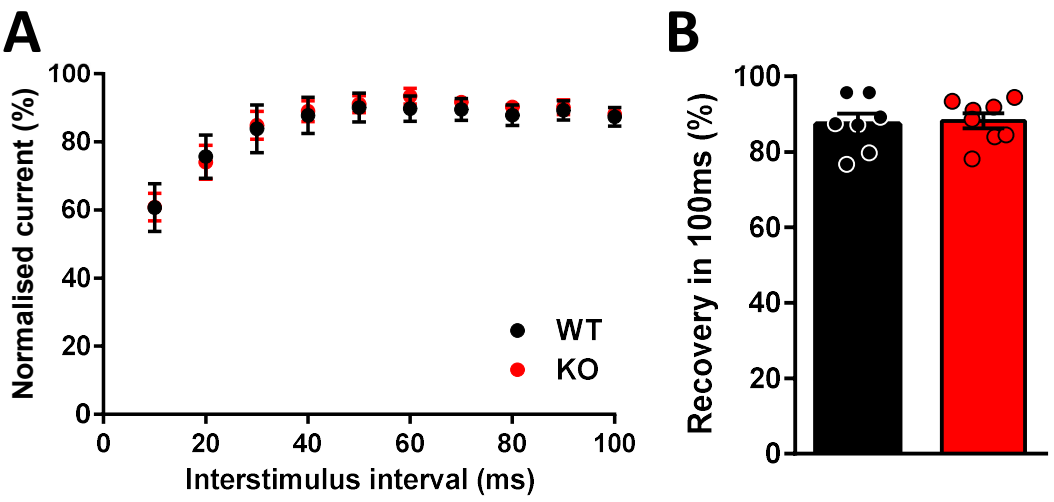

Figure 5.11 Putative $K_v4.2$ component of A-type K^+ current is comparable between genotypes (A) Peak A-type recovery from inactivation was comparable between genotypes. (B) Current recovery at 100ms was not significantly different in *Fmr1* KO neurons (WT: 87.38 ± 2.73%; n=7 cells/3 animals; KO: 88.24 ± 1.99%; n=8 cells/animals; p>0.05, Student unpaired *t*-test).

5.4 Synaptic currents in *Fmr1* PL-BLA projection neurons

5.4.1 Loss of FMRP does not affect spontaneous but does reduce miniature excitatory postsynaptic current frequency in PL-BLA projection neurons

As well as receiving long range inputs from several different brain regions, layer 5 mPFC pyramidal neurons are interconnected forming a local microcircuit. The local excitatory connectivity of these neurons is also highly correlated with their long range targets (Brown & Hestrin 2009; Morishima et al. 2011). I next investigated if the loss of FMRP leads to any changes in excitatory synaptic transmission in PL-BLA projection neurons. Spontaneous excitatory postsynaptic currents (sEPSC) were recorded at -70mV in the presence of 75µM picrotoxin to block fast inhibitory currents. No significant differences were observed in sEPSC amplitude (Fig 5.11 B; WT: -28.45 ± 2.29pA; n=5; KO: -25.71 ± 3.15pA; n=6; p>0.05) or frequency (Fig 5.11 D; WT: 7.56 ± 0.83Hz; n=5; KO: 7.05 ± 0.98Hz; n=6; p>0.05). sEPSC kinetics were also unaffected in *Fmr1* KO neurons (Fig 5.11 F; WT rise time: 1.73 ± 0.06ms; n=5; KO rise time: 1.78 ± 0.08ms; n=6; p>0.05; Fig 5.11 G; WT decay time: 7.56 ±0.83ms; n=5; KO decay time: 7.05 ± 0.98ms; n=6; p>0.05).

The addition of TTX (300nM) to the external solution allows the isolation of miniature excitatory postsynaptic potentials (mEPSC). As mEPSCs are independent of action potentials, their frequency is thought to reflect both the number of synaptic connections as well as their presynaptic release probability whilst the amplitude is an indicator of postsynaptic strength. Comparison of mEPSC in PL-BLA projection neurons revealed no significant difference in amplitude (Fig 5.12 B; WT: -21.25 ± 1.78pA; n=5; KO: -22.65 ± 2.01pA; n=6; p>0.05) suggesting postsynaptic function is unchanged in *Fmr1* KO neurons. Howeverm mEPSC frequency was significantly greater in *Fmr1* KO neurons compared to WT controls (Fig 5.12 D; WT: 5.23 ± 0.50Hz; n=5; KO: 7.55 ± 0.42Hz; n=6; p=0.001). Similar to sEPSC, no significant differences in mEPSC kinetics were observed (Fig 5.12 F; WT rise time: 1.94 ± 0.06ms; n=5; KO rise time: 1.76 ± 0.07ms; n=6; p>0.05; Fig 5.12 G; WT decay time: 5.45 ± 0.13ms; n=5; KO decay time: 5.51 ± 0.20ms; n=6; p>0.05). This data suggests that despite a reduction in the intrinsic excitability of PL-BLA projection neurons, this does not lead to changes in local network driven synaptic events in *Fmr1* KO neurons. However, the loss of FMRP does result in a reduction in the number of excitatory synaptic inputs or release probability on to PL-BLA projection neurons.

5.4.2 Inhibtory transmission onto *Fmr1* KO PL-BLA projection neurons is unaffected

Network excitability can also be affected by inhibitory transmission in cortical circuits. Previous studies in cortical regions including layer 5 mPFC have revealed that local interneurons can selectively innervate pyramidal neurons depending on their long range targets (Krook-Magnuson et al. 2012; Varga et al. 2009; Lee et al. 2014). Therefore, I investigated inhibitory postsynaptic currents (IPSC) in PL-BLA projection neurons to identify if changes in inhibitory neurotransmission could affect the excitability of cortical microcircuits that project specifically to the BLA. Spontaneous IPSC (sIPSC) showed no significant difference in amplitude (Fig 5.13

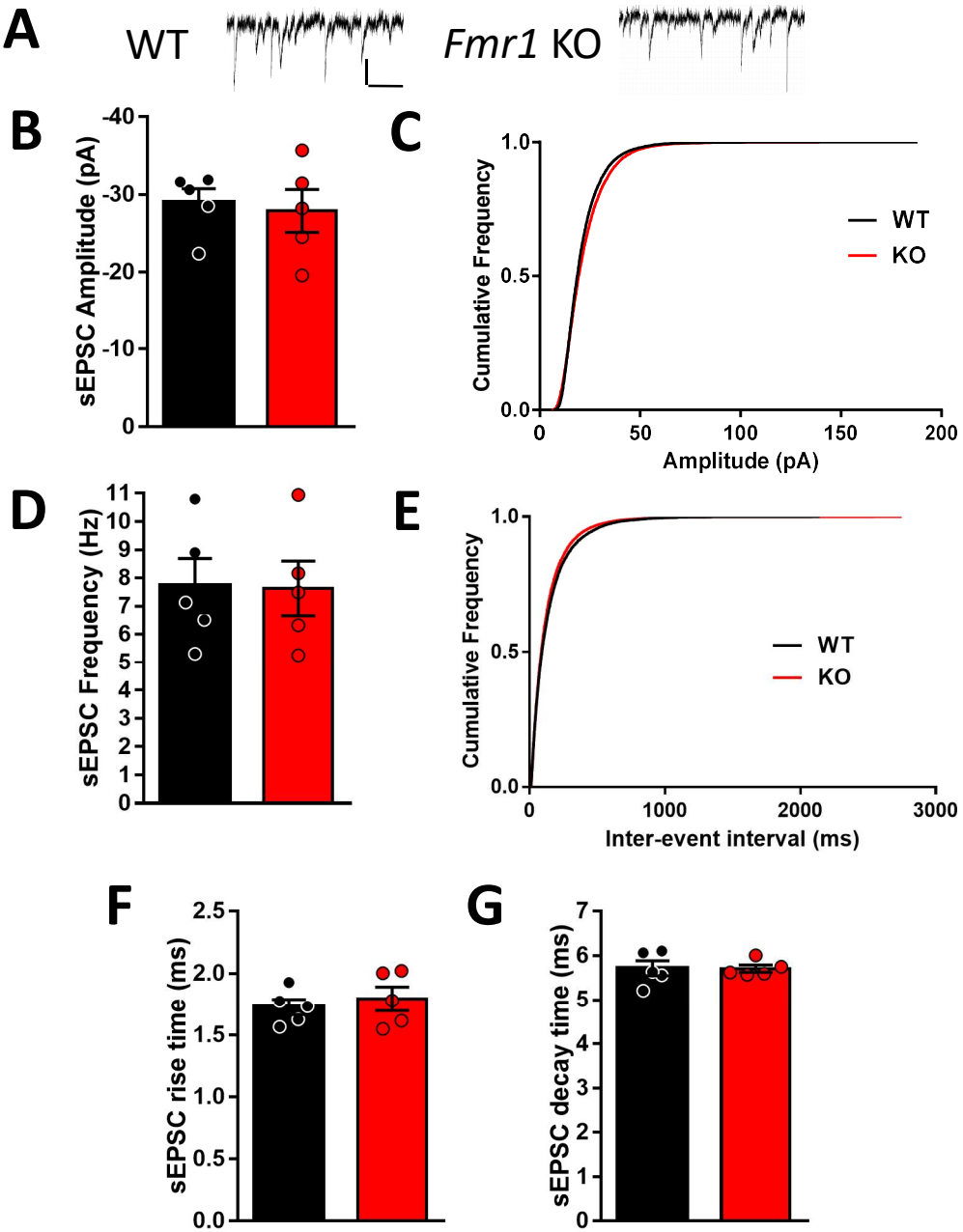

Figure 5.12 sEPSC in L5 PL-BLA were comparable between genotypes (A) Example traces displaying sEPSCs recorded at -70V in the presence of 75µM PTX in both WT and *Fmr1* KO neurons. Scale 200ms, 10pA (B) sEPSC amplitude was unaffected between genotypes (WT: -28.45 ± 2.29pA; n=5 animals/14 cells; KO: -25.71 ± 3.15pA; n=6 animals/11 cells; p>0.05). (C) Cumulative frequency of sEPSC amplitudes in WT and *Fmr1* KO neurons. (D) sEPSC frequency was comparable between genotypes (WT: 7.56 ± 0.83Hz; n=5 animals/14 cells; KO: 7.05 ± 0.98Hz; n=6 animals/11 cells; p>0.05). (E) Cumulative frequency of sEPSC inter-event intervals in WT and *Fmr1* KO neurons. (F) No differences were observed in sEPSC rise time (WT: 1.73 ± 0.06ms; n=5 animals/14 cells; KO: 1.78 ± 0.08ms; n=6 animals/11 cells; p>0.05) or (G) decay time (WT: 7.56 ±0.83ms; n=5 animals/14 cells; KO: 7.05 ± 0.98ms; n=6 animals/11 cells; p>0.05). Statistical tests performed with Student unpaired *t*-test.

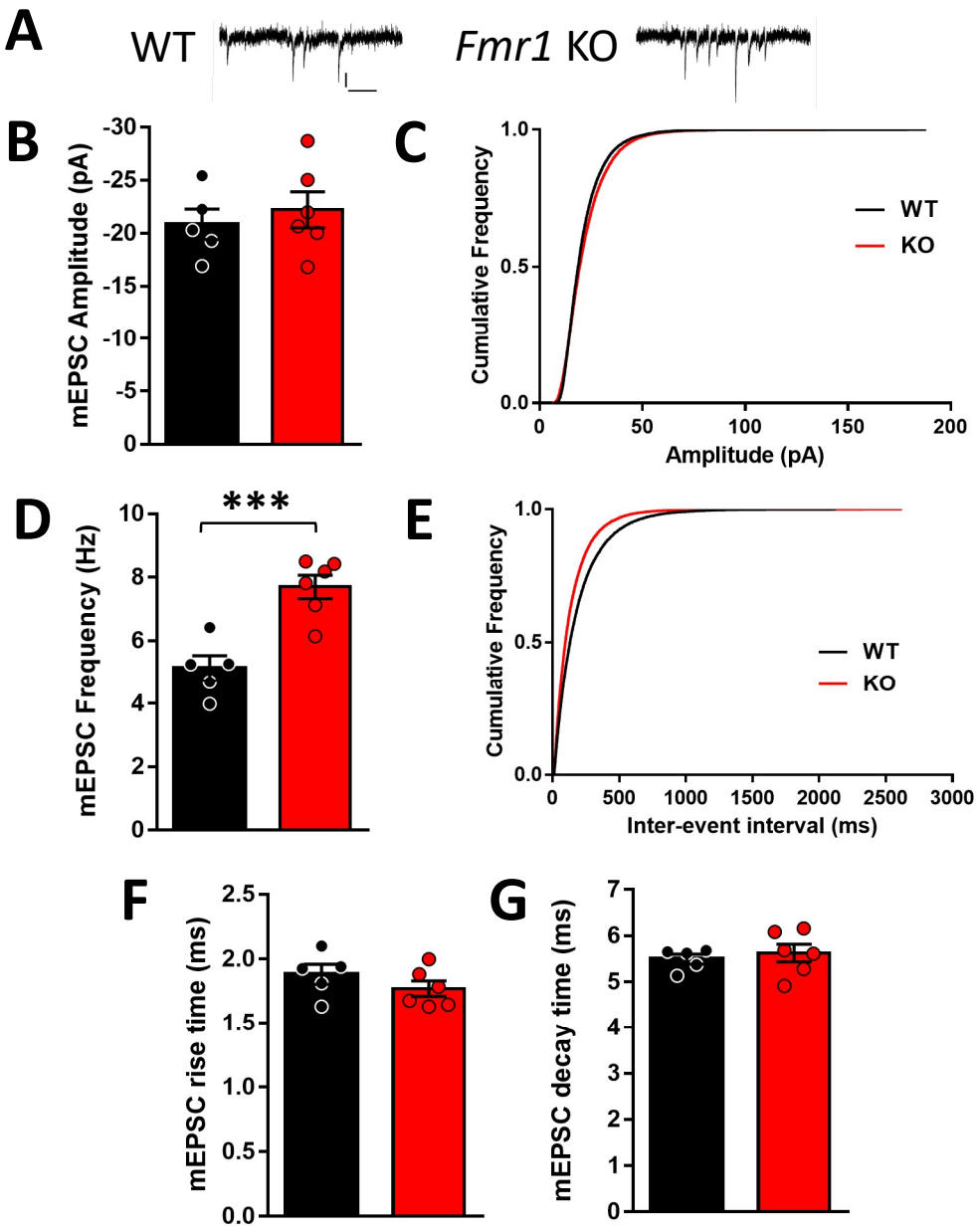

Figure 5.13 mEPSC frequency is increased in *Fmr1* KO PL-BLA projection neurons (A) Example traces displaying mEPSCs recorded at -70V in the presence of 75µM PTX and 300nM TTX in both WT and *Fmr1* KO neurons. Scale 200ms, 5pA (B) mEPSC amplitude was unaffected between genotypes (WT: -21.25 ± 1.78pA; n=5 animals/16 cells; KO: -22.65 ± 2.01pA; n=6 animals/13 cells; p>0.05). (C) Cumulative frequency of mEPSC amplitudes in WT and *Fmr1* KO neurons. (D) mEPSC frequency was significantly increased in *Fmr1* KO neurons (WT: 5.23 ± 0.50Hz; n=5 animals/16 cells; KO: 7.55 ± 0.42Hz; n=6 animals/13 cells; p=0.001). (E) Cumulative frequency of mEPSC inter-event intervals in WT and *Fmr1* KO neurons. (F) No differences were observed in mEPSC rise time (WT: 1.94 ± 0.06ms; n=5 animals/16 cells; KO: 1.76 ± 0.07ms; n=6 animals/13 cells; p>0.05) or (G) decay time (WT: 5.45 ± 0.13ms; n=5 animals/16 cells; KO: 5.51 ± 0.20ms; n=6 animals/13 cells; p>0.05). Statistical tests performed with Student unpaired *t*-test.

B; WT: -41.63 ± 2.35pA; n=6; KO: -52.03 ± 6.86pA; n=5; p>0.05) or frequency (Fig 5.13 D; WT: 5.49 ± 0.76Hz; n=6; KO: 6.56 ± 0.54Hz; n=5; p>0.05) between WT and *Fmr1* KO rats. sIPSC rise time (Fig 5.13 F; WT: 2.11 ± 0.10ms; n=6; KO: 1.83 ± 0.14ms; n=5; p>0.05) and decay time (Fig 5.13 G; WT: 14.45 ± 0.53ms; n=6; KO: 14.69 ± 0.79ms; n=5; p>0.05) were unaffected by the loss of FMRP. Similarly, no significant differences were observed in miniature IPSC properties in *Fmr1* PL-BLA projection neurons. mIPSC amplitude (Fig 5.14 B; WT: -44.17 ± 3.11pA; n=5; KO: -47.29 ± 4.65pA; n=6; p>0.05), mIPSC frequency (Fig 5.14 D; WT: 3.95 ± 0.74Hz; n=5; KO: 4.31 ± 0.53Hz; p>0.05), mIPSC rise time (Fig 5.14 F; WT: 1.63 ± 0.04ms; n=5; KO: 1.67 ± 0.08; n=6; p>0.05) and mIPSC decay time (Fig 5.14 G; WT: 14.54 ± 0.32ms; n=5; KO: 13.97 ± 0.21ms; n=6; p>0.05) were all comparable between genotypes. This data suggests that both inhibitory connectivity onto PL-BLA projection neurons as well as network driven inhibitory activity are unaffected in *Fmr1* KO rats.

5.5 Discussion

5.5.1 Age-dependent plasticity deficits

The mPFC is a cortical region that plays a key role in higher order cognitive functions such as attention, working memory and cognitive flexibility which are affected in FXS. Reports from *Fmr1* KO mice have revealed both biochemical and functional phenotypes in several subregions of the PFC (Zhao et al. 2005; Meredith et al. 2007, Wang et al. 2008). Interestingly, some studies have revealed age-dependent deficits associated with the loss of FMRP in PFC circuits. LTP in the piriform cortex was found to be intact in *Fmr1* mice however showed a progressive deficit as animals aged (Larson et al. 2005). Here I report a similar deficit in the PL cortex, a subregion of the mPFC. LTP was found to be intact in juvenile *Fmr1* KO rats but showed deficits in young adult rats. These findings have also recently been reported in *Fmr1* KO mice mPFC (Martin et al. 2015) suggesting a conserved mechanism associated with the loss of FMRP. This work suggested that this effect

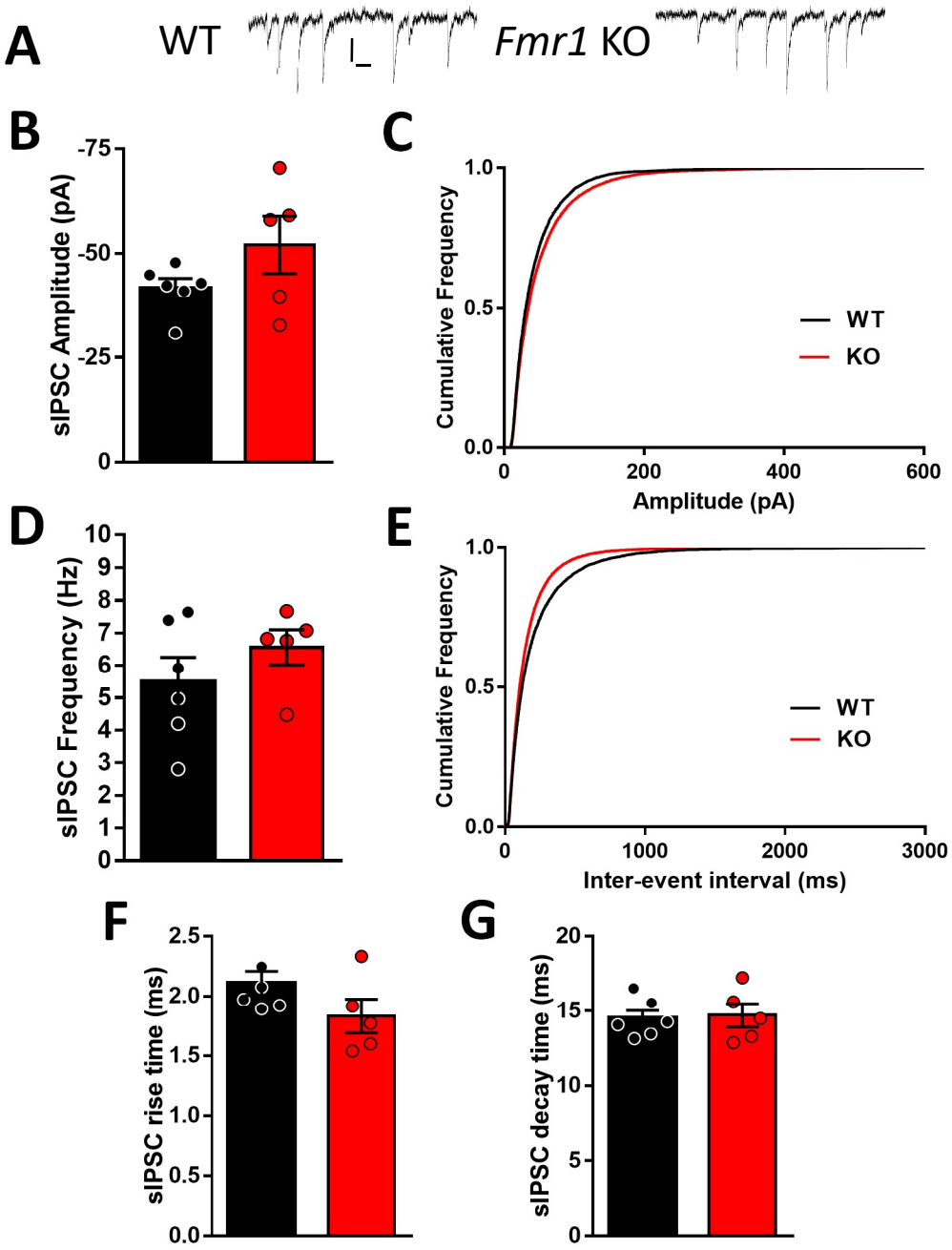

Figure 5.14 sIPSCs are unaffected in *Fmr1* KO PL-BLA projection neurons (A) Example traces displaying sIPSCs recorded at -70V in the presence of 20µM CNQX in both WT and *Fmr1* KO neurons. Scale 20pA, 100ms (B) sIPSC amplitude was unaffected between genotypes (WT: -41.63 ± 2.35pA; n=6 animals/8 cells; KO: -52.03 ± 6.86pA; n=5 animals/9 cells; p>0.05). (C) Cumulative frequency of sIPSC amplitudes in WT and *Fmr1* KO neurons. (D) sIPSC frequency was unaffected in *Fmr1* KO neurons (WT: 5.49 ± 0.76Hz; n=6 animals/8 cells; KO: 6.56 ± 0.54Hz; n=5 animals/9 cells; p>0.05). (E) Cumulative frequency of sIPSC inter-event intervals in WT and *Fmr1* KO neurons. (F) No differences were observed in sIPSC rise time (WT: 2.11 ± 0.10ms; n=6 animals/8 cells; KO: 1.83 ± 0.14ms; n=5 animals/9 cells; p>0.05) or (G) decay time (WT: 14.45 ± 0.53ms; n=6 animals/8 cells; KO: 14.69 ± 0.79ms; n=5 animals/9 cells; p>0.05). Statistical tests performed with Student unpaired *t*-test.

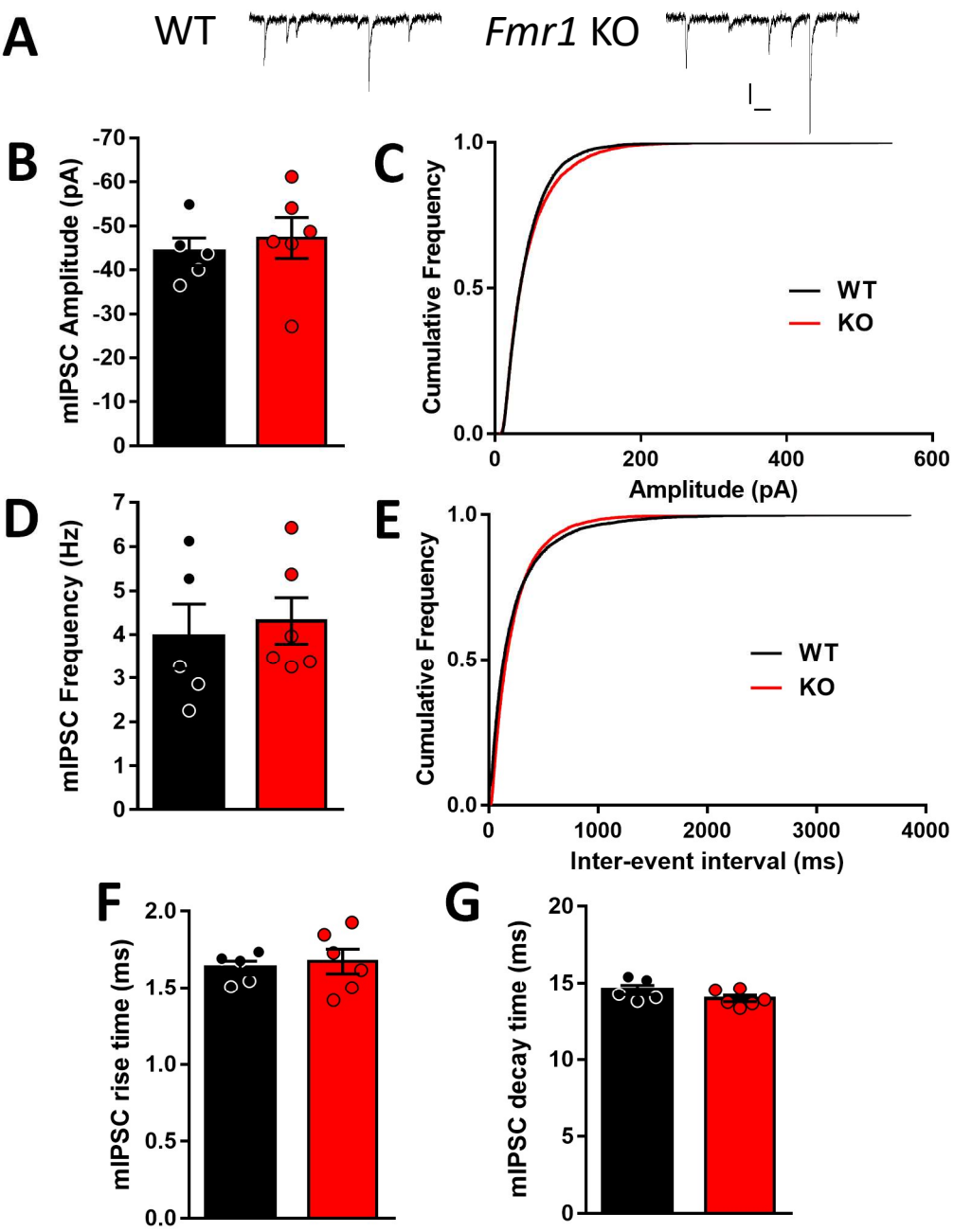

Figure 5.15 mIPSCs are unaffected in *Fmr1* KO PL-BLA projection neurons (A) Example traces displaying mIPSCs recorded at -70V in the presence of 20µM CNQX and 300nM TTX in both WT and *Fmr1* KO neurons. (B) mIPSC amplitude was unaffected between genotypes (WT: -44.17 ± 3.11pA; n=5 animals/9 cells; KO: -47.29 ± 4.65pA; n=6 animals/8 cells; p>0.05). (C) Cumulative frequency of mIPSC amplitudes in WT and *Fmr1* KO neurons. (D) mIPSC frequency was unaffected in *Fmr1* KO neurons (WT: 3.95 ± 0.74Hz; n=5 animals/9 cells; KO: 4.31 ± 0.53Hz; n=6 animals/8 cells; p>0.05). (E) Cumulative frequency of mIPSC inter-event intervals in WT and *Fmr1* KO neurons. (F) No differences were observed in mIPSC rise time (WT: 1.63 ± 0.04ms; n=5 animals/9 cells; KO: 1.67 ± 0.08; n=6 animals/8 cells; p>0.05) or (G) decay time (WT: 14.54 ± 0.32ms; n=5 animals/9 cells; KO: 13.97 ± 0.21ms; n=6 animals/8 cells; p>0.05). Statistical tests performed with Student unpaired *t*-test.

was due to an age dependent decrease in NMDAR signalling, resulting in an increased AMPA/NMDA current ratio. However, this was not observed in our recordings suggesting a reduction in NMDA currents does not contribute to the loss of LTP in *Fmr1* KO rats. This has also not been reported in any other PFC LTP deficit in *Fmr1* KO mice (Larson et al. 2005; Zhao et al. 2005) suggesting other mechanisms may explain the loss of LTP observed here. Preincubation with the $mGluR_5$ antagonist MPEP has been shown to restore adult LTP in mPFC circuits (Martin et al. 2015) suggesting exaggerated mGluR signalling associated with the loss of FMRP plays a role in this LTP deficit (Ronesi & Huber 2008). Given the ability of $mGluR_5$ to enhance NMDAR currents, it is unclear how acute pharmacological inhibition is able to enhance NMDAR currents and restore LTP as reported by Martin et al (2015). However, the ability of $mGluR_5$ activation to potentiate NMDAR currents has not been explored in models of FXS therefore a different mechanism could be taking place in the absence of FMRP that affects this relationship.

Another potential mechanism for LTP loss could be through changes in dopamine (DA) signalling in the absence of FMRP. DA signalling modulates PFC neuronal activity and affects several PFC functions such as working memory and attention (Zahrt et al. 1997; Granon et al. 2000). DA receptor 1 (D1R) signalling has also been shown to be required for the expression of LTP in rat PL mPFC circuits (Huang et al. 2004). D1R activation increases synaptic strength through insertion and phosphorylation of the AMPAR-subtype GluR1 as well as phosphorylation of NMDARs, however both of these effects are diminished in the absence of FMRP (Xu et al. 2012). These effects are associated with a hyperphosphorylation of D1R which prevents activation of downstream pathways in *Fmr1* KO neurons (Xu et al. 2012). Other groups have also reported a reduction in D1R protein levels in PFC neurons suggesting that DA signalling is dampened in *Fmr1* KO PFC (Paul et al. 2013). These findings have been associated with deficits in PFC synaptic plasticity including DA-mediated facilitation of LTP in anterior cingulate cortex (ACC) (Wang et al. 2008) as well as DA-mediated enhancement of inhibitory synaptic activity (Paul et al. 2013). Therefore, one could hypothesise that reduced D1R signalling during LTP induction in *Fmr1* KO rats underlies the loss of LTP. Interestingly, low level group 1 mGluR

antagonists have been shown to restore D1R phosphorylation in *Fmr1* KO neurons to WT levels, restoring DA-mediated facilitation of LTP in the ACC (Xu et al. 2012). This suggests exaggerated mGluR signalling in the absence of FMRP results in diminished DA signalling however the mechanism for this is unclear. Nonetheless, this presents a potential therapeutic strategy to restore LTP in *Fmr1* KO PL circuits and could explain previous observations in mice (Martin et al. 2015). As FXS patients present increasing ID with age (Utari et al. 2010) it is tempting to link this to our finding, however the role that LTP in PL mPFC plays in cognitive function is unknown. Despite this, it is clear that the loss of FMRP results in profound changes in mPFC translaminar communication.

5.5.2 Hypoexcitability of neurons

The mPFC receives and integrates information from a wide range of diverse brain regions as well as providing reciprocal connectivity allowing it to play a role in a variety of cognitive functions. Layer 5 acts as the major output layer of the cortical column, with glutamatergic pyramidal neurons providing long range projections to distinct cortical and subcortical areas. A large body of work has highlighted how these L5 neurons form a heterogeneous population with distinct local circuit organisation, intrinsic properties and neuromodulation depending on their long range target (Wang et al. 2006; Brown & Hestrin 2009; Dembrow et al. 2010; Morishima et al. 2011). This suggests that distinct subcircuits exist within the L5 pyramidal neuron population which regulate specific behaviours through their unique synaptic inputs as well as projection targets.

Here I used retrograde tracing to identify a L5 subpopulation of pyramidal neurons that provide long-range projections to the basolateral amygdala. This projection pathway is known to be important for the expression of fear memories, a behaviour which is known to be affected in *Fmr1* KO animals (Paradee et al. 1999). As $mGluR_5$ activation has been shown to modulate both excitatory and inhibitory transmission in L5 mPFC pyramidal neurons, I predicted several elements of intrinsic and synaptic

physiology would be perturbed in *Fmr1* KO circuits as $mGluR_5$ is thought to be constitutively active in the absence of FMRP (Ronesi & Huber 2008). However, I found none of the physiological phenotypes associated with enhanced $mGluR_5$ signalling in *Fmr1* KO rats. PL-BLA neurons were found to be intrinsically hypoexcitable in the absence of FMRP, firing fewer action potentials in response to current injection than WT control neurons. This is contrary to studies which have shown significant increases in intrinsic excitability in mPFC neurons in the presence of $mGluR_5$ positive allosteric modulators (PAM) (Kiritoshi et al. 2013; Sun & Neugebauer 2011). Similarly, sEPSC amplitude was also unchanged in our recordings but has previously been shown to be increased by $mGluR_5$ PAMs (Kiritoshi et al. 2013). These results suggest that exaggerated $mGluR_5$ signalling does not affect the intrinsic excitability of L5 pyramidal neurons in *Fmr1* KO PL mPFC. However, one must be cautious comparing results using acute pharmacology to a circuit that has possibly undergone development with enhanced $mGluR_5$ signalling as compensatory mechanisms in these animals may mask these effects.

5.5.3 Mechanism underlying hypoexcitability

Despite these results, a clear hypoexcitability was observed in PL-BLA pyramidal neurons in *Fmr1* KO rats. This result is contrary to what is commonly hypothesised in *Fmr1* KO studies which is typically associated with circuit hyperexcitability stemming from increased input resistance (Contractor et al. 2015). Hypoexcitability of PL-BLA neuron in *Fmr1* KO was not associated with changes in intrinsic membrane properties suggesting that subthreshold conductances were unaffected in these neurons. The loss of FMRP has been associated with the dysregulation and dysfunction of several diverse voltage-gated ion channels which have been shown to impact neuronal function in various ways including intrinsic excitability. I_h currents, mediated by HCN-channels, can modulate neuronal excitability through regulation of membrane resistance, synaptic integration and resting membrane potential (Shah, 2014). Studies have revealed opposing changes in dendritic expression of HCN-channels in pyramidal neurons of hippocampus versus cortex of *Fmr1* KO mice emphasising the variability

with which FMRP loss can affect cellular excitability in different brain regions (Brager et al. 2012; Zhang et al. 2014; Kalmbach et al. 2015). I_h currents in PL-BLA neurons appeared to be subtly enhanced in *Fmr1* KO rats however this effect was not significant (Fig 5.5) so it is unclear if this could have an effect on intrinsic excitability. I_h has also been shown to contribute to the generation of mAHP following a burst of action potentials (Oswald et al. 2009). As this was also comparable between genotypes in this study (Fig 5.6), this suggests that I_h changes do not contribute to the observed hypoexcitability of *Fmr1* KO PL-BLA neurons. However, previous studies that have identified changes in I_h currents in *Fmr1* KO neurons have shown that the effect is restricted to the dendritic compartment, with no observable changes in the soma. Therefore, as I recorded currents exclusively in the somatic compartment, I cannot rule out changes in dendritic processes that may contribute to changes in neuronal excitability.

Another channel that can affect neuronal excitability and has been shown to be affected by the loss of FMRP is the A-type K^+ channel $K_v4.2$. Kv4.2 is known to regulate current threshold as well as action potential repolarisation in cortical pyramidal neurons (Carrasquillo et al. 2012) both of which are affected in *Fmr1* KO PL-BLA neurons. FMRP has also been shown to regulate $K_v4.2$ expression (Gross et al. 2011; Lee et al. 2011) leading to functional changes in *Fmr1* KO neurons (Routh et al. 2013) making this a good candidate to underlie the phenotypes observed here. However, I observed no changes in Kv4.2 currents in our cells, or in any other tested K^+ conductance (Fig 5.9). Once again our recordings were limited to soma, as Kv4.2 shows dendritic gradient I cannot rule out changes in this compartment as identified in the *Fmr1* KO CA1 pyramidal neurons are not present (Routh et al. 2013).

FMRP can also directly activate some ion channels via protein-protein interactions. This includes the Slack channel (sequence like a Ca^{2+}-activated K^+ channel) (Brown et al. 2010) and BK channels (large-conductance Ca^{2+}-activated K^+ channel) (Deng et al. 2013). Whilst I did not directly measure either of these conductances, both are known to play a role in the AHP that follows a burst of action potentials. As I observed

no changes in AHP at any frequency, this suggests that changes in these conductances did not contribute to PL-BLA neuron hypoexcitability.

Despite membrane resistance being unchanged in *Fmr1* KO PL-BLA neurons, I observed that rheobase, the minimum current required to trigger an action potential, was significantly larger (Fig 5.4). This was accompanied by an increase in action potential threshold in the absence of FMRP (Fig 5.7) which suggests the availability of voltage-gated Na^+ channels, which influence action potential voltage threshold (Royeck et al. 2008), is affected in *Fmr1* KO neurons. In agreement with this action potential max dv/dt, a measure which reflects underlying Na^+ conductances, was also significantly reduced (Fig 5.7). Action potential threshold is believed to be dependent on the axon initial segment (AIS), a specialised structure with a high density of Na^+ channels approximately 50 times greater than proximal dendrites (Kole & Stuart 2008: Kole et al. 2008). As well as the density of Na^+ channels, the location and length of the AIS are both thought to influence a neurons action potential threshold. Results here suggest a shortening of AIS length in *Fmr1* KO PL-BLA neurons (Fig 5.8). This result is in good agreement with the observed changes in action potential waveform. Further experiments investigating Na^+ currents in PL-BLA neurons could provide support for this mechanism as a shorter AIS length should result in a reduction in Na^+ current density.

Whilst the AIS was classically thought of as a static structure, it is now known that it is able to modulate both its length and distance from soma in response to neuronal activity (Grubb & Burrone 2010). This structural plasticity allows the neuron to fine-tune its excitability according to the level of its synaptic activity thereby homeostatically regulating its input-output relationship. As mEPSC frequency is increased in *Fmr1* KO PL-BLA neurons (Fig 5.12), indicating that the number of inputs or release probability is increased, the decrease in AIS length could represent a compensatory response of KO neurons to normalise their output in response to increased synaptic input. This is supported by the observation that no changes were observed in action potential driven EPSCs (Fig 5.11) suggesting that despite an increase in the frequency of inputs, circuit excitability is maintained possibly through

cell intrinsic properties. However, from these results it is not possible to decipher which of these phenotypes is associated with the loss of FMRP and which is compensatory.

5.5.4 Are changes in neuronal excitability across all mPFC L5 pyramidal neurons or subtype specific?

Whilst L5 pyramidal neurons do show intrinsic differences depending on their long-range targets, it is possible that the results observed here represent a phenotype that is general to all mPFC L5 pyramidal neurons of *Fmr1* KO rats. Previous studies that have investigated neuronal excitability in undefined mPFC L5 pyramidal neurons have found no changes in adult *Fmr1* KO mice (Martin et al. 2015). However others have reported reduced c-fos staining across the *Fmr1* KO mPFC, suggesting neuronal activity is reduced in these circuits (Krueger et al. 2011). If all subtypes are similarly affected, these findings would be counter to the commonly held view that neuronal circuits are hyperexcitable in *Fmr1* KO animals (Contractor et al. 2015). However, these studies are typically confined to early developmental time points with some phenotypes only appearing transiently (Gibson et al. 2008; Zhang et al. 2014; Routh et al. 2013; Brager et al. 2012). As discussed earlier, the intrinsic neuronal hypoexcitability here could represent a compensatory change in response to general circuit hyperexcitability which only becomes apparent at later stages of development. Future work assessing the effect of FMRP loss on other mPFC subcircuits would be of interest in elucidating whether these effects are general to all mPFC L5 pyramidal neurons.

Equally, the phenotypes identified in this chapter could be restricted to be PL-BLA mPFC neurons. Recent work in *Fmr1* KO mice has shown that the loss of FMRP differentially affects two subpopulations of mPFC L5 pyramidal neurons (Kalmbach et al. 2015). This reflects the capability for specific phenotypes in *Fmr1* KO neurons to develop depending on cell extrinsic effects (e.g. synaptic inputs). Previous work has suggested layer 5 pyramidal neurons receive only ~20% of their synaptic inputs from

other local L5 neurons, with the majority of inputs coming from other prefrontal regions, CA1 hippocampus and the BLA (DeNardo et al. 2015). PL-BLA neurons have been shown to receive enhanced input from ascending BLA projections creating a strong reciprocal circuit (Little & Carter 2013; Cheriyan et al. 2016). Therefore in *Fmr1* KO animals where BLA circuits are thought to be hyperexcitable (Olmos-Serrano et al. 2010; Vislay et al. 2013) synaptic inputs onto PL-BLA neurons could be significantly enhanced relative to neighbouring L5 pyramidal neurons. The disparity in synaptic activity between different populations of neurons could result in cell-specific compensatory mechanisms to fine tune neuronal activity as suggested by the results described here.

5.5.5 What could these results mean for behaviour?

The prelimbic mPFC is an important structure in the processing of fear memories. PL-BLA neurons have been shown to be preferentially recruited during fear expression as well as retrieval (Orsini et al. 2011; Knapska et al. 2012). Therefore, hypoexcitability of PL-BLA neurons in *Fmr1* KO rats could contribute to deficits in fear learning as the relevant mPFC circuits are harder to recruit. Similarly, the acquisition of fear memories has been shown to be dependent on intrinsic plasticity of prelimbic circuits. Fear conditioning results in a reduction in intrinsic excitability of PL-BLA neurons similar to that described in *Fmr1* KO neurons. Whilst one study linked this with a decreased input resistance (Song et al. 2015), another found that action potential threshold was depolarised and max dv/dt reduced in PL-BLA neurons following fear conditioning, mirroring the effects of FMRP loss (Szlapczynska, 2014). Interestingly these effects were not present in neighbouring neurons that project to the contralateral mPFC suggesting they may be restricted to PL-BLA neurons. As fear conditioning is known to activate ascending BLA projections to the PL (Senn et al. 2014) this could trigger plasticity of L5 PL-BLA neurons intrinsic excitability as previously hypothesised. Therefore, it is possible that the hypoexcitability of PL-BLA neurons in *Fmr1* KO rats could reflect a circuit that has already adapted to a state of high fear resulting from BLA hyperexcitability. This could occlude any further learning-related

changes in these pathways, contributing to the deficits in fear learning associated with *Fmr1* KO animals (Paradee et al. 1999). Future work focussing on other elements of these pathways and how they are affected by fear learning may reveal changes in the underlying physiology associated with fear memory formation, which are yet to be explored in animal models of FXS.

Chapter 6

Concluding remarks

6.1 mGluR pathophysiology in the *Fmr1* rat

Since its original inception, the mGluR theory of FXS has informed the design and predicted outcomes of many studies attempting to ameliorate phenotypes in models of FXS. It has been corroborated by a wide range of experiments from laboratories around the world at several levels of experimental interrogation and has significantly enhanced our understanding of the underlying pathophysiology of FXS. This data has formed a strong preclinical data set that has resulted in clinical trials targeting $mGluR_5$ signalling in FXS patients. The development of genetically modified rats represent a valuable new tool for the study of NDDs such as FXS. As well as presenting several advantages over mice as preclinical models (discussed earlier), the generation of *Fmr1* KO rats has allowed us directly test the conservation of mGluR-dependent phenotypes across mammalian species.

In this thesis we have been able to recapitulate many of the mGluR dependent phenotypes originally identified in the *Fmr1* KO mouse in both CA1 hippocampus and lateral amygdala. We also report preliminary results showing that pharmaceutical interventions targeting $mGluR_5$, using the negative allosteric modulator CTEP, are able to reverse some of these phenotypes as has commonly been reported in *Fmr1* KO mice literature. This data provides additional support that dysfunction of $mGluR_5$ signalling contributes to pathophysiology of FXS. It also provides validation of the therapeutic strategy of targeting $mGluR_5$ which has been carried forward into clinical trials for treating the human condition. These trials have recently been discontinued as no significant benefit of drug treatment. Here I will discuss these trials and their implications for future work treating $mGluR_5$ as a target in FXS.

6.1.2 $mGluR_5$ as a target in FXS

Mavoglurant (AFQ056), a non-competitive $mGluR_5$ inhibitor, has shown rescue of molecular, dendritic spine and behaviour phenotypes in *Fmr1* KO mice (Levenga et al. 2011; Gantois et al. 2013; Pop et al. 2014). A small scale exploratory cross-over

trial showed no beneficial effect of mavoglurant, however post hoc analysis showed a significant positive outcome in patients with completely methylated *FMR1* promoter (Jacquemont et al. 2011). This resulted in a large-scale double blind, placebo controlled, 3 month trial evaluating the effectiveness of mavoglurant at multiple doses in both adult and adolescent FXS patients stratified by their methylation status of *FMR1*. This trial found no significant benefit of drug treatment in any of the assessed outcome measures. A concurrent phase 2 trial at Roche using the $mGluR_5$ negative allosteric modulator RG7090 also found no significant efficacy in the primary and secondary endpoints assessed in FXS patients. These results suggest that, contrary to over a decade of work in FXS animal models, there is no significant therapeutic action of reduced $mGluR_5$ signalling in FXS.

One possible explanation for this negative result could be that the phenotypes observed in rodent models of FXS are not translatable to humans. Beyond the obvious criticism that rodent and human physiology are not directly comparable, problems in the study of FXS could also stem from the construct validity of the animal models used. The available animal models, including the *Fmr1* KO rats discussed in this thesis, are generated by genetic modification of DNA to resulting in complete transcriptional silencing of the *FMR1* gene. This strategy is in contrast to human FXS which is the result of hypermethylation of the *FMR1* promoter sequence, with only rare instances of FXS resulting from point mutations. Whilst one could argue that the complete disruption of *FMR1* provides good construct validity for the full mutation, this does not reflect the considerable genetic heterogeneity that underlies human FXS. Although clinical severity of FXS typically correlates with CGG repeat number, the methylation status and transcriptional silencing of *FMR1* is not exactly correlated with repeat length (Loesch et al., 2004). Similarly, clinical severity can vary greatly in full mutation carriers and some individuals still show detectable levels of FMRP (Pretto et al. 2014). Individual patients also show multiple repeat lengths in their genomic DNA across different tissues due to somatic mosaicism which again contributes to the genetic heterogeneity (Lokanga et al., 2013). The full KO model also fails to recapitulate the developmental silencing of FMRP in human tissue. FMRP expression is at normal levels until approximately 10 weeks gestation in full mutation males, with

complete silencing occurring by 12.5 weeks (Willemsem et al., 2002). The loss of this complexity represents mechanistic differences between the rodent models and human genotype which may contribute to the difficulty in translating preclinical phenotypes into human trials.

These findings could also result from flaws in trial design which must be addressed in future trials for the treatment of FXS. Firstly, the age of patients used in the trial may have been sub-optimal for therapeutic intervention. Despite the use of adolescents in the mavoglurant trial, the youngest patients were still likely equivalent to a young adult age in mouse studies (Berry-Kravis et al. 2016). Whilst mouse studies have shown rescue of anatomical, biochemical and behavioural phenotypes in young adults with $mGluR_5$ antagonism (Michalon et al. 2012) some groups have reported greater treatment effects at early ages relative to later development (Su et al. 2011). As neuronal plasticity is generally declines with age, therapeutic intervention may be more effective the earlier it is begun. Therefore, in future clinical trials it would be desirable to begin at the earliest possible time point to fully test the age-dependence of $mGluR_5$ inhibition treatment. Secondly, the duration of treatments may not be adequate to see beneficial effects in human FXS trials. Given the obvious expense of clinical trials, durations are limited. As the longest study duration in the $mGluR_5$ trials was 12 weeks it may be informative to use a longer treatment period or extended clinical follow-up window to assess the efficacy of drug targets. Thirdly, the outcome measures used in these studies are typically vulnerable to a strong placebo effect due to the role of parents and caregivers in rating schemes (Berry-Kravis et al., 2015). This is a well-documented issue in trials addressing IDs (Sandler, 2005). Therefore, the use of more objective outcome measures is required to counteract this effect. Finally, the outcome measures used in these studies do not cover all of the symptomatic domains of FXS and are mainly focused on the behavioural symptoms associated with the condition. These features may not show improvement with drug treatment whereas cognitive measures may show more significant improvement to treatments aimed at restoring normal synaptic plasticity. Behaviours that can act as markers of central response, such as pre-pulse inhibition or event related potentials, may also be useful

as non-biased measures of drug treatment. These analyses can also be performed in preclinical models allowing better translation and prediction of effects in human trials.

6.2 Fear and emotionality in FXS

As well as intellectual disability, FXS is associated with a number of emotional symptoms including anxiety, high stress levels and fearfulness. Given the established role of the amygdala in emotional processing as well as the acquisition and storage of fear memories, it has become an area of interest in the study of FXS. Observations that the acquisition of fear memories is reduced in both *Fmr1* KO mice and rats, suggests that the synaptic plasticity underlying this form of memory is affected in the absence of FMRP. It has previously been reported that mGluR-dependent LTP at thalamic inputs to the lateral amygdala is absent in *Fmr1* KO mice. The lateral amygdala receives major cortical and thalamic inputs that are able to undergo synaptic plasticity during fear learning. As these inputs can undergo plasticity independently, it is likely that synaptic potentiation at either input is sufficient for fear learning (Tsvetkov et al., 2004; Romanski & LeDoux, 1992). In this thesis, we report deficits in mGluR-dependent LTP at both the cortical and thalamic inputs to the lateral amygdala in *Fmr1* KO rats. This supports the hypothesis that deficits in plasticity within the lateral amygdala contributes to fear acquisition deficits in *Fmr1* KO rats.

As well as synaptic plasticity and local signalling in the amygdala, the mPFC can also influence fear learning and emotional processing through its long range connectivity with the basolateral amygdala. Whilst the mPFC and amygdala have been studied in isolation in *Fmr1* KO mice, no studies have addressed their reciprocal connectivity and how this can influence FXS behaviours. In this thesis we have taken a first step in investigating how top-down control of the amygdala is affected in the mPFC. We found prelimbic mPFC neurons that send long-range projections to the amygdala are intrinsically hypoexcitable in *Fmr1* KO rats. This appears to be the result of structural changes in the axon initial segment (AIS), resulting in an increased action potential

threshold and dynamics in *Fmr1* KO neurons. These changes are likely the result of homeostatic changes, possibly in response to increased synaptic input in *Fmr1* KO neurons. Future work addressing the correlation of AIS length with intrinsic physiology is required to assess whether this structural change is sufficient to explain the observed neuronal hypoexcitability.

Future work using optogenetics techniques to investigate the synaptic properties of the long range connections to the basolateral amygdala in *Fmr1* KO rats would also be interesting assessing the fidelity of neurotransmission between these two areas. As fear learning has been shown to involve plasticity of both the intrinsic properties of neurons in the mPFC and their synaptic connectivity with the basolateral amygdala, it would be interesting to assess these properties before and after fear learning in *Fmr1* KO rats. As fear circuitry can also be imaged in awake rats using fMRI (Harris et al., 2015), these *in vitro* techniques could be used in complement with *in vivo* imaging to assess how the mPFC and basolateral amygdala interact during acquisition of fear memories and how this is affected in FXS.

6.3 Future modelling of FXS

Appropriate preclinical models are a requirement for the meaningful study of human diseases. Whilst animal models have no doubt contributed greatly to our understanding of FXS, the potential for human derived cell lines as a tool for the study of FXS is also an exciting prospect. Human embryonic stem cells (ESCs) from FXS affected embryos allow the investigation of aspects of FXS that were previously unattainable in other model systems such as CGG region expansion and the developmental timing of *FMR1* silencing (Castren et al. 2005; Eiges et al. 2007). Whilst this makes human ESCs a useful model, the ethical concerns and the difficulty in adequately representing the genetic and clinical variability of FXS in this system presents limitations. Advances in induced pluripotent stem cell (iPSC) technology have allowed the generation of FXS-iPSC lines derived from human FXS patients. Unlike FXS-ESCs, the *FMR1* gene maintains its hypemethylation status following reprogramming meaning it is not a suitable model for studying the silencing mechanisms of FXS (Urbach et al. 2010).

Despite this, FXS-iPSC lines present a unique system for studying subpopulations of FXS individuals with differing genetic and clinical profiles.

The addition of these human cell line technologies to the preclinical animal models of FXS and non-invasive techniques used in FXS patients provides researchers with a powerful toolbox for the study of FXS. However as each of these systems presents its own advantages and limitations, an orchestrated research effort addressing the same question across multiple levels of analysis would be most beneficial. An interesting example of this strategy has been adopted by the Fragile X syndrome research centre, a multi-centre collaborative effort using an integrated approach to test the mechanisms of auditory processing sensitivity. These groups have also attempted to develop complementary tests of auditory processing using auditory event-related potentials that will allow direct comparison between human and animal studies. The ability to perform non-invasive imaging in rats also represents a unique feature of the *Fmr1* KO rat that could be capitalised upon in a similar way. Using a framework like this where phenotypes are followed from multiple levels of analysis and using analogous methods in both preclinical models and human studies will be key to the successful translation of treatments for FXS.

References

Abel, H.J. et al., 2004. Relationships between intracellular calcium and afterhyperpolarizations in neocortical pyramidal neurons. *Journal of. Neurophysiology*, 91(1), pp.324–335.

Abraham, W.C. & Williams, J.M., 2003. Properties and mechanisms of LTP maintenance. *The Neuroscientist*, 9(6), pp.463–474.

Agulhon C. et al., 1999. Expression of *FMR1, FXR1 and FXR2* genes in human prenatal tissues. *Journal of Neuropathology and Experimental Neurology*, 58(8), pp.867-880.

Alger, B.E., 2002. Retrograde signaling in the regulation of synaptic transmission: Focus on endocannabinoids, *Progress in Neurobiology*, 68, pp.247-286.

Anglada-Figueroa, D., 2005. Lesions of the Basal Amygdala Block Expression of Conditioned Fear But Not Extinction. *Journal of Neuroscience*, 25(42), pp.9680–9685.

Ango, F. et al., 2001. Agonist-independent activation of metabotropic glutamate receptors by the intracellular protein Homer. *Nature*, 411(June), pp.962–965.

Antar, L.N. et al., 2006. Local functions for FMRP in axon growth cone motility and activity-dependent regulation of filopodia and spine synapses. *Molecular and Cellular Neuroscience*, 32(1-2), pp.37–48.

Antar, L.N. et al., 2004. Metabotropic Glutamate Receptor Activation Regulates Fragile X Mental Retardation Protein and FMR1 mRNA Localization Differentially in Dendrites and at Synapses. *The Journal of Neuroscience*, 24(11), pp.2648–2655.

Antion, M.D. et al., 2008. mGluR-dependent long-term depression is associated with increased phosphorylation of S6 and synthesis of elongation factor 1A but remains expressed in S6K-deficient mice. *Molecular and cellular biology*, 28(9), pp.2996–3007.

Ashley, C.T. et al., 1993. FMR1 protein: conserved RNP family domains and selective RNA binding. *Science*, 262(5133), pp.563–566.

Auerbach, B.D., Osterweil, E.K. & Bear, M.F., 2011. Mutations causing syndromic autism define an axis of synaptic pathophysiology. *Nature*, 480(7375), pp.63–68.

Bagni, C. et al., 2012. Science in medicine Fragile X syndrome : causes, diagnosis, mechanisms, and therapeutics. *Journal of Clinical Investigation,* 122(12), pp.4314-4322.

Bagni, C. & Greenough, W.T., 2005. From mRNP trafficking to spine dysmorphogenesis: the roots of fragile X syndrome. *Nature reviews. Neuroscience*, 6(5), pp.376–387.

Bailey, D.B. et al., 2009. No Change in the Age of Diagnosis for Fragile X Syndrome: Findings From a National Parent Survey. *Pediatrics*, 124(2), pp.527–533.

Bakker, C. et al., 1994. Fmrl Knockout Mice : A Model to Study Fragile X Mental Retardation. *Cell*, 78(1), pp.23–33.

Bakkker C.E. et al., 2000. Introduction of a *FMR1* transgene in the fragile X knockout mouse. *Neuroscience Research Communications*, 26(3), pp.265-277.

Banko, J.L., 2006. Regulation of Eukaryotic Initiation Factor 4E by Converging Signaling Pathways during Metabotropic Glutamate Receptor-Dependent Long-Term Depression.

Journal of Neuroscience, 26(8), pp.2167–2173.

Barnes, S.A. et al., 2015. Convergence of Hippocampal Pathophysiology in Syngap+/- and Fmr1-/y Mice. *Journal of Neuroscience*, 35(45), pp.15073–15081.

Baranek G.T. et al., 2008. Developmental trajectories and correlates of sensory processing in young boys with fragile X syndrome. *Physical and Occupational therapy in Pediatrics,* 28(1), pp. 79-98.

Bassell, G.J. & Warren, S.T., 2008. Fragile X Syndrome: Loss of Local mRNA Regulation Alters Synaptic Development and Function. *Neuron*, 60(2), pp.201–214.

Bauer, E.P., Schafe, G.E. & LeDoux, J.E., 2002. NMDA receptors and L-type voltage-gated calcium channels contribute to long-term potentiation and different components of fear memory formation in the lateral amygdala. *Journal of neuroscience*, 22(12), pp.5239–5249.

Bear, M.F., Huber, K.M. & Warren, S.T., 2004. The mGluR theory of fragile X mental retardation. *Trends in Neurosciences*, 27(7), pp.370–377.

Beck, H. & Yaari, Y., 2008. Plasticity of intrinsic neuronal properties in CNS disorders. *Nature reviews. Neuroscience*, 9(5), pp.357–69.

Berger, T., Larkum, M.E. & Lüscher, H.R., 2001. High I(h) channel density in the distal apical dendrite of layer V pyramidal cells increases bidirectional attenuation of EPSPs. *Journal of neurophysiology*, 85(2), pp.855–868.

Berry-Kravis, E., 2002. Epilepsy in fragile X syndrome. *Developmental medicine and child neurology*, 44(11), pp.724–728.

Berry-Kravis, E. et al., 2016. Mavoglurant in fragile X syndrome: Results of two randomized, double-blind, placebo-controlled trials. *Science translational medicine*, 8(321), pp. 1-11.

Bianchi, R. et al., 2009. Cellular plasticity for group I mGluR-mediated epileptogenesis. *Journal of neuroscience*, 29(11), pp.3497–3507.

Blair, H.T. et al., 2001. Synaptic plasticity in the lateral amygdala: a cellular hypothesis of fear conditioning. *Learning & memory*, 8(5), pp.229–242.

Bonhoeffer, T. & Yuste, R., 2002. Spine motility: Phenomenology, mechanisms, and function. *Neuron*, 35(6), pp.1019–1027.

Bontekoe, C.J. et al., 2001. Instability of a (CGG)98 repeat in the Fmr1 promoter. *Human molecular genetics*, 10(16), pp.1693–9.

De Boulle, K. et al., 1993. A point mutation in the FMR-1 gene associated with fragile X mental retardation. *Nature genetics*, 3(1), pp.31–35.

Brager, D.H., Akhavan, A.R. & Johnston, D., 2012. Impaired Dendritic Expression and Plasticity of h-Channels in the fmr1-/y Mouse Model of Fragile X Syndrome. *Cell Reports*, 1(3), pp.225–233.

Brown, M.R. et al., 2010. Fragile X mental retardation protein controls gating of the sodium-activated potassium channel Slack. *Nature neuroscience*, 13(7), pp.819–21.

Brown, S.P. & Hestrin, S., 2009. Intracortical circuits of pyramidal neurons reflect their long-range axonal targets. *Nature*, 457(7233), pp.1133–1136.

Bureau, I., Shepherd, G.M.G. & Svoboda, K., 2008. Circuit and plasticity defects in the developing somatosensory cortex of FMR1 knock-out mice. *Journal of Neuroscience*, 28(20), pp.5178–88.

Burgos-Robles, A., Vidal-Gonzalez, I. & Quirk, G.J., 2009. Sustained Conditioned Responses in Prelimbic Prefrontal Neurons Are Correlated with Fear Expression and Extinction Failure. *Journal of Neuroscience*, 29(26), pp.8474–8482.

Carrasquillo, Y., Burkhalter, A. & Nerbonne, J.M., 2012. A-type K+ channels encoded by Kv4.2, Kv4.3 and Kv1.4 differentially regulate intrinsic excitability of cortical pyramidal neurons. *The Journal of physiology*, 590(16), pp.3877–90.

Castren, M. et al., 2003. Augmentation of auditory N1 in children with fragile X syndrome. *Brain Topography*, 15(3), pp.165–171.

Castren M. et al., 2005. Altered differentiation of neural stem cells in fragile X syndrome. *PNAS*, 102(49), pp.17834-9.

Centonze, D. et al., 2008. Abnormal Striatal GABA Transmission in the Mouse Model for the Fragile X Syndrome. *Biological Psychiatry*, 63(10), pp.963–973.

Chen, L. & Toth, M., 2001. Fragile X mice develop sensory hyperreactivity to auditory stimuli. *Neuroscience*, 103(4), pp.1043–1050.

Cheriyan, J. et al., 2016. Specific targeting of the basolateral amygdala to projectionally defined pyramidal neurons in prelimbic and infralimbic cortex. *eNeuro*, 3(2).

Chevaleyre, V., Takahashi, K.A. & Castillo, P.E., 2006. Endocannabinoid-Mediated Synaptic Plasticity in the Cns. *Annual Review of Neuroscience*, 29(1), pp.37–76.

Cho, J.-H. et al., 2011. Coactivation of thalamic and cortical pathways induces input timing–dependent plasticity in amygdala. *Nature Neuroscience*, 15(1), pp.113–122.

Choi, D.C. et al., 2010. Prelimbic cortical BDNF is required for memory of learned fear but not extinction or innate fear. *Proceedings of the National Academy of Sciences of the United States of America*, 107(6), pp.2675–2680.

Chuang, S.-C., 2005. Prolonged Epileptiform Discharges Induced by Altered Group I Metabotropic Glutamate Receptor-Mediated Synaptic Responses in Hippocampal Slices of a Fragile X Mouse Model. *Journal of Neuroscience*, 25(35), pp.8048–8055.

Coetzee, W.A. et al., 1999. Molecular diversity of K+ channels. *Annals of the New York Academy of Sciences*, 868, pp.233–285.

Coffee, B. et al., 2009. Incidence of Fragile X Syndrome by Newborn Screening for Methylated FMR1 DNA. *American Journal of Human Genetics*, 85(4), pp.503–514.

Collins, S.C. et al., 2010. Array-based FMR1 sequencing and deletion analysis in patients with a fragile X syndrome-like phenotype. *PLoS ONE*, 5(3), pp.3–6.

Comery, T. a et al., 1997. Abnormal dendritic spines in fragile X knockout mice. *Proceedings of the National Academy of Sciences of the United States of America*, 94(May), pp.5401–5404.

Contractor, A., Klyachko, V.A. & Portera-Cailliau, C., 2015. Altered Neuronal and Circuit Excitability in Fragile X Syndrome. *Neuron*, 87(4), pp.699–715.

Conway, G.S. et al., 1998. Fragile X premutation screening in women with premature ovarian failure. *Human reproduction (Oxford, England)*, 13(5), pp.1184–7.

Corcoran, K.A. & Quirk, G.J., 2007. Activity in prelimbic cortex is necessary for the expression of learned, but not innate, fears. *Journal of Neuroscience*, 27(4), pp.840–844.

Cordeiro, L. et al., 2011. Clinical assessment of DSM-IV anxiety disorders in fragile X syndrome: prevalence and characterization. *Journal of neurodevelopmental disorders*, 3(1), pp.57–67.

Crair, M.C. & Malenka, R.C., 1995. A critical period for long-term potentiation at thalamocortical synapses. *Nature*, 375(6529), pp.325–328.

Cruz-Martín, A., Crespo, M. & Portera-Cailliau, C., 2010. Delayed stabilization of dendritic spines in fragile X mice. *Journal of neuroscience*, 30(23), pp.7793–7803.

Curia, G. et al., 2009. Downregulation of tonic GABAergic inhibition in a mouse model of fragile X syndrome. *Cerebral Cortex*, 19(7), pp.1515–1520.

Dölen, G. et al., 2007. Correction of Fragile X Syndrome in Mice. *Neuron*, 56(6), pp.955–962.

D'Hulst, C. et al., 2006. Decreased expression of the GABAA receptor in fragile X syndrome. *Brain Research*, 1121(1), pp.238–245.

Dansie, L.E. et al., 2013. Long-lasting effects of minocycline on behavior in young but not adult Fragile X mice. *Neuroscience*, 246, pp.186–198.

Darnell, J.C. et al., 2011. FMRP stalls ribosomal translocation on mRNAs linked to synaptic function and autism. *Cell*, 146(2), pp.247–261.

Darnell, J.C. et al., 2001. Fragile X mental retardation protein targets G quartet mRNAs important for neuronal function. *Cell*, 107, pp.489–499.

Darnell, J.C., Mostovetsky, O. & Darnell, R.B., 2005. FMRP RNA targets: Identification and validation. *Genes, Brain and Behavior*, 4(6), pp.341–349.

David L. Nelson, H.T.O. and S.T.W., 2013. The Unstable Repeats - Three Evolving Faces of Neurological Disease. *Neuron*, 77(5), pp.825–843.

Davidkova, G. & Carroll, R.C., 2007. Characterization of the role of microtubule-associated protein 1B in metabotropic glutamate receptor-mediated endocytosis of AMPA receptors in hippocampus. *Journal of neuroscience*, 27(48), pp.13273–13278.

Davis, M., 2006. Neural systems involved in fear and anxiety measured with fear-potentiated startle. *American Psychologist*, 61(8), pp.741–756.

Dembrow, N.C., Chitwood, R.A. & Johnston, D., 2010. Projection-Specific Neuromodulation of Medial Prefrontal Cortex Neurons. *Journal of Neuroscience*, 30(50), pp.16922–16937.

Deng, P.Y. et al., 2013. FMRP Regulates Neurotransmitter Release and Synaptic Information Transmission by Modulating Action Potential Duration via BK Channels. *Neuron*, 77(4), pp.696–711.

Deng, P.-Y., Sojka, D. & Klyachko, V. a, 2011. Abnormal presynaptic short-term plasticity and information processing in a mouse model of fragile X syndrome. *Journal of neuroscience*, 31(30), pp.10971–10982.

Desai, N.S. et al., 2006. Early Postnatal Plasticity in Neocortex of Fmr1 Knockout Mice Early Postnatal Plasticity in Neocortex of Fmr1 Knockout Mice. *Journal of*

Neurophysiology, 96, pp.1734–1745.

Devys, D. et al., 1993. The FMR-1 protein is cytoplasmic, most abundant in neurons and appears normal in carriers of a fragile X premutation. *Nature genetics*, 4(4), pp.335–340.

Dong, Y. & White, F.J., 2003. Dopamine D1-class receptors selectively modulate a slowly inactivating potassium current in rat medial prefrontal cortex pyramidal neurons. *Journal of Neuroscience*, 23(7), pp.2686–2695.

Doyere, V. et al., 2003. Long-term potentiation in freely moving rats reveals asymmetries in thalamic and cortical inputs to the lateral amygdala. *European Journal of Neuroscience*, 17(12), pp.2703–2715.

Dufner, A. & Thomas, G., 1999. Ribosomal S6 Kinase Signaling and the Control of Translation. *Experimental Cell Research*, 253, pp.100 – 109.

Ehrlich, I. et al., 2009. Amygdala Inhibitory Circuits and the Control of Fear Memory. *Neuron*, 62(6), pp.757–771.

Eiges R. et al., 2007. Developmental study of fragile X syndrome using human embryonic stem cells derived from preimplantation genetically diagnosed embryos. *Cell Stem Cell*, 1, pp.568-577.

Euston, D.R., Gruber, A.J. & McNaughton, B.L., 2012. The Role of Medial Prefrontal Cortex in Memory and Decision Making. *Neuron*, 76(6), pp.1057–1070.

Faas, G.C. et al., 2002. Modulation of presynaptic calcium transients by metabotropic glutamate receptor activation: a differential role in acute depression of synaptic transmission and long-term depression. *Journal of neuroscience*, 22(16), pp.6885–6890.

Fagiolini, M. & Leblanc, J.J., 2011. Autism: A critical period disorder? *Neural Plasticity*, 2011.

Feng, Y. et al., 1997. FMRP associates with polyribosomes as an mRNP, and the I304N mutation of severe fragile X syndrome abolishes this association. *Molecular cell*, 1(1), pp.109–118.

Ferraguti, F. & Shigemoto, R., 2006. Metabotropic glutamate receptors. *Cell and Tissue Research*, 326(2), pp.483–504.

Ferron, L. et al., 2014. Fragile X mental retardation protein controls synaptic vesicle exocytosis by modulating N-type calcium channel density. *Nature communications*, 5, p.3628.

Fitzjohn, S.M. et al., 1999. DHPG-induced LTD in area CA1 of juvenile rat hippocampus; characterisation and sensitivity to novel mGlu receptor antagonists. *Neuropharmacology*, 38(10), pp.1577–1583.

Fombonne, E., 2003. Epidemiological surveys of autism and other pervasive developmental disorders: An update. *Journal of Autism and Developmental Disorders*, 33(4), pp.365–382.

Fontanez-Nuin, D.E. et al., 2011. Memory for fear extinction requires mGluR5-mediated activation of infralimbic neurons. *Cerebral Cortex*, 21(3), pp.727–735.

Frankland, P.W. et al., 2004. Sensorimotor gating abnormalities in young males with fragile

X syndrome and Fmr1-knockout mice. *Molecular psychiatry*, 9(4), pp.417–25.

Frenkel, M.Y. & Bear, M.F., 2004. How monocular deprivation shifts ocular dominance in visual cortex of young mice. *Neuron*, 44(6), pp.917–923.

Fu, Y.H. et al., 1991. Variation of the CGG repeat at the fragile X site results in genetic instability: resolution of the Sherman paradox. *Cell*, 67(6), pp.1047–58.

Gabbott, P.L.A. et al., 2005. Prefrontal cortex in the rat: Projections to subcortical autonomic, motor, and limbic centers. *Journal of Comparative Neurology*, 492(2), pp.145–177.

Gabel, L.A. et al., 2004. Visual Experience Regulates Transient Expression and Dendritic Localization of Fragile X Mental Retardation Protein. *J Neurosci*, 24(47), pp.10579–10583.

Gale, G.D. et al., 2004. Role of the Basolateral Amygdala in the Storage of Fear Memories across the Adult Lifetime of Rats. *Journal of Neuroscience*, 24(15), pp.3810–3815.

Gallagher, S.M., 2004. Extracellular Signal-Regulated Protein Kinase Activation Is Required for Metabotropic Glutamate Receptor-Dependent Long-Term Depression in Hippocampal Area CA1. *Journal of Neuroscience*, 24(20), pp.4859–4864.

Gantois, I. et al., 2013. Chronic administration of AFQ056/Mavoglurant restores social behaviour in Fmr1 knockout mice. *Behavioural Brain Research*, 239(1), pp.72–79.

Gantois, I. et al., 2006. Expression profiling suggests underexpression of the GABAA receptor subunit δ in the fragile X knockout mouse model. *Neurobiology of Disease*, 21(2), pp.346–357.

Geschwind, D.H. & Levitt, P., 2007. Autism spectrum disorders: developmental disconnection syndromes. *Current Opinion in Neurobiology*, 17(1), pp.103–111.

Gibbs, R. a et al., 2004. Genome sequence of the Brown Norway rat yields insights into mammalian evolution. *Nature*, 428(6982), pp.493–521.

Gibson, J.R. et al., 2008. Imbalance of neocortical excitation and inhibition and altered UP states reflect network hyperexcitability in the mouse model of fragile X syndrome. *Journal of neurophysiology*, 100(5), pp.2615–26.

Giuffrida, R., 2005. A Reduced Number of Metabotropic Glutamate Subtype 5 Receptors Are Associated with Constitutive Homer Proteins in a Mouse Model of Fragile X Syndrome. *Journal of Neuroscience*, 25(39), pp.8908–8916.

Gladding, C.M., Fitzjohn, S.M. & Molnar, E., 2009. Metabotropic Glutamate Receptor-Mediated Long- Term Depression : Molecular Mechanisms. *Pharmacological reviews*, 61(4), pp.395–412.

Godfraind, J.M. et al., 1996. Long-term potentiation in the hippocampus of fragile X knockout mice. *American Journal of Medical Genetics*, 64(2), pp.246–251.

Gogolla, N. et al., 2009. Common circuit defect of excitatory-inhibitory balance in mouse models of autism. *Journal of Neurodevelopmental Disorders*, 1(2), pp.172–181.

Gothelf, D. et al., 2008. Neuroanatomy of fragile X syndrome is associated with aberrant behavior and the fragile X mental retardation protein (FMRP). *Annals of Neurology*, 63(1), pp.40–51.

Goto, Y., Yang, C.R. & Otani, S., 2010. Functional and Dysfunctional Synaptic Plasticity in

Prefrontal Cortex: Roles in Psychiatric Disorders. *Biological Psychiatry*, 67(3), pp.199–207.

Granon, S. et al., 2000. Enhanced and impaired attentional performance after infusion of D1 dopaminergic receptor agents into rat prefrontal cortex. *Journal of neuroscience*, 20(3), pp.1208–1215.

Gross, C. et al., 2010. Excess phosphoinositide 3-kinase subunit synthesis and activity as a novel therapeutic target in fragile X syndrome. *Journal of neuroscience*, 30(32), pp.10624–10638.

Gross, C. et al., 2011. Fragile X mental retardation protein regulates protein expression and mRNA translation of the potassium channel Kv4.2. *Journal of neuroscience*, 31(15), pp.5693–5698.

Grubb, M.S. & Burrone, J., 2010. Activity-dependent relocation of the axon initial segment fine-tunes neuronal excitability. *Nature*, 465(7301), pp.1070–4.

Hagerman, R.J. & Hagerman, P.J., 2002. The fragile X premutation: Into the phenotypic fold. *Current Opinion in Genetics and Development*, 12(3), pp.278–283.

Hanson, J.E. & Madison, D. V, 2007. Presynaptic FMR1 genotype influences the degree of synaptic connectivity in a mosaic mouse model of fragile X syndrome. *Journal of neuroscience*, 27(15), pp.4014–4018.

Harlow, E.G. et al., 2010. Critical Period Plasticity Is Disrupted in the Barrel Cortex of Fmr1 Knockout Mice. *Neuron*, 65(3), pp.385–398.

Harris, A.P. et al., 2015. Imaging learned fear circuitry in awake mice using fMRI. *The European journal of neuroscience*, 42(5), pp.2125–34.

Hazlett, H.C. et al., 2009. Teasing apart the heterogeneity of autism: Same behavior, different brains in toddlers with fragile X syndrome and autism. *Journal of Neurodevelopmental Disorders*, 1(1), pp.81–90.

Hefner, K. et al., 2008. Impaired Fear Extinction Learning and Cortico-Amygdala Circuit Abnormalities in a Common Genetic Mouse Strain. *Journal of Neuroscience*, 28(32), pp.8074–8085.

Hessl, D., Rivera, S.M. & Reiss, A.L., 2004. The Neuroanatomy and Neuroendocrinology of Fragile X Syndrome. *Mental Retardation and Developmental Disabilities Research Reviews*, 10(1), pp.17–24.

Heulens, I. et al., 2012. Pharmacological treatment of fragile X syndrome with GABAergic drugs in a knockout mouse model. *Behavioural Brain Research*, 229(1), pp.244–249.

Hinton V.J. et al., 1991. Analysis of neocortex in three males with the fragile X syndrome. *American journal of medical genetics*, 41(3), pp.289-294.

Hoffman, D. a et al., 1997. K+ channel regulation of signal propagation in dendrites of hippocampal pyramidal neurons. *Nature*, 387(6636), pp.869–875.

Hoover, W.B. & Vertes, R.P., 2007. Anatomical analysis of afferent projections to the medial prefrontal cortex in the rat. *Brain Structure and Function*, 212(2), pp.149–179.

Hoppa, M.B. et al., 2015. Connectivity of mouse somatosensory and prefrontal cortex examined with trans-synaptic tracing. *Nature Neuroscience*, 84(4), pp.778–789.

Hou, L. et al., 2006. Dynamic Translational and Proteasomal Regulation of Fragile X Mental

Retardation Protein Controls mGluR-Dependent Long-Term Depression. *Neuron*, 51(4), pp.441–454.

Hou, L. & Klann, E., 2004. Activation of the Phosphoinositide 3-Kinase – Akt – Mammalian Target of Rapamycin Signaling Pathway Is Required for Metabotropic Glutamate Receptor-Dependent Long-Term Depression. *Journal of Neuroscience*, 24(28), pp.6352–6361.

Huang, Y.-Y. et al., 2004. Genetic evidence for the bidirectional modulation of synaptic plasticity in the prefrontal cortex by D1 receptors. *Proceedings of the National Academy of Sciences of the United States of America*, 101(9), pp.3236–3241.

Hubel, D.H. & Wiesel, T.N., 1970. The period of susceptibility to the physiological effects of unilateral eye closure in kittens. *The Journal of physiology*, 206(2), pp.419–436.

Huber, K.M. et al., 2002. Altered synaptic plasticity in a mouse model of fragile X mental retardation. *Proceedings of the National Academy of Sciences of the United States of America*, 99(11), pp.7746–50.

Huber, K.M., 2000. Role for Rapid Dendritic Protein Synthesis in Hippocampal mGluR-Dependent Long-Term Depression. *Science*, 288(5469), pp.1254–1256.

Huber, K.M., Kayser, M.S. & Bear, M.F., 2000. Role for rapid dendritic protein synthesis in hippocampal mGluR-dependent long-term depression. *Science*, 288(5469), pp.1254–1257.

Huber, K.M., Roder, J.C. & Bear, M.F., 2001. Chemical Induction of mGluR5- and Protein Synthesis-Dependent Long-Term Depression in Hippocampal Area CA1. *Journal of Neurophysiology*, 86(1), pp.321–325.

Humeau, Y. et al., 2007. A Pathway-Specific Function for Different AMPA Receptor Subunits in Amygdala Long-Term Potentiation and Fear Conditioning. *Journal of Neuroscience,* 27(41), pp.10947-10956.

El Idrissi, A. et al., 2005. Decreased GABAA receptor expression in the seizure-prone fragile X mouse. *Neuroscience Letters*, 377(3), pp.141–146.

Irwin, S.A. et al., 2001. Abnormal dendritic spine characteristics in the temporal and visual cortices of patients with fragile-X syndrome: A quantitative examination. *American Journal of Medical Genetics*, 98(2), pp.161–167.

Jacquemont, S. et al., 2011. Epigenetic modification of the FMR1 gene in fragile X syndrome is associated with differential response to the mGluR5 antagonist AFQ056. *Science translational medicine*, 3(64),

Jacquemont, S. et al., 2004. Penetrance of the Fragile X – Associated Tremor / Ataxia Syndrome in a. *JAMA*, 291(4), pp.460-69.

Jung, K.-M. et al., 2012. Uncoupling of the endocannabinoid signalling complex in a mouse model of fragile X syndrome. *Nature Communications*, 3, p.1080.

Kalmbach, B.E. et al., 2013. Dendritic Generation of mGluR-Mediated Slow Afterdepolarization in Layer 5 Neurons of Prefrontal Cortex. J*ournal of Neuroscience*, 33(33), pp.13518–32.

Kalmbach, B.E., Johnston, D. & Brager, D.H., 2015. Cell-Type Specific Channelopathies in the Prefrontal Cortex of the fmr1-/y Mouse Model of Fragile X Syndrome(1,2,3). *eNeuro*, 2(6)

Kang, J., Huguenard, J.R. & Prince, D. a, 2000. Voltage-gated potassium channels activated during action potentials in layer V neocortical pyramidal neurons. *Journal of neurophysiology*, 83(1), pp.70–80.

Kates, W.R. et al., 1997. Reliability and validity of MRI measurement of the amygdala and hippocampus in children with fragile X syndrome. *Psychiatry Research - Neuroimaging*, 75(1), pp.31–48.

Kaufmann, W.E. & Moser, H.W., 2000. Dendritic anomalies in disorders associated with mental retardation. *Cerebral cortex*, 10(10), pp.981–991.

Kemp, N. & Bashir, Z.I., 1999. Induction of LTD in the adult hippocampus by the synaptic activation of AMPA/kainate and metabotropic glutamate receptors. *Neuropharmacology*, 38(4), pp.495–504.

Kim, G.E. & Kaczmarek, L.K., 2014. Emerging role of the KCNT1 Slack channel in intellectual disability. *Frontiers in cellular neuroscience*, 8(July), p.209.

Kim, J.J. et al., 2002. The stressed hippocampus, synaptic plasticity and lost memories. *Nature reviews. Neuroscience*, 3(6), pp.453–62.

Kiritoshi, T. et al., 2013. Modulation of pyramidal cell output in the medial prefrontal cortex by mGluR5 interacting with CB1. *Neuropharmacology*, 66, pp.170–178.

Knapska, E. et al., 2012. Functional anatomy of neural circuits regulating fear and extinction. *Proceedings of the National Academy of Sciences*, 109(42), pp.17093–17098.

Koekkoek, S.K.E. et al., 2005. Deletion of FMR1 in purkinje cells enhances parallel fiber LTD, enlarges spines, and attenuates cerebellar eyelid conditioning in fragile X syndrome. *Neuron*, 47(3), pp.339–352.

Koga, K. et al., 2015. Impaired Presynaptic Long-Term Potentiation in the Anterior Cingulate Cortex of Fmr1 Knock-out Mice. *Journal of Neuroscience*, 35(5), pp.2033–2043.

Kole, M.H.P. et al., 2008. Action potential generation requires a high sodium channel density in the axon initial segment. *Nature neuroscience*, 11(2), pp.178–86.

Kole, M.H.P. & Stuart, G.J., 2008. Is action potential threshold lowest in the axon? *Nature neuroscience*, 11(11), pp.1253–1255.

Korngreen, a & Sakmann, B., 2000. Voltage-gated K+ channels in layer 5 neocortical pyramidal neurones from young rats: subtypes and gradients. *The Journal of physiology*, 525(3), pp.621–639.

Kramvis, I. et al., 2013. Hyperactivity, perseveration and increased responding during attentional rule acquisition in the Fragile X mouse model. *Frontiers in behavioral neuroscience*, 7(November), p.172.

Kratovac, S. & Corbin, J.G., 2013. Developmental changes in expression of inhibitory neuronal proteins in the Fragile X Syndrome mouse basolateral amygdala. *Brain Research*, 1537, pp.69–78.

Kremer, E.J. et al., 1991. Mapping of DNA Instability at the Fragile-X to a Trinucleotide Repeat Sequence P(CCG)N. *Science*, 252(5013), pp.1711–1714.

Kronk, R. et al., 2010. Prevalence, nature, and correlates of sleep problems among children with fragile X syndrome based on a large scale parent survey. *Sleep*, 33(5), pp.679–

687.

Krook-Magnuson, E. et al., 2012. New dimensions of interneuronal specialization unmasked by principal cell heterogeneity. *Trends in Neurosciences*, 35(3), pp.175–184.

Krueger, D.D. et al., 2011. Cognitive dysfunction and prefrontal synaptic abnormalities in a mouse model of fragile X syndrome. *Proceedings of the National Academy of Sciences of the United States of America*, 108(6), pp.2587–2592.

Larson, J. et al., 2005. Age-Dependent and Selective Impairment of Long-Term Potentiation in the Anterior Piriform Cortex of Mice Lacking the Fragile X Mental Retardation Protein. *J Neurosci*, 25(41), pp.9460–9.

Lauterborn, J.C. et al., 2007. Brain-Derived Neurotrophic Factor Rescues Synaptic Plasticity in a Mouse Model of Fragile X Syndrome. *J Neurosci*, 27(40), pp.10685–94.

Laviolette, S.R., 2005. A Subpopulation of Neurons in the Medial Prefrontal Cortex Encodes Emotional Learning with Burst and Frequency Codes through a Dopamine D4 Receptor-Dependent Basolateral Amygdala Input. *Journal of Neuroscience*, 25(26), pp.6066–6075.

LeDoux, J., 2003. The emotional brain, fear, and the amygdala. *Cellular and Molecular Neurobiology*, 23(4-5), pp.727–738.

LeDoux, J. et al., 1990. The lateral amygdaloid nucleus: sensory interface of the amygdala in fear conditioning. *Journal of Neuroscience*, 10(4)(4), pp.1062–1069.

Lee, A.T. et al., 2014. A Class of GABAergic Neurons in the Prefrontal Cortex Sends Long-Range Projections to the Nucleus Accumbens and Elicits Acute Avoidance Behavior. *Journal of Neuroscience*, 34(35), pp.11519–11525.

Lee, H.Y. et al., 2011. Bidirectional Regulation of Dendritic Voltage-Gated Potassium Channels by the Fragile X Mental Retardation Protein. *Neuron*, 72(6), p.1091.

Lee, U.S. & Cui, J., 2010. BK channel activation: Structural and functional insights. *Trends in Neurosciences*, 33(9), pp.415–423.

Leonard, H. & Wen, X., 2002. The epidemiology of mental retardation: Challenges and opportunities in the new millennium. *Mental Retardation and Developmental Disabilities Research Reviews*, 8(3), pp.117–134.

Levenga, J. et al., 2011. AFQ056, a new mGluR5 antagonist for treatment of fragile X syndrome. *Neurobiology of Disease*, 42(3), pp.311–317.

Li, C. et al., 2007. The different roles of cyclinD1-CDK4 in STP and mGluR-LTD during the postnatal development in mice hippocampus area CA1. *BMC developmental biology*, 7, p.57.

Li, J. et al., 2002. Reduced cortical synaptic plasticity and GluR1 expression associated with fragile X mental retardation protein deficiency. *Molecular and cellular neurosciences*, 19(2), pp.138–151.

Little, J.P. & Carter, a. G., 2012. Subcellular Synaptic Connectivity of Layer 2 Pyramidal Neurons in the Medial Prefrontal Cortex. *Journal of Neuroscience*, 32(37), pp.12808–12819.

Little, J.P. & Carter, A.G., 2013. Synaptic Mechanisms Underlying Strong Reciprocal Connectivity between the Medial Prefrontal Cortex and Basolateral Amygdala. *Journal*

of Neuroscience current issue, 33(39), pp.15333–15342.

Liu, Z.-H., Chuang, D.-M. & Smith, C.B., 2011. Lithium ameliorates phenotypic deficits in a mouse model of fragile X syndrome. *The international journal of neuropsychopharmacology / official scientific journal of the Collegium Internationale Neuropsychopharmacologicum (CINP)*, 14(5), pp.618–30.

Loesch, D.Z. et al., 2004. Phenotypic variation and FMRP levels in fragile X. *Mental Retardation and developmental disabilities research reviews,* 10(1), pp.31-41.

Lokanga R.A. et al., 2013. Somatic expansion in mouse and human carriers of fragile X permutation alleles. *Human mutation*, 34(1), pp.157-66.

Lubs, H. a, 1969. A marker X chromosome. *American journal of human genetics*, 21(3), pp.231–244.

Lubs, H.A., Stevenson, R.E. & Schwartz, C.E., 2012. Fragile X and X-linked intellectual disability: Four decades of discovery. *American Journal of Human Genetics*, 90(4), pp.579–590.

Lujan, R. et al., 1996. Perisynaptic location of metabotropic glutamate receptors mGluR1 and mGluR5 on dendrites and dendritic spines in the rat hippocampus. *The European journal of neuroscience*, 8(7), pp.1488–1500.

Maccarrone, M. et al., 2010. Abnormal mGlu 5 receptor/endocannabinoid coupling in mice lacking FMRP and BC1 RNA. *Neuropsychopharmacology : official publication of the American College of Neuropsychopharmacology*, 35(7), pp.1500–9.

Marek, G.J; Zhang, C., 2009. activation of metabotropic glutamate5 receptors induces spontaneous excitatory synaptic currents in layer V pyrmidal cells of the rat prefrontal cortex. , 442(3), pp.239–243.

Marek, G.J. & Zhang, C., 2008. Activation of metabotropic glutamate 5 (mGlu5) receptors induces spontaneous excitatory synaptic currents in layer V pyramidal cells of the rat prefrontal cortex. *Neuroscience Letters*, 442(3), pp.239–243.

Martin, B.S., Corbin, J.G. & Huntsman, M.M., 2014. Deficient tonic GABAergic conductance and synaptic balance in the Fragile-X Syndrome Amygdala. *Journal of neurophysiology*, 3(303), pp.890–902.

Martin, H.G.S. et al., 2015. Age-Dependent Long-Term Potentiation Deficits in the Prefrontal Cortex of the Fmr1 Knockout Mouse Model of Fragile X Syndrome. *Cerebral cortex*, pp.1–9.

Martin, J.P. & Bell, J., 1943. A Pedigree of Mental Defect Showing Sex-Linkage. *Journal of neurology and psychiatry*, 6(3-4), pp.154–157.

McBride, S.M.J. et al., 2005. Pharmacological rescue of synaptic plasticity, courtship behavior, and mushroom body defects in a Drosophila model of Fragile X syndrome. *Neuron*, 45(5), pp.753–764.

Mcdonald, A.J., 1998. Cortical Pathways To the Mammalian Amygdala. *Progress in Neurobiology*, 55(3), pp. 257-332.

McKay, B.M. et al., 2009. Intrinsic neuronal excitability is reversibly altered by a single experience in fear conditioning. *Journal of neurophysiology*, 102(5), pp.2763–70.

McNaughton, C.H. et al., 2008. Evidence for social anxiety and impaired social cognition in

a mouse model of fragile X syndrome. *Behavioral Neuroscience*, 122(2), pp.293–300.

Meredith, R.M. et al., 2007. Increased Threshold for Spike-Timing-Dependent Plasticity Is Caused by Unreliable Calcium Signaling in Mice Lacking Fragile X Gene Fmr1. *Neuron*, 54(4), pp.627–638.

Merenstein, S.A. et al., 1996. Molecular-clinical correlations in males with an expanded FMR1 mutation. *American Journal of Medical Genetics*, 64(2), pp.388–394.

Michalon, A. et al., 2014. Chronic metabotropic glutamate receptor 5 inhibition corrects local alterations of brain activity and improves cognitive performance in fragile X mice. *Biological Psychiatry*, 75(3), pp.189–197.

Michalon, A. et al., 2012. Chronic Pharmacological mGlu5 Inhibition Corrects Fragile X in Adult Mice. *Neuron*, 74(1), pp.49–56.

Miller, E.K., 2000. The prefrontal cortex and cognitive control. *Nature reviews: Neuroscience*, 1(1), pp.59–65.

Moon, J. et al., 2006. Attentional dysfunction, impulsivity, and resistance to change in a mouse model of fragile X syndrome. *Behavioral neuroscience*, 120(6), pp.1367–79.

Morishima, M. et al., 2011. Highly Differentiated Projection-Specific Cortical Subnetworks. *Journal of Neuroscience*, 31(28), pp.10380–10391.

Moult, P.R. et al., 2008. Co-activation of p38 mitogen-activated protein kinase and protein tyrosine phosphatase underlies metabotropic glutamate receptor-dependent long-term depression. *Journal of Physiology*, 586(10), pp.2499–2510.

Muddashetty, R.S. et al., 2007. Dysregulated metabotropic glutamate receptor-dependent translation of AMPA receptor and postsynaptic density-95 mRNAs at synapses in a mouse model of fragile X syndrome. *Journal of neuroscience*, 27(20), pp.5338–5348.

Muigg, P. et al., 2008. Impaired extinction of learned fear in rats selectively bred for high anxiety - Evidence of altered neuronal processing in prefrontal-amygdala pathways. *European Journal of Neuroscience*, 28(11), pp.2299–2309.

Muly, E.C., Maddox, M. & Smith, Y., 2003. Distribution of mGluR1 and mGluR5 Immunolabeling in Primate Prefrontal Cortex. *Journal of Comparative Neurology*, 467(4), pp.521–535.

Musumeci, S.A. et al., 2000. Audiogenic seizures susceptibility in transgenic mice with fragile X syndrome. *Epilepsia*, 41(1), pp.19–23.

Myrick, L.K. et al., 2015. Independent role for presynaptic FMRP revealed by an FMR1 missense mutation associated with intellectual disability and seizures. *Proceedings of the National Academy of Sciences of the United States of America*, 112(4), pp.949–56.

Nakamoto, M. et al., 2007. Fragile X mental retardation protein deficiency leads to excessive mGluR5-dependent internalization of AMPA receptors. *Proceedings of the National Academy of Sciences of the United States of America*, 104(39), pp.15537–42.

Narayanan, U. et al., 2007. FMRP phosphorylation reveals an immediate-early signaling pathway triggered by group I mGluR and mediated by PP2A. *Journal of Neuroscience*, 27(52), pp.14349–14357.

Narayanan, U. et al., 2008. S6K1 phosphorylates and regulates fragile X mental retardation protein (FMRP) with the neuronal protein synthesis-dependent mammalian target of

rapamycin (mTOR) signaling cascade. *Journal of Biological Chemistry*, 283(27), pp.18478–18482.

Neves-Pereira, M. et al., 2009. Deregulation of EIF4E: a novel mechanism for autism. *Journal of Medical Genetics*, 46(11), pp.759–65.

Nimchinsky, E. a, Oberlander, a M. & Svoboda, K., 2001. Abnormal development of dendritic spines in FMR1 knock-out mice. *Journal of Neuroscience*, 21(14), pp.5139–5146.

Oliet, S.H., Malenka, R.C. & Nicoll, R.A., 1997. Two distinct forms of long-term depression coexist in CA1 hippocampal pyramidal cells. *Neuron*, 18(6), pp.969–982.

Olmos-Serrano, J.L. et al., 2010. Defective GABAergic neurotransmission and pharmacological rescue of neuronal hyperexcitability in the amygdala in a mouse model of fragile X syndrome. *Journal of neuroscience*, 30(29), pp.9929–38.

Olmos-Serrano, J.L., Corbin, J.G. & Burns, M.P., 2011. The GABA A receptor agonist THIP ameliorates specific behavioral deficits in the mouse model of fragile X syndrome. *Developmental Neuroscience*, 33(5), pp.395–403.

Orsini, C. a. et al., 2011. Hippocampal and Prefrontal Projections to the Basal Amygdala Mediate Contextual Regulation of Fear after Extinction. *Journal of Neuroscience*, 31(47), pp.17269–17277.

Osterweil, E.K. et al., 2010. Hypersensitivity to mGluR5 and ERK1/2 leads to excessive protein synthesis in the hippocampus of a mouse model of fragile X syndrome. *Journal of neuroscience*, 30(46), pp.15616–27.

Oswald, M.J. et al., 2009. IH current generates the afterhyperpolarisation following activation of subthreshold cortical synaptic inputs to striatal cholinergic interneurons. *Journal of Physiology*, 587(24), pp.5879–97.

Palmer, M.J. et al., 1997. The group I mGlu receptor agonist DHPG induces a novel form of LTD in the CA1 region of the hippocampus. *Neuropharmacology*, 36(11-12), pp.1517–1532.

Paluszkiewicz, S.M. et al., 2011. Impaired inhibitory control of cortical synchronization in fragile X syndrome. *Journal of neurophysiology*, 106(5), pp.2264–72.

Pan, F. et al., 2010. Dendritic spine instability and insensitivity to modulation by sensory experience in a mouse model of fragile X syndrome. *Proceedings of the National Academy of Sciences of the United States of America*, 107(41), pp.17768–17773.

Paradee, W. et al., 1999. Fragile X mouse: Strain effects of knockout phenotype and evidence suggesting deficient amygdala function. *Neuroscience*, 94(1), pp.185–192.

Parvez, S., Ramachandran, B. & Frey, J.U., 2010. Functional differences between and across different regions of the apical branch of hippocampal CA1 dendrites with respect to long-term depression induction and synaptic cross-tagging. *Journal of Neuroscience*, 30(14), pp.5118–23.

Patel, A.B. et al., 2014. Postsynaptic FMRP promotes the pruning of cell-to-cell connections among pyramidal neurons in the L5A neocortical network. *Journal of Neuroscience*, 34(9), pp.3413–8.

Paul, K., Venkitaramani, D. V & Cox, C.L., 2013. Dampened dopamine-mediated neuromodulation in prefrontal cortex of fragile X mice. *Journal of Physiology*, 591(4),

pp.1133–43.

Pavlov, I., Riekki, R. & Taira, T., 2004. Synergistic action of GABA-A and NMDA receptors in the induction of long-term depression in glutamatergic synapses in the newborn rat hippocampus. *The European Journal of Neuroscience*, 20(11), pp.3019–26.

Paxinos G. & Watson C., 2006. *The rat brain in stereotaxic co-ordinates*. 6th ed. Academic press.

Pfeiffer, B.E. & Huber, K.M., 2007. Fragile X mental retardation protein induces synapse loss through acute postsynaptic translational regulation. *Journal of Neuroscience*, 27(12), pp.3120–3130.

Pieretti, M. et al., 1991. Absence of expression of the FMR-1 gene in fragile X syndrome. *Cell*, 66(4), pp.817–822.

Pilpel, Y. et al., 2009. Synaptic ionotropic glutamate receptors and plasticity are developmentally altered in the CA1 field of Fmr1 knockout mice. *Journal of Physiology*, 587(4), pp.787–804.

Pitkänen, A., Savander, V. & LeDoux, J.E., 1997. Organization of intra-amygdaloid circuitries in the rat: An emerging framework for understanding functions of the amygdala. *Trends in Neurosciences*, 20(11), pp.517–523.

Poncer, J.C. & Malinow, R., 2001. Postsynaptic conversion of silent synapses during LTP affects synaptic gain and transmission dynamics. *Nature neuroscience*, 4(10), pp.989–96.

Pop, A.S. et al., 2014. Rescue of dendritic spine phenotype in Fmr1 KO mice with the mGluR5 antagonist AFQ056/Mavoglurant. *Psychopharmacology*, 231(6), pp.1227–1235.

Pretto, D.I. et al., 2014. Differential increases of specific FMR1 mRNA isoforms in premutation carriers. *Journal of medical genetics*, pp.1–11.

Qin, M. et al., 2011. A mouse model of the fragile X premutation: Effects on behavior, dendrite morphology, and regional rates of cerebral protein synthesis. *Neurobiology of Disease*, 42(1), pp.85–98.

Qin, M., 2005. Postadolescent Changes in Regional Cerebral Protein Synthesis: An In Vivo Study in the Fmr1 Null Mouse. *Journal of Neuroscience*, 25(20), pp.5087–5095.

Quirk, G.J., Armony, J.L. & LeDoux, J.E., 1997. Fear conditioning enhances different temporal components of tone-evoked spike trains in auditory cortex and lateral amygdala. *Neuron*, 19(3), pp.613–624.

Rauch, A. et al., 2012. Range of genetic mutations associated with severe non-syndromic sporadic intellectual disability: An exome sequencing study. *The Lancet*, 380(9854), pp.1674–1682.

Rodrigues, S.M. et al., 2002. The group I metabotropic glutamate receptor mGluR5 is required for fear memory formation and long-term potentiation in the lateral amygdala. *Journal of Neuroscience*, 22(12), pp.5219–5229.

Rohde, M. et al., 2009. GABAA receptor inhibition does not affect mGluR-dependent LTD at hippocampal Schaffer collateral-CA1 synapses. *Neuroscience Letters*, 467(1), pp.20–25.

Romanski, L.M. & LeDoux, J.E., 1993. Information cascade from primary auditory cortex to the amygdala: corticocortical and cortico-amygdaloid projections of temproal cortex in the rat. *Cereb Cortex*, 3, pp.515–532.

Ronesi, J.A. et al., 2012. Disrupted Homer scaffolds mediate abnormal mGluR5 function in a mouse model of fragile X syndrome. *Nature Neuroscience*, 15(3), pp.431–440.

Ronesi, J.A. & Huber, K.M., 2008. Homer Interactions Are Necessary for Metabotropic Glutamate Receptor-Induced Long-Term Depression and Translational Activation. *Journal of Neuroscience*, 28(2), pp.543–547.

Ropers, H.-H. & Hamel, B.C.J., 2005. X-linked mental retardation. *Nature Reviews Genetics*, 6(1), pp.46–57.

Rouach, N. & Nicoll, R.A., 2003. Endocannabinoids contribute to short-term but not long-term mGluR-induced depression in the hippocampus. *European Journal of Neuroscience*, 18(4), pp.1017–1020.

Routh, B.N., Johnston, D. & Brager, D.H., 2013. Loss of functional A-type potassium channels in the dendrites of CA1 pyramidal neurons from a mouse model of fragile X syndrome. *Journal of Neuroscience*, 33(50), pp.19442–50.

Royall, D.R. et al., 2002. Executive control function: A review of its promise and challenges for clinical research. *Journal of Neuropsychiatry and Clinical Neurosciences*, 14(4), pp.377–405.

Royeck, M. et al., 2008. Role of Axonal Na V 1 . 6 Sodium Channels in Action Potential Initiation of CA1 Pyramidal Neurons. *Journal of Neurophysiology*, pp.2361–2380.

Rudelli, R.D. et al., 1985. Adult fragile X syndrome. Clinico-neuropathologic findings. *Acta Neuropathologica*, 67(3-4), pp.289–295.

S, P.R.I.N. et al., 2004. Rap1-induced p38 Mitogen-activated Protein Kinase Activation Facilitates AMPA Receptor Trafficking via the GDI Rab5 Complex. *Biochemistry*, 279(13), pp.12286–12292.

Sah, P. & Louise Faber, E.S., 2002. Channels underlying neuronal calcium-activated potassium currents. *Progress in Neurobiology*, 66(5), pp.345–353.

Schulz, B. et al., 2001. The metabotropic glutamate receptor antagonist 2-methyl-6-(phenylethynyl)-pyridine (MPEP) blocks fear conditioning in rats. *Neuropharmacology*, 41, pp.1–7.

Selby, L., Zhang, C. & Sun, Q.Q., 2007. Major defects in neocortical GABAergic inhibitory circuits in mice lacking the fragile X mental retardation protein. *Neuroscience Letters*, 412(3), pp.227–232.

Semyanov, A. et al., 2004. Tonically active GABAA receptors: Modulating gain and maintaining the tone. *Trends in Neurosciences*, 27(5), pp.262–269.

Senn, V. et al., 2014. Long-range connectivity defines behavioral specificity of amygdala neurons. *Neuron*, 81(2), pp.428–437.

Shah, M.M., 2014. Cortical HCN channels: function, trafficking and plasticity. *The Journal of Physiology*, 592(13), pp.2711–9.

Sharma, A. et al., 2010. Dysregulation of mTOR signaling in fragile X syndrome. *Journal of Neuroscience*, 30(2), pp.694–702.

Shin, L.M. & Liberzon, I., 2010. The neurocircuitry of fear, stress, and anxiety disorders. *Neuropsychopharmacology*, 35(1), pp.169–191.

Shiraishi-Yamaguchi, Y. & Furuichi, T., 2007. The Homer family proteins. *Genome biology*, 8(2), p.206.

Sidorov, M.S. et al., 2014. Extinction of an instrumental response: A cognitive behavioral assay in Fmr1 knockout mice. *Genes, Brain and Behavior*, 13(5), pp.451–458.

Siomi, H. et al., 1993. The protein product of the fragile X gene, FMR1, has characteristics of an RNA-binding protein. *Cell*, 74(2), pp.291–298.

Snyder, E.M. et al., 2001. Internalization of ionotropic glutamate receptors in response to mGluR activation. *Nature Neuroscience*, 4(11), pp.1079–1085.

Song, C., Ehlers, V.L. & Moyer, J.R., 2015. Trace Fear Conditioning Differentially Modulates Intrinsic Excitability of Medial Prefrontal Cortex-Basolateral Complex of Amygdala Projection Neurons in Infralimbic and Prelimbic Cortices. *Journal of Neuroscience*, 35(39), pp.13511–13524.

Spencer, C.M. et al., 2008. Social behavior in Fmr1 knockout mice carrying a human FMR1 transgene. *Behavioral neuroscience*, 122(3), pp.710–715.

Stanton, P.K. & Sarvey, J.M., 1984. Blockade of long-term potentiation in rat hippocampal CA1 region by inhibitors of protein synthesis. *Journal of Neuroscience*, 4(12), pp.3080–3088.

Stefani, G. et al., 2004. Fragile X Mental Retardation Protein Is Associated with Translating Polyribosomes in Neuronal Cells. *Journal of Neuroscience*, 24(33), pp.9272–9276.

Su, T. et al., 2011. Early continuous inhibition of group 1 mGlu signaling partially rescues dendritic spine abnormalities in the Fmr1 knockout mouse model for fragile X syndrome. *Psychopharmacology*, 215(2), pp.291–300.

Sun, H. & Neugebauer, V., 2011. mGluR1, but not mGluR5, activates feed-forward inhibition in the medial prefrontal cortex to impair decision making. *Journal of Neurophysiology*, 106(2), pp.960–73.

Suvrathan, A. et al., 2010. Characterization and reversal of synaptic defects in the amygdala in a mouse model of fragile X syndrome. *Proceedings of the National Academy of Sciences of the United States of America*, 107(25), pp.11591–11596.

Szlapczynska M., 2014. *Long range connectivity defines learning-induced intrinsic plasticity of prelimbic neurons*. Unpublished PhD thesis, University of Bordeaux.

Testa-Silva, G. et al., 2012. Hyperconnectivity and slow synapses during early development of medial prefrontal cortex in a mouse model for mental retardation and Autism. *Cerebral Cortex*, 22(6), pp.1333–1342.

Tian, D. et al., 2015. Contribution of mGluR5 to pathophysiology in a mouse model of human chromosome 16p11.2 microdeletion. *Nature Neuroscience*, 18(2), pp.16–19.

Till, S.M. et al., 2012. Altered maturation of the primary somatosensory cortex in a mouse model of fragile X syndrome. *Human Molecular Genetics*, 21(10), pp.2143–2156.

Till, S.M. et al., 2015. Conserved hippocampal cellular pathophysiology but distinct behavioural deficits in a new rat model of FXS. *Human Molecular Genetics*, 24(21), pp.5977–5984.

Todd, P.K., Mack, K.J. & Malter, J.S., 2003. The fragile X mental retardation protein is required for type-I metabotropic glutamate receptor-dependent translation of PSD-95. *Proceedings of the National Academy of Sciences of the United States of America*, 100(24), pp.14374–8.

Tsvetkov, E. et al., 2002. Fear conditioning occludes LTP-induced presynaptic enhancement of synaptic transmission in the cortical pathway to the lateral amygdala. *Neuron*, 34(2), pp.289–300.

Urbach A. et al., 2010. Differential modelling of fragile X syndrome by human embryonic stem cells and induced pluripotent stem cells. *Cell Stem Cell*, 6, pp.407-412.

Utari, A. et al., 2010. Aging in fragile X syndrome. *Journal of Neurodevelopmental Disorders*, 2(2), pp.70–76.

Van Aerde, K.I. & Feldmeyer, D., 2015. Morphological and physiological characterization of pyramidal neuron subtypes in rat medial prefrontal cortex. *Cerebral Cortex*, 25(3), pp.788–805.

Van Der Zwaag, B. et al., 2010. A co-segregating microduplication of chromosome 15q11.2 pinpoints two risk genes for autism spectrum disorder. *American Journal of Medical Genetics, Part B: Neuropsychiatric Genetics*, 153(4), pp.960–966.

Varga, V. et al., 2009. Fast synaptic subcortical control of hippocampal circuits. *Science*, 326(5951), pp.449–53.

Varma, N. et al., 2001. Metabotropic glutamate receptors drive the endocannabinoid system in hippocampus. *Journal of Neuroscience*, 21(24), p.RC188.

Verheij, C. et al., 1993. Characterization and localization of the FMR-1 gene product associated with fragile X syndrome. *Nature*, 363(6431), pp.722–724.

Verkerk, A. et al., 1991. Identification of a Gene (FMR-1) Containing a CGG Repeat Coincident with a Breakpoint Cluster Region Exhibiting Length Variation in Fragile X Syndrome. *Cell*, 65, pp.905–914.

Vertes, R.P., 2004. Differential Projections of the Infralimbic and Prelimbic Cortex in the Rat. *Synapse*, 51(1), pp.32–58.

Vidal-Gonzalez, I. et al., 2006. Microstimulation reveals opposing influences of prelimbic and infralimbic cortex on the expression of conditioned fear. *Learning & Memory*, 13(6), pp.728–733.

Vislay, R.L. et al., 2013. Homeostatic Responses Fail to Correct Defective Amygdala Inhibitory Circuit Maturation in Fragile X Syndrome. *Journal of Neuroscience*, 33(17), pp.7548–7558.

Vissers, L.E.L.M., Gilissen, C. & Veltman, J.A., 2015. Genetic studies in intellectual disability and related disorders. *Nature Reviews Genetics*, 17(1), pp.9–18.

Volk, L.J. et al., 2006. Differential Roles for Group 1 mGluR Subtypes in Induction and Expression of Chemically Induced Hippocampal Long-Term Depression Differential Roles for Group 1 mGluR Subtypes in Induction and Expression of Chemically Induced Hippocampal Long-Term Depressi. *Journal of Neurophysiology*, 95, pp.2427–2438.

Volk, L.J. et al., 2007. Multiple Gq-coupled receptors converge on a common protein synthesis-dependent long-term depression that is affected in fragile X syndrome mental

retardation. *Journal of Neuroscience*, 27(43), pp.11624–11634.

de Vries, B.B. a. et al., 1997. Screening and Diagnosis for the Fragile X Syndrome among the Mentally Retarded: An Epidemiological and Psychological Survey. *The American Journal of Human Genetics*, 61(3), pp.660–667.

Wang, H. et al., 2008. FMRP Acts as a Key Messenger for Dopamine Modulation in the Forebrain. *Neuron*, 59(4), pp.634–647.

Wang, Y. et al., 2006. Heterogeneity in the pyramidal network of the medial prefrontal cortex. *Nature Neuroscience*, 9(4), pp.534–542.

Watson, C. et al., 2008. Aberrant Brain Activation During Gaze Processing in Boys With Fragile X Syndrome. *Archives of General Psychiatry*, 65(11), p.1315.

Weiler, I.J. et al., 2004. Fragile X mental retardation protein is necessary for neurotransmitter-activated protein translation at synapses. *Proceedings of the National Academy of Sciences of the United States of America*, 101(50), pp.17504–17509.

Weiler, I.J. et al., 1997. Fragile X mental retardation protein is translated near synapses in response to neurotransmitter activation. *Proceedings of the National Academy of Sciences of the United States of America*, 94(10), pp.5395–5400.

Weiler, I.J. & Greenough, W.T., 1993. Metabotropic glutamate receptors trigger postsynaptic protein synthesis. *Proceedings of the National Academy of Sciences of the United States of America*, 90(15), pp.7168–7171.

Wijetunge, L.S. et al., 2014. Stimulated emission depletion (STED) microscopy reveals nanoscale defects in the developmental trajectory of dendritic spine morphogenesis in a mouse model of fragile X syndrome. *Journal of Neuroscience*, 34(18), pp.6405–12.

Willemsem R. et al., 2002. Timing of the absence of *FMR1* expression in full mutation chorionic villi. *Human Genetics*, 110, pp.601-605.

Wilson, B.M. & Cox, C.L., 2007. Absence of metabotropic glutamate receptor-mediated plasticity in the neocortex of fragile X mice. *Proceedings of the National Academy of Sciences of the United States of America*, 104(7), pp.2454–9.

Wright-Talamante, C. et al., 1996. A controlled study of longitudinal IQ changes in females and males with fragile X syndrome. *American journal of medical genetics*, 64(2), pp.350–5.

Xu, Z.-H. et al., 2012. Group I mGluR antagonist rescues the deficit of D1-induced LTP in a mouse model of fragile X syndrome. *Molecular Neurodegeneration*, 7(1), p.24.

Yan, Q.J. et al., 2005. Suppression of two major Fragile X Syndrome mouse model phenotypes by the mGluR5 antagonist MPEP. *Neuropharmacology*, 49(7), pp.1053–1066.

Yuste, R., 2011. Dendritic spines and distributed circuits. *Neuron*, 71(5), pp.772–781.

Zahrt, J. et al., 1997. Supranormal stimulation of D-1 dopamine receptors in the rodent prefrontal cortex impairs spatial working memory performance. *Journal of Neuroscience*, 17(21), pp.8528–8535.

Zang, J.B. et al., 2009. A mouse model of the human fragile X syndrome I304N mutation. *PLoS Genetics*, 5(12).

Zhang, L. & Alger, B.E., 2010. Enhanced endocannabinoid signaling elevates neuronal

excitability in fragile X syndrome. *Journal of Neuroscience*, 30(16), pp.5724–5729.

Zhang, Y. et al., 2008. The tyrosine phosphatase STEP mediates AMPA receptor endocytosis after metabotropic glutamate receptor stimulation. *Journal of Neuroscience*, 28(42), pp.10561–6.

Zhao, M.-G., 2005. Deficits in Trace Fear Memory and Long-Term Potentiation in a Mouse Model for Fragile X Syndrome. *Journal of Neuroscience*, 25(32), pp.7385–7392.

Zhuo D. et al., 1998. Ankyrin G is required for clustering of voltage gates Na channels at axon initial segments and for normal action potential firing. *Journal of Cell Biology*, 143(5), pp. 1295-1304.

Zucker, R.S. & Regehr, W.G., 2002. Short term plasticity. *Annual Review of Physiology*, 64(1), pp.355–405.